2017

Investigating the Feedstock Properties and Process Conditions Influencing the Characteristics of Products Generated from the Hydrothermal Carbonization of Organic Feedstocks

Liang Li
University of South Carolina

INVESTIGATING THE FEEDSTOCK PROPERTIES AND PROCESS CONDITIONS INFLUENCING THE CHARACTERISTICS OF PRODUCTS GENERATED FROM THE HYDROTHERMAL CARBONIZATION OF ORGANIC FEEDSTOCKS

by

Liang Li

Bachelor of Engineering
East China University of Science and Technology, 2008

Master of Inorganic Chemistry
Chinese Academy of Sciences, 2011

Submitted in Partial Fulfillment of the Requirements

For the Degree of Doctor of Philosophy in

Civil Engineering

College of Engineering and Computing

University of South Carolina

2017

Accepted by:

Nicole D. Berge, Major Professor

Juan Caicedo, Committee Member

Joseph Flora, Committee Member

Kyoung S. Ro, Committee Member

Cheryl L. Addy, Vice Provost and Dean of the Graduate School

ACKNOWLEDGEMENTS

First I want to give my greatest acknowledgement to my advisor Dr. Nicole D. Berge, for her constant support during my Ph.D. study and for her patience and motivation. I cannot imagine how I could finish my Ph.D. study without her guidance and help and I am truly fortunate to have her as my advisor.

I also want to acknowledge my Ph.D. committee, Dr. Juan Caicedo, Dr. Joseph Flora, Dr. Kyoung S. Ro for their great help and encouragement. My sincere thanks also go to all professors in the environmental area in our department. I want to thank my former lab mate and roommate Xiaowei Lu, who supported and encouraged me a lot. I also want to thank fellow graduate students in our department who always support and encourage me.

Many friends gave me great help during my Ph.D. study: Yang Cao, Yuan Hong, Junxiu Liu, Yating Mao, Yiying Wang, Jiting Xu, Mr. and Mrs. Rice, Mr. and Mrs. Aluri, and I am grateful for many other friends not named here.

I give my whole-hearted thanks to my dear husband Chen Zhou and our little girl Iris Zhou. I also would like to express my gratitude to my parents and parents in law for everything they have given to me. I would not have completed this long journey without their unconditional love and support. They have always been by my side.

ABSTRACT

Hydrothermal carbonization (HTC) is a novel environmentally beneficial thermal conversion process for the transformation of organic feedstocks to value-added products. However, little is known about the role of feedstock properties and/or process conditions during carbonization. This study was conducted to determine the parameters most influential during the HTC of organic feedstocks. Experiments and statistical analyses were conducted to: (1) determine the effect of specific feedstocks, feedstock interactions, and process conditions on carbonization product characteristics; (2) understand how initial liquid characteristics influence product characteristics and evaluate the significance of these initial liquid characteristics in predicting product characteristics; and (3) develop statistical models to predict product characteristics and determine parameter influence on carbonization product characteristics when carbonizing various feedstocks at different reaction conditions. Results from laboratory-scale experiments evaluating the carbonization of food waste and packaging materials indicate solid concentration influences carbon distribution. The presence of packaging materials significantly influences hydrochar carbon content. Laboratory-scale experiment results from the carbonization of wastes in the presence of different initial liquids suggest activated sludge and landfill leachate impart minimal impact on the evaluated carbonization product characteristics. Multiple linear regression and regression tree models were developed and indicate process conditions are more influential to the hydrochar yield, liquid and gas-

phase carbon content, while feedstock proximate and ultimate properties are more influential on hydrochar carbon, energy contents, and the normalized carbon content of the solid. Additional linear and nonlinear (e.g., regression tree and random forest) models were developed with a larger number of feedstock properties to describe hydrochar yield, carbon content, and energy content. Results from Sobol analysis of these models suggests the most influential parameters to hydrochar yield are solid concentration, temperature, feedstock lignin, polarity, hydrogen, carbon, time and ash. The most influential parameters to hydrochar carbon content are feedstock hydrogen, carbon, solid concentration and ash or volatile matter. The most influential parameters to hydrochar energy content are feedstock hydrogen, carbon, oxygen, ash, temperature and time. These most influential feedstock properties should be considered during feedstock selection. Overall, results from this work provide models that can be used to predict carbonization product characteristics.

TABLE OF CONTENTS

LIST OF TABLES

LIST OF FIGURES

LIST OF ABBREVIATIONS

Ash_{feed} ..... Ash content in feedstock

BOD ..... Biological oxygen demand

C_{feed} ..... Carbon content in feedstock

Cel_{feed} ..... Cellulose content in feedstock

COD ..... Chemical oxygen demand

FC_{feed} ..... Fixed carbon in feedstock

FSI ..... First order Sobol index

H_{feed} ..... Hydrogen content in feedstock

Hem_{feed} ..... Hemicellulose content in feedstock

HR ..... Heating rate

HTC ..... Hydrothermal carbonization

HT ..... Heating time

HT/t ..... Heating time over reaction time

Lig_{feed} ..... Fixed carbon content in feedstock

MAPE ..... mean absolute percentage error

MLR ..... multiple linear regression

OOB RMSE ..... out-of-bag root mean squared error

O_{feed} ..... Oxygen content in feedstock

Pol_{feed} ..... Polarity of feedstock

RF ..... Random forest model

RMSE ..... Root mean squared error

$RMSE_{CV}$ ..... Cross validated root mean squared error

RT ..... Regression tree model

$Solids_{initial}$ ..... Initial solids concentration

T_{final} ..... Reaction temperature

TOC ..... Total organic carbon

TSI ..... Total order Sobol index

t ..... Reaction time

V ..... Reactor volume

VR ..... Volume ratio

VM_{feed} ..... Volatile matter in feedstock

CHAPTER 1.

INTRODUCTION

1.1 MOTIVATION

Hydrothermal carbonization (HTC) is a novel thermal conversion process that has been shown to be environmentally beneficial for the transformation of organic feedstocks, such as biomass, carbohydrates and organic components of waste streams, into value-added products. This wet, relatively low temperature thermal conversion process occurs in the temperature range of 180 – 350 ^{o}C in closed systems for a certain time under autogenous pressures. Hydrothermal carbonization can potentially be a viable option for the production of such materials. During HTC, wet organic feedstocks (e.g., biomass and wastes) undergo a series of simultaneous reactions, including hydrolysis, dehydration, decarboxylation, aromatization, and recondensation (Funke et al., 2010; Libra et al., 2011; Sevilla and Fuertes, 2009; Titirici et al., 2007 and 2012). Carbon-rich, energy-dense carbonaceous materials, referred to as hydrochar, with attractive surface functionalization are ultimately generated. Hydrochar has been reported to be used in a variety of environmentally-relevant applications, including as a soil amendment (Libra et al., 2011), energy source (Berge et al., 2011; Heilmann et al., 2010; Reza et al., 2014; Hrncic et al., 2016), environmental sorbent (Román et al., 2012 and 2013; Jain et al., 2016), and/or a material for energy and/or hydrogen storage (Falco et al., 2013). Along with hydrochar, a liquid stream that contains appreciable concentrations of valuable compounds (e.g., organic acids, hydroxymethylfurfural (HMF)) and nutrients can be formed. The number of published papers reporting on different aspects of HTC has increased significantly over the past ten years. As the exploration of the HTC process continues, there is a great need for understanding the parameters that influence the characteristics of products generated from the HTC of organic feedstocks.

Feedstock types have been reported to play an important role during hydrothermal carbonization (Asghari and Yoshida, 2006; Akalın et al., 2012; Becker et al., 2013; Nizamuddin, et al., 2017), and lead to the diversified characteristics of value-added products. Feedstocks studied during HTC vary from pure compounds (e.g., cellulose and glucose) to complex feedstocks (e.g., wood and plant materials). Pure compounds are often carbonized when it is necessary to identify the carbonization mechanisms. Titirici et al. (2008) have reported that hexose sugars degrade to hydroxymethyl furfural and then condense to solid carbonaceous materials with similar chemical and structural composition during HTC, while solids formed from the carbonization of different pentoses are relatively different from one another. The majority of the HTC studies have focused on the complex feedstocks. Complex feedstocks such as wood and grass have different compositions (e.g., the different proportions of cellulose, hemicellulose and lignin) and likely influence the carbonization products characteristics such as recovered solids yield, energy content, carbon distribution in solid, liquid and gas phases (Kang, et al., 2012; Nizamuddin, et al., 2017).

Along with feedstock properties, the hydrothermal conversion process also depends on process conditions such as reaction temperature (Tian, et al., 2012; Wiedner, et al., 2013, Sabio, et al., 2016; Nizamuddin, et al., 2017), time (Asghari and Yoshida, 2006; Lu, et al., 2012 and 2013), and other process-related parameters (Sevilla and Fuertes, 2009; Heilmann et al., 2000 and 2011). Changes in process conditions are likely to influence the carbonization kinetics and have been shown to affect hydrochar chemical characteristics and morphology (Akiya and Savage, 2002; Siskin and Katritzky, 2001; Sevilla and Fuertes, 2009), hydrochar energy content (Román et al., 2012; Akalin et al.,

2012; Hwang et al., 2012; Kieseler et al., 2013), and liquid-phase organic concentrations (Asghari and Yoshida, 2006; Hrncic et al., 2016; Lu et al., 2013; Luo et al., 2011; Watchararuji et al., 2008). An important and required component of HTC is the presence of adequate moisture/liquid. Results from previously conducted experiments also indicate that changes in initial liquid composition may favorably impact carbonization product yields and composition (Lynam et al., 2011 and 2012). These multiple parameters influence the hydrothermal carbonization process, and competing influences of the carbonization parameters lead to carbonization products with varied properties.

Although the influences of feedstock properties, process conditions and liquid characteristics have been previously investigated in many HTC studies, their specific role on carbonization product characteristics remains unclear and the reported conclusions/trends that detail the influence of feedstock properties, process conditions and liquid characteristics cannot be universally applied. This is likely due to the changes in process kinetics, which likely vary with feedstocks, reactor volumes, and reactor heating mechanisms/rates. Conflicting conclusions about the influence of specific process conditions, such as reaction time, on carbonization product characteristics have been reported. Solid yields have been shown to decrease with reaction time, while the carbon and energy contents of the solids have been shown to increase with reaction time (Heilmann et al., 2010 and 2011; Lu et al., 2012 and 2013). Others have reported that reaction time does not have a significant impact on carbonization product formation/characteristics (Heilmann et al., 2010; Román et al., 2012). Similarly, conflicting reports about the influence of feedstocks have been documented. Hoekman et al. (2013) report the difference in energy content when carbonizing woody and

herbaceous feedstocks respectively, while Wiedner et al. (2013) report that changes in feedstock type have little influence on solids characteristics.

Nizamuddin et al., 2017 recently conducted a literature review to investigate the influence of reaction temperature, feedstock (e.g., cellulose, hemicellulose and lignin), reaction time, catalyst presence, and pressure on solid fuel production during HTC. As part of this study, only 105 HTC related papers were reviewed. Based on the literature information, the authors suggest reaction temperature, time and type of feedstocks are the primary parameters that influence the HTC process. However, no analytical techniques were used to determine the most critical parameters and a limited set of feedstock properties (e.g., cellulose, hemicellulose and lignin) and process conditions (e.g., temperature and time) were considered.

It is very important to understand the specific role of the individual influential parameter to design carbonization work that can meet the desired carbonization goal. Therefore, this dissertation focuses on investigating the critical parameters that influence the carbonization product characteristics using statistical models. Potential influential parameters, with specific attention paid to feedstock properties, will be investigated in this work. Few HTC studies have focused on developing statistical models to understand parameter importance or to predict product characteristics given a specific feedstock and a set of reaction conditions. Furthermore, the reported HTC models are somewhat limited to their specific study conditions (e.g., range of temperatures, times, reactor sizes, and types of feedstock) and the ability to expand the models to other feedstocks and process conditions has not been studied. Through this work, prediction models of carbonization product characteristics, which can be widely used, will be developed by collecting

literature on hydrothermal carbonization. The investigation of critical parameters influencing carbonization product characteristics and development of predictive statistical models based on such critical influential parameters would allow for the prediction of carbonization product characteristics prior to the carbonization work. It would also allow for the predetermination of the suitable operational conditions required to meet the desired carbonization purpose.

1.2 RESEARCH OBJECTIVES

The overall goal associated with the work described in this dissertation is to determine the parameters most influential during the hydrothermal carbonization (HTC) of organic feedstocks and to describe how each of these parameters influences the final product characteristics. Although some literature has studied the parameters influencing HTC, none of the previously published literature elucidates the specific role of individual feedstock properties and/or process conditions when carbonizing a series of feedstocks under various process conditions. Laboratory-scale experiments will be conducted to investigate how various feedstocks (e.g., paper, yard waste, food waste and packaging materials), liquid characteristics (e.g., pH, conductivity, COD and TOC) and process conditions (e.g., temperature, time and initial solids concentration) influence carbonization product characteristics. To further understand the general effects of the specific parameters including feedstock properties (e.g., ultimate and proximate properties, cellulose, hemicellulose, lignin and polarity) and process conditions (e.g., temperature, time and initial solids concentration) and to determine which parameters are critical to the HTC process, carbonization data will be collected from literature, and

statistical models will be developed to explain the role of critical parameters in predicting carbonization product characteristics. Results from this work will play an important role in selecting appropriate operational parameters during the HTC process to meet specific application objectives and predicting carbonization product characteristics. The specific objectives of this work include:

Objective 1: Determine the effect of specific feedstocks (e.g., paper, yard waste and food waste) (Chapter 3, 4 and 5) and process conditions (e.g., temperature, time and solids concentration) (Chapter 2-5) on the carbonization product characteristics and determine whether interactions between feedstocks are present during carbonization (Chapter 3 and 5).

Objective 2: Understand how liquid characteristics (e.g., pH, conductivity, COD and TOC) influence carbonization product characteristics and evaluate the significance of liquid characteristics in predicting these carbonization product characteristics (e.g., hydrochar yield, carbon content, energy content as well as the mass of carbon in the liquid and gas phase) (Chapter 4).

Objective 3: Develop statistical models to predict product characteristics when carbonizing a variety of feedstocks over a range of reaction conditions and to study the parameters significantly influencing the carbonization product characteristics using different methods (Chapter 3 - 5).

1.3 DISSERTATION ORGANIZATION

This dissertation consists of six chapters. Chapters 2 – 6 contain results from laboratory experiments and statistical models of product characteristics aimed at meeting

the specific research objectives of this study. Chapter 6 contains overall conclusions from this study. The following outlines the information represented in each chapter:

In Chapter 2, laboratory-scale experiments evaluating the carbonization of food waste and packaging materials were conducted over time (0 - 96 hr) and at different temperatures (225, 250 and 275^{o}C) and solids concentrations (5 - 47%). Results from these experiments are used to help understand how feedstocks (e.g., food waste and packaging materials) and process conditions (e.g., temperature, time and initial solids concentration) influence carbonization product properties and composition. This work has been published in Waste Management (Li et al., 2013).

In Chapter 3, results from laboratory experiments aimed at evaluating the influence of different initial moisture sources (e.g., DI water, landfill leachate and activated sludge) during the carbonization of yard waste, paper, and food waste are described. Statistical analyses were conducted to evaluate whether changes in initial liquid characteristics (e.g., pH, conductivity, COD and TOC) have a significant influence on carbonization product characteristics and to assess the relationship between carbonization product characteristics, initial liquid source characteristics, feedstock type, and process conditions. This work has been published in Waste Management (Li et al., 2014).

In Chapter 4, linear (multiple linear regression) and non-linear (regression tree) models developed to describe the role of process conditions and feedstock properties (e.g., ultimate and proximate properties) on carbonization product characteristics based on experimental data collected from HTC-related literature are described. The influence of

feedstock properties and process conditions were evaluated using parameter importance. This work has been published in Bioresource Technology (Li et al., 2015).

In Chapter 5, additional linear and non-linear (regression tree and random forest models) statistical methods based on data collected from HTC-related literature to describe hydrochar characteristics (e.g., hydrochar yield, carbon content, and energy content) are described. Sobol analysis was conducted to evaluate the sensitivity of feedstock properties (e.g., feedstock ultimate properties, proximate properties, cellulose, hemicellulose, lignin and polarity) and process conditions (e.g., temperature, time and initial solids concentration) on each hydrochar characteristic to identify the most influential parameters on the studied hydrochar properties. This work will be submitted to Bioresource Technology.

Chapter 6 contains the overall conclusions of this study, as well as recommendations for future studies.

CHAPTER 2.

HYDROTHERMAL CARBONIZATION OF FOOD WASTE AND ASSSOCIATED PACKAGING MATERIALS FOR ENERGY SOURCE GENERATION

Li, L., Diederick, R., Flora, J. R., and Berge, N. D. 2013. Hydrothermal carbonization of food waste and associated packaging materials for energy source generation. *Waste management*, *33*(11), 2478-2492.

Reprinted here with permission of publisher.

ABSTRACT

Hydrothermal carbonization (HTC) is a thermal conversion technique that converts food wastes and associated packaging materials to a valuable, energy-rich resource. Food waste collected from local restaurants was carbonized over time at different temperatures (225, 250 and 275oC) and solids concentrations to determine how process conditions influence carbonization product properties and composition. Experiments were also conducted to determine the influence of packaging material on food waste carbonization. Results indicate the majority of initial carbon remains integrated within the solid-phase at the solids concentrations and reaction temperatures evaluated. Initial solids concentration influences carbon distribution because of increased compound solubilization, while changes in reaction temperature imparted little change on carbon distribution. The presence of packaging materials significantly influences the energy content of the recovered solids. As the proportion of packaging materials increase, the energy content of recovered solids decreases because of the low energetic retention associated with the packaging materials. HTC results in net positive energy balances at all conditions, except at a 5% (dry wt.) solids concentration. Carbonization of food waste and associated packaging materials also results in net positive balances, but energy needs for solids post-processing are significant. Advantages associated with carbonization are not fully realized when only evaluating process energetics. A more detailed life cycle assessment is needed for a more complete comparison of processes.

2.1 INTRODUCTION

Food waste represents a significant and largely underutilized fraction of municipal solid waste (MSW). The National Resources Defense Council (NRDC, 2012) recently reported that approximately 40% of food in the US is wasted during its processing and distribution and/or while at commercial institutions and/or households. In 2010, the United States (US) discarded approximately 30.8 million tonnes of food waste, accounting for 14 percent of total generated MSW (EPA, 2011). Food wastes also represent large fractions of MSW in other developed countries, such as England (15% of waste, DEFRA, 2011) and Belgium (7.6% of waste, European Commission, 2010). Waste streams in developing countries generally contain even larger fractions of food waste. Bangladesh and Kuwait, for example, generate waste with 62 (Sujauddin et al., 2008) and 51% (Abdulla and Mahrous, 2001) of food, respectively.

A large fraction of discarded food in the US is landfilled, where food waste degradation rates coupled with low initial gas collection efficiencies result in little recovery of methane gas generated by decomposition of the food (Amini and Reinhart, 2011; Levis and Barlaz, 2011). The desire for greater environmental stewardship and policy requirements are leading to greater diversion of food wastes from MSW landfills. Food waste diversion is currently being practiced and promoted in several countries (e.g., Japan (Takata et al., 2012), European Union (EU Council, 1999)), in several states within the United States (e.g., California (Moore and Edgar, 2008)), at several commercial institutions/restaurants, and is becoming prevalent on many college campuses.

Diverted food wastes are primarily treated/managed using biological approaches, including composting (e.g., Büyüksönmez, 2012; Jambeck et al., 2006; Levis et al., 2010;

Lundie and Peters, 2005; Namkoong, 1999; Sullivan, 2010; Witt, 2011; Yespan, 2009) and anaerobic digestion (Banks et al., 2011; Bernstad and la Cour Jansen, 2012; Ike et al., 2010; Levis et al., 2010). These techniques result in reductions in fugitive greenhouse gas emissions when compared to landfilling and lead to the generation of valuable resources (e.g., fertilizer, methane gas). However, these techniques also impart several operational challenges. Mixed wastes present a critical issue with these techniques (Levis et al., 2010), thus packaging wastes (often comingled with the food wastes) must be separated prior to treatment. Other disadvantages associated with these techniques include the need for large treatment footprints, little volume reduction of the wastes, and process-related odors. Although each of these techniques does result in production of a value added product, the future market for large amounts of compost is unknown (Levis et al. 2010) and the capital costs associated with anaerobic digestion facilities may be prohibitive (Kelleher, 2007; Levis et al., 2010).

Hydrothermal carbonization (HTC) is a thermal conversion technique that has the potential to overcome many of the challenges associated with the biological treatment of discarded food. Carbonization may allow for smaller required treatment footprints, more efficient conversion of mixed wastes, and greater waste volume reductions. In addition, carbonization results in the production of an easily stored energy-rich resource. HTC is a wet, relatively low temperature (~180 – 350 ^{o}C) thermal conversion process that occurs under autogeneous pressures (Berge et al., 2011; Funke and Ziegler, 2010; Hoekman et al., 2011; Libra et al., 2011; Titirici and Antonietti, 2010; Titirici et al., 2007). During HTC, wet feedstocks undergo a series of simultaneous reactions, including hydrolysis, dehydration, decarboxylation, aromatization, and recondensation (e.g., Berge et al., 2011;

Funke and Zeigler. 2010; Libra et al., 2011). A result of this process is the formation of a high carbon and energy density material (often termed hydrochar) that has been reported to have an energy content and composition equivalent to that of lignite coal (Berge et al., 2011). The produced chars may be easily stored and used for energy generation as needed. Because HTC is a thermochemical technique, mixed wastes may not be as significant of an operational issue as in composting and anaerobic digestion. In addition, because of the moisture requirement, food wastes are more suited for conversion via HTC than other dry, more common thermal conversion techniques.

Carbonization of feedstocks ranging from pure substances to components found in MSW has been evaluated (e.g., (Berge et al., 2011; Falco et al., 2011; Kang et al., 2012; Ramke et al., 2009; Sevilla and Fuertes, 2009). Few studies have focused on the carbonization of food wastes. Berge et al. (2011), Goto et al. (2004) and Lu et al. (2012) evaluated the carbonization of rabbit food, while Hwang et al. (2012) carbonized dog food. These experiments were conducted at different conditions, spanning a range of reaction temperatures (200 – 350^{o}C) and times (0.5 – 120 hrs), and demonstrate that carbonization of model food wastes is beneficial, resulting in the generation of hydrochar that has high carbon (45 - 93% of initial carbon) and energy (15 – 30 kJ/g dry solids) contents. Lu et al. (2012) suggest energy derived from hydrochar resulting from model food waste carbonization may be greater than that expected during incineration.

A detailed study evaluating the carbonization of collected food wastes, and associated packaging materials, is needed to determine the feasibility of this technique. The purpose of this study is to evaluate the carbonization of food waste and typical food packaging materials to determine how process conditions (e.g., feedstock

concentration/composition, reaction time/temperature) influence product properties and composition. The specific objectives of this study include: 1) determine the effect of food waste concentration and reaction temperature on food waste carbonization; 2) evaluate the effect of packaging materials on mixed food waste carbonization; 3) evaluate and compare energy balances associated with HTC and incineration of food wastes.

2.2 MATERIALS AND METHODS

2.2.1 Feedstocks

Food waste was periodically collected from restaurants located near the University of South Carolina (Columbia, SC). All collected waste was weighed and immediately separated into four categories: (1) all food materials, except those containing bones, (2) food containing bones (e.g., chicken wings), (3) packaging materials (e.g., paper, plastic, condiment containers, paper/plastic cups), and (4) others (e.g., plastic utensils, glass bottles). Each separated fraction of the waste was weighed to allow the determination of waste composition (Table 2.1). Visual observation of the collected food indicates the waste consists of a variety of cooked foods (e.g., chicken, seafood, french fries, vegetables), uncooked foods (e.g., vegetables, seafood) and condiments (e.g., salad dressing, ketchup, cocktail sauce). Because of processing limitations, food containing bones (e.g., chicken bones) was not used in these experiments. Packaging materials were subsequently separated into three additional categories: (1) paper, (2) cardboard and (3) plastics (Table 2.1). Following separation, the food and packaging materials were shredded to ensure uniform composition and particle size. The food waste was mixed and homogenized with a food-grade blender (Ninja Master Prep, Euro-Pro Operating LLC).

All packaging materials (e.g. paper, plastic, cardboard) were shredded using a titanium paper shredder (25 by 4 mm strips).

The moisture, energy, and carbon, hydrogen and nitrogen contents of these materials were measured. The moisture content of the separated components was measured using a gravimetric technique. A mass of each component was dried in a laboratory oven at 80℃ for at least 48 hours, or until the dried sample mass remains constant. The carbon, hydrogen, and nitrogen contents of the samples were measured using an elemental analyzer (Perkin Elmer 2400). The energy content of the dried waste components was measured using bomb calorimetry (C-200 Calorimeter, IKA, Inc.).

2.2.2 Batch HTC Experiments

All batch carbonization experiments were conducted following procedures previously described (Berge et al., 2011; Lu et al., 2012). Briefly, shredded wet feedstocks (e.g., food waste and/or packaging materials) were placed in 160-mL stainless steel tubular reactors (2.54 cm i.d., 25.4 cm long, MSC, Inc.) fitted with gas-sampling valves (Swagelock, Inc.). If required, deinonized (DI) water was subsequently added to each reactor to achieve desired moisture contents. All reactors were then sealed and heated in a laboratory oven at the desired temperature. Reactors were sacrificially sampled over a period of 96 hr. All experiments were conducted in duplicate. The relative percent difference (RPD) associated with duplicate samples is less than 15%, with the majority of the duplicate RPDs less than 5%. This low level of difference suggests the sample volumes used in this study are sufficient for obtaining reproducible results.

Two sets of experiments were conducted: (1) experiments in which separated food waste was carbonized at various solid contents and temperatures and (2)

experiments containing food and packaging materials to evaluate the influence of packaging on food waste carbonization. A list of the experiments conducted in this work is included in Table 2.2. The first set of experiments was conducted to understand how solids concentration and temperature influence the carbonization of food waste. Solids concentrations (%, dry wt.) of 32% (representing the as-received waste), 20%, and 5% were evaluated. These experiments were conducted at 250 ^{o}C. Reactors containing 32% solids (as-received food waste) were also conducted at 225 ^{o}C and 275 ^{o}C to evaluate the influence of temperature on carbonization.

To evaluate the influence of packaging materials on food waste carbonization, mixed packaging materials (added in the proportion collected, see Table 2.1) were mixed with food waste. Packaging concentrations of 7, 14, and 27% (dry wt.) were evaluated. Control experiments containing only packaging materials (in the proportion reported in Table 2.1) were also conducted. All experiments were conducted at 250^{o}C. Samples were sacrificially taken over a period of 96 hours.

2.2.3 Analytical Techniques

At each sampling time, reactors were removed from the oven and placed in a cold water bath. Following cooling, the produced gas was collected in either a 1 or 3-L foil gas sampling bag. Gas composition of these samples was analyzed using GC-MS (Agilent 7890). Gas samples were routed through a GS-CarbonPlot column (30m long and 0.53 mm id, J&W Scientific). Initial oven temperature was 35^{o}C. After 5-min, the temperature was increased at a rate of 25^{o}C/min until a final temperature of 250^{o}C was achieved. Carbon dioxide and trace gas standards (i.e., methane, ethane, propane, butane) (Matheson Trigas) were used to determine gas concentrations. Results from this analysis

were also used to provide qualitative data associated with the composition of the gas stream. Another gas sample was injected into a gas chromatograph (HP5890) equipped with a TCD and a Carboxen 1010 Plot column (30m x 0.53mm i.d., Supelco) for determination of hydrogen concentration (carrier gas was argon). Initial oven temperature was held constant at 35^{o}C for 7.5 min and subsequently increased to 240^{o}C at a rate of 24^{o}C/min. Gas volumes were measured with a volume syringe (S-1000, Hamilton Co.).

The process liquid and solid were separated via vacuum filtration through a 0.45 µm cellulose nitrate membrane filter (Whatman International Ltd.). Liquid conductivity and pH were measured using electrodes (Thermo Scientific Orion). Liquid chemical oxygen demand (COD) was measured using HACH reagents (HR + test kit, Loveland, CO). Liquid total organic carbon (TOC) was measured using a TOC analyzer (TOC-Vcsn, Shimadzu). All collected solids were dried at 80°C. Solid carbon, hydrogen, and nitrogen content (Perkin Elmer 2400 Elemental Analyzer) and energy content (C-200 bomb calorimeter, IKA, Inc.) were measured.

All collected data were used to calculate carbon and energy-related properties associated with the recovered solids, including: carbon fraction, carbon densification, carbon conversion fraction, energy density, and energetic retention efficiency (see Table 2.3 for parameter definitions and equations).

2.3 RESULTS AND DISCUSSION

2.3.1 Influence of Solids Concentration on Food Waste Carbonization

2.3.1.1 Carbon distribution

Experiments at three solids concentrations (5, 20 and 32%, dry wt.) were conducted to determine how solids concentration influences food waste carbonization. Mass balance

analyses indicate food waste carbonization results in a significant fraction (> 70%) of initially present carbon retained within the solid-phase over the 96-hour reaction period at all solids concentrations evaluated. This observation is consistent with carbonization studies reported in the literature associated with model food wastes (e.g., rabbit and dog food) and other feedstocks, such as cellulose, xylose, and glucose (e.g., Goto et al., 2004; Hwang et al., 2012; Kang et al., 2012; Lu et al., 2012; Sevilla and Fuertes, 2009). Smaller fractions of carbon were transferred to the liquid (10-40%) and gas-phases (<10%), also consistent with previous studies (e.g., Berge et al., 2011; Hoekman et al., 2011; Lu et al., 2012). Carbon recoveries in all experiments range from 93-116%.

Results indicate that initial solids concentration influences carbon distribution. Solids concentration imparts a large influence on the mass of carbon transferred to the liquid-phase (Figure 2.1), particularly at low initial solids concentrations. As the volume of water initially present increases (Table 2.2), so does the potential for increased feedstock dissolution/solubilization. A linear relationship between initial water volume and carbon mass (normalized by dry initial solids) transferred to the liquid results at each sampling time, with the coefficient of determination ranging from 0.88 to 0.90. Results from analysis of variance (ANOVA, Sigma Plot, Inc., at a level of significance of 0.05) tests indicate there is not a statistically significant ($p>0.05$) difference between the carbon content in the liquid (normalized by initial dry mass) in the 20 and 32% solids experiments at times greater than 16 hours. However, the liquid-phase carbon content resulting from the experiments conducted at 5% initial solids concentration is significantly different from that obtained at 20 and 32% solids concentration at all reaction times ($p < 0.05$).

Except for at 96 hours, there is a noticeable decrease of the fraction of carbon integrated within the solid-phase when carbonizing food waste at an initial concentration of 5% (dry wt.). There is little difference between the solid and gas-phase carbon distribution resulting from the carbonization of 20 and 32% (dry wt.) food waste. Results from ANOVA tests indicate the recovered solids carbon content (normalized by mass of initial solids) varies as a function of time and initial solids concentration. There is also a significant interaction between the time and initial solids concentration when comparing these data. Results suggest the difference between the carbon content (normalized by the mass of initial dry solids) of the char at 20 and 32% solids concentration is similar ($p > 0.05$) at 10 of the 11 reaction times evaluated. The carbon content of the recovered solids resulting from the experiments conducted at 5% initial solids concentration are statistically different from those at 20 and 32% solids at 6 of the 11 reaction times evaluated. ANOVA results also indicate that at 9 of the 11 reaction times evaluated the carbon in the gas (normalized by initial solids) from the 5% initial solids test is similar to that in obtained in both the 20 and 32% tests; the carbon content of the gas from the 20 and 32% tests results are similar in 5 of the 11 reaction times evaluated.Carbon conversion fractions were calculated following Lu et al. (2012) and reflect the extent of solid-phase carbon conversion as a result of HTC. Carbon conversion fractions greater than one are indicative of feedstock solubilization. Results from this analysis (Figure 2.2) suggest some initial solubilization of the food waste occurs. This observation is consistent with that reported by others. Lu et al. (2012) and Knezevic et al. (2010; 2009) report that feedstock solubilization is an important initial step for carbonization. Components of the food waste likely solubilized during early time include proteins,

carbohydrates, and lipids, following that reported by Ren et al. (2006) when heating restaurant garbage in water at 180^{o}C. Following initial solubilization, the conversion fractions associated with 20 and 32% solids (dry wt.) decrease and remain at or below one. The conversion fractions associated with the 5% initial solids experiments, however, remain above one, indicating the transfer of carbon from the liquid to the solid controls solid-phase carbon content/carbon distribution.

Based on carbon distribution data (Figure 2.1), the period of greatest conversion occurs during the first 8 hours of carbonization, with complete conversion resulting after 16-24 hours. It appears the rate of carbon transfer to the liquid, and thus to the solid, is influenced by initial solids concentration, as evidenced by changes in carbon distribution trends over time.

2.3.1.2 Gas composition

Carbon dioxide is the most predominant gas produced. This is consistent with reports associated with the carbonization of other feedstocks (e.g., Berge et al., 2011; Funke and Ziegler, 2010; Lu et al., 2012; Ramke et al., 2009) and indicates decarboxylation is a predominant pathway during food waste carbonization. Carbon dioxide accounts for approximately 30% (vol.) at early reaction times to 85% (vol.) at longer reaction times of the gas produced at all solids concentrations evaluated. The most predominant trace gases identified (via GC/MS) include methane, ethane, propane, propene, butane and furan. It should be noted that there are likely additional significant trace gases present that have not been identified with the current analytical method. This is evident when conducting a gas balance. The quantified trace gases (e.g., methane,

ethane, propane, butane, Figure 2.3) account for up to 1% (vol.) of the produced gas, indicating that approximately 14% of the produced gas is composed of unidentified gases.

Quantified gases are presented in Figure 2.3. The normalized mass of these gases is similar at all solids concentrations evaluated. These energy-rich gases increase with reaction time, suggesting longer reaction times correlate to greater energy that can be recovered from the gas-phase. The current analysis can also be used as a tool to qualitatively compare unquantified detected/identified gases over time. The gas peak areas associated with the identified gases were multiplied by the gas volume produced at each sampling time to represent changes in individual gas mass. The normalized mass of these gases (e.g., furan, propene) is similar at all solids concentrations (data not shown). The trend of furan mass in the gas differs from that of the other detected gases. Furan mass in the gas initially increases and then decreases with time. Gas-phase furan content is likely related to the presence of furfurals (such as 5-Hydroxymethyl furfural) in the liquid. Although specific liquid composition was not measured in this study, others have reported the presence of furfurals as a result of carbonization (e.g., (Chuntanapum and Matsumura, 2010; Falco et al., 2011; Titirici et al., 2008). As furfural is heated, it decomposes to form furan (Asghari and Yoshida, 2006). Over time, gas-phase furans may be incorporated into the solid-phase carbon (Baccile, 2009; Falco et al., 2011; Titirici et al., 2008).

2.3.1.3 Recovered solids

Solids recovery is calculated based on the total mass of dry solids recovered at each sampling time divided by the dry mass of the initial feedstock (Figure 2.4a). Recoveries from these experiments fit within the reported range of solids recovered

following carbonization of various feedstocks (e.g., Berge et al., 2011; Falco et al., 2011; Hoekman et al., 2011). Solids recovered during early times are comprised of both unconverted food waste and hydrochar. Such differences cannot be distinguished via gravimetric or solid-phase carbon measurements. Visual inspection of recovered solids at early times confirms this phenomenon. Solids recovery decreases with decreasing initial feedstock concentration (Figure 2.4a). This decrease in solids recovered results from a combination of initial feedstock solubilization and component partitioning to the gas and liquid-phases. Results from ANOVA tests indicate that solids recoveries at an initial solids concentration of 5% are statistically different from those at 20 and 32% at all reaction times, while solids recoveries obtained at 20 and 32% initial solids concentrations are similar in 6 of the 11 reaction times evaluated.

The hydrogen and nitrogen contents (defined in Table 2.3) of the recovered solids were measured and used to determine the mass of each released to the gas and/or liquid-phases. The majority of the initially present nitrogen mass remains within the solids; the mass of nitrogen released from the solid-phase decreases with decreasing initial moisture content, indicative of greater nitrogen compound dissolution in the liquid-phase (data not shown). At 96 hours and an initial solids concentration of 5% (dry wt.), approximately 37% of the initially present nitrogen is released, while only 24 and 18% is released at 20 and 32% (dry wt.) initial solids, respectively. This release of nitrogen from the solid-phase has also been observed by Ren et al. (2006). The mass of hydrogen in the recovered solids also declines, indicating dehydration of the feedstock occurs, as observed in other carbonization studies (e.g., Berge et al., 2011; Falco et al., 2011). Hydrogen transfer from the solid-phase appears to be dependent on initial moisture content. After 48 hours, an

average of approximately 54, 61, and 65% of initially present hydrogen remains integrated within the solid-phase when carbonizing 5, 20, and 32% solids (dry wt.), respectively.

The carbon in the recovered solids densifies with time. After 96 hours, the carbon densification of the recovered solids is 1.50, 1.45, and 1.30 for experiments conducted with 5, 20 and 32% (dry wt.) solids, respectively. Carbon densities decrease with increasing solids concentration, likely resulting from the lower mass of solids recovered at low initial solids concentrations. This densification has important energy-related implications (e.g., Channiwala and Parikh, 2002; Hwang et al., 2012; Ramke et al., 2009). The energy value of the recovered solids increases over time for all solids concentrations evaluated, with energy densities approaching 1.5 at all solids contents evaluated (Figure 2.5). After 96 hours, the average energy content of the char material is 33,570 J/g dry char. Solids energy densification has been reported when carbonizing a variety of feedstocks (Berge et al., 2011; Hoekman et al., 2011; Ramke et al., 2009; Román et al., 2012). Although the energy contents of the solids resulting from carbonization are similar at all solids concentrations, the amount of energy stored per gram of initial dry solids differs. Results indicate that normalized energy yield (as defined in Table 2.3) from recovered solids increases with solids concentration. Results from ANOVA tests indicate that the normalized energy yields from experiments conducted at an initial solids concentration of 5% are statistically different than those obtained when carbonizing with initial solids concentrations of 20 and 32% at all reaction times. There is not a statistically significant difference between the normalized energy yields obtained at initial solids concentrations of 20 and 32% at 10 of the 11 reaction times evaluated.

2.3.2 Influence of Temperature on Food Waste Carbonization

Experiments to determine the influence of reaction temperature (225, 250 and 275 ^{o}C) on food waste carbonization were conducted at 32% (dry wt.) solids. Results indicate that changes in final reaction temperature only slightly influence food waste carbonization.

The temperatures evaluated impart a similar effect on the carbon content of the recovered solids (normalized by dry initial solids) ($p = 0.103$, note there is no statistically significant interaction between temperature and time) (Figure 2.6). The carbon content of the liquid is slightly lower and carbon content of the gas is slightly higher at 275^{o}C because at higher temperatures gas evolution via decarboxylation and/or volatilization of organics is increased (Falco et al., 2011; Funke and Ziegler, 2010; Hoekman et al., 2011). The statistical significance associated with changes in the liquid and gas-phase carbon contents (normalized by initial dry solids) resulting from carbonization at different temperatures depends on reaction time. A comparison of these data indicates that the liquid-phase carbon contents at 225^{o}C are similar to those at 250^{o}C in 10 of the 11 reaction times evaluated and similar to those at 275^{o}C at 9 of the 11 reaction times evaluated; the liquid-phase data at 250^{o}C are statistically different from those at 275^{o}C after a reaction time of 24 hours. The gas-phase carbon contents (normalized by mass of initial solids) at 250^{o}C are similar to those at 275^{o}C at 9 of the 11 reaction times evaluated, while the data at 225^{o}C are statistically different from those at 250^{o}C in 6 of the 11 reaction times and different from those at 275^{o}C at 8 of the 11 reaction times.

Carbon dioxide remained the predominant gas at all temperatures evaluated. Temperature had little influence on the volume of carbon dioxide produced (~80% (vol.)

at longer reaction times). The masses of quantified trace gases produced normalized per gram of initial dry feedstock increase as reaction temperature increases, accounting for approximately 3% (vol.) of the gas produced at 275^{o}C and only 0.6% (vol.) at 225^{o}C (Figure 2.3). This increase in trace gas production at higher temperatures is likely a result of greater cracking of the long-chain hydrocarbons found in the food as reaction temperatures increase (Jia et al., 2004; Zhong et al., 2012).

Solids recovery (Figure 2.4b) is lowest at 275^{o}C. It is generally expected that as reaction temperatures increase, final solids recovery decreases (Figure 2.4b). A similar influence of temperature on solids recovery has also been reported in the literature when carbonizing feedstocks such as cellulose, glucose and wood (Hoekman et al., 2011; Kang et al., 2012; Knežević et al., 2009). ANOVA test results indicate that changes between the solid recoveries obtained from the experiments conducted at 225 and 250^{o}C are not statistically different at all reaction times, while changes between those obtained from experiments conducted at 225 and 275^{o}C and 250 and 275^{o}C are each only statistically significant at 3 of the 11 reaction times.

The average retained hydrogen and nitrogen in the recovered solids after 48 hours decreases with increasing reaction temperature, with 77% and 66% of nitrogen retained in the recovered solids at 225 and 275 ^{o}C, respectively, and 65 and 60% of hydrogen retained in the recovered solids at 225 and 275 ^{o}C, respectively. After 96 hours, the carbon densities of the recovered solids increase slightly with temperature and are 1.27, 1.30, and 1.42 for solids recovered at 225, 250 and 275 ^{o}C, respectively. Similar to the experiments conducted at different initial solids concentrations, these carbon densities increase as recovered solids decrease. Accordingly, the energy content of the recovered

solids from all experiments increases with time and, after 96 hours, the hydrochar energy contents at 250 and 275^{o}C are similar (33,909 and 34,791 J/g, respectively), with that associated with solids recovered when carbonizing at 225^{o}C approximately 17% lower (28,360 J/g dry solids). However, temperature does not impart a statistically different ($p = 0.160$) change in recovered solids energy content. Solids energy densities of 1.29, 1.54 and 1.58 at 225, 250 and 275 ^{o}C, respectively, result (Figure 2.5).

2.3.3. Influence of Packaging Materials on Food Waste Carbonization

Food waste often contains packaging materials that cause operational challenges when anaerobically digesting or composting these materials (Appels et al., 2011; Favoino, 2000; Levis et al., 2010). Waste collected from restaurants around the University of South Carolina campus contained approximately 13% (wet wt.) of packaging materials with the following composition (%, wet wt.): 27% plastic, 24% paper, and 49% cardboard. Experiments were conducted to evaluate how the presence of varying proportions of packaging materials influence food waste carbonization, specifically carbon distribution, gas composition, and solids energy content. For comparative purposes, carbonization of packaging materials (mixed in the proportion in which was found) was conducted separately, at a total solids content of 14% (dry wt.). Table 2.2 contains information regarding each of the conducted experiments.

2.3.3.1 Carbon distribution

The majority of initially present carbon remains integrated within the solid (> 74%) following carbonization in the presence of packaging material, while smaller fractions of carbon are transferred to the liquid (8 - 25%) and gas-phases (< 7%) in the presence of 7 and 14% (dry wt.) packaging materials (experiments 6 and 7, Table 2.2).

Carbon recoveries from these experiments range from 91 – 103%. Packaging materials impart a statistically different ($p<0.001$) influence on the solid-phase carbon content (normalized by mass of initial dry solids) at all reaction times. The statistical significance of changes in the carbon content in the gas-phase (normalized by mass of initial dry solids) depends on both reaction time and the percentage of packaging materials. The carbon content of the gas-phase resulting from experiments conducted with 27% (dry wt.) packaging materials are statistically different from those at 7% in 9 of the 11 reaction times and in 8 of the 11 reaction times at 14% packaging. Results from experiments containing 7% packaging materials are similar to those containing 14% packaging materials at 7 of the 11 reaction times evaluated. Because some liquid-phase samples were not obtainable, statistics associated with that data were not conducted.

As observed when evaluating the influence of solids content on carbonization, the percentage of carbon ultimately transferred to the liquid-phase depends on system initial moisture content. As the packaging percentage increases, the initial moisture content decreases (Table 2.2) and so does the fraction of carbon transferred to the liquid. It is important to note that as initial moisture content decreases, the amount of recoverable liquid also decreases (Table 2.4). In the studies containing 47% (dry wt.) total solids (27% (dry wt.) packaging materials, experiment 8), no liquid was recoverable via gravity drainage. The initial moisture remained bound in the char material, rendering liquid-phase carbon measurements impossible. An artifact of the bound liquid is high percentages of solid-phase carbon, as the carbon in the bound liquid is integrated within the solid-phase measurement. This bound liquid has important implications associated with process energetics, as discussed in subsequent sections.

The absolute mass of carbon found in each phase (solid, liquid, and gas) is influenced by the fraction of food and packaging materials (Figures 2.7a,c,e), with systems containing greater packaging resulting in greater masses of carbon in each phase. This is an artifact of the larger moisture content of the food waste. The carbon masses in the gas, liquid and solid-phases resulting from the experiments containing only food waste and only packaging materials (experiments 3 and 9, Table 2.2) can be used to predict the mass of carbon expected in the solid, liquid, and gas-phases in the mixed food and packaging experiments (experiments 6-8, Table 2.2). Results from this analysis are present in Figures 2.7 b,d,f. As shown, approximations associated with the carbon integrated within the solid are similar to the measured data, suggesting there is no interaction between the food and packaging materials during carbonization. To approximate the carbon in the solids resulting from the experiments containing 27% packaging material, the mass of carbon in the liquid needs to be accounted for. The theoretical carbon in the solid values vary by less than 5% from the experimental values (Figure 2.7d).

There are some deviations from these theoretical approximations in the gas and liquid-phases (Figure 2.7 b,f). These deviations likely result from changes in system moisture content. The theoretical approximations are based on experiments with larger moisture contents (Table 2.2), overestimating the mass of carbon in the liquid-phase. The majority of these points differ from the experimental value by less than 30%. Because more carbon is integrated within the liquid-phase, less is transferred to the gas, resulting in the underestimation of carbon in the gas-phase in the presence of packaging materials

(Figure 2.7f). The majority of these predictions differ from the experimental values by less than 20%.

2.3.3.2 Gas composition

Carbon dioxide remains the predominant component of the gas stream, equating to approximately 85% (vol.) of the produced gas after 96 hours. This is similar to the experiments containing only food waste (experiment 3, Table 2.2). The quantified trace gases (e.g., methane, ethane, propane, butane) account for up to 1% (vol.) of the produced gas. The normalized mass of methane, ethane, propane and butane (Figure 2.8) are lower than that obtained when carbonizing only food waste, likely due to the cracking of fewer long-chain hydrocarbons in the more complex packaging materials. A larger normalized mass of propene is produced with the presence of packaging material (data not shown). Previous studies indicate propene is the most abundant component in the gas obtained by the decomposition of plastics (Hájeková et al., 2007). When comparing the propene mass during HTC, Lu et al. (2012) found paper products released more propene than a model food waste.

2.3.3.3 Solids recovered

Solids recovered are influenced by the presence of packaging material (Figure 2.4c). There is a statistically significant difference between the solids recovered when carbonizing at the different concentrations of packaging materials ($p<0.001$). The mass of solids recovered can be approximated using results from the food and packaging only experimental results (Figure 2.9) and supports the hypothesis that there is no interaction between the food and packaging materials during carbonization. The majority of these predictions differ from the experimental values by less than 10%.

The presence of packaging materials does influence recovered solids carbon and energy densifications. The carbon densification when carbonizing with 7% (dry wt.) packaging materials is 1.33, while the densifications at 14% (dry wt.) packaging materials is 1.16 and close to that of the carbon densification associated with solids recovered when carbonizing packaging materials alone (1.17). Carbon densifications associated with the 27% (dry wt.) packaging materials are skewed by the carbon in the bound liquid.

The presence of packaging material also influences recovered solids energy content (statistically significant, $p<0.001$). Solids energy content decreases as the percentage of packaging materials increases, as do solids energy densities (Figure 2.5c). The decrease in normalized solids energy content is a result of the lower energy content of carbonized packaging materials. The total energy in the recovered solids can also be approximated by the initial mass of food and packaging materials. The approximations differ from the measured values by less than 20% (Figure 2.10). After 16 hrs, changes between the solid-phase hydrogen and nitrogen content of the recovered solids in these experiments are minimal (differences are less than 10%). A greater fraction of nitrogen remains integrated within the solids in the presence of packaging materials (average of 86%) than that associated with food waste, while less hydrogen is retained (average of 59%).

2.3.4 Carbonization Energy Balances

Energy balances associated with HTC and incineration of food and mixed food and packaging materials were calculated and compared (Figures 2.11 and 2.12). Energy balances from HTC were performed by calculating the energy required to ultimately

convert the food waste to heat, including (as shown in Figure 2.11a): (1) energy required to heat the water and solids for carbonization, (2) energy in the recovered solids and gases (assuming 100% energy recovery), (3) post-processing needs (i.e., char drying), and (4) subsequent combustion of the char material.

The energy required to heat water for carbonization was calculated by accounting for the mass distribution of water at the target temperature and by evaluating the enthalpy difference of the system at the final and initial temperatures (following procedures outlined by Berge et al., (2011)). During HTC, the phase change from water to steam is largely avoided, thus the energy required to heat the water (in a closed system to saturation conditions) is small in comparison to that required to evaporate the same mass of water needed for other thermal conversion processes. The energy required to heat the solids was calculated using specific heat capacities for food and the packaging materials (Table 2.5). The energy content of the gas was estimated based on measured concentrations and their respective energy densities (Table 2.5).

Because post-processing of recovered solids is necessary to obtain the final product, energy associated with the drying of the char and subsequent combustion were also considered. It is assumed that following carbonization, a portion of water will be removed from the material via gravity drainage (Figure 2.11a), requiring no energy. The amount of water retained in the solids following drainage will need to be evaporated. For these calculations, the mass of water remaining in char following drainage during the experiments was used (Table 2.4). Note that as initial system water content decreases, the amount of water drained via gravity also decreases. It should be noted that a lower energy alternative to evaporation of the wet recovered solids is air-drying of the char, which

would ultimately decrease post-processing energy requirements. Once dried, the char is combusted to obtain heat. The energy required to heat the solids to the combustion temperature (1,100^{o}C) was calculated using an assumed specific heat value for the char (Table 2.5). Any heat losses were neglected, as was the energy required to heat the reactor.

For comparison, an energy balance on waste material combustion was also completed. The following processes were accounted for (Figure 2.11b): (1) the energy required to evaporate the water, (2) the energy required to heat the solids to the combustion temperature of 1,100^{o}C, and (3) the energy content of the waste materials (based on laboratory measurements). It is assumed there is 100% efficiency of conversion. Any heat losses were neglected, as was the energy required to heat the reactor.

Results from these analyses indicate that carbonization of food waste containing 5% solids results in a net loss of energy. This unfavorable result is in large part due to the energy required to heat the large mass of liquid present (Figure 2.12a). Although the carbonization of food waste containing 20% solids is energetically positive, it is not more favorable than the incineration of food waste (as received, moisture content of approximately 68%). The largest contributing factor to this difference is the amount of energy required to heat the water in excess of what is initially present (Figure 2.12a). Carbonization of as received food waste (32% solids, dry wt.) is energetically positive and more energetically advantageous than incineration because there is a lower amount of energy required to heat the water during HTC than evaporation during incineration (Figure 2.12a). In addition, the recoverable energy from the char and gas is comparable to that expected to be derived from incineration. Drying of the recovered solids is the most

energy intensive component of the process at 32% (dry wt.) food waste, requiring approximately 1.42 times more energy than the heating of the water. It should be noted that if the recovered solids are air dried (e.g., energy requirements become zero), the net energy from HTC would be even more advantageous than incineration. Mechanically dewatering of the solids recovered from carbonization has been shown to be more efficient than its precursor material (Ramke et al., 2009) and thus may provide a means to reduce process energy needs if the energy associated with the mechanical process does not exceed that required to evaporate all bound moisture. Air-drying of the initial food waste stream (prior to incineration) could also be air-dried, however the length of such a process may lead to odor and additional greenhouse gas emission issues. It is also possible that air-drying of the recovered solids may result in odor-related issues. It should also be noted that heat may be recovered from the carbonization process (step 1) that may also offset energy requirements associated with any step of the carbonization and/or post-processing processes.

Carbonization is energetically positive at all temperatures evaluated with as received food waste (32%, wet wt.). It appears the most energetically favorable carbonization temperature is 275^{o}C. Although the recovered solids and gas produced at this temperature yield a slightly lower value that that at 250^{o}C, carbonization at 275^{o}C yields a solid material that retains less moisture than that at lower temperatures (Table 2.4), ultimately requiring less energy for post-solids processing. Carbonization at 250^{o}C is also more energetically favorable than incineration, despite the high energy required for post-processing of the solids recovered (Figure 2.12b). Although energetically positive, carbonization at 225^{o}C is not as favorable as incineration of food. At 225^{o}C,

more water remains bound within the char material, requiring greater post-processing energy needs. In addition, the solids at 225^{o}C yield a slightly lower energy content (Figure 2.12b).

Carbonization of food and associated packaging materials results in net energetically positive energy balances (Figure 2.12c). However, these scenarios appear to be less favorable than incineration of the same wastes. At 7% (dry wt.) packaging materials, the difference between the net energy associated with HTC and incineration of the same material is only 2%. As the fraction of packaging materials increases, so does the difference between HTC and incineration (9.5 and 10.8% difference at 14 and 27% (dry wt.) packaging, respectively). The following contributes to this result: (1) the energetic retention efficiency associated with packaging materials (~84%) is not as large as that associated with food (>95%) and (2) more liquid remains bound within the solid material (Table 2.4), requiring greater post-processing energy needs. If the recovered solids are completely air dried, carbonization processes are always more favorable than incineration. Using the data obtained from these experiments, a final recovered solids moisture content of less than approximately 60% (by wet weight) is required to result in the same net energy as incineration. Approximately one fourth of the moisture remaining bound within the char material needs to be air dried for HTC of the food and associated packaging to be at least as energetically favorable as incineration. As noted previously, mechanically dewatering of the solids may aid in achieving this level of moisture. Experiments containing packaging materials were only conducted at 250^{o}C. It is possible that at 275^{o}C less liquid remains bound in the recovered solids, requiring lower post-processing energy.

There are advantages associated with carbonization that are not included in these energy balance calculations. The solid energy source produced as a result of HTC can be easily stored, transported, and used for energy generation as needed. Because the char is more energy dense than its corresponding feedstock, transportation costs/requirements per mass of char will be less (McKendry, 2002). It is also likely that energy can also be recovered from the liquid, increasing the energetics of HTC (Wirth et al., 2012). Another benefit associated with HTC is nutrient recovery from the liquids (e.g., contains nitrogen species), and the potential for using it as a fertilizer (Lilliestråle, 2007).

2.4 CONCLUSIONS

Results indicate carbonization of food waste results in the majority of initial carbon remaining within the solid-phase (> 70% of initially present carbon), with small fractions remaining in the liquid and gas-phases. Carbon dioxide is the predominant gas detected, with methane, ethane, propane, propene, butane and furan also detected. Initial solids concentration (or moisture content) influences carbon distribution because, as initial liquid volume increases, so does the potential for increased compound solubilization. Changes in reaction temperature, however, impart a small change on carbon distribution. Energy contents associated with the recovered solids are similar to high-value coals. The energy yields (also accounting for the mass of solids recovered) associated with the recovered solids were greatest at a food waste concentration of 32% solids (dry wt.) and 250 ^{o}C.

The presence of packaging materials has a significant influence on the energy content of the recovered solids. As the proportion of packaging materials increases, the energy content of recovered solids decreases because of the low energetic retention

associated with the packaging materials. Results from these experiments can be approximated using results from experiments conducted with food and packaging only, suggesting there is no synergistic interaction during the HTC of these materials.

Results from energy balances suggest HTC results in net positive energy balances at all conditions, except at a 5% solids concentration. HTC is most energetically favorable with as received food waste (32% solids, wet wt.) and at 275 ^{o}C. Carbonization of food waste and associated packaging materials is also energetically positive. As the fraction of packaging materials increases, so does the difference between HTC and incineration because of energy needs for solids post-processing. It should be noted that advantages associated with carbonization, such as reduced transportation costs and nutrient recovery from process waters are not fully realized when only comparing process energetics. A more detailed life cycle assessment is needed for a complete comparison of processes.

Table 2.1 Collected food waste/packaging waste composition and properties.

Category		Composition (%)	Moisture Content (%, dry wt.)	Initial Energy Content (J/g dry wt.)	Composition (%, dry wt.) C	H	N
Food waste (without bones)		52	68	22,036	52.4	8.3	2.8
Food waste (with bones)		1.6	45	NM	NM	NM	NM
Packaging Materials	Paper	3.5	46	15,670	40.6	6.4	0.08
	Cardboard	6.5	37	13,029	40.0	6.0	0.13
	Plastic	3.2	5.9	25,523	62.0	4.8	0.10
Others		33	NM	NM	NM	NM	NM

NM: not measured

Table 2.2 Initial conditions associated with conducted experiments.

			Solids Composition (% dry wt.)			Initial Solids Properties				
Exp #	Temp (^{o}C)	Total mass of dry solids added to the reactor (g)	Food Waste	Packaging[1]	Total Solids	Moisture Content (%)	Energy Content (J/g dry solids)	Carbon (%, dry wt.)	Hydrogen (%, dry wt.)	Nitrogen (%, dry wt.)
1	250	2	5[2]	0	5	95	22,036	52.4	8.3	2.8
2	250	8	20[2]	0	20	80	22,036	52.4	8.3	2.8
3	250	12.8	32	0	32	68	22,036	52.4	8.3	2.8
4	225	12.8	32	0	32	68	22,036	52.4	8.3	2.8
5	275	12.8	32	0	32	68	22,036	52.4	8.3	2.8
6	250	14.8	30	7	37	63	21,262	51.5	7.8	2.3
7	250	16.4	27	14	41	59	20,621	50.8	7.4	1.9
8	250	18.8	20	27	47	53	19,623	49.7	6.7	1.3
9	250	5.6	0	14[2]	14	86	17,850	47.7	5.6	0.1

[1]Packaging wastes have the following composition (%, wet wt): 27% plastic, 24% paper, and 49% cardboard
[2]Additional moisture was added to these experiments.

Table 2.3 Terminology and associated equations for determination of carbon and energy-related properties.

Term	Definition	Equation
Carbon fraction	Mass of carbon in the solid, liquid or gas-phase normalized by mass of initially present carbon (dry wt).	$\frac{\text{mass carbon in solid, liquid or gas phase}}{\text{mass of carbon in initial feedstock}}$
Normalized carbon mass	Mass of carbon in the solid, liquid or gas-phase normalized by mass of initially present feedstock.	$\frac{\text{mass carbon in solid, liquid or gas phase}}{\text{mass of dry initial feedstock}}$
Carbon conversion fraction	Measure of the extent of solid-phase carbon conversion (defined by Lu et al. 2012)	$\eta = \frac{C_{feed} - C_t}{C_{feed} - C_\infty}$ where C_{feed} is the mass of carbon in the initial feedstock, C_t is the carbon in the recovered solids at time t, and C_∞ is the carbon in the recovered solids after 96 hours
Carbon densification	Densification of carbon in the recovered solids	$\frac{\%\text{ carbon in the recovered solids}}{\%\text{ carbon in the initial feedstock}}$
Carbon content	Measured carbon concentration in solids (%)	$\frac{\text{mass of carbon in solids}}{\text{mass of dry solids}} \times 100$
Hydrogen content	Measured hydrogen concentration in solids (%)	$\frac{\text{mass of hydrogen in solids}}{\text{mass of dry solids}} \times 100$
Nitrogen content	Measured nitrogen concentration in solids (%)	$\frac{\text{mass of nitrogen in solids}}{\text{mass of dry solids}} \times 100$
Solids recovery	Mass of solids recovered normalized by mass of initial feedstock	$\frac{\text{mass of dried solids recovered}}{\text{mass of dry initial feedstock}} \times 100$
Energy densification	Densification of solid energy content	$\frac{\text{measured energy content of recovered solids}}{\text{measured energy content of feedstock}}$

Energetic retention efficiency	Measure of the fraction of feedstock energy retained within the solid material.	$\frac{\text{Energy content of recovered solids}}{\text{Energy content of feedstock}}$ X solids recovery
Normalized energy yield	Calculation of the total energy associated with the recovered solids normalized by mass of initial dry feedstock	$\text{Energy content of recovered solids X } \frac{\text{mass of recovered solids}}{\text{mass of dry initial feedstock}}$
Total energy	Calculation of the total energy of the solids material	$\text{Energy content of recovered solids X } \frac{}{\text{mass of solids recovered}}$

Table 2.4 Fraction of water remaining bound within the solids.

Exp #	Temp (^{o}C)	Total Solids (%, dry wt.)	Moisture retained within solids (% of initially present moisture)[1,2]
1	250	5	2.0 (0.44)
2	250	20	6.6 (0.83)
3	250	32	61.7 (18.51)
4	225	32	59.2 (7.09)
5	275	32	16.5 (6.30)
6	250	37	44.7 (6.41)
7	250	41	94.2 (6.79)
8	250	47	100 (0)

[1]based on average of water retained from 72 – 96 hours

[2]values in parentheses represent the standard deviations

Table 2.5 Input information and assumptions associated with energy balance calculations.

Hydrothermal Carbonization				
Step	*Process*	*Parameters/Assumptions*		
1	Water and solids heating	Water/Vapor Properties		Solids Properties
		Water densities (g/mL):[a]	Vapor densities (g/mL):[a]	Heat Capacities (kJ/kg-^{o}C):
		225^{o}C: 0.835	225^{o}C: 0.0128	Food waste: 3.3[b]
		250^{o}C: 0.799	250^{o}C: 0.0199	Packaging: 1.75[c]
		275^{o}C: 0.756	275^{o}C: 0.0352	
2	Energy recovery from solids and gas	Solids calculation: Energy content of recovered solids x the mass of recovered solids.		Gas energy densities:[d] Methane:55.528 kJ/g Ethane: 51.901 kJ/g Propane: 50.368 kJ/g Butane: 49.546 kJ/g
		Note: 100% efficiency/recovery is assumed.		
3	Water evaporation from recovered char	Heat capacity of water = 4.186 kJ/kg-K[a] Heat of vaporization of water = 2270 kJ/kg[a] *Volume of water taken from experimental data (Table 4)*		
4	Solids combustion	Heat capacity of char = 1.3 kJ/kg-^{o}C[e] Combustion temperature = 1,100^{o}C		

Incineration		
Step	*Process*	*Parameters/Assumptions*
1	Water evaporation	Heat capacity of water = 4.186 kJ/kg-K Heat of vaporization of water = 2270 kJ/kg
2	Heat solids	Heat capacity of food = 3.3 kJ/kg-^{o}C

		Heat capacity of packaging = 1.75 kJ/kg-^{o}C Combustion temperature = 1,100^{o}C
3	Energy generation	Food waste = 22.04 kJ/g dry feedstock Paper = 15.595 kJ/g dry feedstock Cardboard = 13.209 kJ/g dry feedstock Plastic = 25.522 kJ/g dry feedstock *Note: these are based on laboratory measurements. 100% efficiency/recovery is assumed.*

[a] Sandler, 2006
[b] Rodriguez et al., 1995
[c] Hatakeyama, 1982; Morikawa and Hashimoto, 2011
[d] Turns, 2000
[e] Hanrot et al., 1994

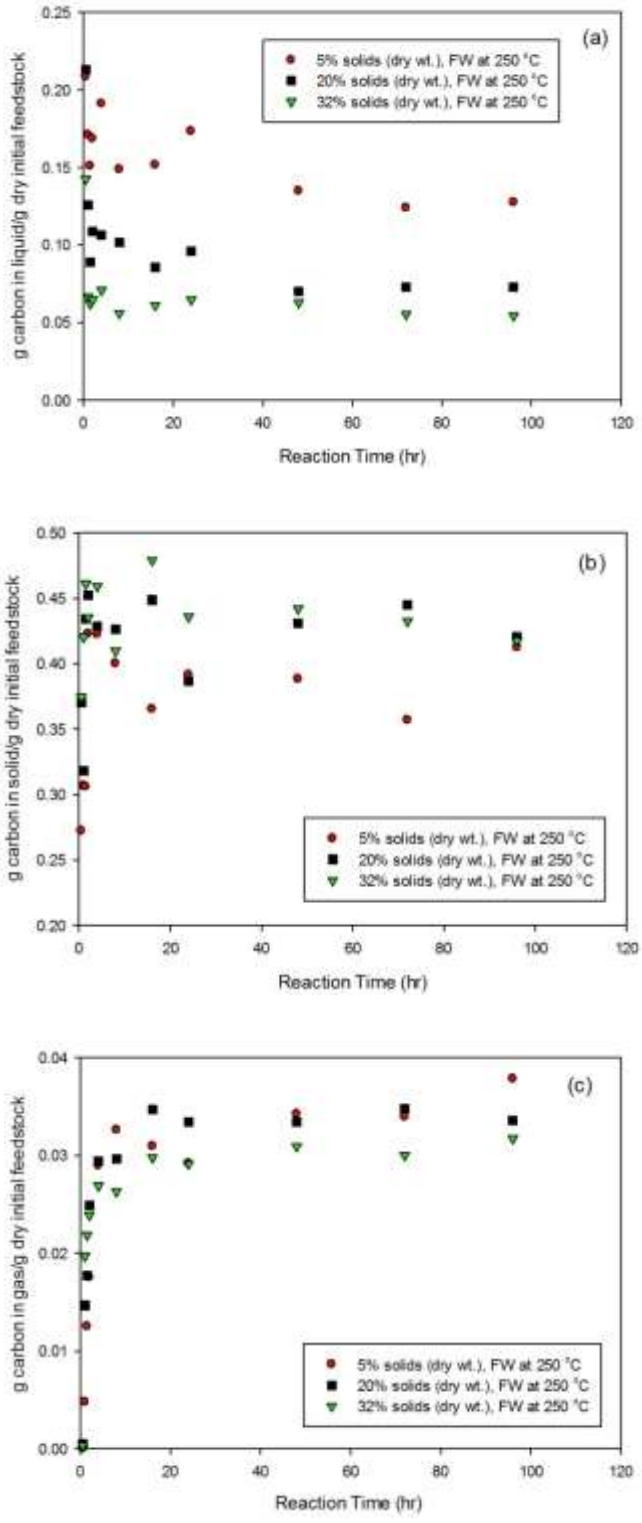

Figure 2.1 Carbon distribution (normalized by initial dry feedstock mass) in the: (a) liquid, (b) solid, and (c) gas-phases resulting from the carbonization of food wastes (FW) at 5, 20, and 32% (dry wt.) solids at 250^{o}C.

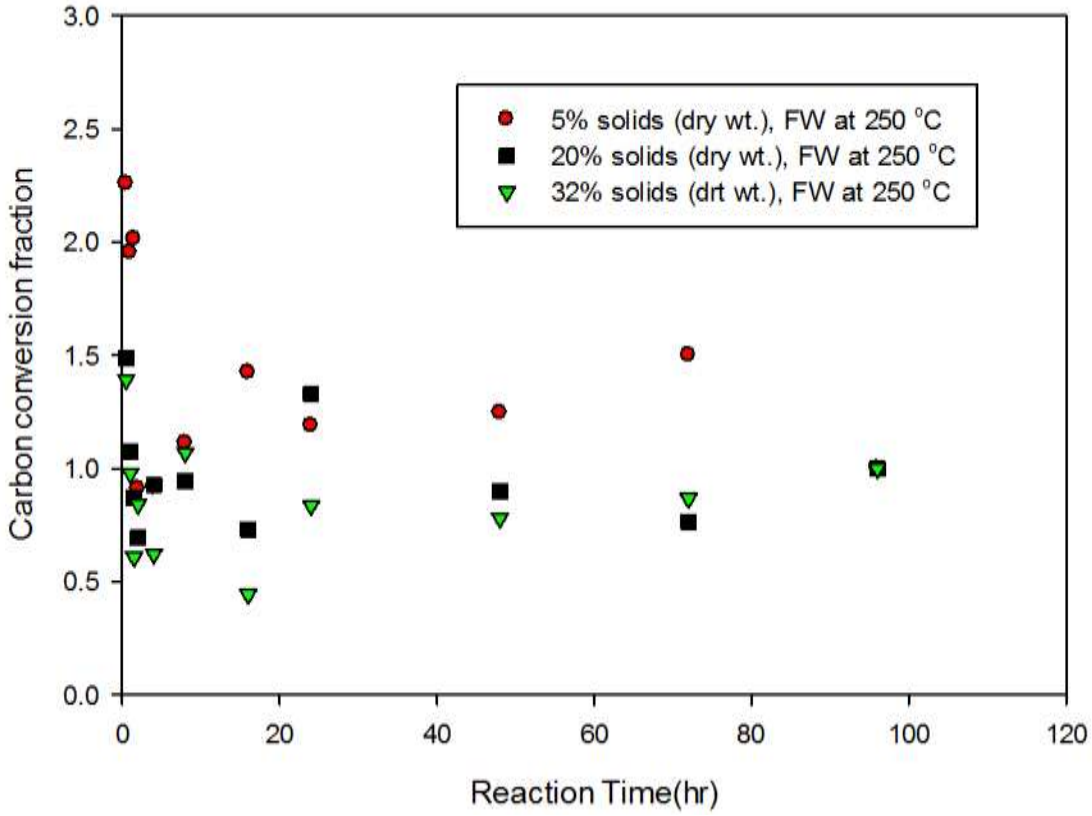

Figure 2.2 Carbon conversion fractions associated with food waste conversion at different solids concentrations at 250^{o}C.

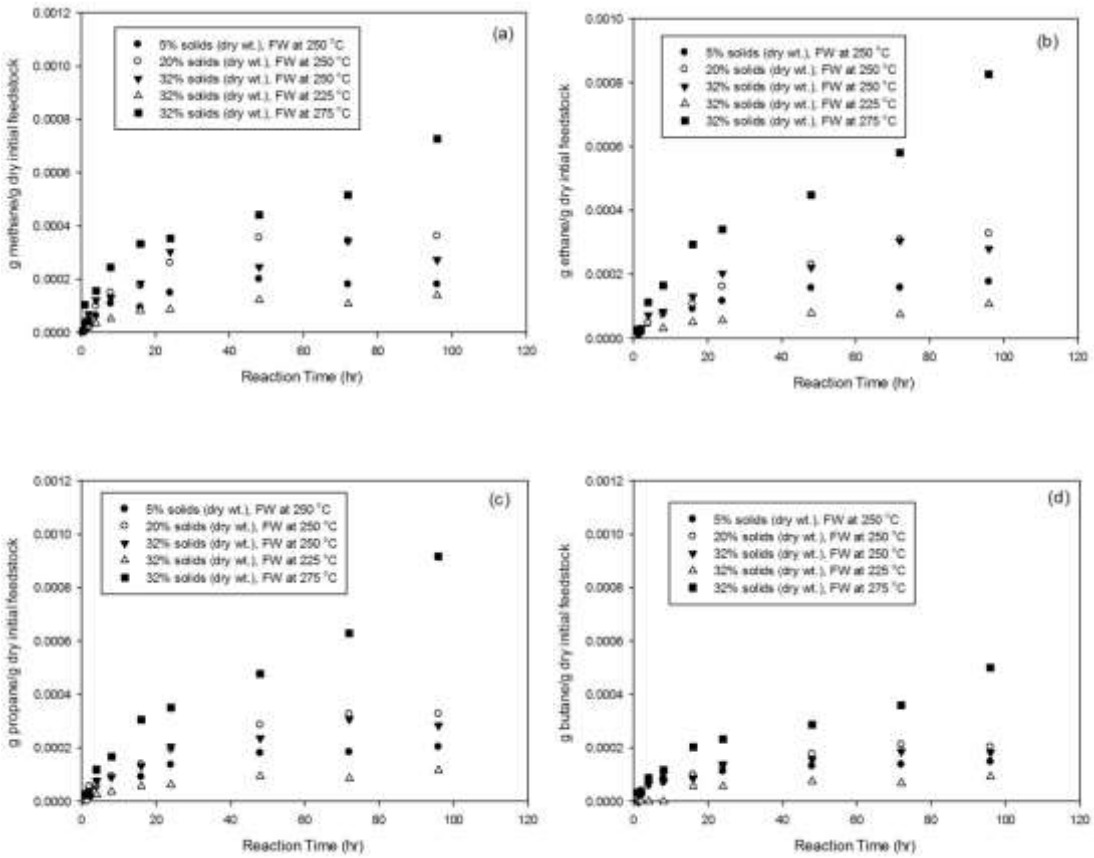

Figure 2.3 Normalized trace gas production resulting from experiments conducted with varying initial solids concentrations and temperatures: (a) methane, (b) ethane, (c) propane, and (d) butane. FW represents food waste. PM represents packaging materials.

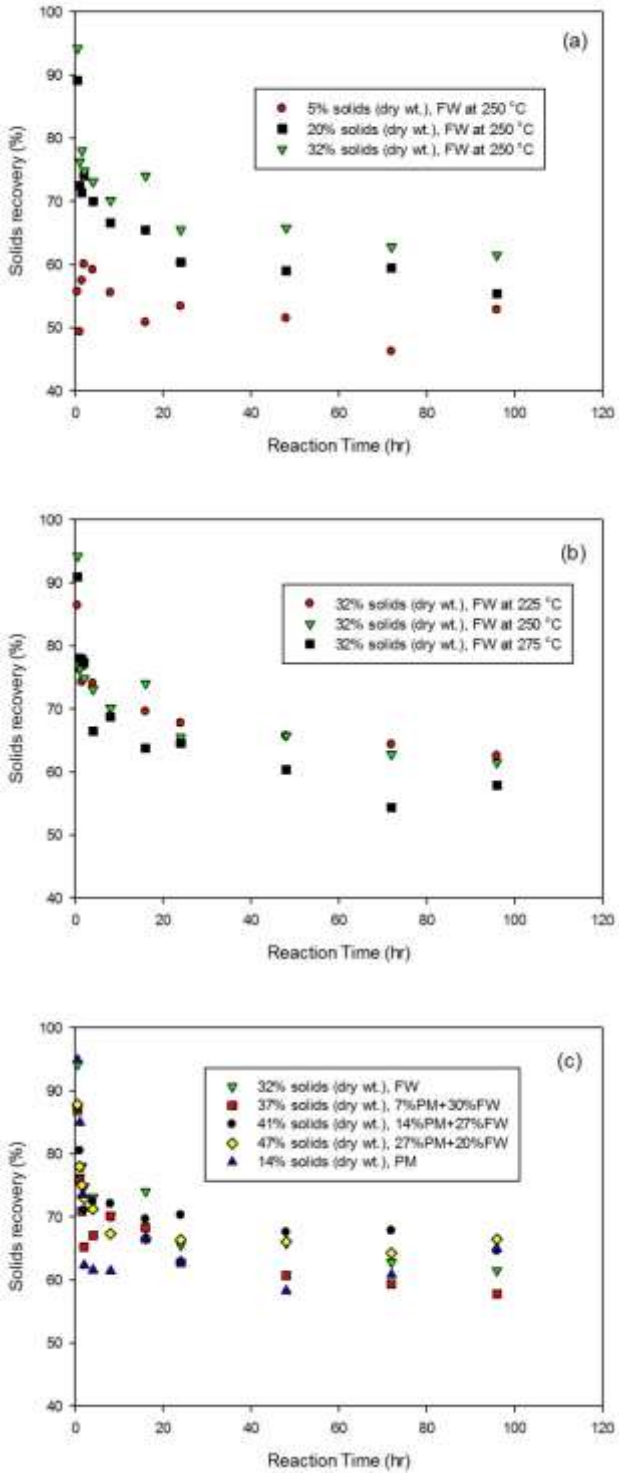

Figure 2.4 Solids recovery resulting from carbonization at: (a) different initial solids concentrations, (b) different reaction temperatures, and (c) in the presence of various fractions of packaging materials. FW represents food waste. PM represents packaging.

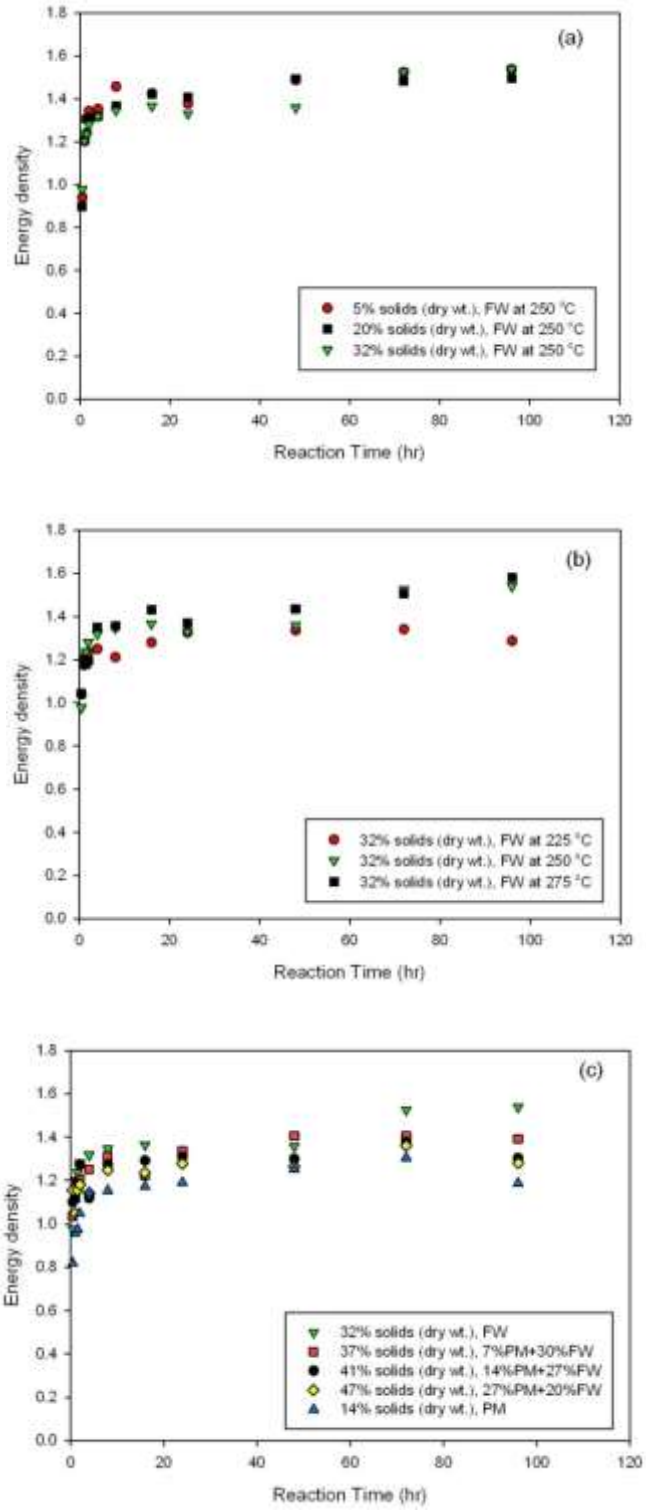

Figure 2.5 Energy densities at: (a) different initial solids concentrations, (b) different reaction temperatures, and (c) in the presence of various fractions of packaging materials. FW represents food waste. PM represents packaging materials.

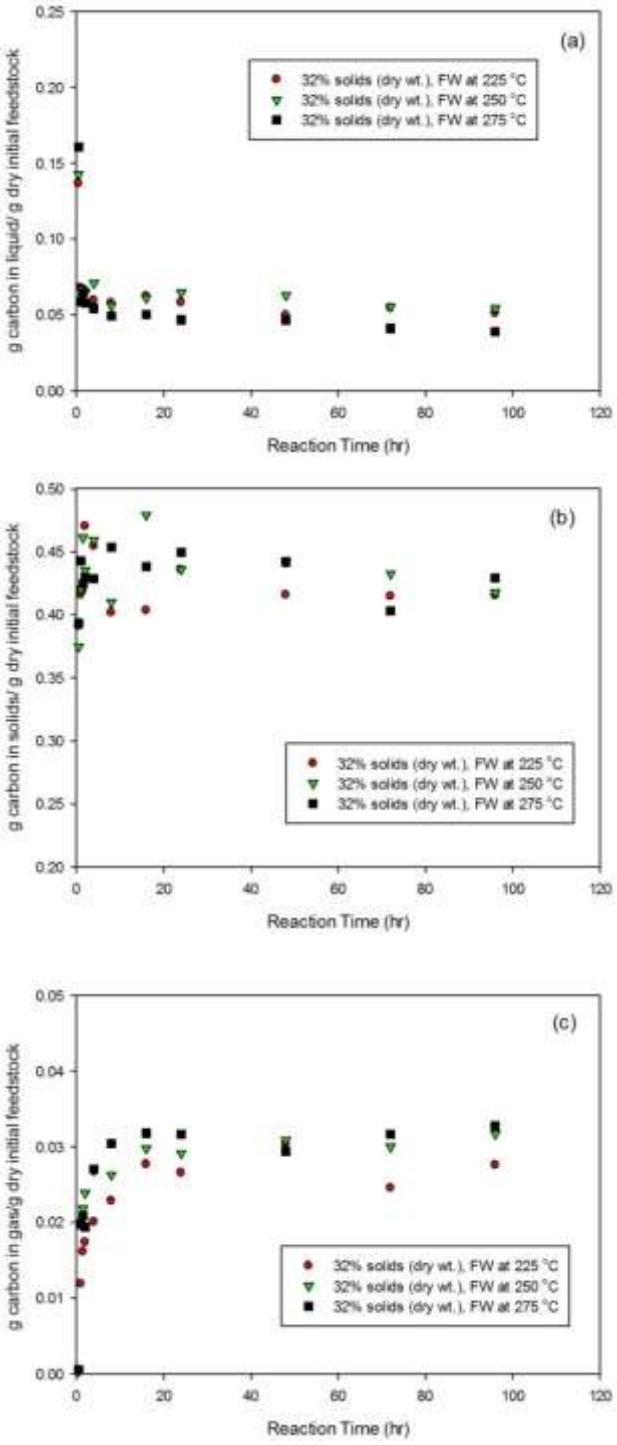

Figure 2.6 Carbon distribution (normalized by initial dry feedstock mass) in the: (a) liquid, (b) solid, and (c) gas-phases resulting from the carbonization of food wastes at 225, 250, and 275oC. FW represents food waste. PM represents packaging materials.

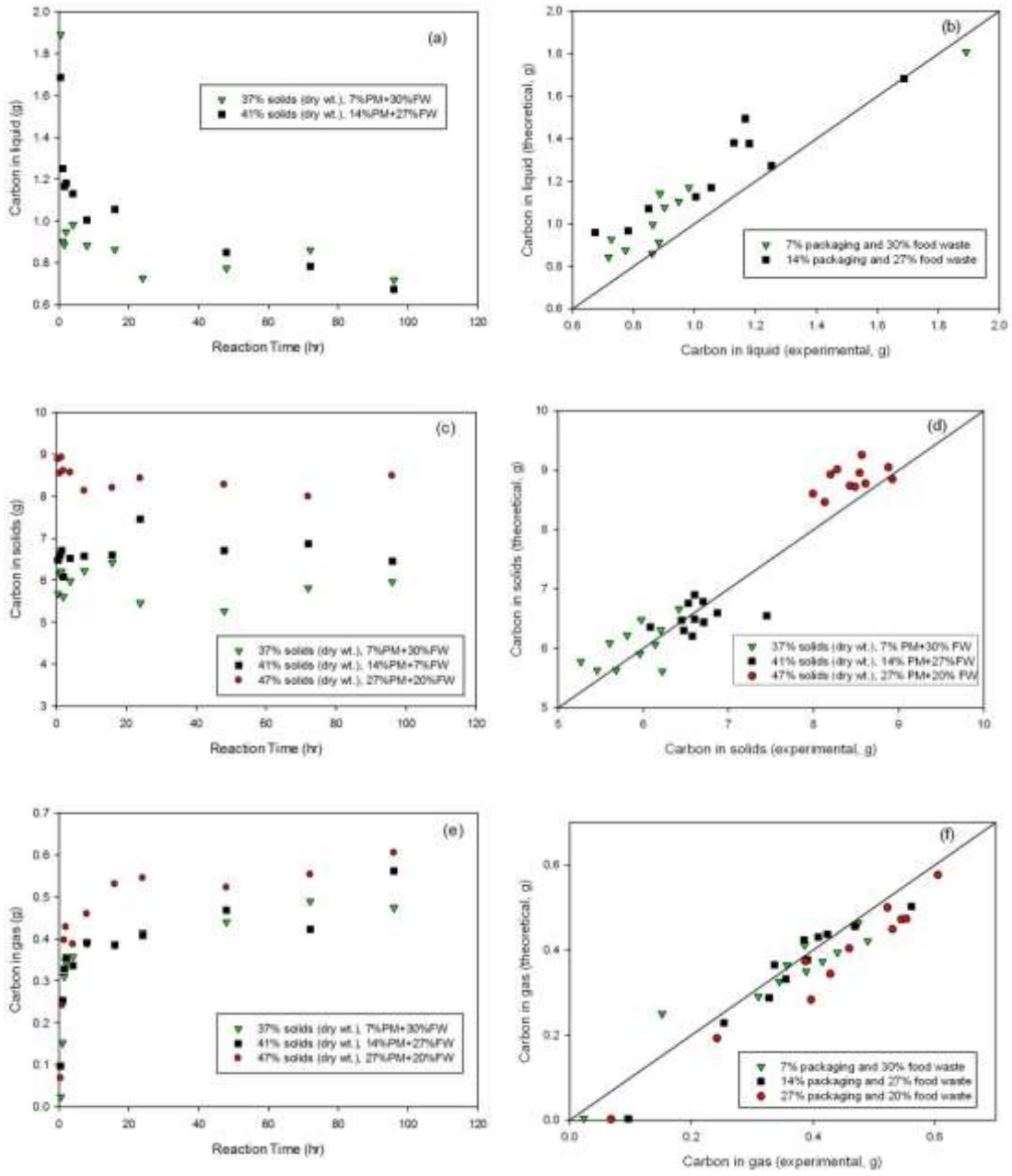

Figure 2.7 Results from experiments with food waste and differing percentages of packing materials: (a) normalized carbon mass in the liquid-phase, (b) comparison between the actual and predicted carbon in the liquid-phase, (c) normalized carbon mass in the solid-phase, (d) comparison between the actual and predicted carbon in the solid-phase, (e) normalized carbon mass gas-phase, and (f) comparison between the actual and predicted carbon in the gas-phase. FW represents food waste. PM represents packaging materials.

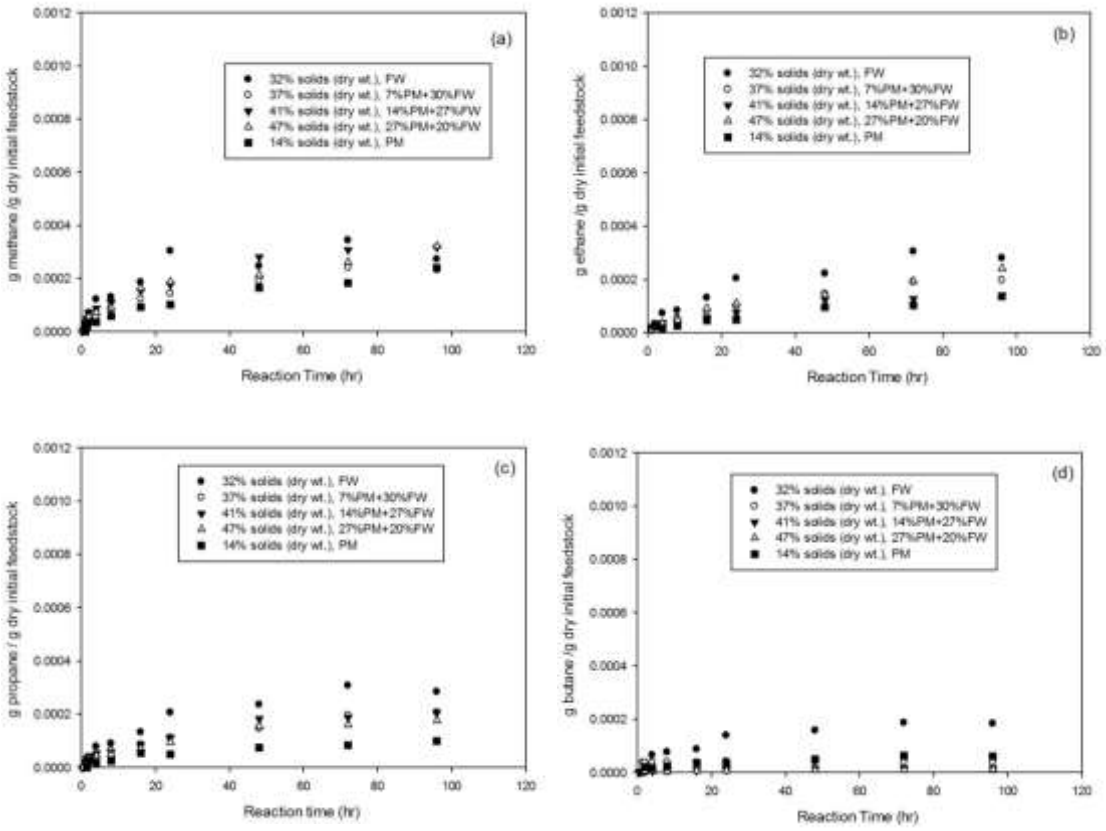

Figure 2.8 Normalized trace gas production resulting from experiments conducted with different fractions of packaging materials: (a) methane, (b) ethane, (c) propane, and (d) butane. FW represents food waste. PM represents packaging materials.

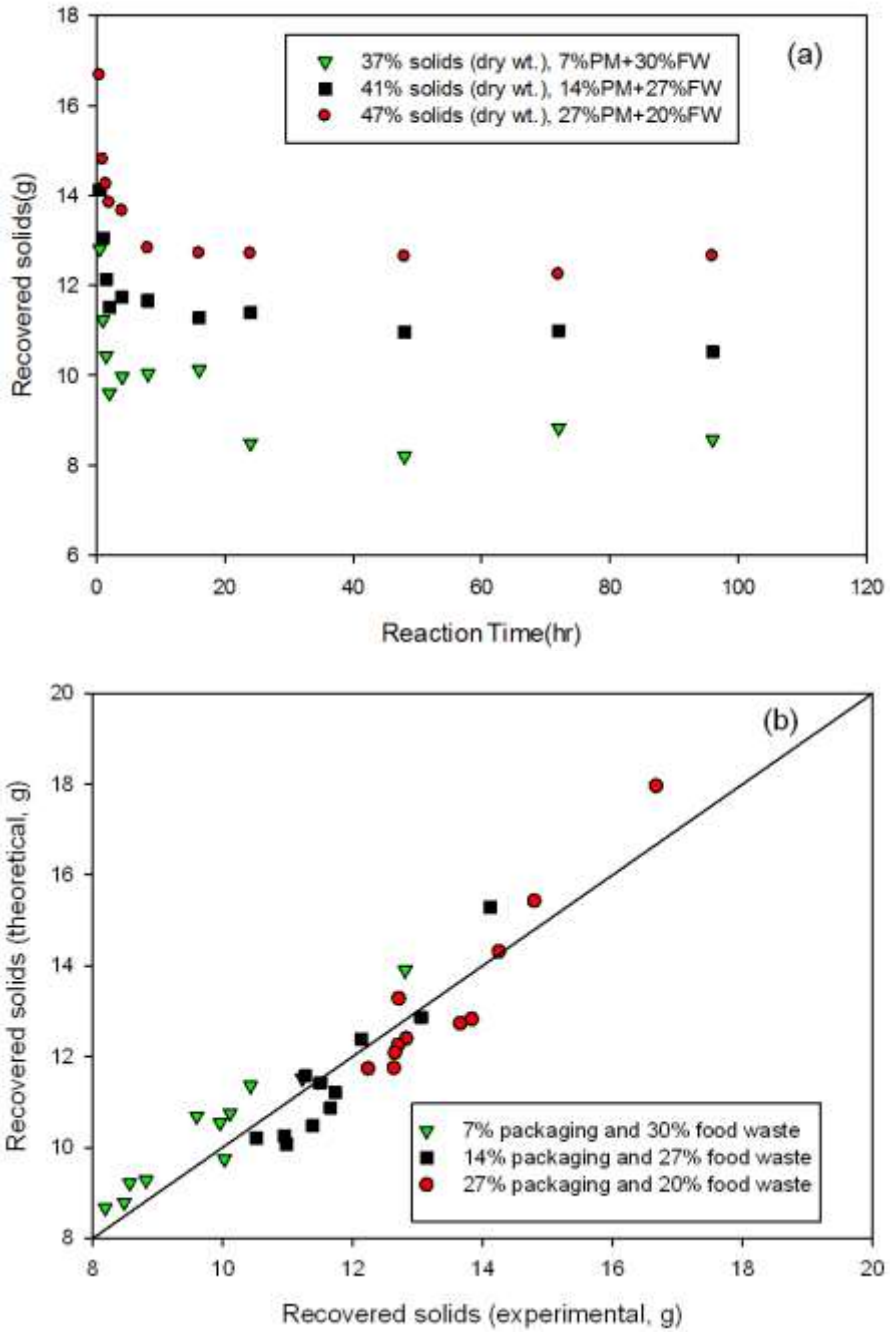

Figure 2.9 Solids recovery results from experiments with food waste and differing percentages of packing materials: (a) mass of solids recovered resulting from the carbonization of food wastes mixed with different fractions of packaging materials and (b) comparison between experimental and predicted values. FW represents food waste. PM represents packaging materials.

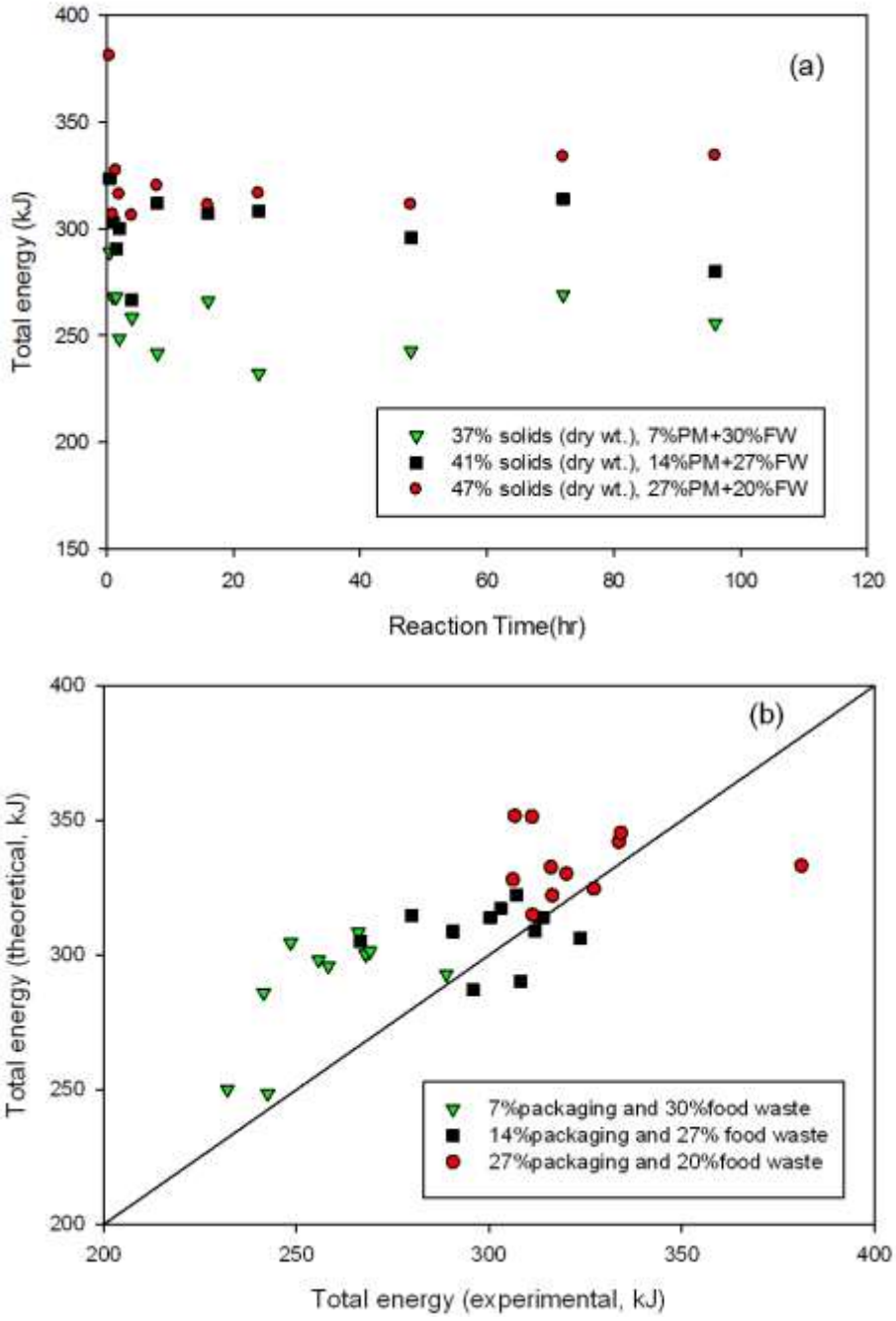

Figure 2.10 Energy results from experiments with food waste and differing percentages of packing materials: (a) total energy in the recovered solids and (b) comparison between experimental and predicted values. FW represents food waste. PM represents packaging materials.

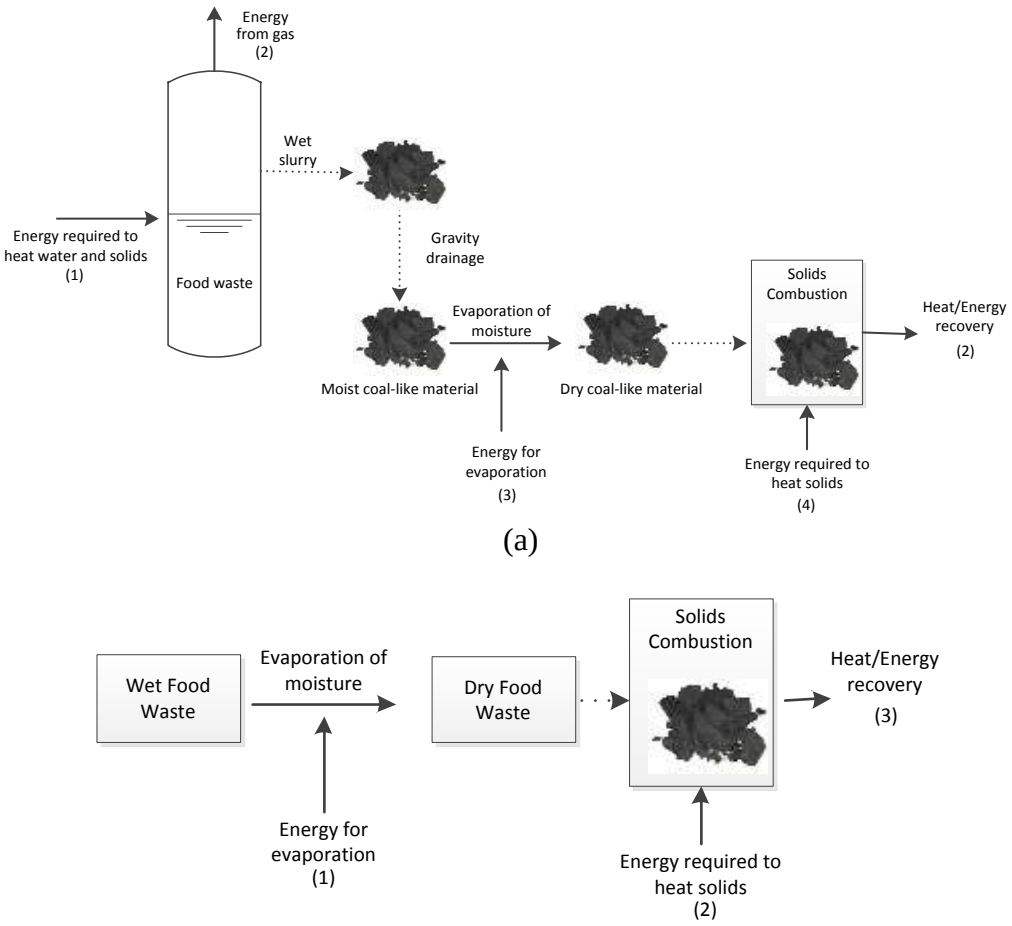

Figure 2.11 Energy balances associated with: (a) hydrothermal carbonization and (b) incineration. The numbers represent the steps of each process, as described in the text. Dotted lines represent processes with no energy requirement.

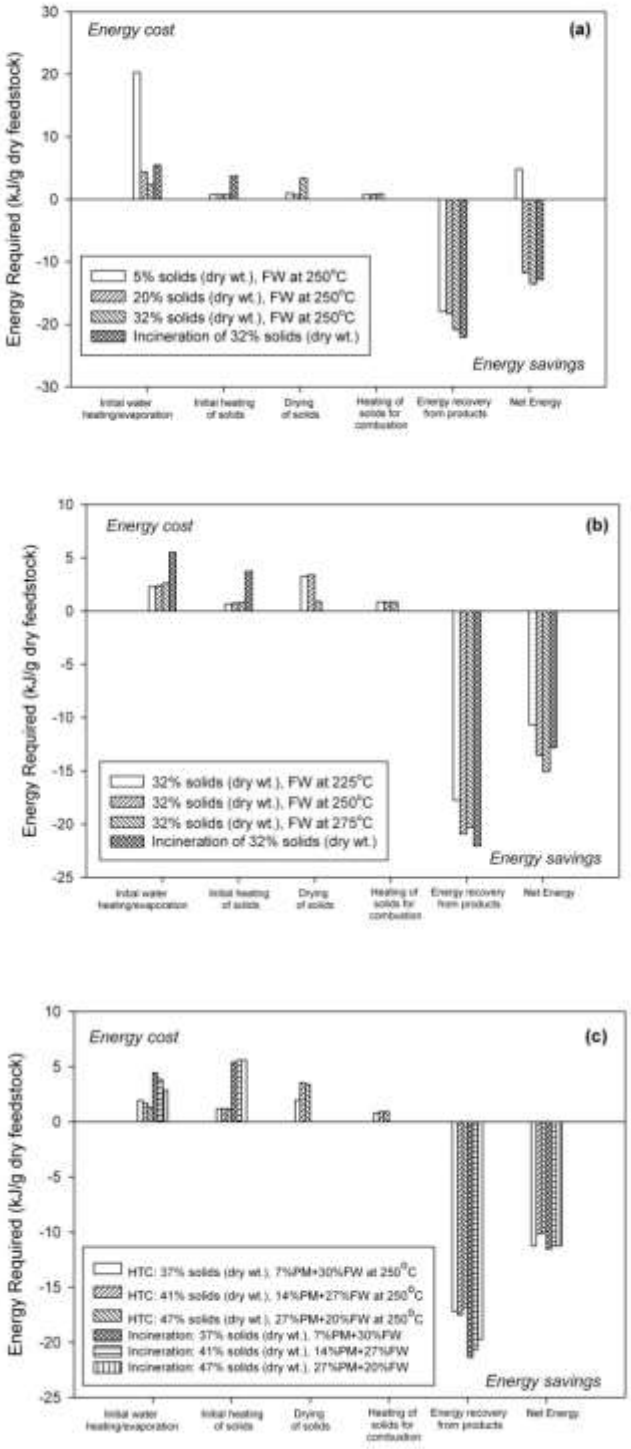

Figure 2.12 Energy balance results associated with: (a) the influence of initial solids concentration, (b) influence of reaction temperature, and (c) the influence of the presence of various fractions of packaging materials. FW represents food waste. PM represents packaging materials.

CHAPTER 3.

USING LIQUID WASTE STREAMS AS THE MOISTURE SOURCE DURING THE HYDROTHERMAL CARBONIZATION OF MUNICIPAL SOLID WASTES

Li, L., Hale, M., Olsen, P., and Berge, N. D. (2014). Using liquid waste streams as the moisture source during the hydrothermal carbonization of municipal solid wastes. *Waste management*, *34*(11), 2185-2195.

Reprinted here with permission of publisher.

ABSTRACT

Hydrothermal carbonization (HTC) is a thermal conversion process that can be an environmentally beneficial approach for the conversion of municipal solid wastes to value-added products. The influence of using activated sludge and landfill leachate as initial moisture sources during the carbonization of paper, food waste and yard waste over time at 250oC was evaluated. Results from batch experiments indicate that the use of activated sludge and landfill leachate are acceptable alternative supplemental liquid sources, ultimately imparting minimal impact on carbonization product characteristics and yields. Regression results indicate that the initial carbon content of the feedstock is more influential than any of the characteristics of the initial liquid source and is statistically significant when describing the relationship associated with all evaluated carbonization products. Initial liquid-phase characteristics are only statistically significant when describing the solids energy content and the mass of carbon in the gas-phase. The use of these alternative liquid sources has the potential to greatly increase the sustainability of the carbonization process. A life cycle assessment is required to quantify the benefits associated with using these alternative liquid sources.

3.1 INTRODUCTION

Hydrothermal carbonization (HTC) is a relatively low temperature thermal conversion process that has been shown to be an environmentally beneficial approach for the transformation of biomass, carbohydrates, and waste streams to value-added products (e.g., Berge et al., 2011; Hwang et al., 2012; Li et al., 2013; Libra et al., 2011; Román et al., 2013; Titirici et al., 2012; Sevilla and Fuertes, 2009). Results from recent research indicate that conversion of municipal solid wastes (MSW) via HTC, particularly wet waste components, is energetically advantageous. As a result of HTC, a solid carbon-rich, energy-dense material referred to as hydrochar is generated. Berge et al. (2011), Lu et al. (2012), Hwang et al. (2012) and Li et al. (2013) report that when carbonizing different MSW components, the majority of initially present carbon remains integrated within the hydrochar and that the hydrochar has an energy content and structure resembling a low-grade coal material. Other advantages associated with using HTC as a waste conversion technique include the formation of a liquid stream that contains appreciable concentrations of valuable compounds (e.g., organic acids, hydroxymethylfurfural (HMF)) and nutrients (e.g., Berge et al., 2011; Li et al., 2013) and that carbonization has the potential to convert compounds of concern found in waste streams (i.e., pesticides, pharmaceuticals) to less harmful products (Weiner et al., 2013).

An important and required component of HTC is the presence of adequate moisture/liquid. At typical HTC system temperatures, the properties of liquid differ significantly from water, ultimately mimicking that of an organic solvent (Akiya and Savage, 2002; Siskin et al., 2001; Wantanabe et al., 2004). The liquid properties/behavior during carbonization play a key role in the carbonization process, leading to increased

saturation concentrations of dissolved organic and inorganic compounds and promotion of ionic reactions. Funke and Ziegler (2010) report that for hydrothermal carbonization to proceed the feedstocks need to be completely submerged. Often, to achieve feedstock submersion, the moisture requirement for HTC is greater than that naturally present in the feedstock, particularly for dry components of MSW, such as paper. It should be noted that carbonization reactions will proceed under limited moisture contents, but the carbon content of the solid materials is reduced and solids yields are increased (Funke et al., 2013).

To date, water (often deionized) is the liquid used as the moisture source in the majority of reported hydrothermal carbonization studies. As concerns associated with water scarcity increase, the need for identifying alternative carbonization liquid sources increases. Using liquid waste streams as moisture sources during carbonization would be advantageous. Liquid waste streams, such as municipal wastewater and landfill leachates, represent wastes streams that are plentiful and require extensive treatment prior to their discharge to the environment. In addition, use of these liquid waste streams during HTC may be beneficial to carbonization, potentially increasing carbonization kinetics and enhancing the properties of the generated solids. Stemann et al. (2013) conducted experiments in which carbonization process water was recirculated and report that changes in initial process water quality catalyze dehydration reactions and that organics in the liquid stream are further polymerized, increasing the carbon and energy content of the recovered solids. Catalyst addition to the initial process water has also been shown to positively influence carbonization. Lynam et al. (2012) found that when adding salt to carbonization systems, the energy value of the solids increases. In another study, Lynam

et al. (2011) report that the addition of acetic acid and lithium chloride also increase the energy value of the recovered solids.

Using municipal waste streams as the initial moisture source for HTC has not been previously investigated. The purpose of this work is to evaluate the influence of substituting activated sludge and landfill leachate as the moisture source for HTC and to determine their influence on carbonization product characteristics. Laboratory-scale experiments evaluating the influence of using landfill leachate and activated sludge as initial moisture sources during the carbonization of yard waste, paper, and food waste were conducted. Characteristics of the solid, liquid, and gas-phases were measured and used to determine if these alternative moisture sources can be used to increase the sustainability of the HTC process. Statistical analyses were conducted to evaluate whether changes in initial liquid properties results in a statistically significant change in carbonization product characteristics and to assess the relationship between carbonization products, initial liquid source characteristics, feedstock type, and process conditions.

3.2 MATERIALS AND METHODS

3.2.1 Liquid Source and Solid Waste Material Characteristics

Activated sludge and landfill leachate are the liquid waste streams evaluated in this study. Each waste stream was obtained from either a local wastewater treatment plant or a municipal solid waste landfill. Typical properties of each liquid stream were measured and are reported in Table 3.1 using the analytical methods described in subsequent sections.

The solid waste materials used in this work include paper, food waste, and yard waste. Before use, the office paper was shredded into 25 by 4 mm strips using a titanium

paper shredder (micro-cut shredder, Staples, Inc.). Food wastes were collected from local restaurants. The collected waste was sorted, as reported by Li et al. (2013), and the food component subsequently homogenized with a food-grade blender (Ninja Master Prep Model #: QB900, Euro-Pro Operating LLC). Yard waste is comprised of a mixture of 50% (dry wt.) of grass clippings and 50% (dry wt.) shredded shrubs. The shrubs were chipped using an electric shredder (Chicago Electric Power Tools, Inc., 1.5 inch, 14 Amp Shredder). The properties of each of these waste materials are presented in Table 3.2.

3.2.2 Batch HTC experiments

All batch carbonization experiments were conducted following procedures previously described (Berge et al., 2011; Li et al., 2013; Lu et al., 2012; Lu et al., 2013; Flora et al., 2013). Briefly, the feedstocks (e.g., paper, food, and yard wastes) were placed in 160-mL stainless steel tubular reactors (2.54 cm i.d., 25.4 cm long, MSC, Inc.) fitted with gas-sampling valves (Swagelock, Inc.). A mass of 8 g of dry solids was added to all reactors. Moisture was subsequently added to achieve the desired solid material concentration of 20 % (dry wt.). The moisture sources evaluated include: (1) deionized (DI) water, (2) landfill leachate, and (3) activated sludge. In addition, control experiments containing only activated sludge and landfill leachate were conducted. All reactors were sealed and heated in a laboratory oven (Heratherm model, Fisher Scientific, Inc.) at 250^{o}C. The desired in-situ temperature of the reactors was achieved after 90 min. Experiments for each feedstock and moisture source were conducted over three carbonization times (2, 8, and 24 hours) to evaluate how reaction time influences carbonization. These sampling times include the period of reactor heating. All experiments were conducted in triplicate.

3.2.3 Analytical Techniques

At each sampling time, reactors were removed from the oven and placed in a cold water bath. Following cooling, the produced gas was collected in either a 1 or 3-L foil gas sampling bag (SKC, Inc.). Gas composition of these samples was analyzed using GC-MS (Agilent 7890). Gas samples were routed through a GS-CarbonPlot column (30m long and 0.53 mm id, J&W Scientific). Initial oven temperature was 35^{o}C. After 5-min, the temperature was increased at a rate of 25^{o}C/min until a final temperature of 250^{o}C was achieved. Carbon dioxide standards (Matheson Trigas) were used to determine concentrations in the gas. Results from this analysis were also used to provide qualitative data associated with the composition of the gas stream. Gas volumes were measured with a large volume syringe (S-1000, Hamilton Co.).

The process liquid and solid were separated via vacuum filtration through a 0.45 µm cellulose nitrate membrane filter (Whatman International Ltd.). Liquid conductivity and pH were measured using electrodes (Thermo Scientific Orion). Liquid chemical oxygen demand (COD) was measured using HACH reagents (HR + test kit, HACH Co.). Liquid total organic carbon (TOC) was measured using a TOC analyzer (TOC-Vcsn, Shimadzu). The 5-day biological oxygen demand (BOD) of the liquids collected after the 24-hour reaction time was measured using the HACH BODTrak technique (BODTrack II, HACH Co.).

All collected solids were dried at 80^{o}C. Solid carbon, hydrogen, and nitrogen content (Perkin Elmer 2400 Elemental Analyzer) and energy content (C-200 bomb calorimeter, IKA, Inc.) were measured.

3.2.4 Description of Theoretical Predictions

Theoretical masses of recovered solids resulting from the carbonization of feedstocks in the presence of liquid waste streams were calculated based on experimental results from the carbonization of each feedstock (paper, food waste or yard waste) in the presence of DI water and those in which only the liquid waste stream (activated sludge or landfill leachate) was carbonized. The relationship used for the prediction of recovered solid mass is presented in equation 1:

$$Solids_{pred} = SR_{feed} \times Mass_{feed} + SR_{liquid} \times Mass_{liquid} \quad (1)$$

where, $Solids_{pred}$ represents the predicted solids recovered (g), SR_{feed} represents the solids recovery (%, dry wt.) from the carbonization of feedstock in the presence of DI water, SR_{liquid} represents the solids recovery (%, dry wt.) from the carbonization of liquid waste stream only, $Mass_{feed}$ represents the mass of feedstock used in the experiment (g), and $Mass_{liquid}$ represents the mass of liquid waste stream added to the reactor (g). Standard deviations associated with these predictions were determined using the Delta Method. The variances associated with the theoretical recovered solids obtained from the feedstock ($SR_{feed} \times M_{feed}$) and liquid waste stream ($SR_{liquid} \times M_{liquid}$) were calculated separately based on a first-order Taylor expansion. Standard deviations were determined by taking the square root of the variances.

Similarly, the theoretical liquid-phase COD resulting from the carbonization of each feedstock in the presence of the liquid waste streams was determined using the relationship described in equation 2:

$$COD_{pred} = COD_{feed} + COD_{liquid} \times \frac{Mass_{liquid}}{Mass_{liquid-control}} \quad (2)$$

where, COD_{pred} represents the predicted COD (g/L), COD_{feed} represents the COD (g/L) from the carbonization of feedstock in the presence of DI water, COD_{liquid} represents the COD (g/L) from the carbonization of liquid waste stream only, $Mass_{liquid}$ represents the mass of liquid stream added to the experiment (g), and $Mass_{liquid\text{-}control}$ represents the mass of liquid added to the control experiment (g). Standard deviations associated with these predictions were calculated using the procedure described previously.

3.2.5 Statistical Analysis

Statistical analyses were used to determine whether differences between groups of obtained data and/or calculated parameters are statistically significant. Analysis of variance (ANOVA) test were conducted using SigmaPlot (version 11) to evaluate whether, from a statistics point of view, differences between the means of obtained solid, liquid and gas-phase data and/or related calculated parameters obtained when carbonizing the different feedstocks in the presence of the different waste streams are statistically significant at a decision level of 0.05.

In addition, a series of multiple linear regressions were performed to assess the predictive relationship between carbonization products, initial liquid source characteristics (Table 3.1), feedstock type, and process conditions to ultimately determine which, if any, of the liquid-waste stream characteristics are statistically significant in the describing the relationship of the following carbonization product parameters/characteristics: (1) solids recovery, (2) solids energy content, (3) solids carbon content (%, dry basis), (4) mass of carbon in the liquid-phase, and (5) mass of carbon in the gas-phase. In each regression, reaction time, initial solid material (e.g., yard waste, paper, and food waste), and carbon content (%, dry basis) were used to represent

the changing process conditions and properties of the initial solid materials. Reaction temperature was not included in this analysis because it remained constant throughout the duration of the experiments.

All multiple linear regressions were performed using SAS (version 9.3). The liquid-phase characteristics (i.e., pH, conductivity, COD, and TOC) were individually added to the model to determine if the inclusion improved the adjusted R^2 and/or the parameter was statistically significant. Parameter influence within each regression was determined by comparing the absolute value of the standardized regression coefficients. Standardized regression coefficients allow such comparison because they account for the standard deviations of both the dependent and independent variables.

3.3 RESULTS AND DISCUSSION

3.3.1 Liquid Source Influence on Carbon Distribution

Carbon recoveries (based on the masses of carbon recovered in the solid, liquid, and gas-phases) range from 80 to 101% (Figure 3.1). Results indicate that the percentage of initially present carbon remaining in the solid-phase ranges between 32 and 80% when carbonizing each solid material with all liquid sources, and decreases with reaction time, which is in-line with that reported by others evaluating the carbonization of waste materials and biomass (e.g., Berge et al., 2011; Hoekman et al., 2011; Hwang et al., 2012; Li et al., 2013; Lu et al., 2012). Results from ANOVA tests indicate that the fractions of initially present carbon found in the solid-phase resulting when carbonizing in the presence of the alternative liquid sources (e.g., leachate and activated sludge) are not statistically significant from those obtained when carbonizing in the presence of DI water at a decision level of 0.05. It should be noted, however, that feedstock type (e.g., paper, food waste, yard waste) does influence the fraction of initially present carbon remaining

in the solid-phase. The percentage of carbon remaining in the solid-phase is greater when carbonizing food and yard wastes than that associated with carbonizing paper (Figure 3.1).

The fraction of initially present carbon transferred to the liquid-phase ranges between 12 and 42%, depending on feedstock and reaction time. The fraction of carbon found in the liquid is greater when carbonizing paper, than when carbonizing food and yard wastes. ANOVA test results indicate that the fraction of carbon in the liquid-phase resulting when carbonizing food and yard wastes in the presence of leachate at a reaction time of 2 hours is statistically significant from the liquid-phase carbon when carbonizing in with DI ($p < 0.05$).

A smaller fraction of carbon is transferred to the gas-phase. The percentage of initially present carbon found in the gas when carbonizing paper ranges between 8 and 14%, while the percentage of carbon found in the gas when carbonizing food and yard wastes is smaller, ranging from 3 to 9%. ANOVA test results indicate that the fraction of initially present carbon transferred to the gas-phase at early reaction times in the presence of leachate and/or activated sludge is statistically significant from those obtained when carbonizing in DI (described in more detail in subsequent sections).

3.3.2 Liquid Source Influence on Solid Recoveries and Properties

The influence of alternative liquid sources on the solids generated during carbonization depends on the solid waste material and reaction time. When carbonizing paper in the presence of DI water, the solid recoveries change little at the reaction times of 2, 8 and 24 hours (Figure 3.2). Results from ANOVA tests support this conclusion, indicating the recoveries do not statistically change with reaction time ($p > 0.05$).

When carbonizing paper in the presence of activated sludge and leachate at a reaction time of 2 hours, the solid recoveries are larger than those measured in the presence of DI (Figure 3.2). A statically significance difference between these observations is confirmed via ANOVA tests ($p < 0.05$). Interestingly, the solids recovery when carbonizing in the presence of leachate at 2 hours is greater than that when carbonizing in the presence of activated sludge (ANOVA tests suggest this difference is statistically significant, $p < 0.05$). Results from control experiments, however, indicate that carbonization of activated sludge alone results in significantly greater solids recoveries (16-28%, dry wt.) than those obtained when carbonizing leachate alone (3-9%, dry wt.) (Figure 3.2). The larger mass of solids recovered when carbonizing paper in the presence of leachate suggests that the initial characteristics of the leachate may enhance solids generation at early times. Surprisingly, there appears to be no impact on solid recoveries at reaction times of 8 and 24 hours when carbonizing in the presence of activated sludge and leachate, even though appreciable solids are recovered when carbonizing the leachate and activated sludge alone. These recoveries are similar to that obtained when carbonizing in the presence of DI (supported by ANOVA tests indicating these groups of data are not statistically significant from one another, $p > 0.05$). The theoretical contribution of solids from the carbonization of the liquid waste streams is small (< 0.01 g) in these experiments, and is likely why no statistical impact is observed.

The influence of using activated sludge and leachate as the moisture source on the carbonization of food and yard wastes differs from that observed when carbonizing paper (Figure 3.2). When carbonizing food waste, the solids recoveries are mostly unaffected by the presence of activated sludge and leachate; the recoveries are not statistically

significant from those obtained when carbonizing with DI at a decision level of 0.05. The solids recovery obtained when carbonizing food waste at a reaction time of 24 hours and in the presence of activated sludge is the only recovery deemed statistically significant at a decision level of 0.05 when compared to the recoveries obtained when carbonizing in DI. The presence of activated sludge imparts no statistical impact on solids recoveries when carbonizing yard waste ($p > 0.05$). However, when carbonizing yard waste in the presence of leachate, the solids recoveries at 2 and 8 hours are statistically significant from the recoveries obtained when carbonizing in the presence of DI ($p < 0.05$). As described previously, it is likely that the impact on solids recoveries when carbonizing with the liquid waste streams is small because of the small mass of each in comparison to the solid waste material. These results suggest that the impact of using alternative liquid sources may be kinetic in nature, with ultimate solid recoveries remaining similar.

The theoretical recoverable solids masses were calculated for each experiment based on results from the control experiments containing only leachate and activated sludge and those in which the solid material is carbonized in the presence of DI water (equation 1). A comparison between the theoretically calculated and measured mass of solids is presented in Figure 3.3. It should be noted that the contribution of the solids expected due to carbonization of the leachate and activated sludge alone are small, and difficult to see in each figure. Results from this analysis indicate that when carbonizing in the presence of activated sludge, the solids collected when carbonizing food and yard waste are closely approximated (Figure 3.3a). There is more deviation between the measured and theoretical values when carbonizing in the presence of leachate (Figure 3.3b), especially when carbonizing paper at a reaction time of 2 hours. In both instances,

paper recoveries are generally under-predicted, while the mass of solids collected when carbonizing food and yard waste in the presence of activated sludge are closely predicted, but over-predicted when carbonizing in the presence of leachate. These differences may be a result of unknown interactions associated with constituents in the initial liquid sources and the solid materials being carbonized.

The impact of using activated sludge and leachate as moisture sources on the solids carbon content (%, dry weight, Figure 3.4) and energy content (Figure 3.5) is minimal. Except for a statistically significant difference between the solids carbon contents at a reaction time of 2 hours when carbonizing paper in the presence of leachate and activated sludge ($p < 0.05$), the solids carbon contents do not differ from a statistics point of view at an imposed level of 0.05. It is possible that if a more concentrated or larger volume of the liquid stream is used, a more significant influence on solids carbon content may be observed.

The solids energy contents are also primarily unaffected when carbonizing in the presence of activated sludge and leachate. When compared to experiments conducted in DI water, the only statistically significant changes (at an imposed level of 0.05) in the solids energy contents are at early times when carbonizing food and paper in the presence of activated sludge and leachate. There are no statistically significant differences in the ultimate solids energy contents (at a reaction time of 24 hours) when compared to those obtained when carbonizing in the presence of DI water (at an imposed level of 0,05). Stemann et al. (2013) report that organics in the initial process water may partition into the solids during carbonization, ultimately increasing the recovered solids energy contents. This phenomenon was not observed in these experiments. The carbon content of

the initial process waters used by Stemann et al. (2013) were orders of magnitude greater than those used in this work, suggesting that more concentrated process waters may impart a more positive effect on solids energy contents.

The energetic retention efficiencies (defined as the energy of the recovered solids/energy in the initial feedstock) indicate that the greatest efficiency occurs when carbonizing yard waste (Figure 3.6). Carbonizing in the presence of activated sludge and leachate did not influence the energetic retention efficiency associated with paper and yard waste carbonization; when compared with the efficiencies determined when carbonizing in DI, there is no statistically significant effect when carbonizing in the presence of activated sludge and leachate for each of these solid materials ($p > 0.05$). However, carbonization in the presence of activated sludge and leachate do influence energetic retention efficiencies when carbonizing food waste. ANOVA test results indicate that the efficiencies differ from those obtained when carbonizing in the presence of food waste and leachate and activated sludge ($p < 0.05$) at all times, except at a reaction time of 8 hours in the presence of activated sludge.

3.3.3 Liquid Source Influence on Solids Dewaterability

Results from these experiments indicate that carbonizing in the presence of alternative liquid sources, specifically landfill leachate, may increase the dewaterability of the recovered solids, which is important when considering future uses of the solids and when assessing process energy requirements (Liang et al., 2013). The mass of water remaining within the solid matrix following gravity drainage was determined (Figure 3.7). Results indicate that the mass of water remaining in the solids matrix decreases with time, with the greatest retention of water in the solids recovered from the carbonization of yard waste. ANOVA tests indicate that carbonizing in the presence of activated sludge does

not result in a statistically significant difference on solids water content when compared to that when carbonizing with DI water at all reaction times and for all feedstocks ($p > 0.05$). However, the presence of leachate does result in a statistically significant influence (at an imposed level of 0.05) on solids dewaterability when carbonizing paper (reaction time of 2 hours), food waste (reaction time of 24 hours), and yard waste (reaction times of 2 and 8 hours).

3.3.4 Liquid Source Influence on Water Quality Following Carbonization

The COD and TOC concentrations in the process water are larger when carbonizing paper, than food and yard wastes (Figures 3.8 and 3.9). This result is consistent with that reported by Berge et al. (2011) and Lu et al. (2012). It has been well established that the trend of process water COD and TOC increase and then decrease (e.g., Hoekmann et al., 2011; Knezevic et al., 2009, 2010; Li et al., 2013; Lu et al., 2013). Over time, the COD and TOC in the final process waters decrease when carbonizing paper and food waste. A different trend is observed when carbonizing yard waste in the presence of DI, activated sludge, and landfill leachate. This trend may be observed because it is possible that reaction kinetics are slower when carbonizing yard wastes, resulting in the upward trend of process water organics.

Initial liquid stream quality does not influence the COD or TOC of the process water following carbonization (Figures 3.8 and 3.9). With the exception of one COD (food waste with leachate) and three TOC (paper with leachate; food with leachate; yard waste with leachate) values at a reaction time of 2 hours, the COD and TOC values obtained when carbonizing in the presence of activated sludge and leachate do not differ

from a statistics point of view from those obtained at similar reaction times when carbonizing with DI ($p > 0.05$).

A comparison of the predicted (based on the COD concentrations from the liquid waste stream control and the experiments conducted with DI) and measured COD concentrations in the process water are shown in Figure 3.10. These results indicate that when carbonizing paper in the presence of activated sludge and leachate, the liquid-phase COD is often over-predicted, suggesting that a greater portion of the oxidizable organics are transferred to the solid or gas-phases when carbonizing in the presence of the alternative liquid sources. Previous carbonization studies have reported that HMF (a common dehydration product produced during carbonization) becomes incorporated within the solids via polymerization-polycondensation (Baccile et al., 2009; Falco et al., 2011) over time and has been reported to play a role in solids formation (Falco et a., 2011; Titirici et al., 2008). It is possible a similar phenomenon is occurring, but unable to be detected using the solid-phase carbon measurement.

Conversely, when carbonizing yard waste in the presence of activated sludge, it does not appear that changing the initial liquid source influences the final liquid-phase COD, as the values are closely predicted (Figure 3.10). When carbonizing yard waste in the presence of leachate, the liquid-phase COD is over-predicted, similar to that observed with paper. When carbonizing food waste in the presence of alternative liquid sources, there is no discernable trend; the COD is closely approximated, suggesting the presence of alternative initial liquid sources does not influence final liquid-phase COD.

Process water BOD increases as a result of carbonization (Figure 3.11). Results from the control experiments indicate a greater increase in liquid-phase BOD after

carbonizing with leachate (increases by a factor of 20). Carbonization of food waste results in larger BOD values in the process water following carbonization than that obtained when carbonizing paper and yard wastes. Results from ANOVA tests indicate that changes in initial water source do statistically influence the liquid BOD values when carbonizing food waste ($p < 0.05$), but not when carbonizing paper or yard waste ($p > 0.05$). This result is somewhat surprising, as the BOD associated with the process waters obtained when carbonizing the liquid streams alone is appreciable, indicating that the BOD concentration in the process water following carbonization is not additive.

3.3.5 Liquid Source Influence on Gas Composition

The mass of carbon found in the gas-phase (based on carbon dioxide) increases with reaction time (Figure 3.12), similar to that reported by others (e.g., Li et al., 2013; Lu et al., 2013). ANOVA test results indicate that the addition of activated sludge and leachate do result in statistically significant differences in the carbon content of the gas-phase (at a level of 0.05). Only when carbonizing food waste in the presence of leachate is the carbon content of the gas-phase statistically significant from the carbon in the gas when carbonizing in the presence of DI water ($p < 0.05$) at a reaction time of 24 hours.

The addition of alternative moisture sources does influence gas volumes and thus the production of trace gases. This influence is dependent on feedstock type and reaction time. When carbonizing paper in the presence of activated sludge, the measured gas volumes are statistically different from those obtained when carbonizing DI water at all reaction times ($p < 0.05$). The presence of activated sludge also imparts a statistically significant effect when carbonizing food waste at a reaction time of 2 hours and yard waste at reaction times of 2 and 8 hours (at a level of 0.05). Using leachate as the

moisture source statistically influences the gas volumes when carbonizing paper at 8 hours and yard waste at 2 and 8 hours (level of 0.05). The most significant gases detected as a result of carbonization of all feedstocks and at all reaction times include methane, ethane, propene, propane, butane and furan (data not shown). The relative masses of all the trace gases (evaluated by taking peak areas and multiplying by the total volume of collected gas), except furan, increase with time. The furan decreases with time, similar to that reported by Li et al. (2013), likely being incorporated within the solids. Interestingly, when carbonizing leachate alone, the mass of methane generated is significantly larger than when carbonizing only activated sludge. The impact of alternative liquid sources on individual trace gas production is variable; no discernable trend exists.

3.4 REGRESSION ANALYSIS

Results from the multiple linear regression analysis are shown in Table 3.3 and indicate that the initial liquid source characteristics (Table 3.1) are not statistically significant (at a decision level of 005) in describing the predictive relationship for the solids recovery, solids carbon content, and mass of carbon in the liquid. Initial liquid-phase characteristics, however, are statistically significant (at a decision level of 005) when describing a relationship to predict the solids energy content and the mass of carbon in the gas and the process and feedstock conditions. The linear regression equations obtained are presented in Table 3.3 and only include the parameters deemed statistically significant (at a decision level of 005). The standardized normalized regression coefficients are also included in Table 3.3. A comparison between the predictions resulting from the regression equation associated with the solids recovered and the theoretical (equation 1) and actual measured values is presented in Figure 3.3.

Results from all regressions indicate that that the feedstock (e.g., paper, food waste and yard waste) carbon content is the most influential parameter (greatest standardized regression coefficients). This result is consistent with the experimental results, as there are distinct differences in carbonization products between feedstocks. This result is also consistent with previously published results in which the feedstock was deemed more influential on carbonization products than other process conditions (e.g., Cao et al., 2013; Mumme et al., 2011). In most regressions, the values of the standardized regression coefficients associated with the carbon content of the feedstock are significantly greater than all other regression parameters. An exception to this are the regressions associated with the mass of carbon in the gas-phase. In these regressions, the standardized coefficients associated with reaction time are similar to that of the carbon content of the feedstock, suggesting carbon content of the feedstock and reaction time are of equal importance.

When describing the relationships for solids energy content and the mass of carbon in the gas, the initial liquid-phase parameters found statistically significant (e.g., pH, conductivity, COD, and TOC) appear to be of equal importance in each regression, indicating no one liquid-phase parameter is best suited to describe the influence of initial liquid-phase characteristics. The standardized regression coefficients associated with the initial liquid-phase parameters are similar to those of reaction time in the regression equations describing the relationship of solids energy content. In addition, the adjusted R^2 values associated with these relationships are all similar, suggesting that the influence of time and initial liquid-phase parameters is similar.

3.5 CONCLUSIONS

The use of activated sludge and landfill leachate are acceptable alternative supplemental liquid sources, ultimately imparting minimal impact on the evaluated carbonization product characteristics and yields. The impact of using alternative liquid sources depends on feedstock type, carbonization product, and reaction time. The impact of alternative liquid sources on carbonization products/yields may increase with increases in initial liquid source organics.

Results from linear regressions indicate that the initial carbon content of the feedstock is more influential than any of the characteristics of the initial liquid source in predicting carbonization characteristics and is always statistically significant ($p < 0.05$). Initial liquid-phase characteristics were only deemed statistically significant ($p < 0.05$) when describing the solids energy content and the mass of carbon in the gas-phase. These results are consistent with experimental results, also indicating that the use of activated sludge and leachate have a minimal impact on carbonization the evaluated product properties. The use of these liquid sources has the potential to greatly increase the sustainability of the carbonization process. A life cycle assessment is required to quantify the benefits associated with using these alternative liquid sources.

Table 3.1 Characteristics of liquid sources used this study.

Process Water	Solids Concentration (%, dry wt.)	pH	Conductivity (mS/cm)	COD_{Total} (mg/L)	TOC (mg/L	BOD (mg/L)
DI Water	0	6.85 (0.046)	0.002 (0.0009)	0	0	0
Landfill Leachate	0.79 (0.041)	8.24 (0.090)	12.74 (1.140)	3220 (324.551)	2169 (125.328)	101 (19.788)
Activated Sludge	0.26 (0.041)	7.02 (0.251)	0.61 (0.119)	1830 (172.626)	181 (15.094)	404 (82.902)

Values in parentheses represent standard deviations

Table 3.2 Characteristics of solid wastes using in this study.

Waste		Moisture Content (%, dry wt.)	Carbon (%, dry wt.)	Hydrogen (%, dry wt.)	Nitrogen (%, dry wt.)	Energy Content (MJ/kg)
Paper		0.19 (0.025)	36.34 (1.388)	5.05 (0.532)	0.045 (0.035)	8.50 (1.253)
Yard Waste	Shrubs	66.95 (4.095)	49.76 (0.504)	6.55 (0.166)	1.22 (0.2641)	15.85 (0.635)
	Grass clippings	45.97 (1.942)	45.60 (1.914)	6.08 (0.222)	1.56 (0.087)	13.90 (1.509)
Food Waste		68.41 (2.335)	52.26 (1.321)	8.62 (0.232)	2.65 (0.336)	22.04 (1.365)

Values in parentheses represent standard deviations

Table 3.3 Regression equations and normalized regression coefficients.

Parameter	Regression Equations[1,2]	Adj. R^2	Normalized Regression Coefficients
Solids recovery (%,dry wt.)	$SR = - 0.427\ t + 1.850\ C_{feed} - 29.50$	0.79	t = - 0.271; C_{feed} = 0.848
Solids carbon content (%, dry wt.)	$C_{solid} = 0.206\ t + 1.149\ C_{feed} + 6.80$	0.83	t = 0.220; C_{feed} = 0.888
Solids energy content (J/g dry solids)	$Energy = - 1601.7\ pH + 111.9\ t + 711.9\ C_{feed} + 882.4$	0.84	pH = - 0.183; t = 0.192 ; C_{feed} = 0.881
	$Energy = - 162.6\ Cond + 111.9\ t + 711.9\ C_{feed} - 10198$	0.84	Cond = - 0.176; t = 0.192 ; C_{feed} = 0.881
	$Energy = - 0.844\ COD + 111.9\ t + 711.9\ C_{feed} - 9500.3$	0.85	COD = - 0.206; t = 0.192 ; C_{feed} = 0.881
	$Energy = - 0.989\ TOC + 111.9\ t + 711.9\ C_{feed} - 10147$	0.84	TOC = - 0.180; t = 0.192 ; C_{feed} = 0.881
Mass of carbon in the gas (g C)	$C_{gas} = 0.024\ pH + 0.004\ t - 0.007\ C_{feed} + 0.357$	0.64	pH = 0.189; t = 0.531 ; C_{feed} = -0.583
	$C_{gas} = 0.0027\ Cond + 0.004\ t - 0.007\ C_{feed} + 0.518$	0.65	Cond = 0.207; t = 0.531 ; C_{feed} = -0.583
	$C_{gas} = 0.00002\ TOC + 0.004\ t - 0.007\ C_{feed} + 0.518$	0.65	TOC = 0.199; t = 0.531 ; C_{feed} = -0.583
Mass of carbon in the liquid (g C)	$C_{liquid} = - 0.0044\ t - 0.025\ C_{feed} + 1.95$	0.62	t = -0.188; C_{feed} = -0.772

[1]only statistically significant variables are included in the regression equations; [2]t = reaction time (hr); C_{feed} = carbon content of the initial solid material (%, dry wt.), pH = initial liquid source pH; COD = initial liquid total COD (mg/L); Cond = initial liquid conductivity (mS/cm); TOC = initial liquid TOC (mg/L); C_{solid} = solids carbon content (%, dry wt.), SR = solids recovery (%, dry wt.); Energy = solids energy content (J/g dry solids); C_{gas} = mass of carbon in the gas-phase (g C); C_{liquid} = mass of carbon in the

liquid-phase (g C).

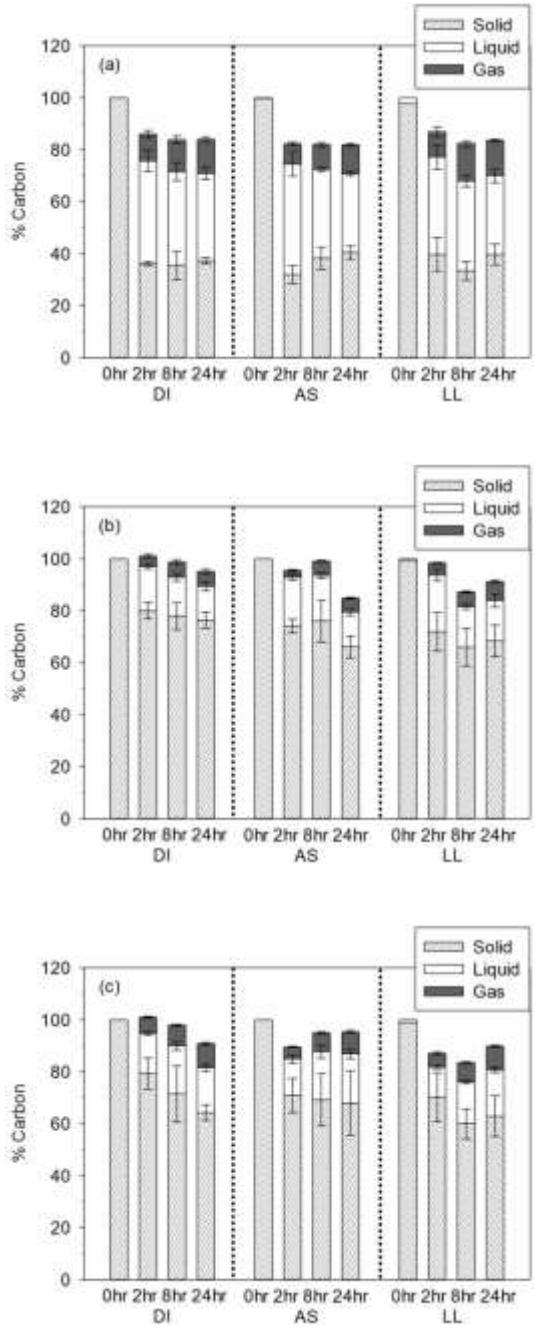

Figure 3.1 Carbon distribution in the solid, liquid and gas-phases resulting from the carbonization of (a) paper, (b) food waste and (c) yard waste in the presence of deionized water (DI), activated sludge (AS) and landfill leachate (LL). All data labeled solid, liquid, and gas represent the percent of initially present carbon found in the generated solids, resulting liquid stream or the generated gas, respectively, at each sampling time and for each liquid source. Error bars represent standard deviations.

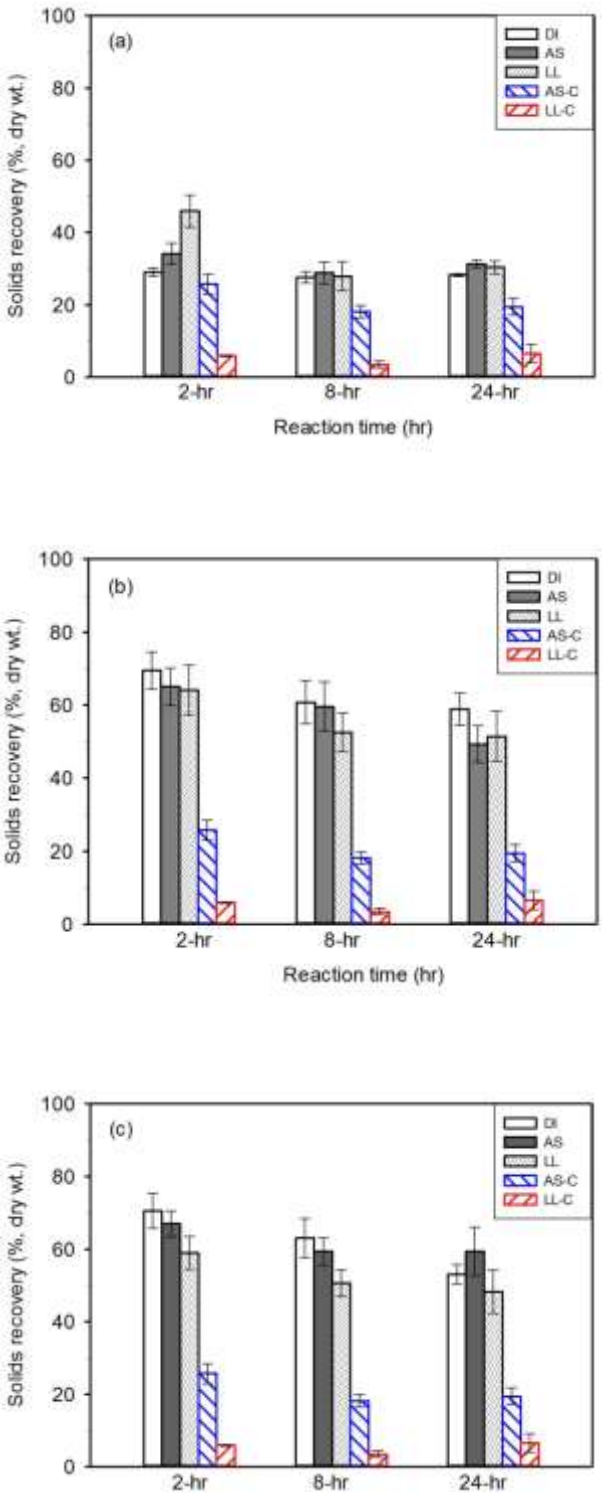

Figure 3.2 Solids recoveries resulting from the carbonization of (a) paper, (b) food waste and (c) yard waste in the presence of deionized water (DI), activated sludge (AS), and landfill leachate (LL). AS-C and LL-C represent activated sludge control and landfill leachate control experiments. Error bars represent standard deviations.

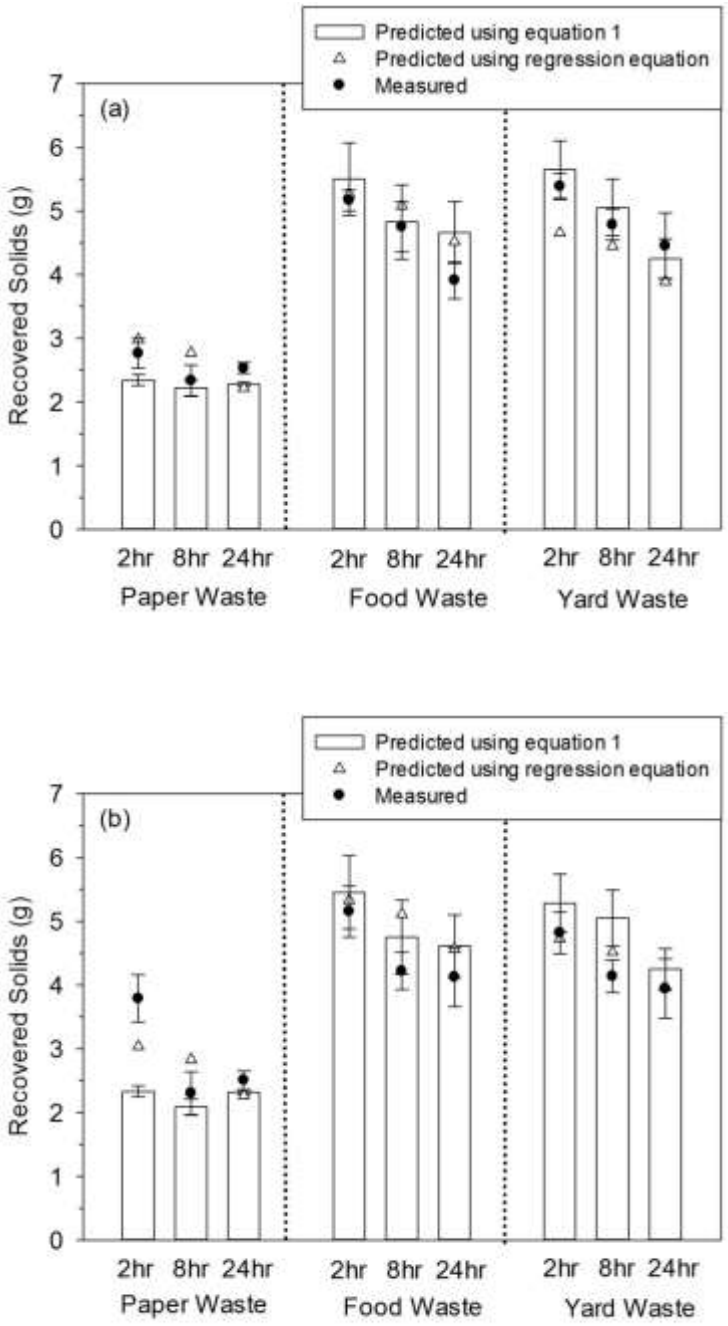

Figure 3.3 Comparison of masses of recovered solids resulting from the carbonization of different feedstocks (paper, food waste and yard waste) in the presence of (a) activated sludge (AS) and (b) landfill leachate (LL). Data included in this figure represent the theoretically calculated (bars) masses, actual mass measurements (filled points), and predicted masses using the regression equation (open points).

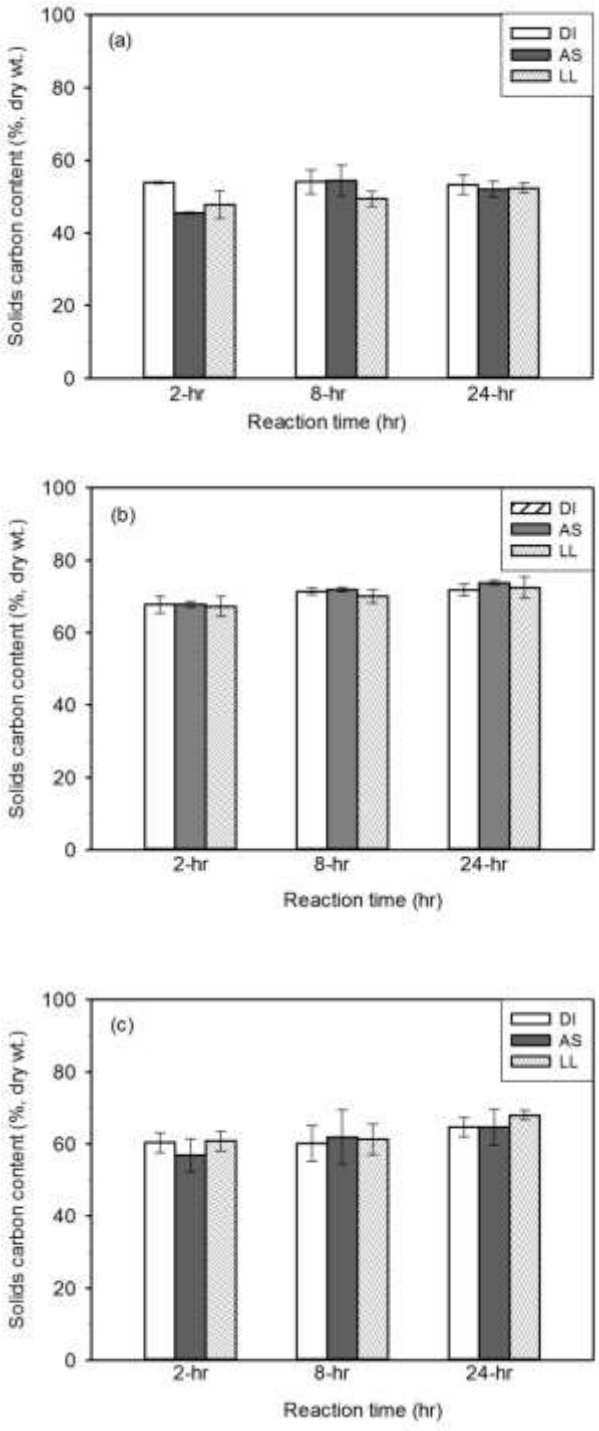

Figure 3.4 Carbon content of recovered solids resulting from the carbonization of (a) paper, (b) food waste and (c) yard waste in the presence of deionized water (DI), activated sludge (AS) and landfill leachate (LL). Error bars represent standard deviations.

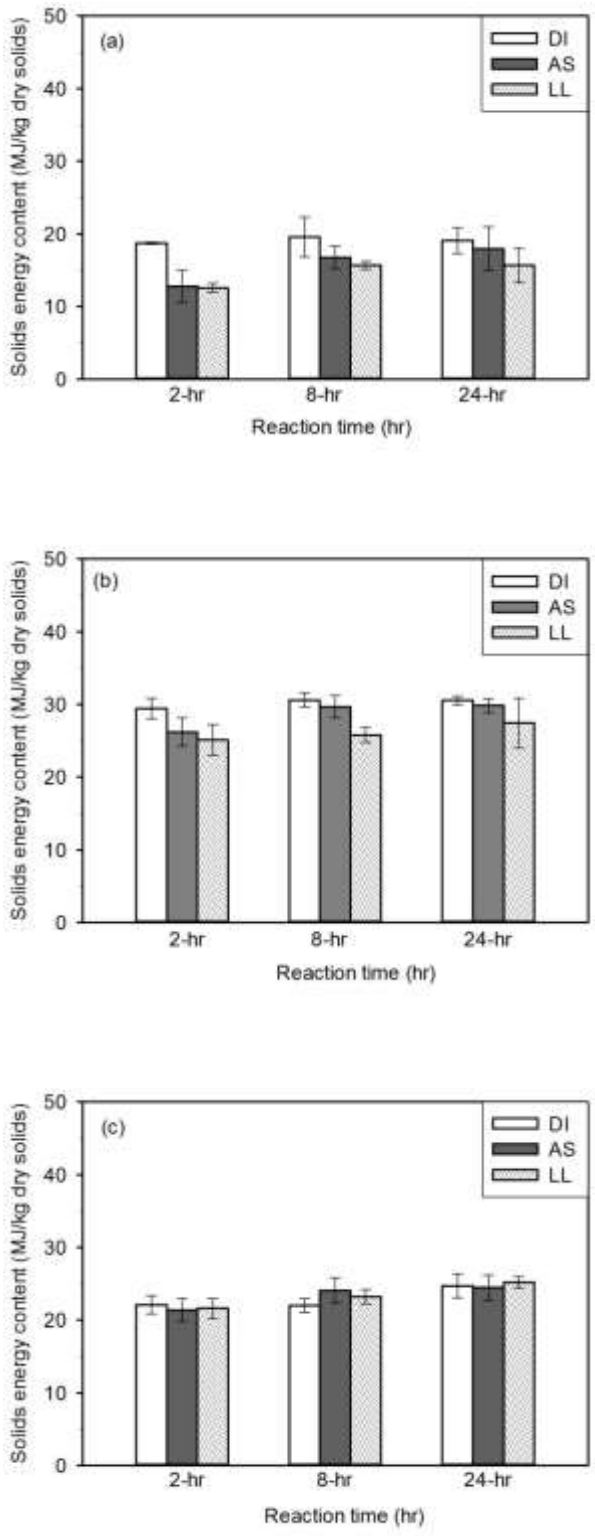

Figure 3.5 Energy content of recovered solids resulting from the carbonization of (a) paper, (b) food waste and (c) yard waste in the presence of deionized water (DI), activated sludge (AS) and landfill leachate (LL). Error bars represent standard deviations.

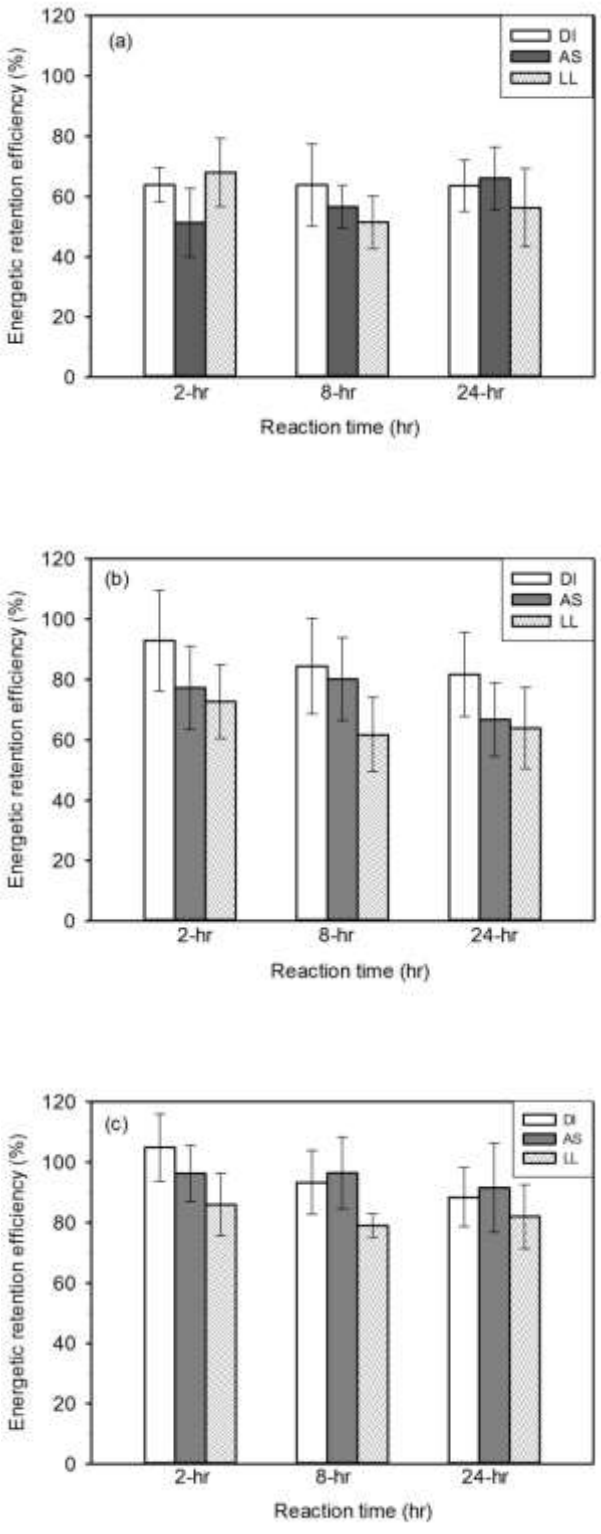

Figure 3.6 Energetic retention efficiencies resulting from the carbonization of (a) paper, (b) food waste and (c) yard waste in the presence of deionized water (DI), activated sludge (AS) and landfill leachate (LL). Error bars represent standard deviations.

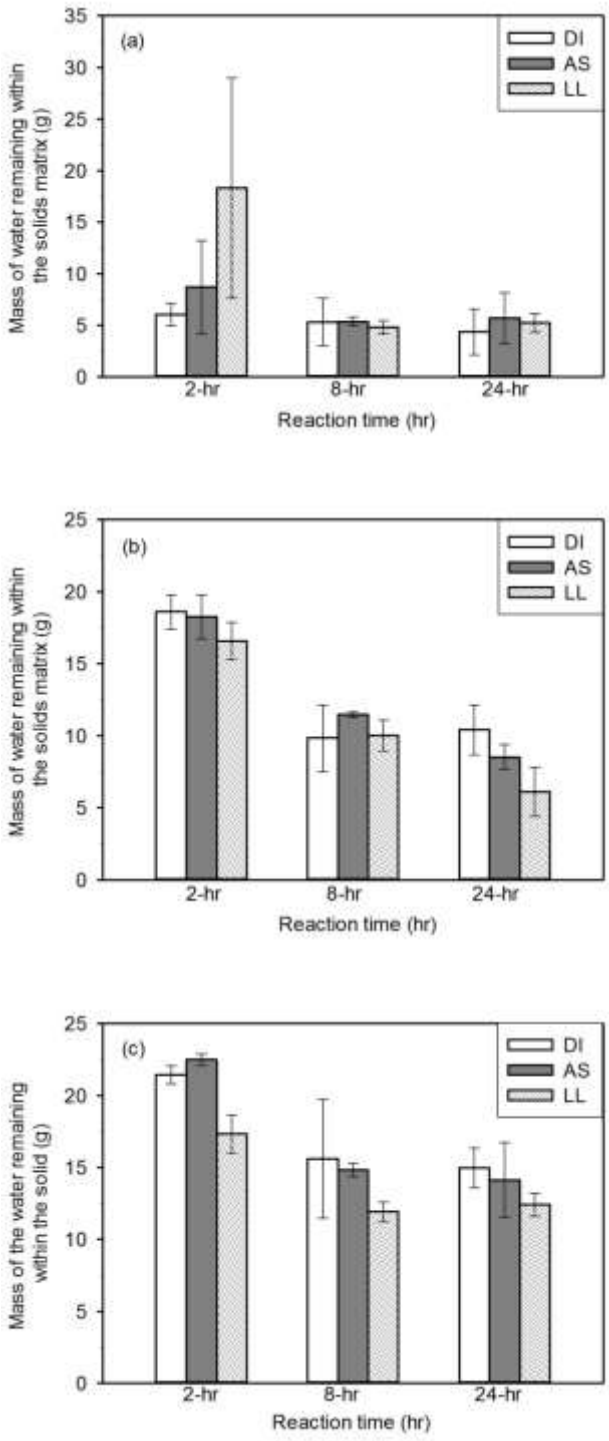

Figure 3.7 Mass of water remaining within the solids matrix after carbonization (a) paper, (b) food waste and (c) yard waste in the presence of deionized water (DI), activated sludge (AS) and landfill leachate (LL). Error bars represent standard deviations.

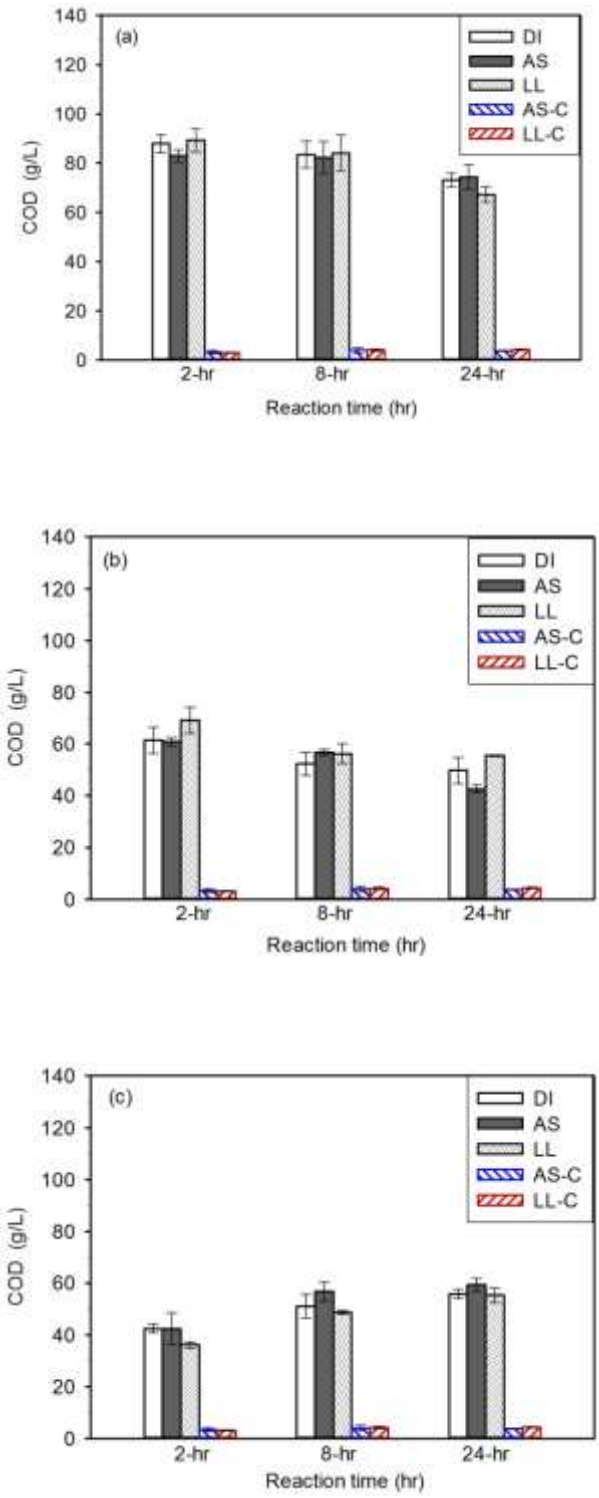

Figure 3.8 COD concentrations in the final process liquid resulting from the carbonization of (a) paper, (b) food waste and (c) yard waste in the presence of deionized water (DI), activated sludge (AS) and landfill leachate (LL). Error bars represent standard deviations.

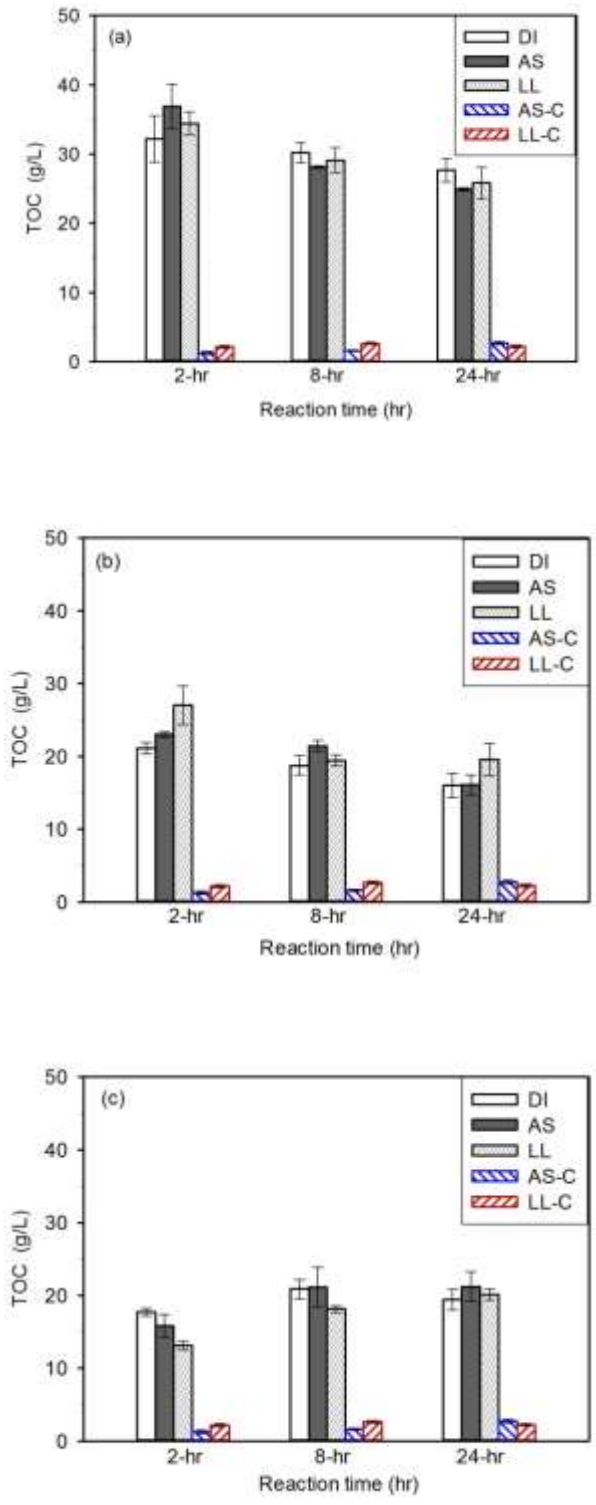

Figure 3.9 TOC concentrations in the final process liquid resulting from the carbonization of (a) paper, (b) food waste and (c) yard waste in the presence of deionized water (DI), activated sludge (AS) and landfill leachate (LL). Error bars represent standard deviations.

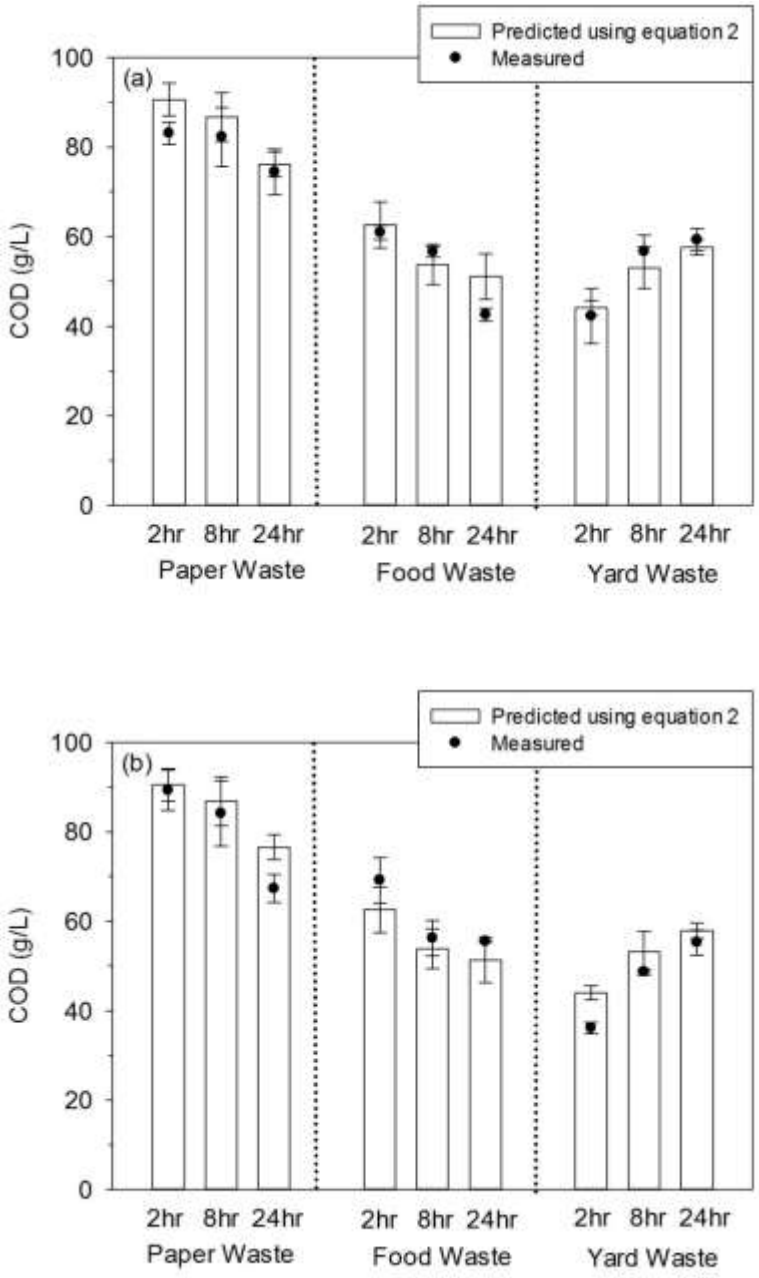

Figure 3.10 Comparison of measured (points) and theoretical (bar) COD concentrations in the final process liquid resulting from the carbonization of different feedstocks (paper, food waste and yard waste) in the presence of (a) activated sludge (AS) and (b) landfill leachate (LL). Error bars represent standard deviations.

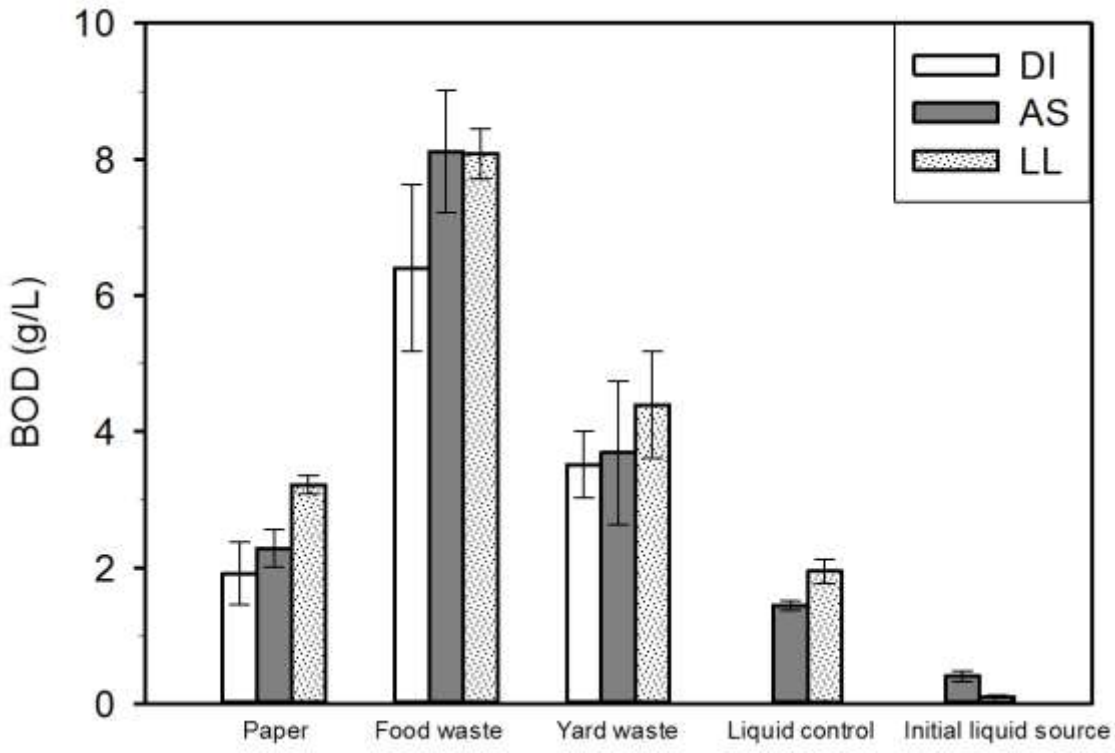

Figure 3.11 BOD concentrations in the final process liquid resulting from the carbonization of activated sludge only, landfill leachate only and paper, food waste, yard waste in the presence of deionized water (DI), activated sludge (AS), and landfill leachate (LL) after a reaction time of 24 hr. Error bars represent standard deviations.

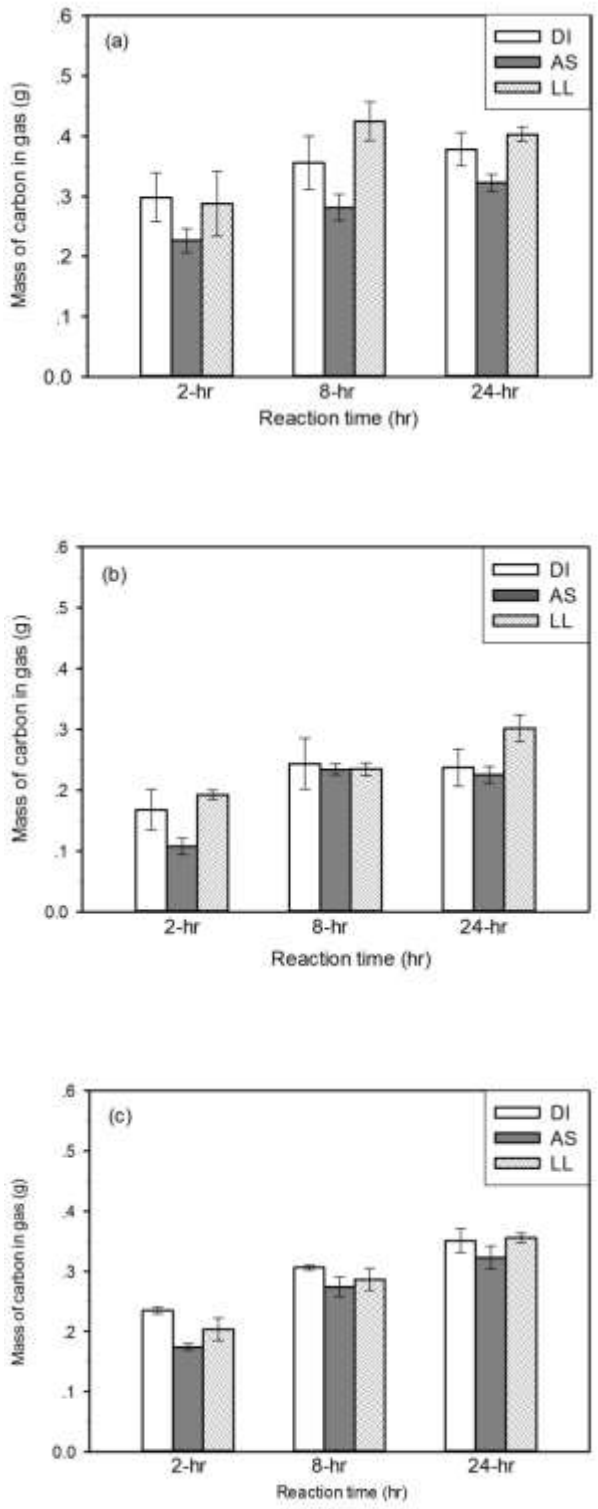

Figure 3.12 Mass of carbon in gas resulting from the carbonization of (a) paper, (b) food waste and (c) leachate in the presence of deionized water (DI), activated sludge (AS) and landfill leachate (LL). Error bars represent standard deviations.

CHAPTER 4.

INVESTIGATING THE ROLE OF FEEDSTOCK PROPERTIES AND PROCESS CONDITIONS ON PRODUCTS FORMED DURING THE HYDROTHERMAL CARBONIZATION OF ORGANICS USING REGRESSION TECHNIQUES

Li, L., Flora, J. R., Caicedo, J. M., and Berge, N. D. 2015. Investigating the role of feedstock properties and process conditions on products formed during the hydrothermal carbonization of organics using regression techniques. *Bioresource Technology*, 187, 263-274.

Reprinted here with permission of publisher.

ABSTRACT

The purpose of this study is to develop regression models that describe the role of process conditions and feedstock chemical properties on carbonization product characteristics. Experimental data were collected and compiled from literature-reported carbonization studies and subsequently analyzed using two statistical approaches: multiple linear regression and regression trees. Results from these analyses indicate that both the multiple linear regression and regression tree models fit the product characteristics data well. The regression tree models provide valuable insight into parameter relationships. Relative weight analyses indicate that process conditions are more influential to the solid yields and liquid and gas-phase carbon contents, while feedstock properties are more influential on the hydrochar carbon content, energy content, and the normalized carbon content of the solid.

4.1 INTRODUCTION

Hydrothermal carbonization (HTC) is a thermal conversion technique that continues to gain significant attention as a sustainable and environmentally beneficial means for biomass and waste transformation to value-added products. HTC is a unique process in which wet feedstocks are thermally converted into value- added products under relatively low temperatures (< 350^{o} C) and with relatively low input energy requirements (Funke and Zieglar, 2010; Libra et al., 2011; Li et al., 2013; Lu et al., 2012; Titirici et al., 2012). Feedstock transformation during HTC occurs through a series of simultaneous reactions, including hydrolysis, dehydration, decarboxylation, aromatization, and recondenstation (Funke and Zieglar, 2010; Libra et al., 2011; Sevilla and Fuertes, 2009a, 2009b; Titirici et al., 2007, 2012), with degree of conversion depending on reaction time and temperature (e.g., reaction severity), as well as other process-related conditions and feedstock type. Carbon-rich, energy-dense carbonaceous materials, referred to as hydrochar, with attractive surface functionalization are ultimately generated and have garnered significant study, as they may be used in a variety of environmentally-relevant applications, including as a soil amendment (e.g., Libra et al., 2011), energy source (e.g., Berge et al., 2011; Heilmann et al., 2010), environmental sorbent (e.g., Román et al., 2012, 2013; Sevilla et al., 2011), and/or a material for energy and/or hydrogen storage (e.g., Falco et al., 2013; Sevilla et al., 2011). Several recent reviews have detailed different aspects of carbonization, including reaction mechanisms (e.g., Funke and Ziegler, 2010; Libra et al., 2011), recovery of valuable liquid and solid products (e.g., Reza et al., 2014), and material synthesis for various material and/or environmental applications (e.g., Libra et al., 2011; Titirici et al., 2007, 2012).

The number of published papers reporting on various aspects of HTC has increased significantly over the past ten years, with carbonization investigations performed on a variety of feedstocks, ranging from pure substances, such as glucose and cellulose, to more complex feedstocks, such as mixed municipal solid waste (MSW), food waste, and animal wastes, and over a range of process conditions (e.g., Berge et al., 2011; Falco et al., 2011; Kang et al., 2012; Li et al., 2013). Results from these individual studies indicate that carbonization product characteristics are greatly influenced by both feedstock properties and processing conditions. However, their specific influence/role on products formed from HTC remains unclear. Because these experimental results are often described with no reference to process kinetics, which likely vary with feedstock, reactor volumes, and reactor heating mechanisms/rates, reported conclusions and trends that detail the influence of specific feedstock properties and process conditions cannot be universally applied. Conflicting reports of the influence of specific process conditions, such as reaction time (e.g., Li et al., 2013; Lu et al., 2013; Roman et al., 2012; Mumme et al., 2011) and feedstock type (e.g., Hoekman et al., 2011; Wiedner et al., 2013), on carbonization product characteristics support this hypothesis.

Despite the large number of peer-reviewed carbonization studies, very few of these studies have focused on developing statistical models to understand parameter/reaction condition importance or to predict product characteristics given a specific feedstock and set of reaction conditions. Kinetic models have been developed to describe product disappearance and generation based on their specific experimental data/conditions (e.g., Knežević et al. 2009, 2010; Alenezi et al., 2009; Pinkowsaka et al., 2012; Reza et al. 2013b; Danso-Boateng et al., 2013). The applicability of these models is

somewhat limited to specific study conditions (e.g., range of temperatures, times, reactor sizes, and types of feedstock) and the ability to expand their models to other feedstocks and process conditions has not been studied. Others have focused on modeling specific aspects of carbonization, such as particle liquefaction (e.g., Kamio et al., 2008). Mumme et al. (2011) conducted regression analyses of data obtained from the carbonization of anaerobic digestate and cellulose to evaluate the statistical significance of process related data. Because they added catalysts and adjusted their initial pH conditions and used only their experimental data in their regression analyses (< 15 points), the universal use of their developed models may be limited.

To date, there has been no attempt to aggregate and subsequently analyze literature reported carbonization data with the intent of developing statistical models to elucidate the importance of feedstock properties and reaction conditions on the hydrothermal carbonization process and to predict product characteristics when carbonizing a variety of feedstocks over a range of reaction conditions. The purpose of the work presented in this manuscript is to use data collected from the literature to develop regression models that describe the role of process conditions (e.g., reaction time, reaction temperature) and feedstock chemical properties (e.g., elemental composition) on carbonization product characteristics (e.g., yields and composition). The specific objectives of this work are to: (1) collect and analyze carbonization data from previously published studies, (2) build parametric and non-parametric statistical models using literature-reported process conditions and feedstock properties and to compare their predictive performance, and (3) highlight the critical feedstock properties and carbonization process conditions by assessing parameter importance and relationships in

these regression models. Data were analyzed using multiple linear regression (MLR) and regression trees (RT). These statistical approaches differ in that the MLR model assumes a linear relationship between variables, while no relationships between variables are assumed in the RT models. Results from these analyses were used to ultimately understand the relationships between process conditions, feedstock properties, and the characteristics of the generated products (e.g., solids recovery, solids energy content and normalized carbon content of the gas, liquid and solid-phases). In addition, a series of models were generated that may be used as a screening tool to meet a specific carbonization objective.

4.2 MATERIALS AND METHODS

4.2.1 Data Collection and Extraction

A survey of existing HTC-related literature was conducted. Studies reporting on hydrothermal treatment processes occurring between 180 and 350 oC were collected. Literature searches were conducted in scientific databases (including Science Direct, Web of Knowledge, and Google Scholar) using key words including: hydrothermal carbonization, hydrothermal conversion, hydrothermal decomposition, subcritical water hydrolysis, hydrolysis, and hot compressed water. Literature available in these databases through May 2014 was collected. The purposes of these collected studies varied, ranging from recovery of liquid-phase intermediates (e.g., acid and/or 5-(Hydroxymethyl)furfural (HMF) recovery) to production of carbon-based materials for use as an energy source or adsorption media.

Process related data (e.g., reaction time, reaction temperature, solids concentration) and experimentally collected carbonization product information from each study were

tabulated. The carbonization product information reviewed and assessed in this study includes: solid-phase carbon content (% carbon in the recovered solids), normalized carbon content of the hydrochar (mass of carbon per mass of initial dry feedstock), energy content of the hydrochar, hydrochar yield (mass of dry recovered solids per mass of initial dry feedstock), gas-phase carbon content (mass of carbon in the gas per mass of initial dry feedstock), and liquid-phase carbon content (mass of carbon in the liquid per mass of initial dry feedstock). These parameters were chosen because they are often reported and critical when carbonizing feedstocks with the purpose of waste and/or biomass conversion.

Data from all collected manuscripts were either extracted from published data tables, the text, or from published figures using Plot Digitizer (version 2.6.1). In some instances, calculations were performed to obtain desired information using data provided in the manuscripts. In this study, a reaction time equal to zero represents the time when reactor heating commences. If required, reported reaction times were corrected to reflect the heating period based on provided heating rate data or other provided temperature-related information. If not reported directly, heating rates were calculated based on provided information assuming a constant and linear rate. Reactor heating times are defined as the time it takes to heat the reactor from room temperature (assumed to be 25oC) to the final desired temperature. All collected data were converted to a consistent set of units. Feedstock ultimate and proximate data were also collected from the published studies. If feedstock data were not reported, literature searches were conducted to obtain average initial feedstock properties.

4.2.2 Development of Statistical Models

MLR is an explicit and frequently used technique for developing predictive relationships between dependent and independent variables. An advantage associated with this technique is the generation of an equation that is easy to use and understand. However, this regression technique assumes a linear relationship between variables, potentially resulting in a model with modeling errors and limited ability to interpret important relationships. RT analyses differ from MLR in that they represent a non-parametric technique in which no a priori relationships between variables are assumed, allowing for the modeling of nonlinearities. This approach produces binary trees through the splitting of dependent variables into nodes following recursive partitioning rules (Breiman et al., 1984). Regression trees provide several advantages, including the generation of a graphical representation that provides insight into the interaction between parameters. A disadvantage to RTs, however, is that they often result in heavily parameterized, discontinuous models that may be more complicated to use.

In this study, MLR models were developed using the "lm" function in the statistical software package R (version 3.1.0, R Development Core Team). A backward elimination procedure was employed to obtain regression models containing only statically significant parameters ($p < 0.05$). RT models were developed using the "rpart" function of the "rpart" package in R.

4.2.2.1 Model evaluation and comparison

The goodness of fit of both MLRs and RTs were evaluated using an adjusted coefficient of determination (adj. R^2). The adj. R^2 is a modified version of R^2 that accounts for the number of explanatory variables in each model. The error associated

with each model was assessed by using the root mean squared error (RMSE), and was calculated according to equation (1) (Kobayashi and Salam, 2000):

$$\text{RMSE} = \sqrt{\frac{\sum_{i=1}^{n}(Y_{pred,i} - Y_{obs,i})^2}{n}} \qquad (1)$$

where, $Y_{pred,i}$ represents the predicted value, $Y_{obs,i}$ represents the experimentally observed value, and n represents the number of observations.

Leave one out cross-validation (LOOCV) was used to validate the MLR and RT models. In LOOCV, a series of models are built based on all observed values except for one. This left out observation is predicted based on the regression model developed without it. This process is repeated until all observations have been left out once and each observation has been independently predicted. LOOCV for MLR was performed using the *cv.lm* function of the "DAAG" package in R. LOOCV for RT was performed using the *rpart* function of the "rpart" package in R. A cross-validated RMSE (referred to as RMSEcv) was calculated and illustrates the ability of each model to predict data not used to build the model.

The relative importance of each variable in the MLR and RT models was assessed using relative weight analysis. Relative weights are a measure of the percentage of predictable variance that can be explained by each independent variable and can be used to rank the relative importance of the variables (Nathans et al., 2012). Relative weights for the MLR models were calculated using the calc.relimp function of the "relaimpo" package in R. Relative weights for the RT models were calculated using the "rpart" function in R.

4.3 RESULTS AND DISCUSSION

4.3.1 Overview of Collected Carbonization Studies

A total of 313 papers associated with hydrothermal carbonization were collected, resulting in a total of 985 data points. Several of the collected papers involved the addition of catalysts (66 papers) (e.g., Mumme et al., 2011) and/or external sources of pressure (37 papers) (e.g., Alenezi et al., 2009) during carbonization. These papers were not considered in this study because these external additives likely impart some effect on carbonization. Catalyst addition, for example, has been shown to modify collected solids characteristics and influence carbonization kinetics (e.g., Asghari et al., 2007), preventing a true evaluation of the influence of process conditions on carbonization product characteristics. In addition, a large fraction of the collected papers (80 papers) did not report sufficient information for inclusion in this study. These unused studies focused on understanding aspects of product formation or properties from hydrothermal carbonization that did not result in the reporting of the desired process parameters and/or product characteristics, such as understanding hydrochar structure via 13C NMR, soil incubation, and/or heat of reactions. Several of the studies in this category also focused on feedstock hydrolysis, rather than carbonization, resulting in the reporting of little information applicable to this study. In addition, a fraction of these unused studies (11 papers) reported carbonization products in units that could not be converted to the units utilized in this work.

Approximately 53% of the relevant collected papers (excluding those in which catalysts and external pressure were added) reported at least one carbonization product parameter of interest (e.g., hydrochar yield, hydrochar carbon content, hydrochar energy

content, or carbon content of the liquid or gas-phases). The majority of these reported studies focused on the carbonization of complex feedstocks (e.g., wood, food, paper). The three most commonly evaluated complex feedstocks in the reported literature include wood, food wastes, and plant material. Cellulose and glucose were the most commonly carbonized pure compounds. These compounds were most often evaluated because they served as model compounds for biomass. Pure compounds were also often carbonized when the identification of carbonization mechanisms was desired (Falco et al., 2011; Knežević et al., 2009; Lu et al., 2013).

The most commonly reported carbonization product parameter was hydrochar yield (71 % of papers). The recovered solids carbon content was the second most reported carbonization product (54 % of papers), while relatively few studies reported carbon-related information in the liquid and gas-phases (< 18% of the relevant papers). Process related parameters were also reported, with the most common being reaction time (100 % of papers) and temperature (100% of papers). The least reported process parameters were heating rate and heating time (54 % of papers reported each).

When assessing these carbonization studies, it was required to separate the results into two main categories, depending on how the recovered solids were collected/processed. Of the papers containing data relevant to this study, 61% reported washing the hydrochar (referred to as washed) with water or some sort of organic solvent (i.e., acetone) prior to analysis. Washing/rinsing of the collected hydrochar alters solids properties (e.g., Cao et al., 2011), complicating the determination of the impact of process parameters on solid product formation and measured characteristics. Therefore, such data were not used when assessing hydrochar properties. Because washing/rinsing

has no effect on the liquid and gas-phase carbon contents, data from studies in which this washing/rinsing occurred were used when assessing these parameters.

4.3.2 Selection of Independent Variables

4.3.2.1 Process conditions

The collected literature was surveyed to determine which process conditions warranted inclusion in this study. The process parameters found in Table 4.1 are the process-related independent variables evaluated in this study and were chosen because they have either been shown to impart some influence on carbonization product composition/generation, as suggested in several previously published studies (e.g., Kang et al., 2012; Lu et al., 2013), or have been suspected to influence carbonization product composition. Reaction temperature, reaction time, and feedstock concentration were three of the most commonly reported process parameters, each documented to impart an influence on carbonization product characteristics (Heilmann et al., 2010; Li et al., 2013; Román et al., 2012). Evaluation of the compiled data also suggests that the influence of reaction time on carbonization product characteristics is likely dependent on reactor heating time (HT, defined as the time to reach the final desired reaction temperature) and/or heating rate (HR). To put the reaction times in context with reactor heating times, a descriptive variable representing the ratio of reactor heating time to reaction time (HT/t) was developed and used as an independent variable in this study. A HT/t ratio greater than 1 indicates that the reactor has not yet reached the final reaction temperature, and is at a point in which the influence of reaction time is likely more important. At HT/t ratios less than 1, the influence of reaction time is likely less significant, as the final reaction time has been reached. Other process parameters including reactor volume, volume ratio

(fraction of reactor volume filled with liquid and feedstock), and reactor heating rate were reported less frequently and their influence on carbonization has not been specifically studied in the existing literature. It is possible these parameters influence carbonization kinetics, ultimately influencing optimal reaction times and carbonization product characteristics, thus these parameters were also included in this study.

Because these chosen independent variables were not reported in all collected studies, the dataset used in this work was modified accordingly. Only points in which all of these parameters were known were used. This resulted in the use of 19% of the relevant papers and a total of 340 data points. Table 4.1 contains the range of reported values associated with each of these parameters.

4.3.2.2 Feedstock chemical composition

There are conflicting reports related to the influence feedstock type imparts to carbonization product composition and yields (Hoekman et al., 2011; Wiedner et al., 2013). Hoekman et al. (2011) report that feedstock type does influence product characteristics, while Wiedner et al. (2013) report that changes in feedstock type have little influence on solids characteristics. In addition, little is known about the role of specific feedstock properties on carbonization product characteristics. In this study, the following typically reported feedstock properties were assessed: carbon, hydrogen, oxygen, ash, volatile matter, and fixed carbon contents (%, dry wt.). If such feedstock data were not reported, literature searches were conducted to obtain average initial feedstock properties.

4.3.3 Regression Models

4.3.3.1 Solid yield

The MLR model developed to explain the relationship between solid yield and reaction conditions/feedstock parameters is presented in Table 4.2. Of the evaluated independent parameters, 11 were deemed statistically significant ($p < 0.05$); only reaction time, system heating time, and reactor volume were determined to be statistically insignificant ($p > 0.05$). Although reaction time was not statistically significant, yields have been shown to change with reaction time (e.g., Knežević et al., 2009, 2010). The influence of reaction time in this MLR model is coupled with the HT/t parameter. The inclusion of the other parameters in this model is consistent with that reported in the literature. Solid yields have been reported to be influenced by reaction temperature (Kang et al., 2012; Knežević et al., 2009, 2010), initial feedstock concentration (Danso-Boateng 2013; Heilmann et al., 2010), and feedstock type (Kang et al., 2012; Toor et al., 2013). This MLR model appears to fit the data well (adj. R2 is 0.63, Table 4.2). The RMSE associated with this model is relatively small, representing approximately 16% of the average solid yield modeled.

The RT model developed to describe the relationships between solid yield and the independent parameters is presented in Figure 4.1 and also appears to fit the data well (adj. R2 is 0.76, Table 4.3). This model is highly branched (20 nodes) and significantly more complex than the MLR model, suggesting there is a high level of interaction between independent variables and that a non-linear model may fit the data better. The main node in this model is defined by the parameter HT/t. The importance of this parameter is not surprising, as the greatest changes in solid yield occur during early

reaction times when the reactor is still heating (e.g., HT/t > 1). The right side of the tree (HT/t ≥ 1.155) represents the solid yields obtained during early reaction times (before the final reaction temperature is attained), and accordingly, the solid yields on the right side of the tree represent the largest of the solid yields measured in the literature (noting the solids recovered are likely a combination of hydrochar and unreacted feedstock). The greatest level of interaction between the process conditions and feedstock properties occurs when the HT/t value is less than 1.155, indicating that feedstock properties and other process conditions impart a more significant influence on solid yields as reaction time increases. After HT/t on the left side of the tree (or when the reactors are heated to the target temperature), the initial feedstock concentration is the next main node, suggesting this parameter also plays an important role on solid yields. The RMSE associated with this the overall RT model is relatively low, representing only approximately 13% of the average solid yield value modeled, suggesting it can be used to reasonably predict yields.

When comparing the MLR and RT models, it appears that the RT model fits the solid yield data better than the MLR model, as evidenced by a larger goodness of fit (adj. R2) and lower RMSE value (Table 4.3). The RMSE associated with the RT model is approximately 21% lower than that obtained from the MLR model. The RMSEcv values for each model remain less than 18% of the average solid yield value modeled, suggesting each model is fairly robust.

Relative weights were calculated and used to assess variable importance in each model. Results from this analysis are shown in Table 4.4 and indicate that for both regression models, HT/t is the parameter of greatest importance (represents the greatest

percentage of predicted variance in each model). In the MLR model, the contribution of the HT/t parameter is 1.9 times greater than that of all other independent parameters. The second most important parameter in the MLR model is initial feedstock concentration. In the RT model, the difference in the contribution of the HT/t parameter and other independent parameters is not as significant, indicating a greater level of interaction between parameters than that described in the MLR model. When comparing the combined relative weights of process conditions and feedstock properties associated with both regression models, it is clear that process conditions (e.g., HT/t, feedstock concentration, reaction time, etc.) play a more important role on solid yields than the feedstock properties.

4.3.3.2 Hydrochar carbon content

Table 4.2 contains the MLR model describing the relationship associated with hydrochar carbon content (%C, dry wt). Of the evaluated independent parameters, 10 were deemed statistically significant ($p < 0.05$). All of the evaluated feedstock properties were deemed statistically significant, while initial feedstock concentration, final temperature, heating time, and volume ratio were determined to be statistically insignificant ($p > 0.05$). This regression model appears to be fairly consistent with relationships reported in the literature. Final reaction temperature is an exception. This parameter was not determined to be statistically significant, but it has been documented that increases in reaction temperature lead to increases in hydrochar carbon content (Cao et al., 2013; Hwang et al., 2012; Sevilla and Fuertes, 2009b). This regression model appears to fit the data quite well (adj. R2 is 0.79, Table 4.2). In addition, the RMSE associated with this model is relatively small, representing only approximately 8% of the

average hydrochar carbon content modeled.

The RT model developed to describe hydrochar carbon content is presented in Figure 4.2 and also appears to fit the data well (adj. R2 is 0.84, Table 4.3) and better than that associated with the MLR model. As with the RT associated with solid yield, the RT model associated with hydrochar carbon content is highly branched (20 nodes). This model is significantly more complex than the MLR model, which demonstrates a higher level of interaction between the independent variables than that represented in the MLR model. The main node in this model is defined by the feedstock ash content (%, dry wt.). When inspecting the tree structure, it is apparent that when the ash content of the feedstock is greater than or equal to 26.4% (dry wt.), the carbon content of the hydrochar is at its lowest point (~34%, dry wt.). This observation is logical and indicates that as the feedstock ash content increases, the carbon content of the hydrochar decreases. When the feedstock ash content (%, dry wt.) is less than 26.4% (right side of the tree), a greater level of interaction between process and feedstock parameters exists. The main nodes at smaller feedstock ash contents (> 26.4 %, dry wt.) are the feedstock hydrogen content (%, dry wt.), HT/t, and the feedstock carbon content (%, dry wt.). The RMSE associated with this model is relatively low, representing approximately only 6% of the average hydrochar carbon content modeled.

As with solid yield, it appears that the RT model fits the hydrochar carbon content data better than the MLR model, as evidenced by a larger goodness of fit value. The RMSE values associated with both models vary by less than 16%, suggesting the models are similar (Table 4.3). The low RMSE values also suggest that they can be used to predict hydrochar carbon contents reasonably well. The cross-validated RMSE values for

each model suggest each model is fairly robust, as they remain less than 8% of the average hydrochar carbon content.

The relative weights calculated to assess variable importance in each model are shown in Table 4.4. Results from this analysis indicate that the parameter of greatest importance in the MLR model is feedstock carbon content, while the most important variable in the RT model is feedstock ash content. Although the most important values in each model differ, the combined contribution of the evaluated feedstock properties is more than three times greater than the combined contribution associated with the process condition parameters evaluated for both models (Table 4.4). This result suggests that if carbonizing to maximize (or minimize) the carbon sequestered in the hydrochar, it is more critical to consider feedstock properties than specific process conditions. These results also suggest that choosing a feedstock with low ash and high initial carbon contents will result in greater hydrochar carbon contents.

4.3.3.3 Hydrochar energy content

The MLR model describing the hydrochar energy content (kJ/g dry wt., Table 4.2) contains 10 statistically significant ($p < 0.05$) parameters. Feedstock carbon and oxygen contents, initial feedstock solid concentration, and reactor volume were deemed statistically insignificant ($p > 0.05$). The influence of feedstock parameters on solids energy content has been well documented (Danso-Boateng et al., 2013; Toor et al., 2013). Changes in reaction temperature (Hwang et al., 2012; Reza et al., 2013a, 2013b), and reaction time (Danso-Boateng et al., 2013; Reza et al., 2013b) have been documented to influence hydrochar energy content. This regression model appears to fit the data quite well (adj. R2 is 0.79, Table 4.2). The RMSE associated with this model is relatively small,

representing only approximately 8% of the average hydrochar energy content modeled.

The RT model developed to describe hydrochar energy content (Figure 4.3) also appears to fit the data well (adj. R2 is 0.80, Table 4.3) and better than that associated with the MLR model. As with previously described RT models, the RT model associated with hydrochar energy content is highly branched (18 nodes). The main node in this model is defined by the feedstock property fixed carbon content (%, dry wt.). The tree structure suggests that there is a great level of interaction between parameters at all feedstock fixed carbon content values, with a spitting value of 11.21 % (dry wt.). The next two nodes are represented by HT/t (feedstock fixed carbon content $\geq$ 11.21%) and feedstock carbon content (feedstock fixed carbon content < 11.21%). This complex relationship between parameters is not observed in the MLR model. The RMSE associated with this model is essentially the same as that associated with the MLR model, suggesting both models can be used to predict hydrochar energy contents.

The cross-validated RMSE values for each model suggest the models are robust, as the RMSEcv values remain less than 10% of the average energy content value modeled. More significant information about parameter relationships with hydrochar energy content can be determined from the calculated relative weights (Table 4.4). Results from this analysis indicate that the parameter of greatest influence in the MLR model is feedstock hydrogen content, while the most influential variable in the RT model is feedstock oxygen content. It has been previously documented that feedstock oxygen content plays an important factor in hydrochar energy content (Hwang et al., 2012; Lu et al., 2013). Although this relationship is present in the RT model, this relationship is not shown in the MLR model (feedstock oxygen content was statistically insignificant, p >

0.05). The combined relative weights of the evaluated feedstock properties is two to three times greater than the combined weights associated with the process conditions for each model (Table 4.4), suggesting that if carbonizing to maximize hydrochar energy content, feedstock selection is more critical than choosing specific process conditions.

4.3.3.4 Normalized carbon in the liquid

The MLR model describing the normalized carbon in the liquid (g C in liquid/g dry feedstock, Table 4.2) contains 10 statistically significant ($p < 0.05$) parameters. The parameters deemed statistically insignificant are: feedstock fixed carbon and volatile matter contents, HT/t, and reactor volume. Many of the statistically significant parameters have been documented to influence the liquid-phase carbon content, such as reaction time (Li et al., 2013; Möller et al., 2013), temperature (Hoekman et al., 2011), and initial feedstock concentration (Li et al., 2013). This regression model appears to fit the data reasonably well (adj. R2 is 0.68, Table 4.2). However, the RMSE associated with this model is relatively large, representing approximately 44% of the average normalized carbon in the liquid values modeled. This suggests that although the MLR model may fit this dataset, the ability to use this equation to predict liquid-phase carbon contents will be hindered by a large amount of error/variability. This result is not surprising, as the relationship between liquid-phase carbon content and process conditions, such as reaction time, is not linear. Lu et al. (2013) and Möller et al. (2013) report an increase and subsequent decrease in liquid-phase carbon content with reaction time.

The RT model developed to describe the normalized carbon content in the liquid (Figure 4.4) appears to fit the data (adj. R2 is 0.88, Table 4.3) significantly better than that associated with the MLR model. This result is not surprising, as the relationship

between liquid-phase carbon content and reaction time has been shown to be non-linear (Lu et al., 2013; Möller et al., 2013). The RMSE value associated with this model is relatively large, but almost half of that associated with the MLR model (approximately 25% of the average normalized carbon in the liquid values modeled). The RT model does provide some valuable information associated with the interaction/relationships between different independent parameters. This regression tree is highly branched (19 nodes), with the main node defined by the initial feedstock concentration (% solids, dry wt.). The importance associated with the initial feedstock concentration has been documented in the literature (e.g., Li et al., 2013). The tree structure (Figure 4.4) indicates that there is a great level of interaction between parameters, independent of the initial feedstock concentration. The next two nodes in the tree are represented by the final reaction temperature (initial feedstock concentration < 11.11%) and feedstock fixed carbon content (initial feedstock concentration ≥11.11%).

More significant information about parameter relationships with normalized liquid-phase carbon content can be determined from the calculated relative weights (Table 4.4). Results from this analysis for both models indicates that the combined contribution of the process conditions is approximately two times greater than that of the combined weights associated with the feedstock properties (Table 4.4).

4.3.3.5 Normalized carbon in the gas

The MLR model describing the normalized carbon in the gas (g C in gas/g dry feedstock, Table 4.2) contains 10 statistically significant ($p < 0.05$) parameters. Only the feedstock ash content, initial feedstock concentration, heating time, and reactor volume were determined to be statistically insignificant ($p > 0.05$). This regression model appears

to fit the data reasonably well (adj. R2 is 0.79, Table 4.2). The RMSE associated with this model is relatively small, representing approximately 20% of the average normalized carbon in the gas values modeled.

The RT model developed to describe the normalized carbon content in the gas (Figure 4.5) appears to fit the data (adj. R2 is 0.79, Table 4.3) at a level equivalent to that of the MLR model. The RMSE value associated with this model is smaller than that associated with the MLR model, representing approximately 16% of the average normalized carbon in the gas values modeled. The RT model does provide some valuable information associated with the interaction/relationships between different independent parameters. The main node in this model is defined by reaction time. The importance associated with reaction time has been documented in the literature; gas-phase carbon content has been found to generally increase with reaction time (Lu et al., 2012). After reaction time, the next node is represented by HT/t, suggesting that the carbon content in the gas-phase is dependent on system heating rate and/or process kinetics.

Results from the relative weights analysis indicate that the parameter of greatest importance in the MLR model is HT/t, while the most important variable in the RT model is reaction time (Table 4.4). The second most important variable in the regression model is HT/t. These process conditions contribute to greater than 50% of the predicted variance associated with the models of normalized carbon in the gas-phase. Interestingly, the combined relative weights of the evaluated process conditions are 93 and 77% for the MLR and RT models, respectively (Table 4.4). The difference in these combined relative weights may be due to a lack of differentiation between variables in the MLR model. These results indicate that when evaluating the carbon partitioning to the gas-phase,

process conditions are more important than the feedstock properties.

4.3.3.6 Normalized carbon in the solid

The MLR model describing the normalized carbon in the solid (g C in solid/g dry feedstock, Table 4.2) contains 11 statistically significant ($p < 0.05$) parameters. All feedstock properties evaluated were determined to be statistically significant ($p < 0.05$); only reaction time, heating rate, and reactor volume were determined to be statistically insignificant. The influence of initial solids concentration and temperature on normalized carbon content have been previously documented (Hwang et al., 2012; Li et al., 2013). Although not statistically significant in this model, reaction time has been reported to influence carbon distribution (Li et al., 2013; Knežević et al., 2010). This regression model appears to fit the data reasonably well (adj. R2 is 0.78, Table 4.2). The RMSE associated with this model is approximately 13% of the average normalized solid-phase carbon values modeled.

The RT model developed to describe the normalized carbon content in the solid (Figure 4.6) appears to fit the data (adj. R2 is 0.85, Table 4.3) as well as the MLR model. The RMSE value associated with this model is smaller than that associated with the MLR model, representing approximately 8% of the average normalized carbon in the solid values modeled. The RT model provides some valuable information associated with the interaction/relationships between different independent parameters. The main node in this model is defined by feedstock carbon content, followed by secondary nodes represented by initial feedstock concentration (feedstock carbon content ≥ 42.7) and feedstock hydrogen content (feedstock carbon content < 42.7).

More significant information about parameter relationships with normalized solid-

phase carbon content can be determined from the calculated relative weights (Table 4.4). Results from this analysis indicate that the parameter of greatest importance in both the MLR and RT model is feedstock carbon content, followed by the feedstock hydrogen content. Results from this analysis also indicate that the combined relative weights of the evaluated feedstock properties is approximately three times greater than that of the process conditions (Table 4.4).

4.4 CONCLUSIONS

Results indicate that both the MLR and RT models fit the carbonization product characteristics data well. Relative weight analyses indicate that process conditions are more influential to the solid yields and liquid and gas-phase carbon contents, while feedstock properties are more influential on hydrochar carbon and energy contents, and the normalized carbon content of the solid. These conclusions are based on aggregate trends over varying feedstocks and can be used as a general guide or screening tool to meet a specific carbonization objective. Trends associated with the carbonization of a particular feedstock should be evaluated when optimizing a specific objective.

Table 4.1 Overview of collected data used in this regression analysis.

Category	Reported Parameters	Range of Reported Values[a]
Feedstock	Feedstocks Carbonized	Agricultural residues Animal feed Cellulose Digestate Food waste Municipal solid waste Paper Plant residue Poultry manure Sludge Straw Wood Yard waste
Carbonization Product Properties	Carbon content of recovered solids (%, db)	26 – 79 (61)
	Normalized carbon in the solids (g C/g initial dry feedstock)	0.13 – 0.54 (0.36)
	Solids Yield (%, db)	20 – 98 (58)
	Solids Energy Content (kJ/g, db)	14 – 35 (25)
	Liquid carbon content (g C /g initial dry feedstock)	0.0006 – 0.42 (0.11)
	Gas carbon content (g C/g initial dry feedstock)	1.02×10^{-6} – 0.04 (0.02)
Process Parameters	Time (t) (min)	5 – 7,200 (920)
	Temperature (T_{final}) (^{o}C)	180 – 320 (240)
	Initial feedstock concentration (% solids)	1 – 47 (18)
	Reactor heating rate (HR) (^{o}C/min)	0.6 – 580 (28)
	Heating time (HT) (min)	0.4 – 310 (81)
	Heating time/reaction time (HT/t)	0.01 – 4 (0.5)
	Reactor volume (V) (mL)	5 – 25,000 (2870)
	Volume ratio (VR) (fraction of reactor volume filled with liquid and feedstock)	0.04 – 0.98 (0.40)

[a]value in parentheses represents the average value

db = dry basis

Table 4.2 Summary of multiple linear regression models determined for all dependent parameters.

Dependent Parameter	Equation[1]	Data Points	Adj. R^2
Solid yield (%, db)	$\text{yield} = -1.12\text{Ash}_{\text{feed}} - 1.22\text{VM}_{\text{feed}} - 1.58\text{FC}_{\text{feed}} + 1.63\text{C}_{\text{feed}} - 4.89\text{H}_{\text{feed}} - 0.73\text{O}_{\text{feed}} + 0.43\text{Solids}_{\text{initial}} - 0.21\text{T}_{\text{final}} + 9.70\,\frac{\text{HT}}{\text{t}} + 1.36\text{HR} - 22.19\text{VR} + 212.76$	263	0.63
Hydrochar carbon content (%C, db)	$\%\text{C in char} = -0.94\text{Ash}_{\text{feed}} - 0.75\text{VM}_{\text{feed}} + 0.55\text{FC}_{\text{feed}} + 0.40\text{C}_{\text{feed}} + 4.18\text{H}_{\text{feed}} + 0.30\text{O}_{\text{feed}} + 0.0005\text{t} - 5.65\,\frac{\text{HT}}{\text{t}} - 0.36\text{HR} - 0.00009\text{V} - 12.68$	248	0.79
Energy content (kJ/g, db)	$\text{Energy} = -0.45\text{Ash}_{\text{feed}} - 0.43\text{VM}_{\text{feed}} + 0.41\text{FC}_{\text{feed}} + 2.35\text{H}_{\text{feed}} - 0.16\text{T}_{\text{final}} + 0.0005\text{t} + 0.52\text{HT} - 2.11\,\frac{\text{HT}}{\text{t}} + 25.25\text{HR} - 12.73\text{VR} - 22.74$	220	0.79
Norm. C in solid (g C/g dry feedstock)	$\text{g C in solid/g dry feedstock} = -0.0058\text{Ash}_{\text{feed}} - 0.0072\text{VM}_{\text{feed}} - 0.0061\text{FC}_{\text{feed}} + 0.0181\text{C}_{\text{feed}} - 0.0331\text{H}_{\text{feed}} - 0.0031\text{O}_{\text{feed}} + 0.0027\text{Solids}_{\text{initial}} - 0.0013\text{T}_{\text{final}} - 0.0005\text{HT} + 0.0133\,\frac{\text{HT}}{\text{t}} - 0.1447\text{VR} + 0.9220$	244	0.78
Norm. C in liquid (g C/g dry feedstock)	$\text{g C in liquid/g dry feedstock} = 0.0049\text{Ash}_{\text{feed}} + 0.0137\text{C}_{\text{feed}} - 0.0469\text{H}_{\text{feed}} + 0.0043\text{O}_{\text{feed}} - 0.0033\text{Solids}_{\text{initial}} + 0.0006\text{T}_{\text{final}} - 7.39 \times 10^{-6}\text{t} - 0.0007\text{HT} - 0.0002\text{HR} + 0.2209\text{VR} - 0.5406$	203	0.68

Norm. C in gas (g C/g dry feedstock)	$\text{g C in gas/g dry feedstock} = 0.0005\text{VM}_{\text{feed}} + 0.0030\text{FC}_{\text{feed}} - 0.0012\text{C}_{\text{feed}} + 0.0058\text{H}_{\text{feed}} + 0.0006\text{O}_{\text{feed}} + 0.0002\text{T}_{\text{final}} + 9.53 \times 10^{-7} \times \text{t} - 0.0082\frac{\text{HT}}{\text{t}} - 0.00006\text{HR} - 0.0220\text{VR} - 0.0995$	188	0.79

[1]C_{feed}=carbon content of the feedstock (%, db); H_{feed}=hydrogen content of the feedstock (%, db); O_{feed}=oxygen content of the feedstock (%, db); Ash_{feed}=ash content of the feedstock (%, db); VM_{feed}=volatile matter content of the feedstock (%,db); FC_{feed}=fixed carbon content of the feedstock (%, db); $Solids_{initial}$=initial feedstock concentration (%, solid); T_{final}=final reaction temperature (^{o}C); t=reaction time (min); HT=heating time (min); HT/t=heating time to reaction time ratio; HR=heating rate (^{o}C/min); V=volume (mL); VR=volume ratio

Table 4.3 Summary of regression model evaluation parameters.

Parameter	Solid yield (%, db)		Hydrochar carbon content (%C, db)		Energy content (kJ/g, db)		Norm. C in solid (g C/g dry feedstock)		Norm. C in liquid (g C/g dry feedstock)		Norm. C in gas (g C/g dry feedstock)	
	MLR	RT	MLR	RT	MLR	RT	MLR	RT	MLR	RT	MLR	RT
Adj. R^2	0.63	0.76	0.79	0.84	0.79	0.80	0.78	0.85	0.68	0.88	0.79	0.79
RMSE	9.41	7.47	4.66	3.94	1.92	1.83	0.047	0.027	0.049	0.028	0.004	0.004
$RMSE_{cv}$	10.10	9.79	4.81	4.39	2.17	2.53	0.053	0.032	0.057	0.030	0.005	0.005

RT is regression tree

MLR is multiple linear regression

Table 4.4 Summary of independent parameter relative weights (%) in each regression model.

Independent parameter	Solid yield (%, db)		Hydrochar carbon content (%C, db)		Energy content (kJ/g, db)		Norm. C in solid (g C/g dry feedstock)		Norm. C in liquid (g C/g dry feedstock)		Norm. C in gas (g C/g dry feedstock)	
	MLR	RT	MLR	RT	MLR	RT	MLR	RT	MLR	RT	MLR	RT
Ash_{feed}	3	10	8	21	3	12	2	12	4	4	NS	7
VM_{feed}	2	8	5	8	5	13	2	10	NS	4	1	3
FC_{feed}	1	4	7	10	12	13	1	5	NS	13	3	6
C_{feed}	14	7	30	18	NS	11	38	25	10	10	1	3
H_{feed}	9	5	24	19	45	11	26	18	20	2	2	2
O_{feed}	5	10	2	2	NS	15	3	6	2	2	0.5	2
Combined contribution of feedstock properties:[a]	34	44	76	78	65	75	72	76	36	35	7.5	23
$Solids_{initial}$	17	13	NS	1	NS	NS	14	8	16	18	NS	1
T_{final}	9	5	NS	NS	2	NS	4	2	6	6	21	8
t	NS	14	4	5	9	10	NS	2	6	2	15	28
HT	NS	2	NS	NS	2	NS	1	2	13	12	NS	12
HR	3	2	NS	6	2	NS	NS	NS	4	9	1	1
HT/t	32	17	16	6	16	11	4	1	NS	4	55	23
V	NS	3	2	NS	NS	NS	NS	1	NS	1	NS	1
VR	3	NS	2	3	3	3	4	9	18	11	1	3
Combined contribution of process conditions:[b]	64	56	24	21	34	24	27	25	63	63	93	77

[a]summation of the relative weight percentages from all feedstock properties; [b]summation of the relative weight percentages from all process conditions. RT is regression tree; MLR is multiple linear regression; NS is not statistically significant.

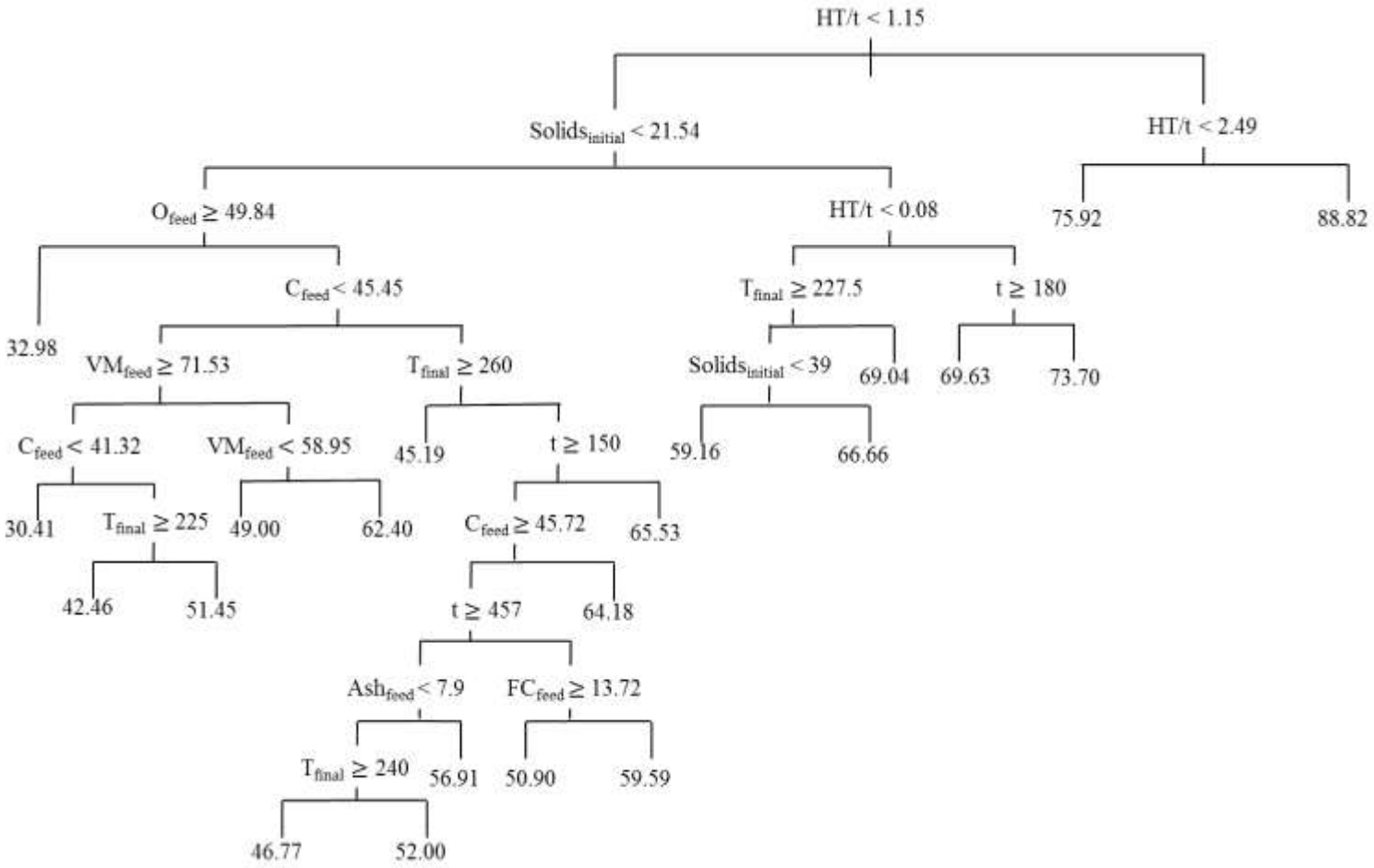

Figure 4.1 Regression tree model associated with solid yield (%, dry wt.). Mean values are represented at the end of each branch. Each node corresponds to a binary split. If the node condition is true, the left side of the split should be followed.

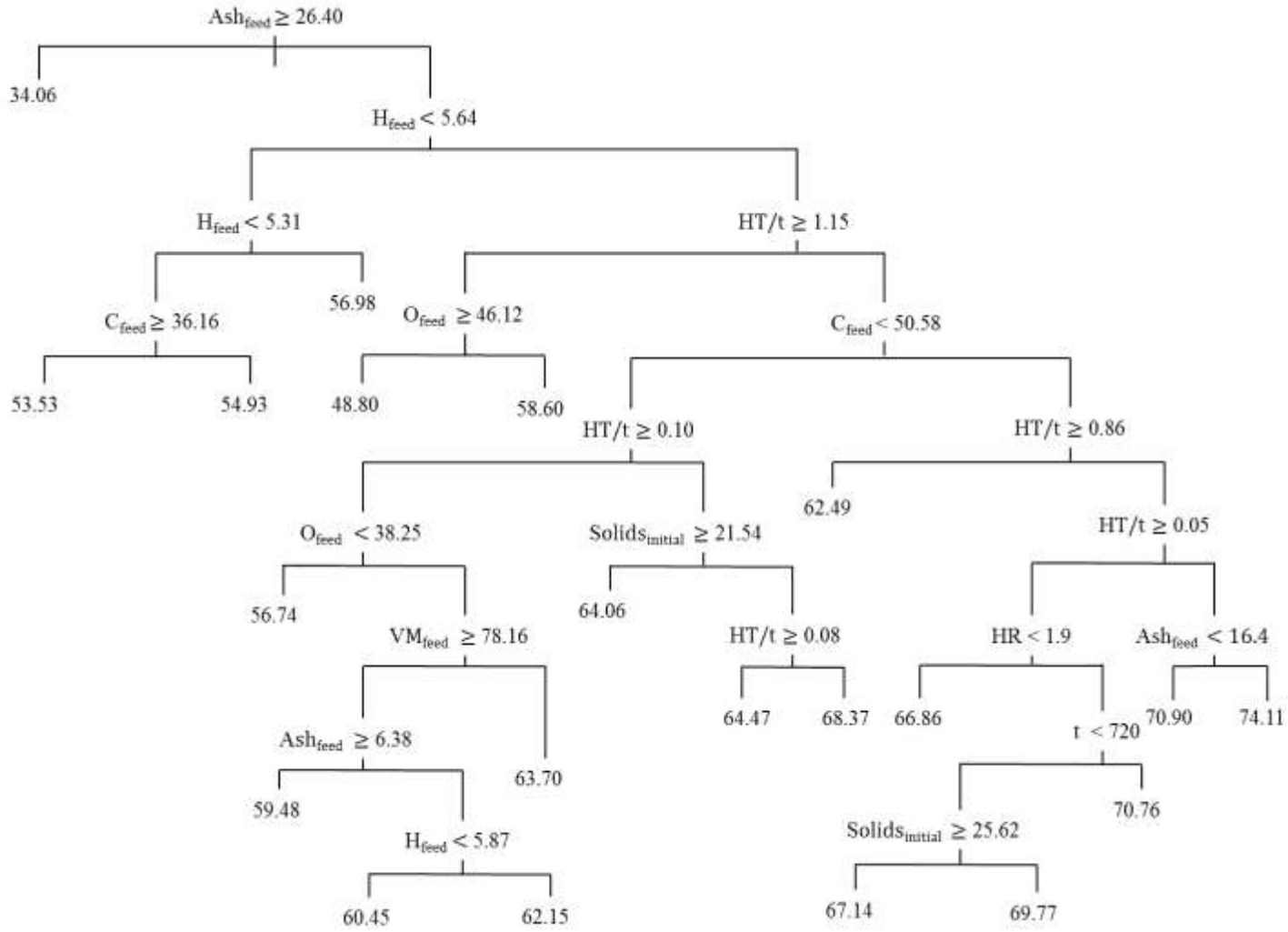

Figure 4.2 Regression tree model associated with hydrochar carbon content (%, dry wt.). Mean values are represented at the end of each branch. Each node corresponds to a binary split. If the node condition is true, the left side of the split should be followed.

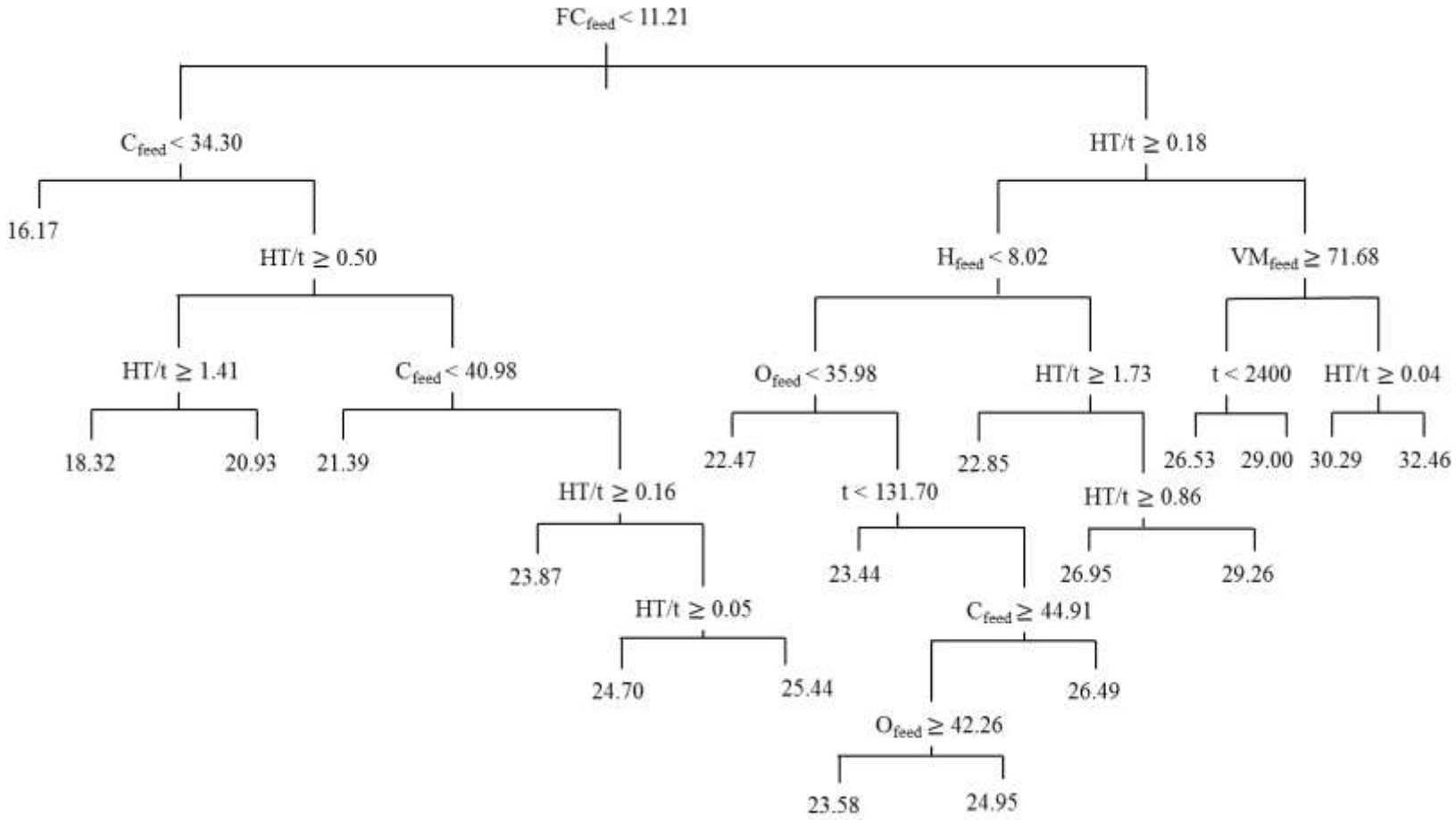

Figure 4.3 Regression tree model associated with hydrochar energy content (kJ/g dry solids). Mean values are represented at the end of each branch. Each node corresponds to a binary split. If the node condition is true, the left side of the split should be followed.

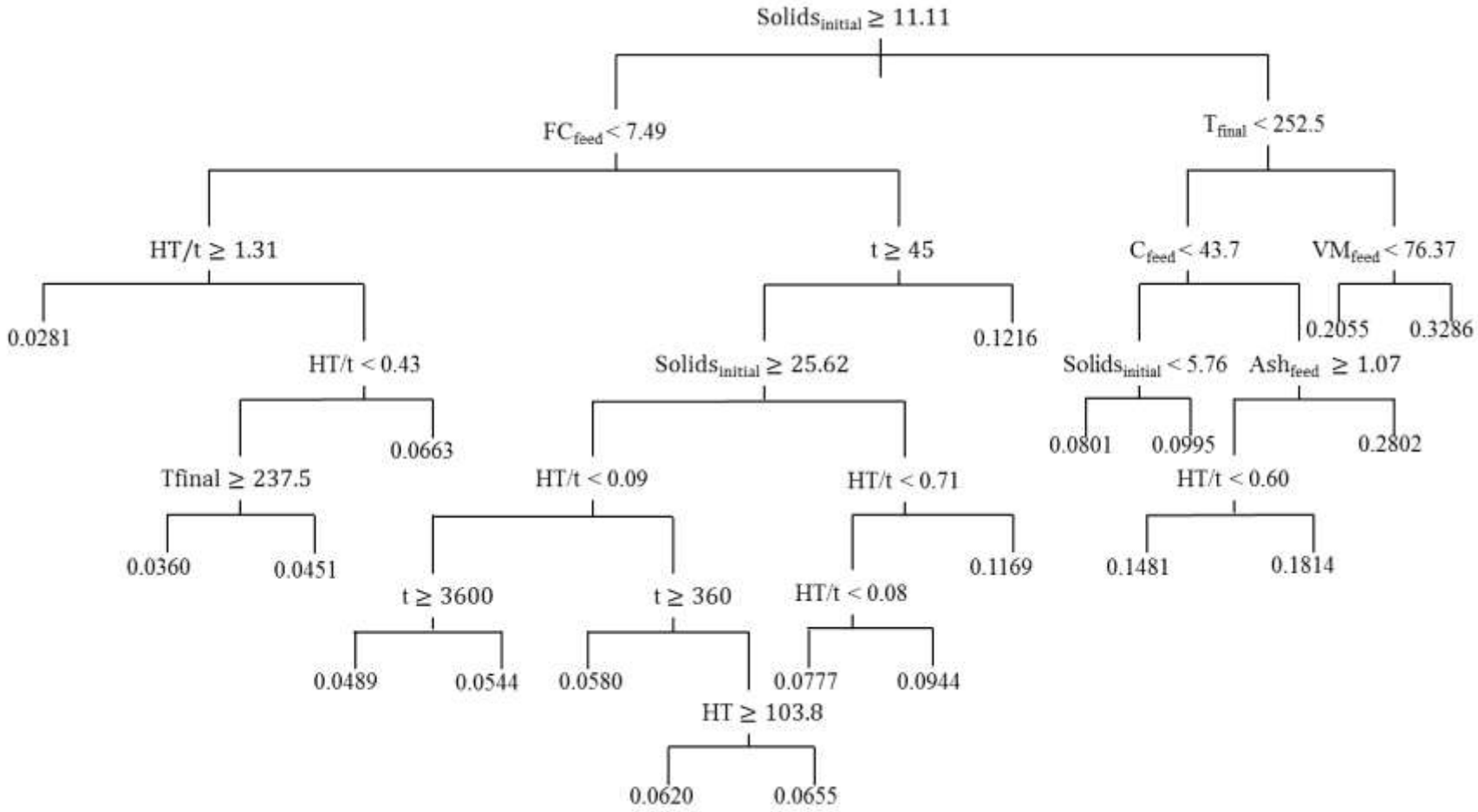

Figure 4.4 Regression tree model associated with normalized carbon content in the liquid (g C/g dry feedstock). Mean values are represented at the end of each branch. Each node corresponds to a binary split. If the node condition is true, the left side of the split should be followed.

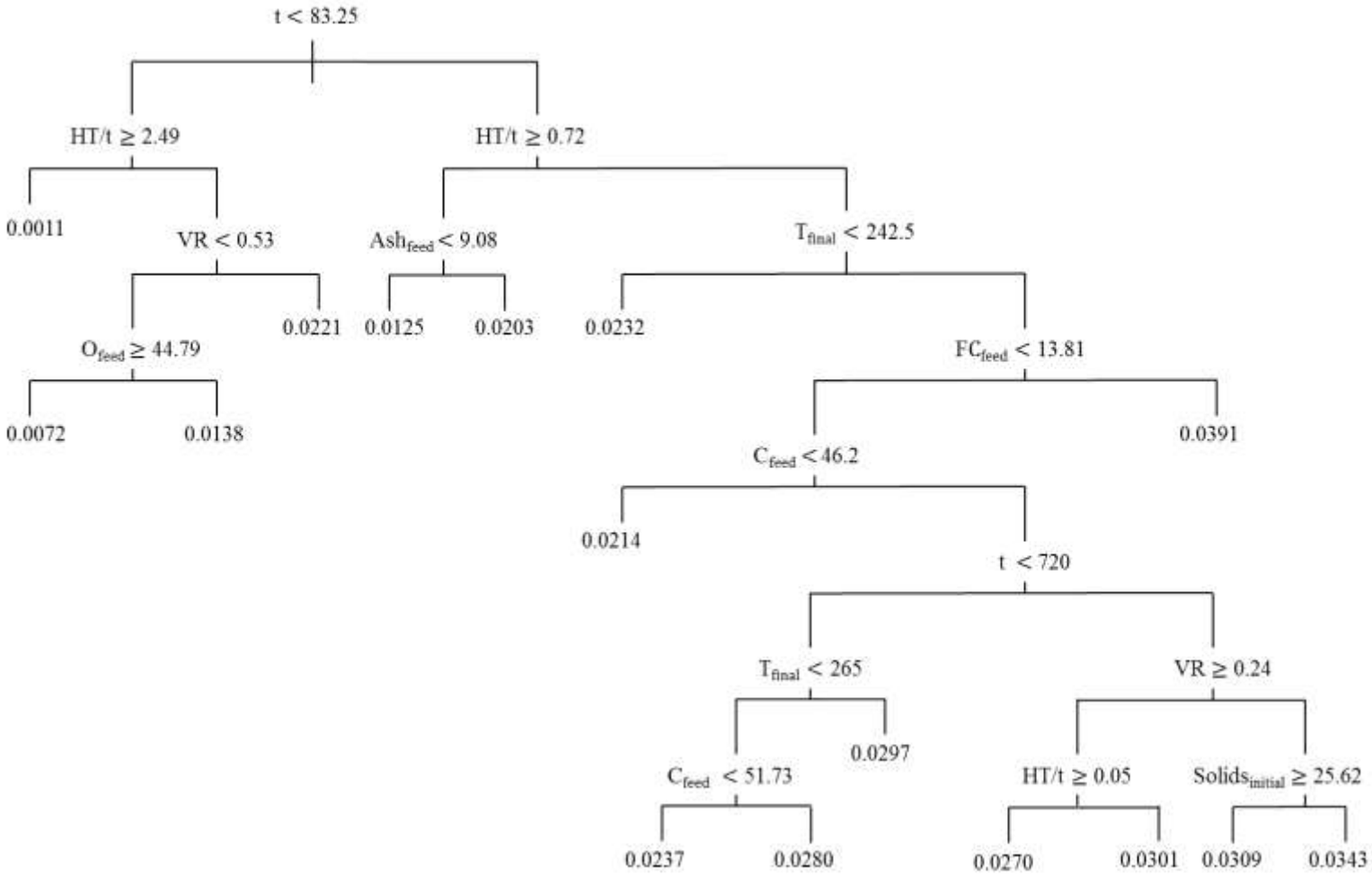

Figure 4.5 Regression tree model associated with normalized carbon content in the gas (g C/g dry feedstock). Mean values are represented at the end of each branch. Each node corresponds to a binary split. If the node condition is true, the left side of the split should be followed.

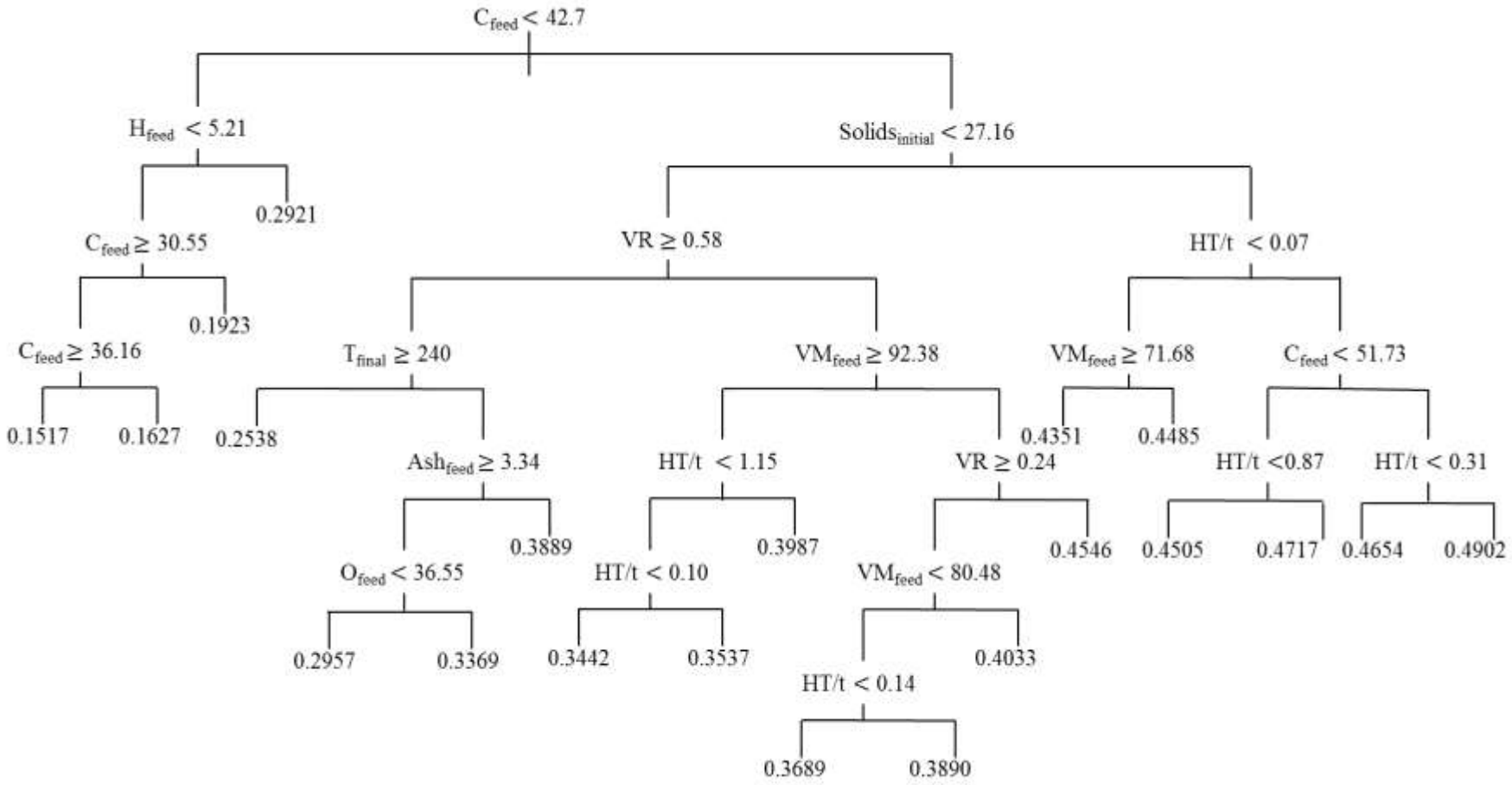

Figure 4.6 Regression tree model associated with normalized solid-phase carbon content (g C/g dry feedstock). Mean values are represented at the end of each branch. Each node corresponds to a binary split. If the node condition is true, the left side of the split should be followed.

4.6 SUPPLEMENTARY INFORMATION

4.6.1 Overview of Collected Studies and Feedstock Properties

Table 4.5 Feedstock properties.

Feedstock	% Ash (db)	% Volatile matter (db)	% Fixed carbon (db)	%C (db)	%H (db)	% O (db)
Agricultural residues[a]	11.52	71.89	14.36	45.26	5.77	36.64
Algae[b]	17.82	68.65	11.31	41.90	6.40	35.11
Animal waste[c]	18.50	60.60	8.10	47.19	6.00	22.60
Animal feed[d]	7.51	77.80	14.69	44.14	5.81	41.39
Cellulose[e]	0.05	93.77	6.23	45.41	6.95	48.18
Coal/lignite[f]	9.80	48.23	42.12	54.52	47.62	18.96
Digestate[g]	26.2	55.9	8.2	40.39	5.65	32.99
Food and food waste[h]	7.44	75.11	16.32	44.19	5.79	40.92
Fructose[i]	0.5	94.23	5.77	39.90	6.64	53.15
Glucose[j]	0.02	94.23	5.77	39.99	6.67	54.79
Lactose[k]	0.20	94.23	5.77	39.97	5.68	54.15
Lignin[l]	1.45	59.75	38.80	45.36	5.07	42.94
Municipal Solid Waste[m]	16.73	74.71	8.33	31.36	4.13	40.35
Pyrolysis Oil[n]	0.01	64.50	35.50	40.60	7.60	51.76
Paper[o]	9.43	81.95	8.70	36.58	5.26	52.69
Plant[p]	8.40	77.23	14.08	43.78	5.57	41.97
Silk[q]	1.19	89.00	9.81	50.8	3.4	34
Sludge[r]	28.34	67.58	3.89	33.01	5.56	33.17
Starch[s]	0.27	90.17	9.56	44.32	6.15	36.92
Straw[t]	5.37	78.97	15.08	45.76	5.70	42.85
Sucrose[u]	0.03	94.23	5.77	42.10	6.41	51.27

Wood[v]	1.67	84.80	13.13	49.13	6.03	44.36
Xylose[w]	0.00	94.23	5.77	39.88	6.86	53.24
Yard wastes[x]	9.1	79.28	14.6	47.68	6.31	44.61

a. Agricultural residues characteristics are the average value from Oliveira et al. (2013).
b. Algae characteristics are the average value from collected papers (Daneshvar et al., 2012; Du et al., 2012a, 2012b; Heilmann et al., 2010, 2011; Lilliestråle, 2007; Toor et al., 2013); References for ash content is from database for biomass and waste (2012); References for volatile matter and fixed carbon is from database for biomass and waste (2012).
c. Animal waste characteristics are the average value from collected papers (Cao et al., 2011; Lilliestråle, 2007; Oliveira et al., 2013; Sun et al., 2011).
d. Animal feed are the average value from collected papers (Berge et al., 2011; Flora et al., 2013; George et al., 2012; Goto et al., 2004; Heilmann et al., 2011; Hwang et al., 2012; Lu et al., 2012; Oliveira et al., 2013; Reza et al., 2014).
e. Cellulose characteristics are the average value from collected papers (Falco et al., 2011; Kang et al., 2012; Karagöz et al., 2005; Kong et al., 2013; Lu et al., 2013, 2014; Möller et al., 2013; Pavlovic et al., 2013; Sevilla and Fuertes, 2009a; Yin et al., 2011).
f. Coal/lignite characteristics are the average value from collected papers (Blazso et al., 1986; Fujino et al., 2002; Parshetti et al., 2013); Reference for ash content is from database for biomass and waste (2012); Reference for volatile matter and fixed carbon is from database for biomass and waste (2012) and Nikkhah et al. (1993).
g. Digestate characteristics are the average value from collected papers (Berge et al., 2011; Becker et al., 2013; Eibisch et al., 2013; Funke et al., 2013a, 2013b; Oliveira et al.,2013).
h. Food characteristics are the average value from collected papers (Akalın et al., 2012; Aydıncak et al., 2012; Cao et al., 2013; Chen et al., 2012; Fiori et al., 2014; Hoekman et al., 2013; Karagoz et al., 2005; Khuwijitjaru et al., 2012; Lamoolphak et al., 2006; Li et al., 2013; Liu and Balasubramanian, 2013; Liu et al., 2013a, 2013b; Oliveira et al.,2013; Pala et al., 2014; Pari, et al., 2014; Pourali et al., 2009, 2010; Reza et al., 2013; Román et al., 2012; Salak et al., 2013; Tian et al., 2012; Watchararuji et al., 2008; Wiedner et al., 2013; Yoshida et al., 1999); References for ash content are from Tchobanoglous (1993), Bhattacharjee et al. (2013) and database for biomass and waste (2012); References for volatile matter and fixed carbon are from Demirbaş (1997), Miranda et al. (2008), whole food catalog (2011) and database for biomass and waste (2012); References for ultimate analysis are from SuÁrez et al. (2000) and Tchobanoglous (1993).
i. Fructose characteristics are the average value from collected paper (Asghari and Yoshida, 2006); Reference for ash content is from certificate of analysis fructose (1993).
j. Glucose characteristics are the average value from collected papers (Aydıncak et al., 2012; Falco et al., 2011, 2013; Knežević, et al., 2009, 2010; Paraknowitsch et al., 2009; Sevilla and Fuertes, 2009).
k. Lactose characteristics is the average value from collected paper (Aydıncak et al., 2012); Reference for volatile matter and fixed carbon is from Kang et al. (2012).

l. Lignin characteristics are the average value from collected papers (Falco et al., 2011; Kang et al., 2012; Karagöz et al., 2005; Nonaka and Funaoka, 2011; Pinkowska et al., 2012).
m. Municipal solid waste characteristics are the average value from collected papers (Berge et al., 2011; Li et al., 2013; Lu et al., 2012; Lu et al.,2011); References for ash content is from Tchobanoglous (1993); References for volatile matter and fixed carbon is from Tchobanoglous (1993).
n. Pyrolysis oil characteristics is the average value from Knežević et al. (2010); Reference for ash content is from database for biomass and waste (2012); Reference for volatile matter and fixed carbon is from database for biomass and waste (2012).
o. Paper characteristics are the average value from collected papers (Berge et al., 2011; Hwang et al., 2012; Li et al., 2014; Lu et al., 2012).
p. Plant characteristics are the average value from collected papers (Aydıncak et al., 2012; Chen et al., 2012; Eibisch et al., 2013; Gao et al., 2013; Jamari and Howse, 2012; Karagöz et al., 2005; Kumar et al., 2011; Liu and Balasubramanian, 2013; Liu et al., 2013a, 2014; Luo et al., 2011; Miyazawa and Funazukuri, 2006; Parshetti et al., 2013b; Ramsurn et al., 2011; Regmi et al., 2012; Reza et al., 2013a; Román et al., 2012; Wang et al., 2014; Xiao et al., 2012, 2013). Reference for ash content is from Parikh et al. (2007); References for volatile matter and fixed carbon are from database for biomass and waste (2012), Ogden et al. (2006) and Parikh et al. (2007); Reference for ultimate analysis is from Parikh et al. (2007).
q. Silk characteristics is the average value from Lamoolphak et al. (2008); Reference for ash content is from Mondal (2007); Reference for volatile matter and fixed carbon is from silk protein product data sheet (2008); Reference for ultimate analysis is from Henry et al. (1814).
r. Sludge characteristics are the average value from collected papers (Alatalo et al., 2013; Areeprasert et al., 2014; Danso-Boateng et al., 2013; Escala et al., 2013; He et al., 2013; Kang et al., 2012; Parshetti et al., 2013a; Zhang et al., 2014; Zhao et al., 2014); Reference for volatile matter and fixed carbon is from database for biomass and waste (2012).
s. Starch characteristics are the average value from collected papers (Nagamori and Funazukuri, 2004; Sevilla and Fuertes, 2009b); Reference for ash content is from Kaur et al. (2007); Reference for volatile matter and fixed carbon is from database for biomass and waste (2012).
t. Straw characteristics are the average value from collected papers (Abdelmoez et al., 2014; Becker et al., 2013; Eibisch et al., 2013; Falco et al., 2011; Funke et al., 2013a, 2013b; Oliveira et al., 2013; Sevilla et al., 2011; Wiedner et al., 2013); References for ash content are from Dinjus (2011) and database for biomass and waste (2012); References for volatile matter and fixed carbon is from database for biomass and waste (2012); References for ultimate analysis are from Dinjus (2011).
u. Sucrose characteristics are the average value from Sevilla and Fuertes (2009b); References for ash content are from production specification of sucrose; References for volatile matter and fixed carbon is from Kang et al. (2012).
v. Wood characteristics are the average value from collected papers (Becker et al., 2013; Brand et al., 2014; Cao et al., 2013; Chang et al., 2013; Eibisch et al., 2013; Erlach et al., 2012; Hoekman et al., 2011, 2013; Hwang et al., 2012; Kang et al., 2012; Karagöz et al., 2005; Kim et al., 2013; Knežević et al., 2010; Karagöz et al., 2006; Kobayashi et al.,

2008; Liu et al., 2010, 2013a, 2013b, 2014; Liu and Li, 2014; Lynam et al., 2011, 2012; Oliveira et al., 2013; Reza et al., 2013b, 2014a; Sevilla et al., 2011; Stemann et al., 2013; Sun et al., 2011; Tremel et al., 2012; Wiedner et al., 2013; Yan et al., 2009); Reference for ash content is from database for biomass and waste (2012); Reference for volatile matter and fixed carbon is from database for biomass and waste (2012).
w. Xylose characteristics are the average value from Kang et al. (2012).
x. Yard waste characteristics are from Li et al. (2014); Reference for ash content is from Tchobanoglous (1993); References for volatile matter and fixed carbon is from Tchobanoglous (1993).

Table 4.6 Overview of all collected carbonization data from the literature.

Category	Reported Parameters	% of Papers Reporting
Feedstock	Feedstocks Carbonized	Agricultural residues: 0.89; Algae: 6.25; Animal feed: 8.04; Animal waste: 3.57; Cellulose: 8.93; Coal/Lignite: 2.68; Digestate: 5.36; Food: 22.32; Fructose: 0.89; Glucose: 6.25; Lactose: 0.89; Lignin: 4.46; Municipal Solid Waste: 3.57; Pyrolysis oil: 0.89; Paper: 3.57; Plant: 16.96; Silk: 0.89; Sludge: 8.03; Starch: 1.78; Straw: 8.04; Sucrose: 0.89; Wood: 27.68; Xylose: 0.89; Yard waste: 0.89
Carbonization Product Properties	Carbon content of recovered solids (%, db)	53.57
	Normalized carbon in the solids (g C/g initial dry feedstock)	33.04
	Solids Yield (%, db)	70.54
	Solids Energy Content (MJ/kg, db)	42.86
	Liquid carbon content(g C/g initial dry feedstock)	17.86
	Gas carbon content (g C/g initial dry feedstock)	9.82
Process Parameters	Time (min)	100
	Temperature (^{o}C)	100
	Initial feedstock concentration (% solids)	95.54
	Reactor heating rate (^{o}C/min)	54.46
	Heating time (min)	54.46
	HT/t	54.46
	Reactor volume (mL)	89.29
	Volume ratio (VR)	66.96
Feedstock Properties	Ash (%, db)	50.89
	Volatile matter (%, db)	24.11
	Fixed carbon (%, db)	24.11
	Carbon (%, db)	61.61

	Hydrogen (%, db)	58.93
	Oxygen (%, db)	58.93

Table 4.7 Carbonization studies used in modelling effort.

No.	Carbonization Studies	Ref.
1	Adding value to onion (Allium cepa L.) waste by subcritical water treatment	Salak et al., 2013
2	Application of subcritical water for conversion of macroalgae to value-added materials	Daneshvar et al., 2012
3	Carbohydrate content and composition of product from subcritical water treatment of coconut meal	Khuwijitjaru et al., 2012
4	Chemical modification of biomass residues during hydrothermal carbonization – What makes the difference, temperature or feedstock?	Wiedner et al., 2013
5	Experimental comparison of hydrothermal and vapothermal carbonization	Funke et al., 2013
6	Hydrothermal carbonization of agricultural residues	Oliveira et al., 2013
7	Hydrothermal carbonization (HTC) of lignocellulosic biomass	Hoekman et al., 2011
8	Hydrothermal carbonization (HTC) of selected woody and herbaceous biomass feedstocks	Hoekman et al., 2013
9	HTC of food waste and associated packaging materials for energy source generation	Li et al., 2013
10	Hydrothermal carbonization of municipal waste streams	Berge et al., 2011
11	Hydrothermally carbonized plant materials: Patterns of volatile organic compounds detected by gas chromatography	Becker et al., 2013
12	Hydrothermal carbonization as an energy-efficient alternative to established drying technologies for sewage sludge: A feasibility study on a laboratory scale	Escala et al., 2013
13	Hydrothermal carbonization: Process water characterization and effects of water recirculation	Stemann et al., 2013

14	Hydrothermal carbonization (HTC): Near infrared spectroscopy and partial least-squares regression for determination of selective components in HTC solid and liquid products derived from maize silage	Reza et al., 2014
15	Hydrothermal conversion of cellulose to 5-hydroxymethyl furfural	Yin et al., 2011
16	Hydrothermal liquefaction of cellulose in subcritical water: The role of crystallinity on the cellulose reactivity	Möller et al., 2013
17	Influence of process water quality on hydrothermal carbonization of cellulose	Lu et al., 2014
18	Influence of reaction time and temperature on product formation associated with the hydrothermal carbonization of cellulose	Lu et al., 2013
19	Sub-critical water treatment of rice bran to produce valuable materials	Pourali et al., 2009
20	Thermal conversion of municipal solid waste via hydrothermal carbonization: Comparison of carbonization products to products from current waste management techniques	Lu et al., 2012
21	Using liquid waste streams as the moisture source during the hydrothermal carbonization of municipal solid wastes	Li et al., 2014

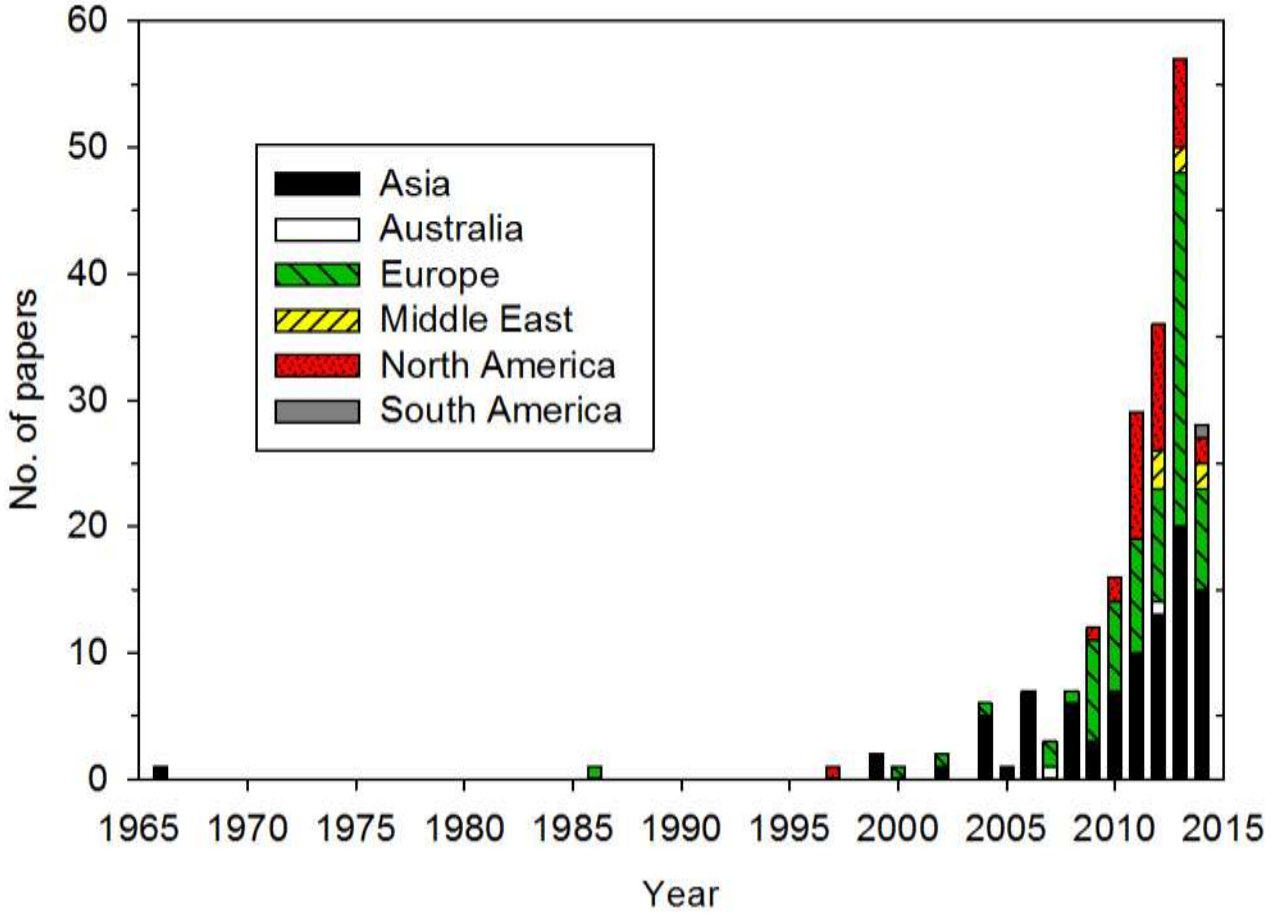

Figure 4.7 Overview of collected studies (catalyst and pressure papers not included).

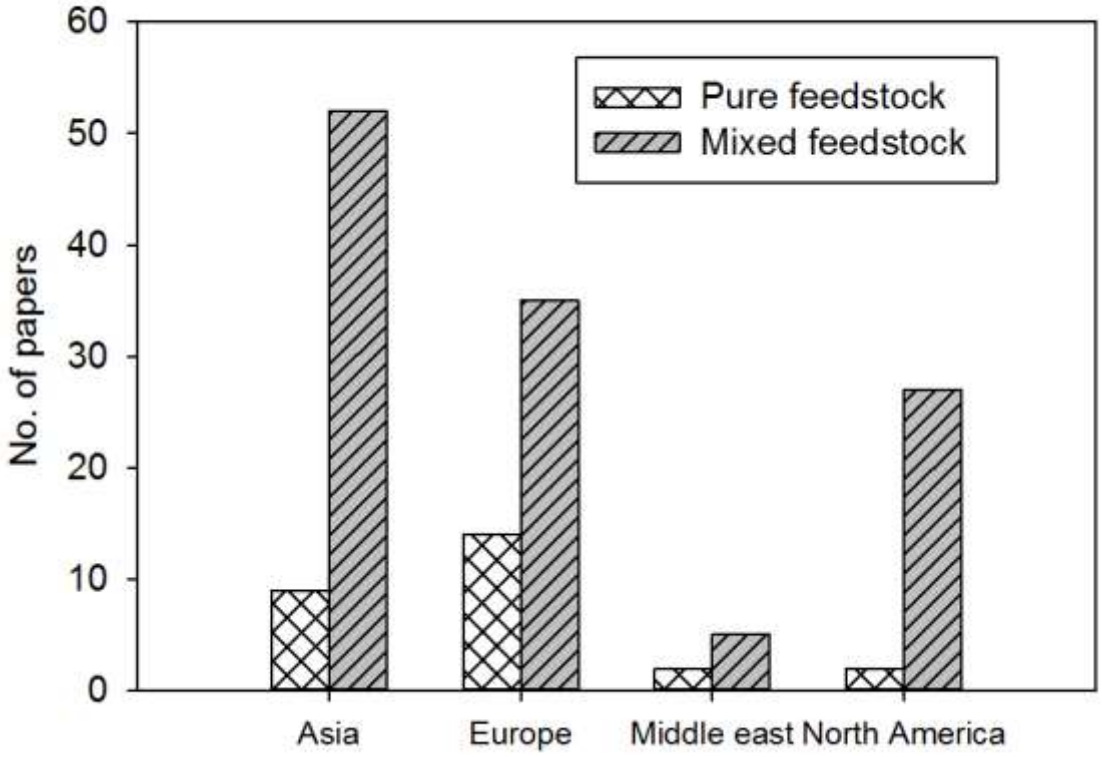

Figure 4.8 The number of papers that report carbonization on mixed and pure feedstocks.

4.6.2 Variability of Independent Parameters Related to Variability of Each Dependent Parameter

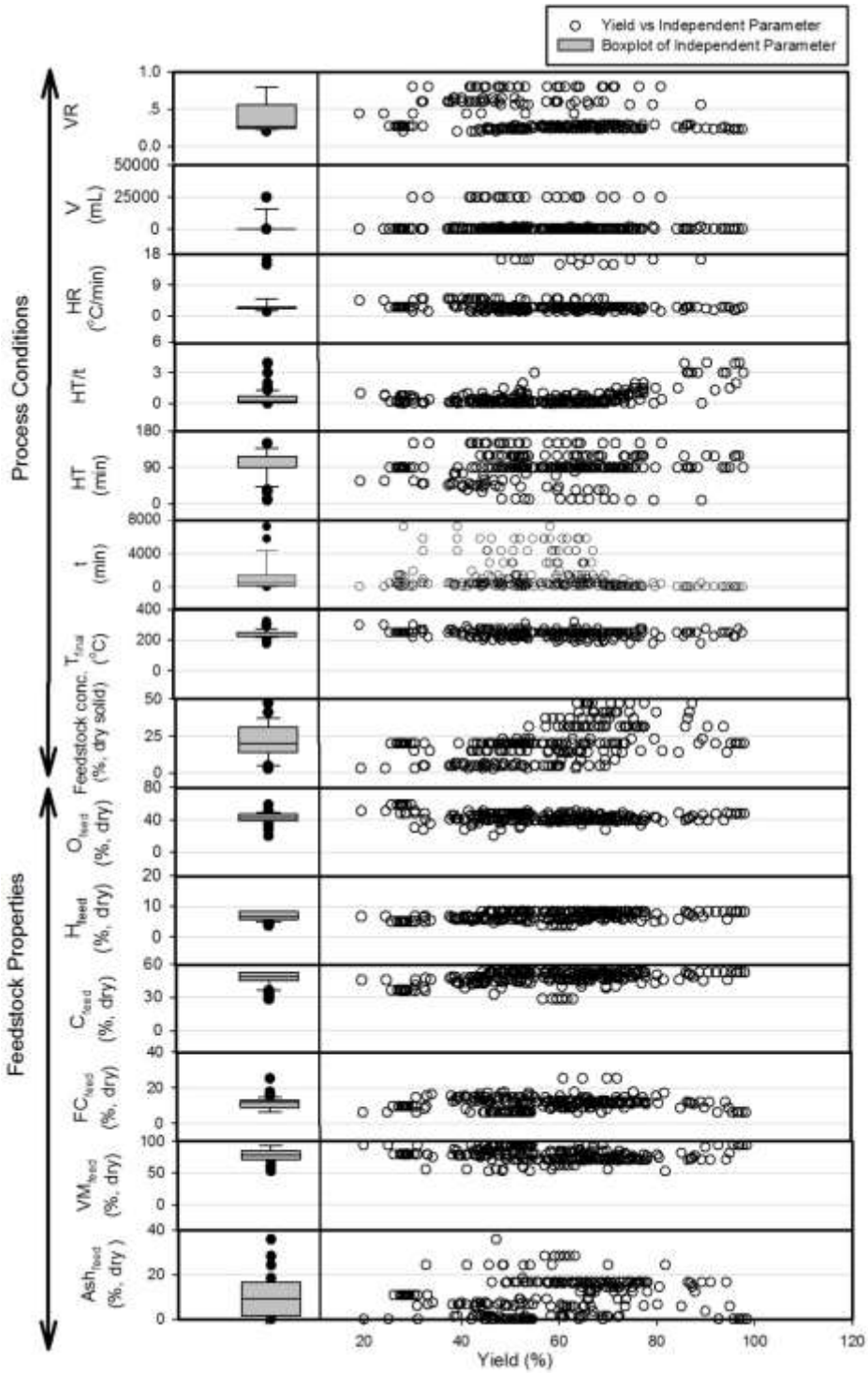

Figure 4.9 Variability of independent variables related to variability of solid yield.

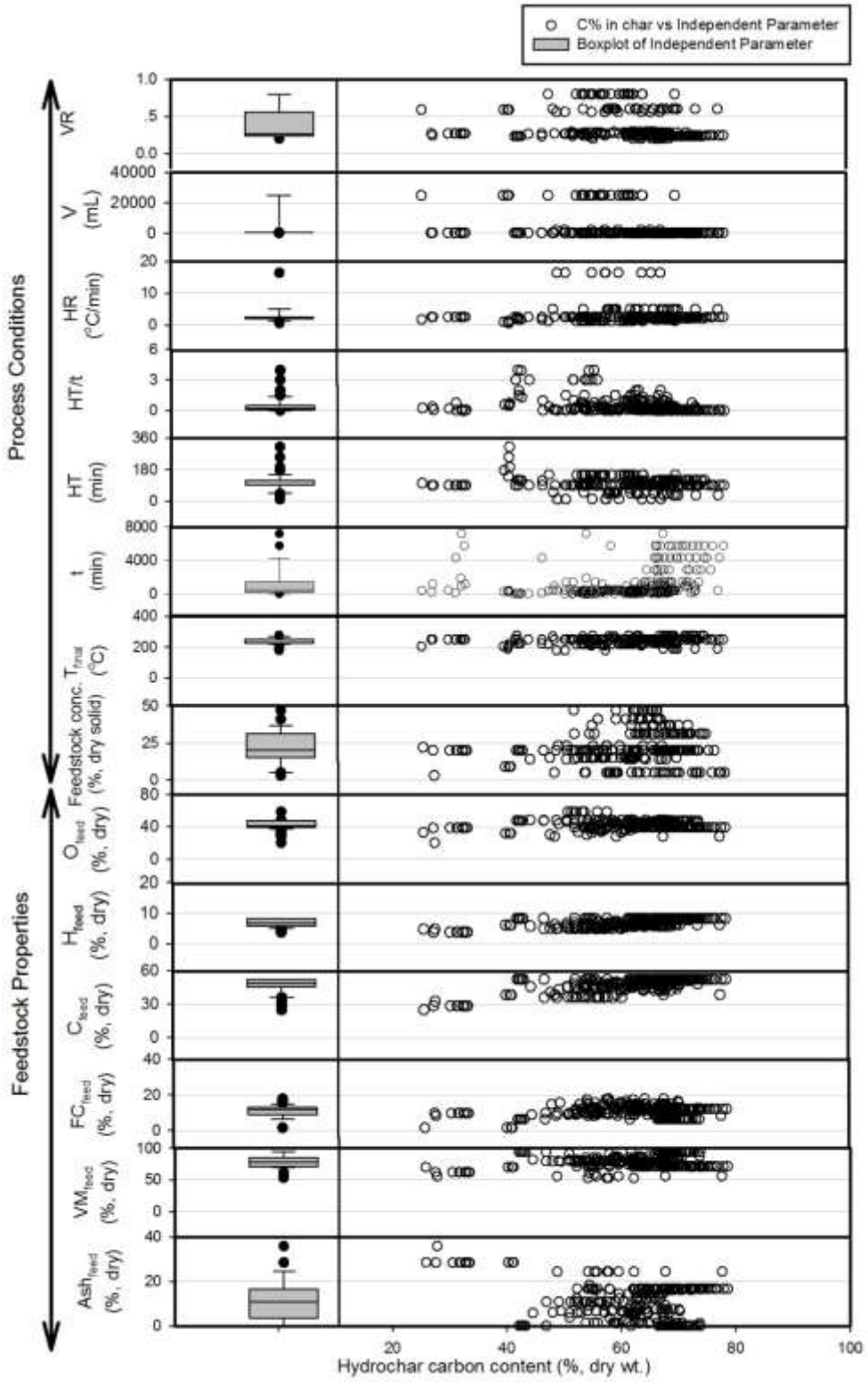

Figure 4.10 Variability of independent variables related to variability of hydrochar carbon content.

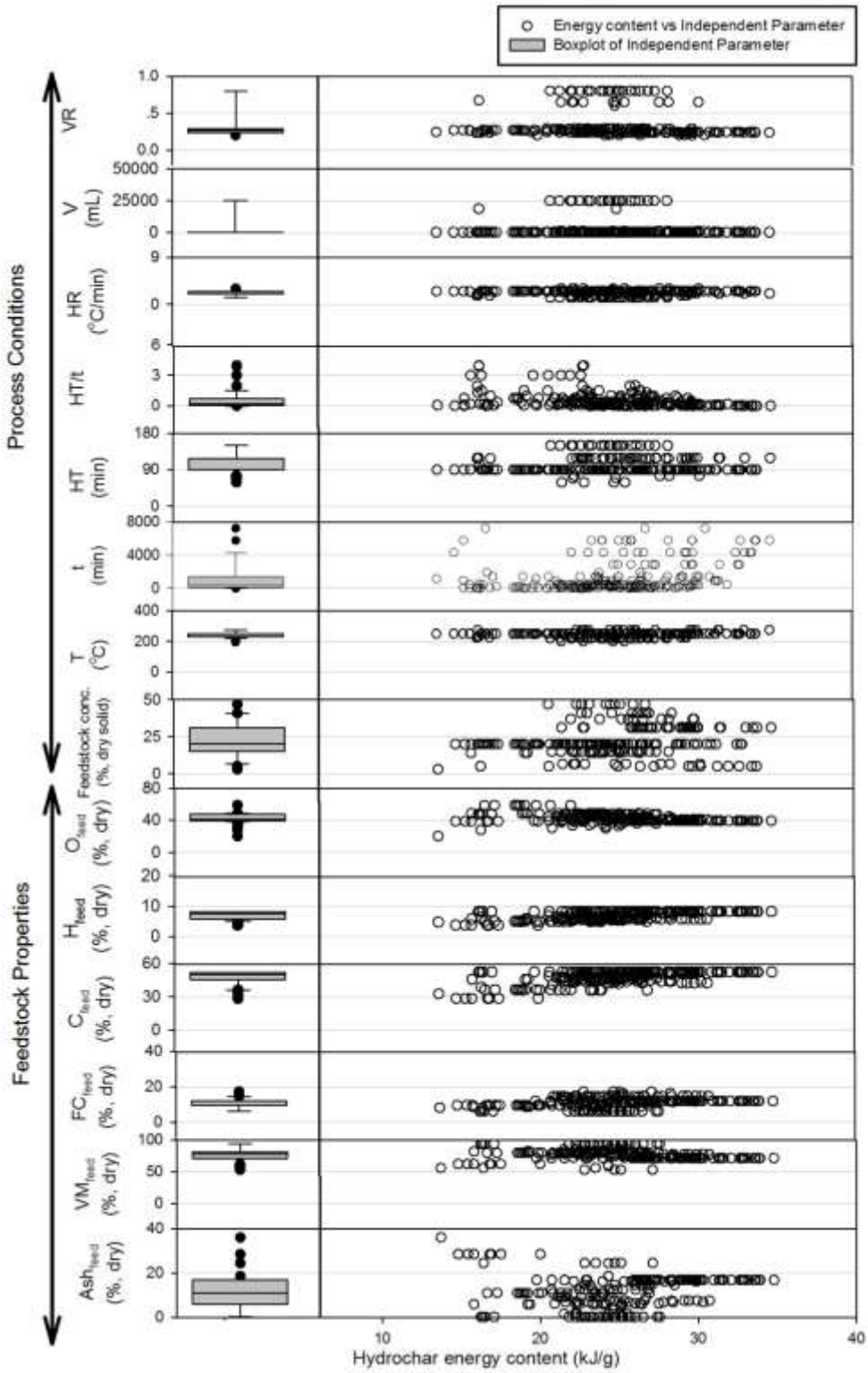

Figure 4.11 Variability of independent variables related to variability of hydrochar energy content.

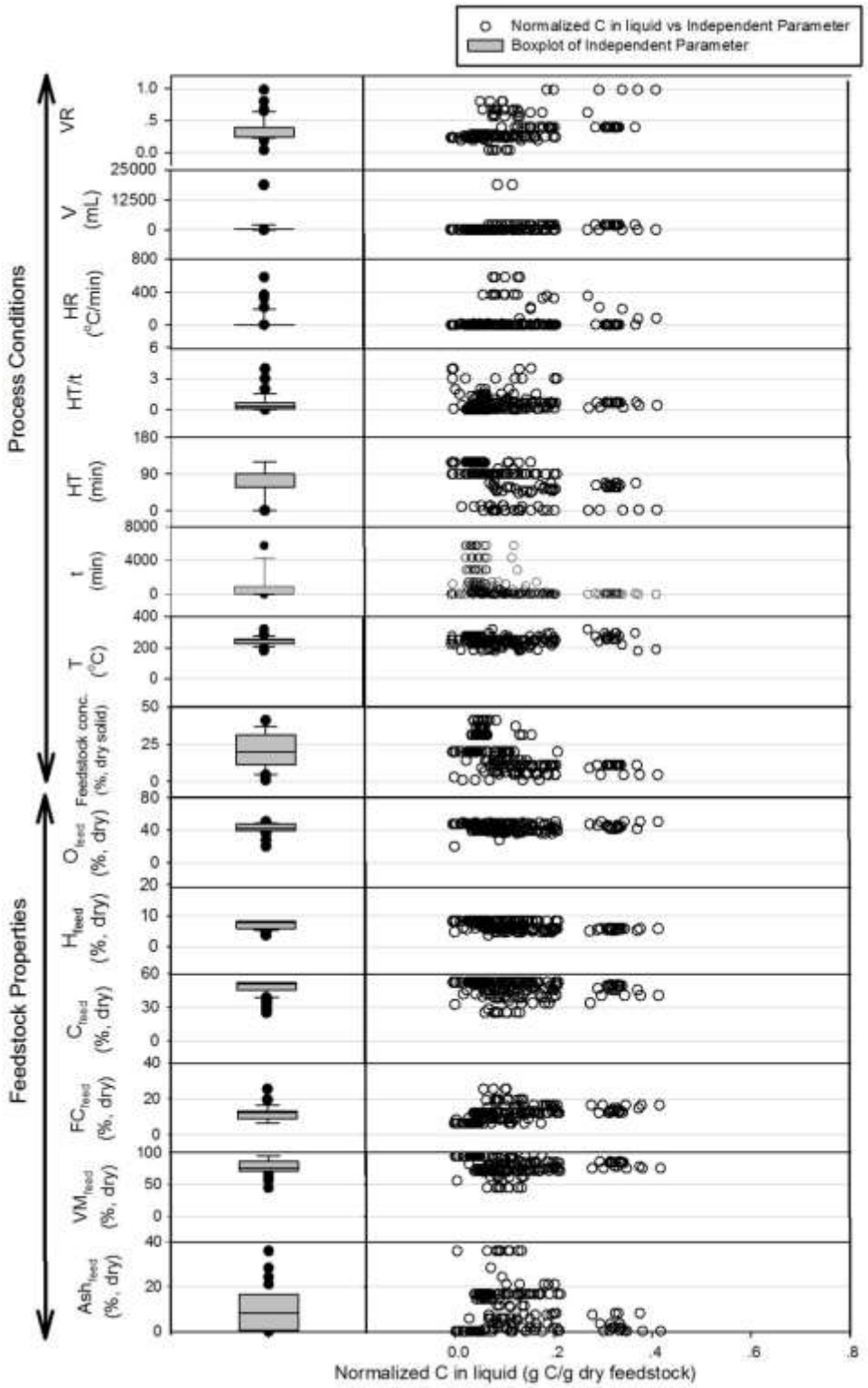

Figure 4.12 Variability of independent variables related to variability of normalized carbon in the liquid.

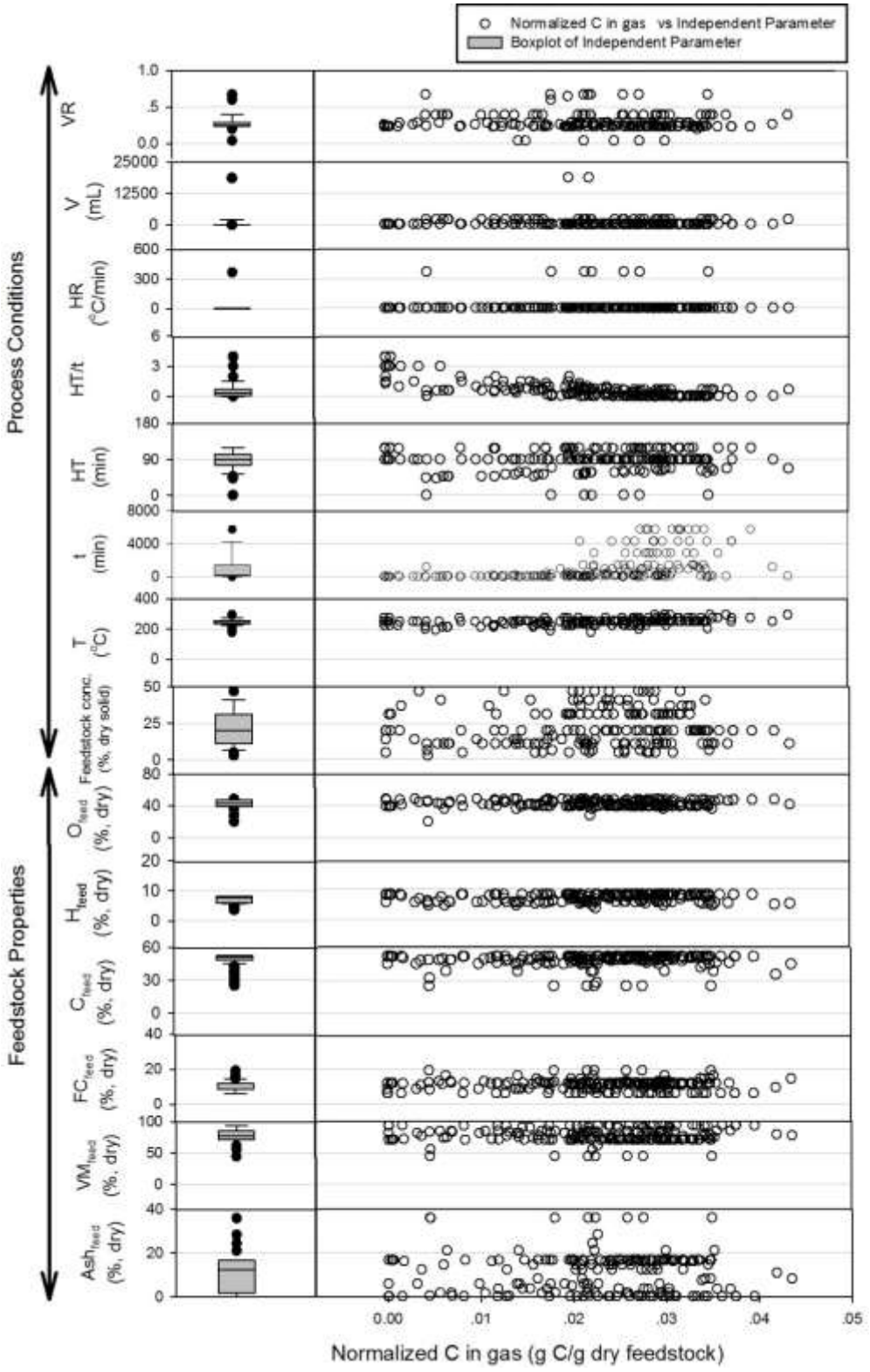

Figure 4.13 Variability of independent variables related to variability of normalized carbon in the gas.

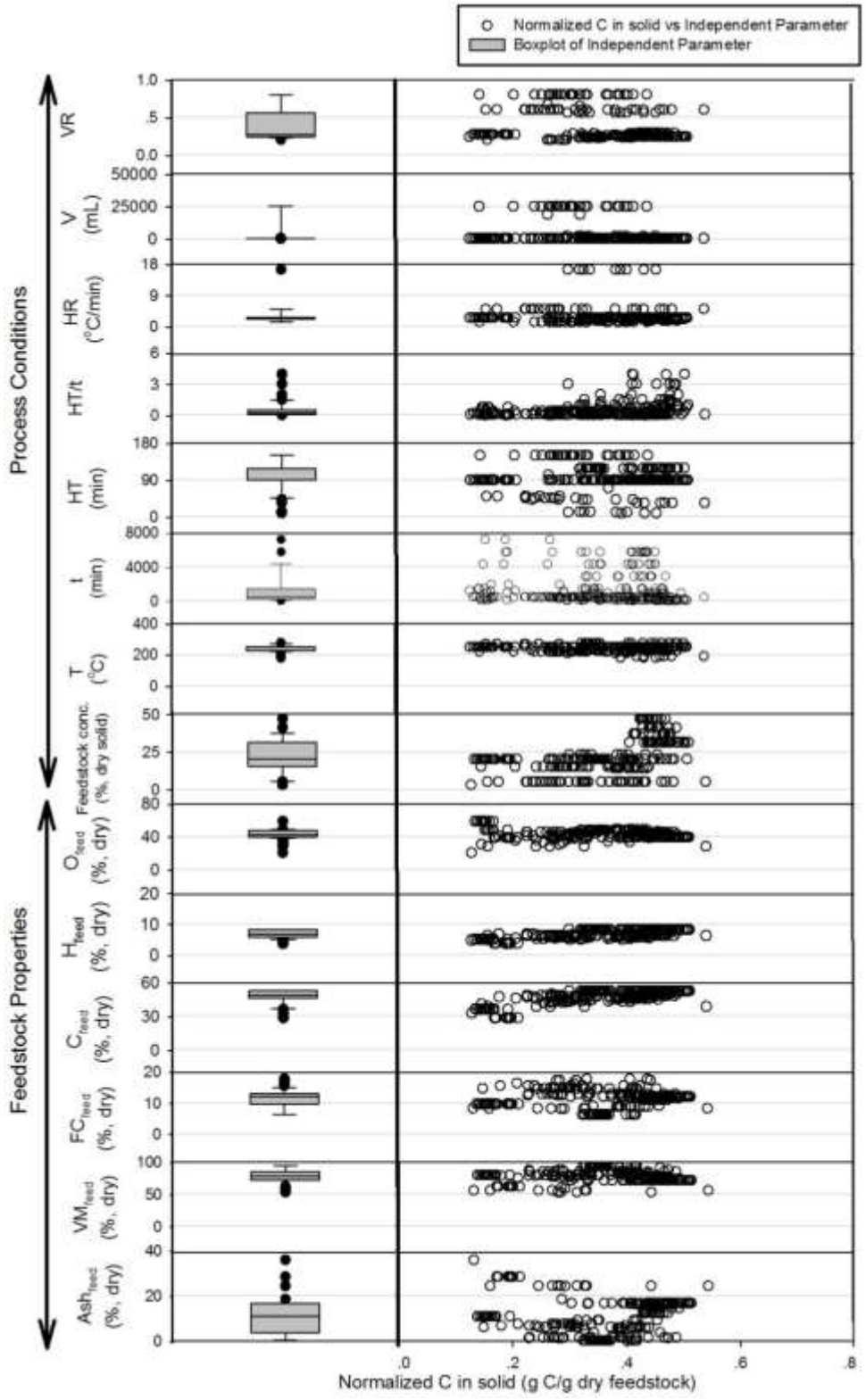

Figure 4.14 Variability of independent parameters related to variability of normalized carbon in the solid.

4.6.3 Comparison between Prediction and Observation

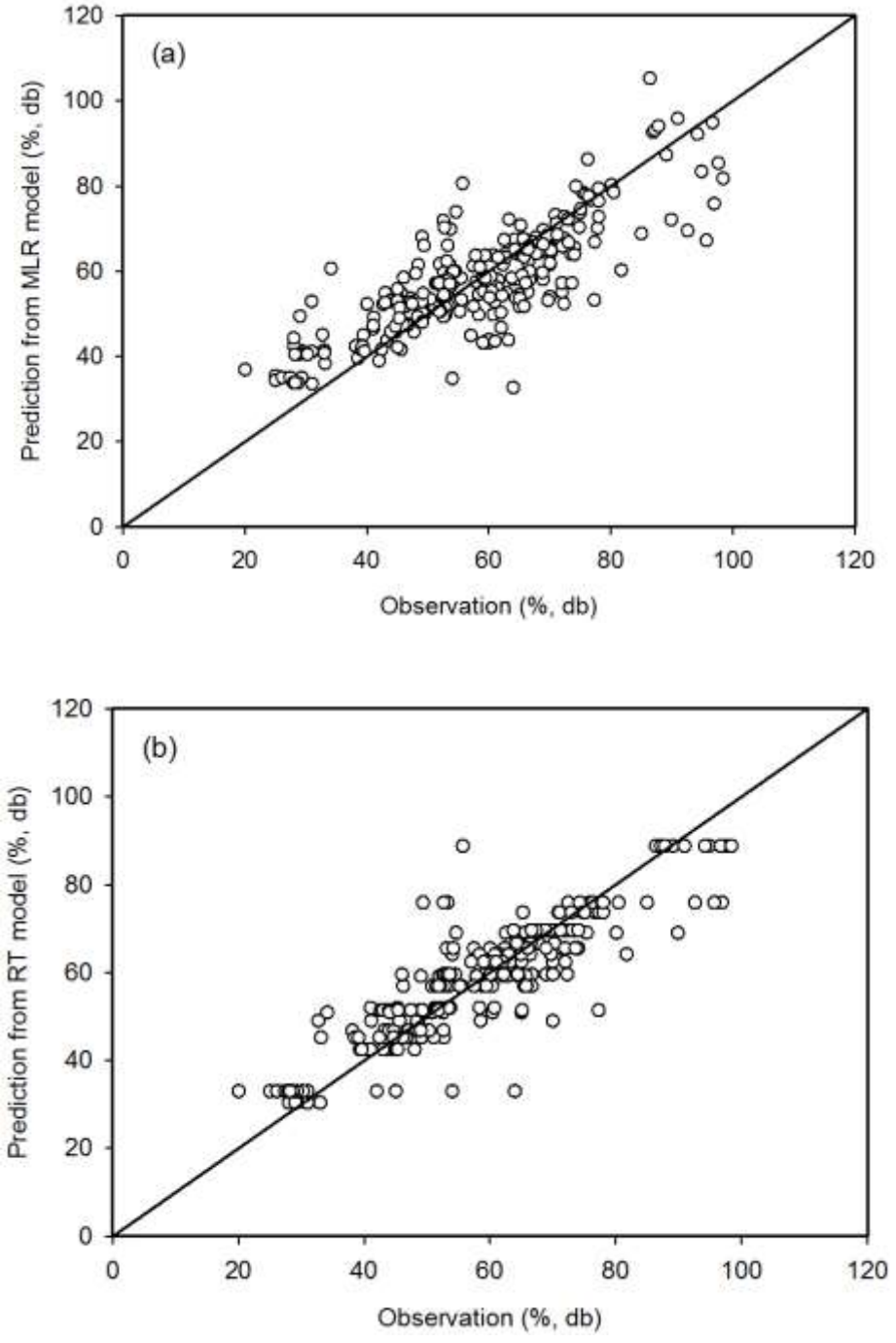

Figure 4.15 Comparison between observed solid yield and predicted solid yield from (a) multiple linear regression (MLR) model and (b) regression tree (RT) model.

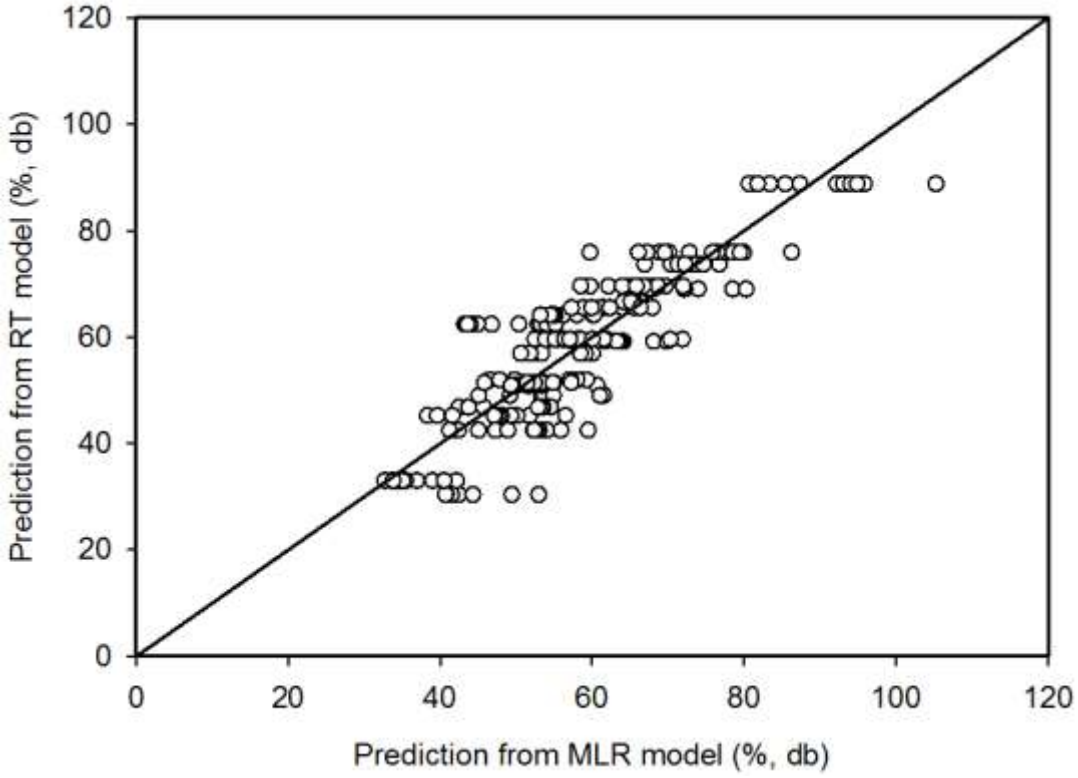

Figure 4.16 Comparison between predicted solid yield from regression tree (RT) model and multiple linear regression (MLR) model.

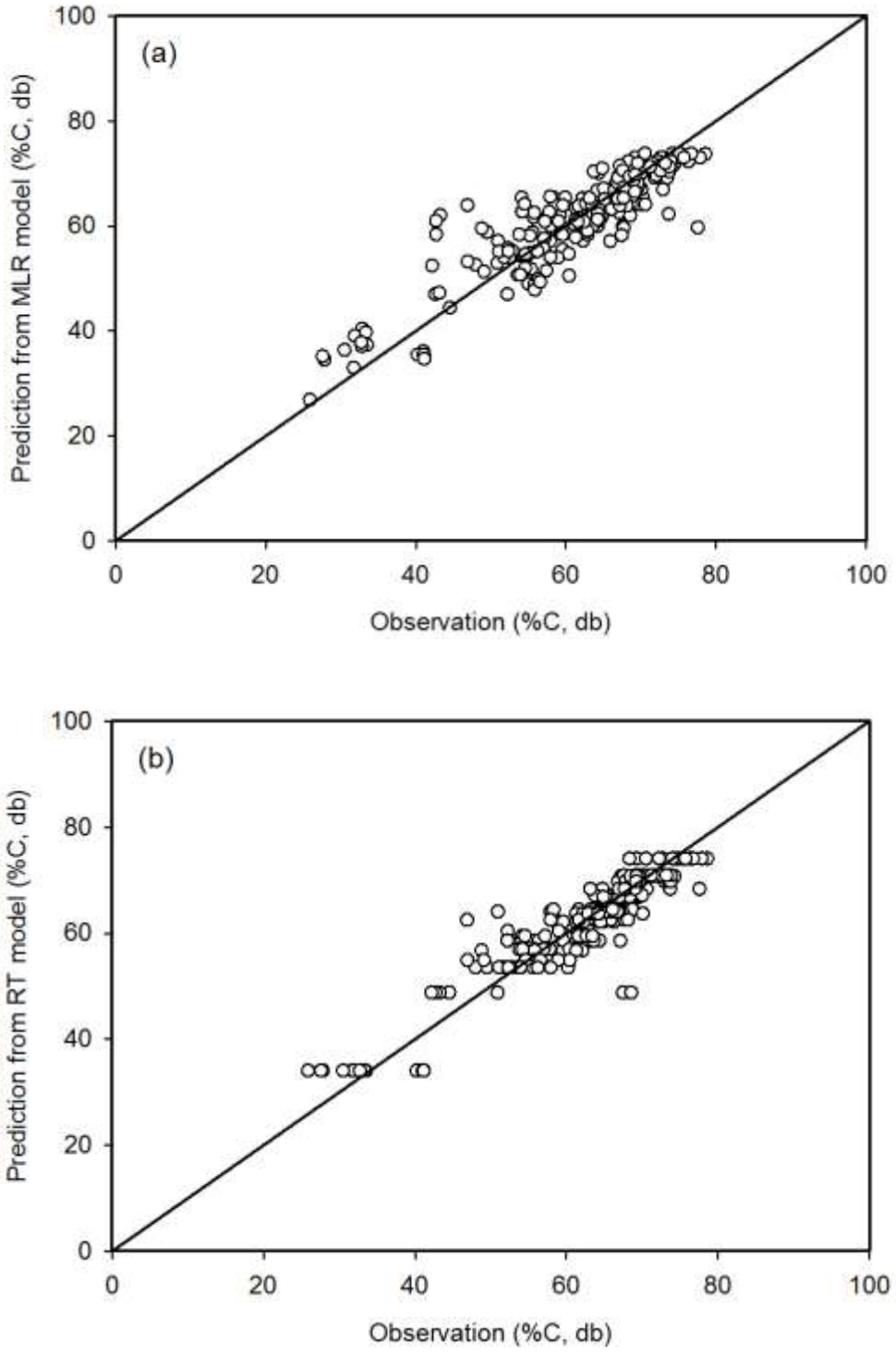

Figure 4.17 Comparison between observed hydrochar carbon content and predicted hydrochar carbon content from (a) multiple linear regression (MLR) model and (b) regression tree (RT) model.

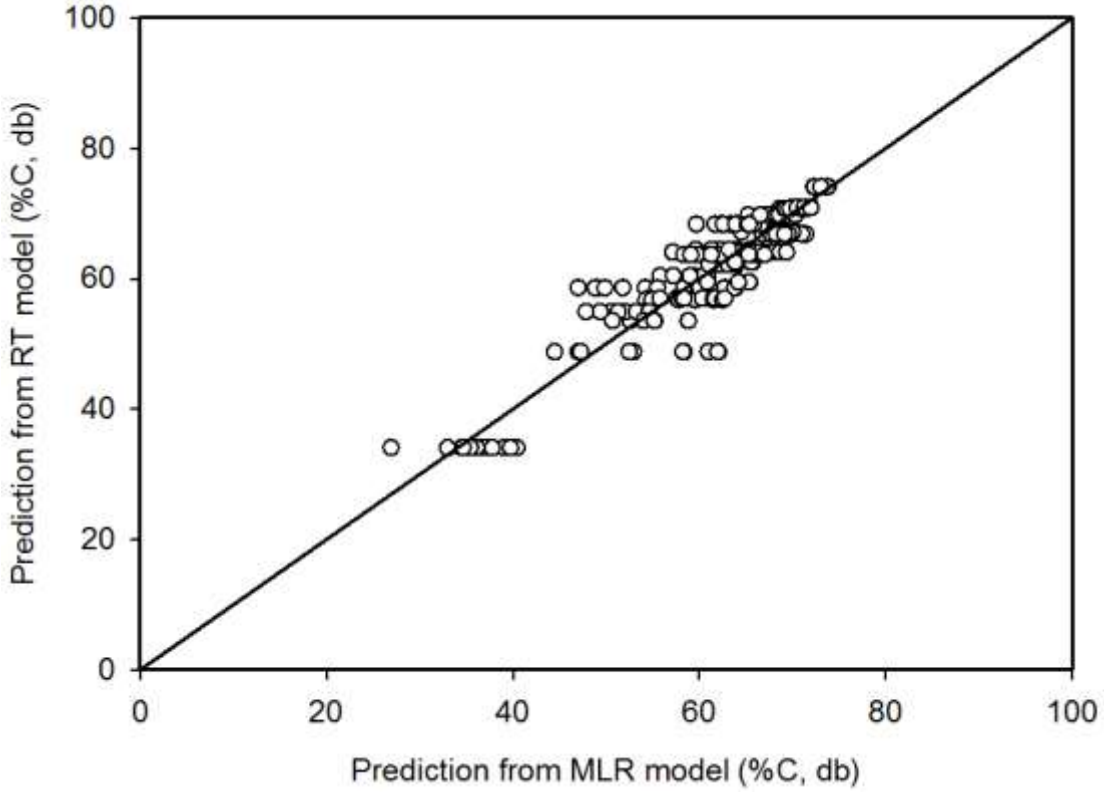

Figure 4.18 Comparison between predicted hydrochar carbon content from regression tree (RT) model and multiple linear regression (MLR) model.

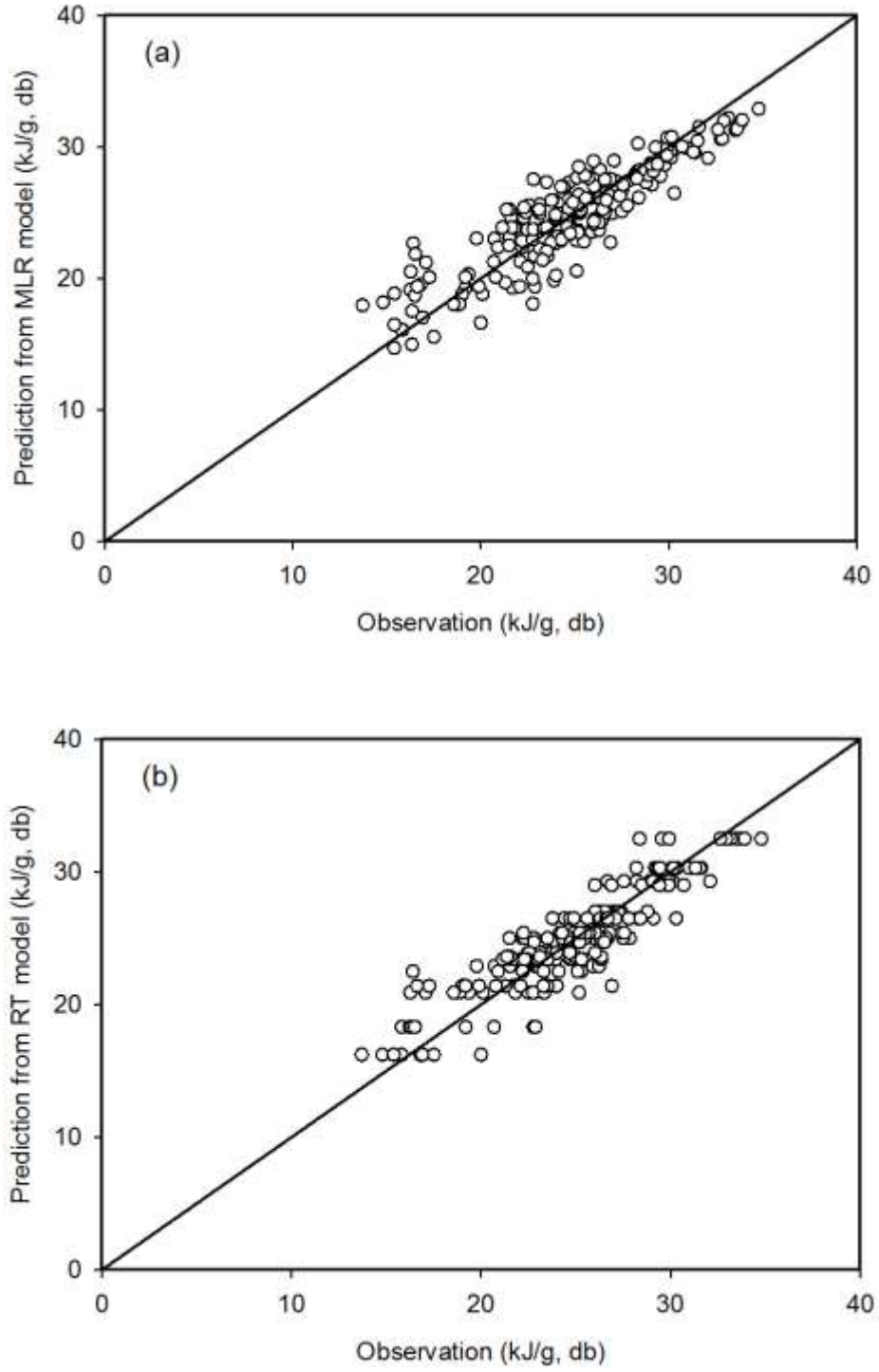

Figure 4.19 Comparison between observed hydrochar energy content and predicted hydrochar energy content from (a) multiple linear regression (MLR) model and (b) regression tree (RT) model.

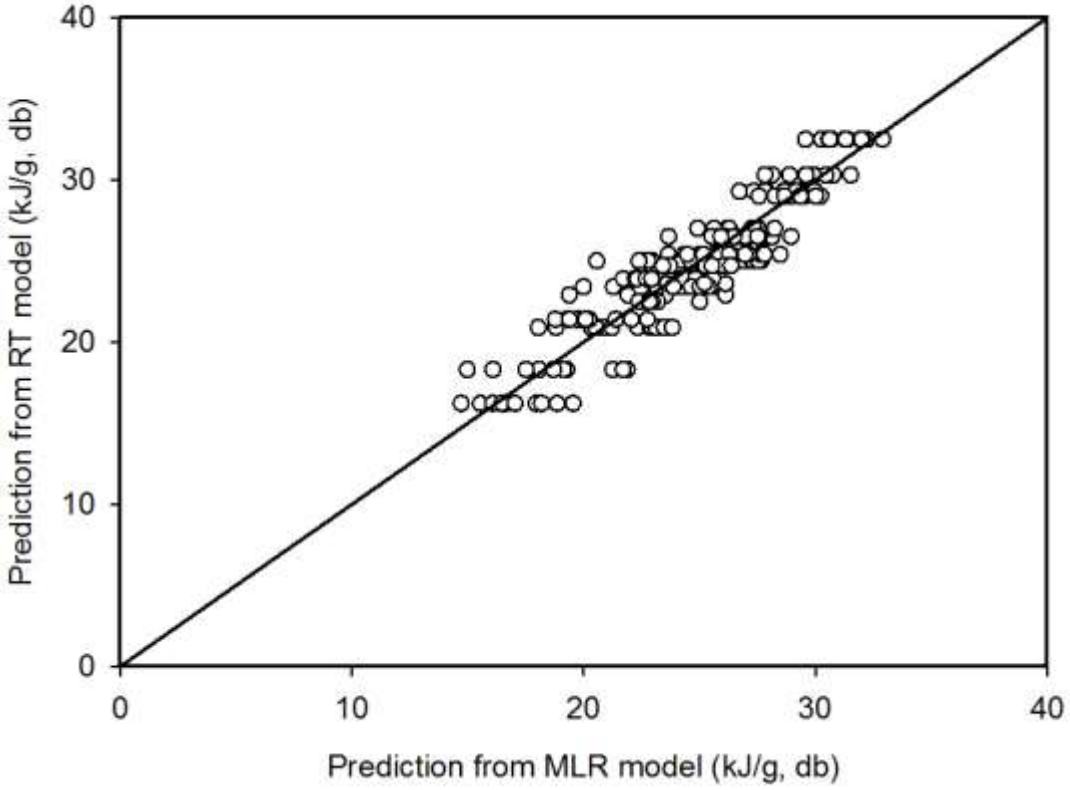

Figure 4.20 Comparison between predicted hydrochar energy content from regression tree (RT) model and multiple linear regression (MLR) model.

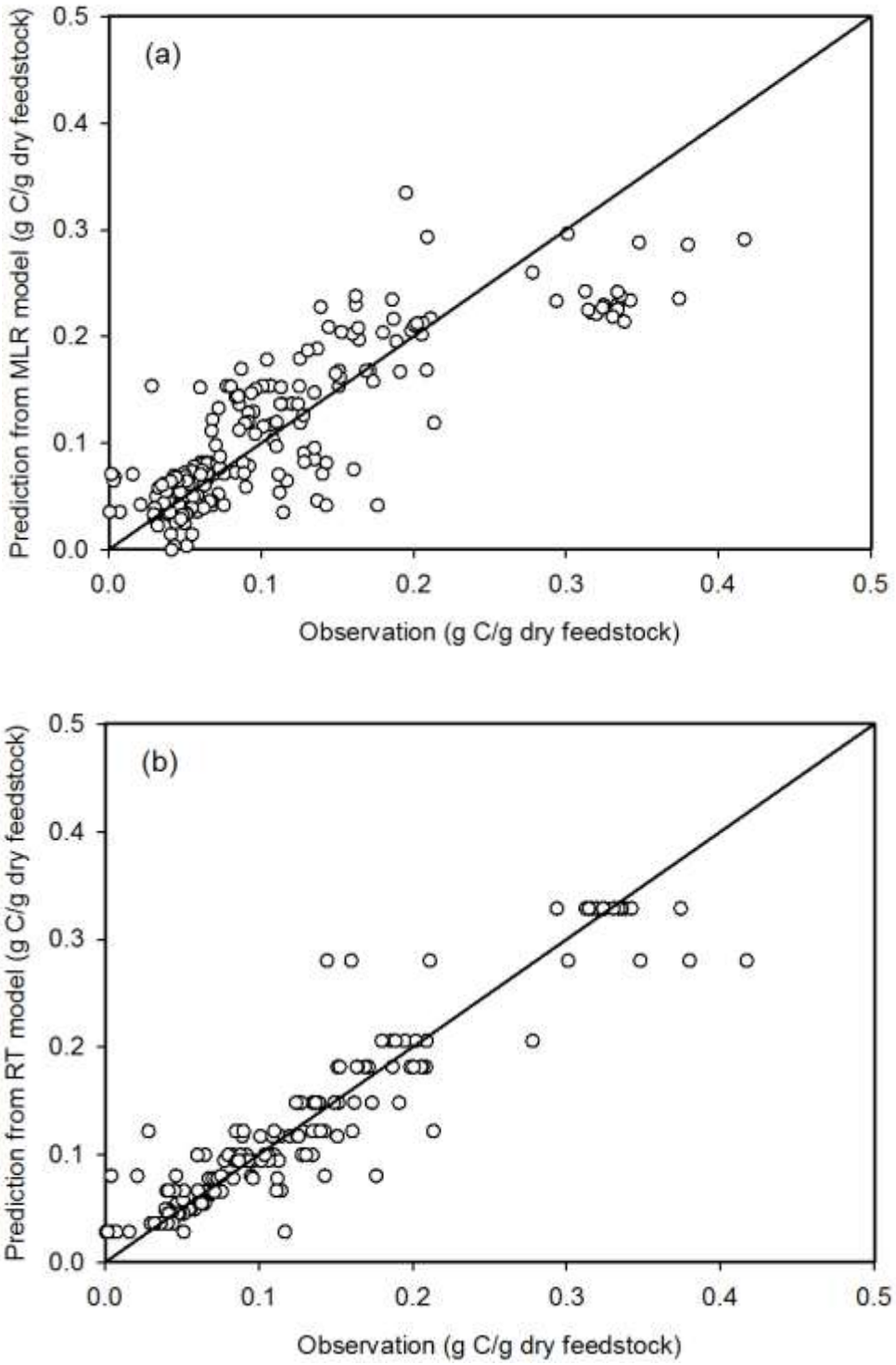

Figure 4.21 Comparison between observed normalized carbon in the liquid and predicted normalized carbon in the liquid from (a) multiple linear regression (MLR) model and (b) regression tree (RT) model.

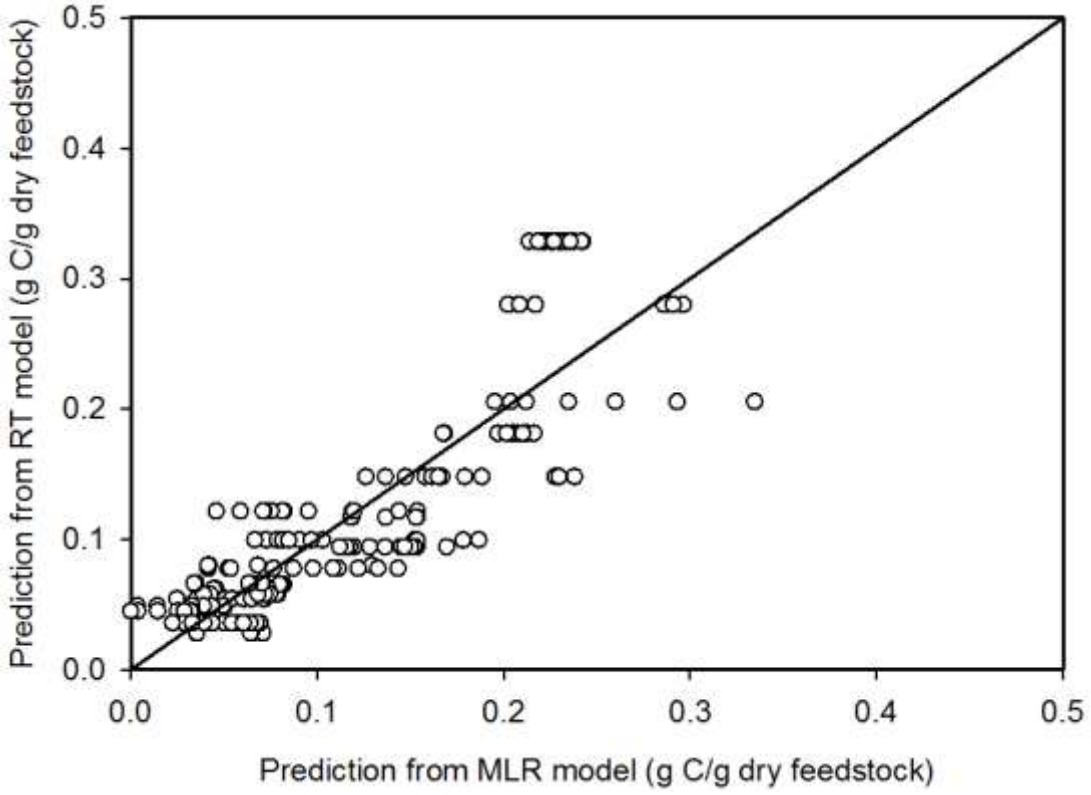

Figure 4.22 Comparison between predicted normalized carbon in the liquid from regression tree (RT) model and multiple linear regression (MLR) model.

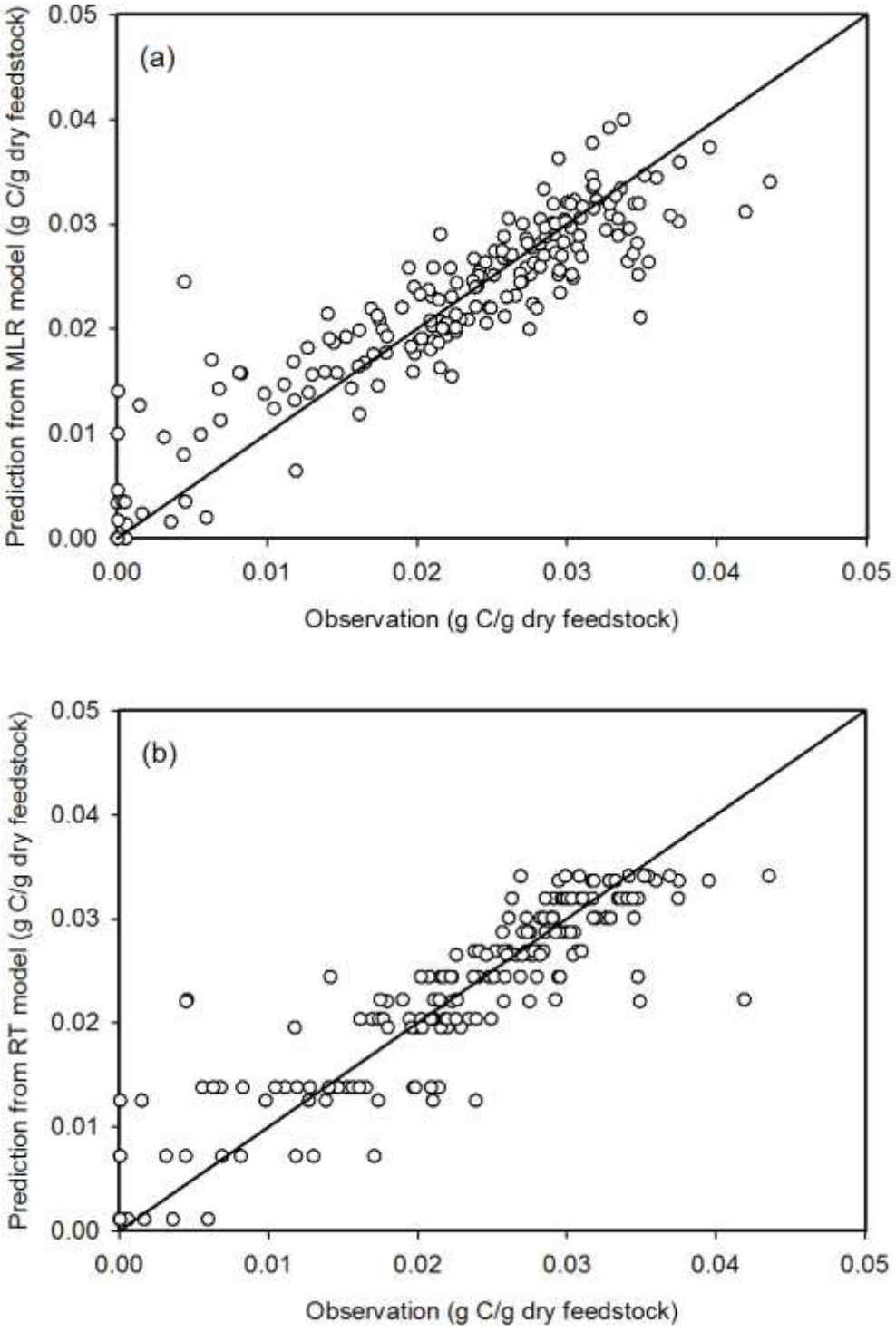

Figure 4.23 Comparison between observed normalized carbon in the gas and predicted normalized carbon in the gas from (a) multiple linear regression (MLR) model and (b) regression tree (RT) model.

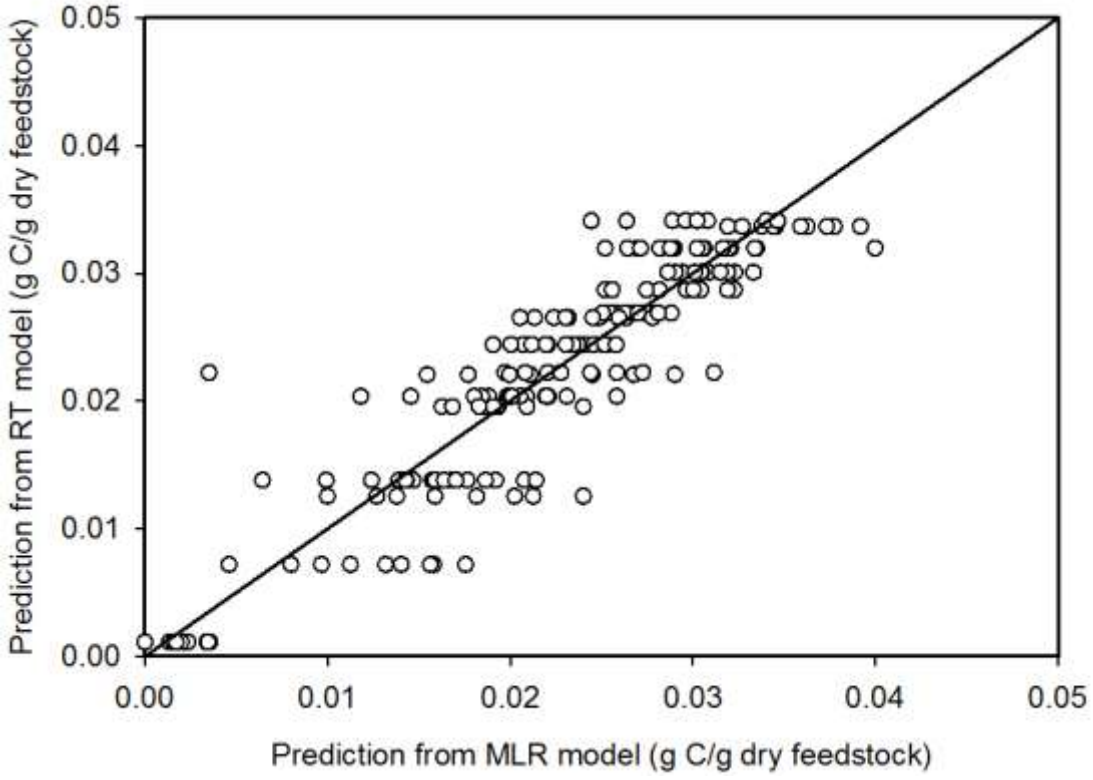

Figure 4.24 Comparison between predicted normalized carbon in the gas from regression tree (RT) model and multiple linear regression (MLR) model.

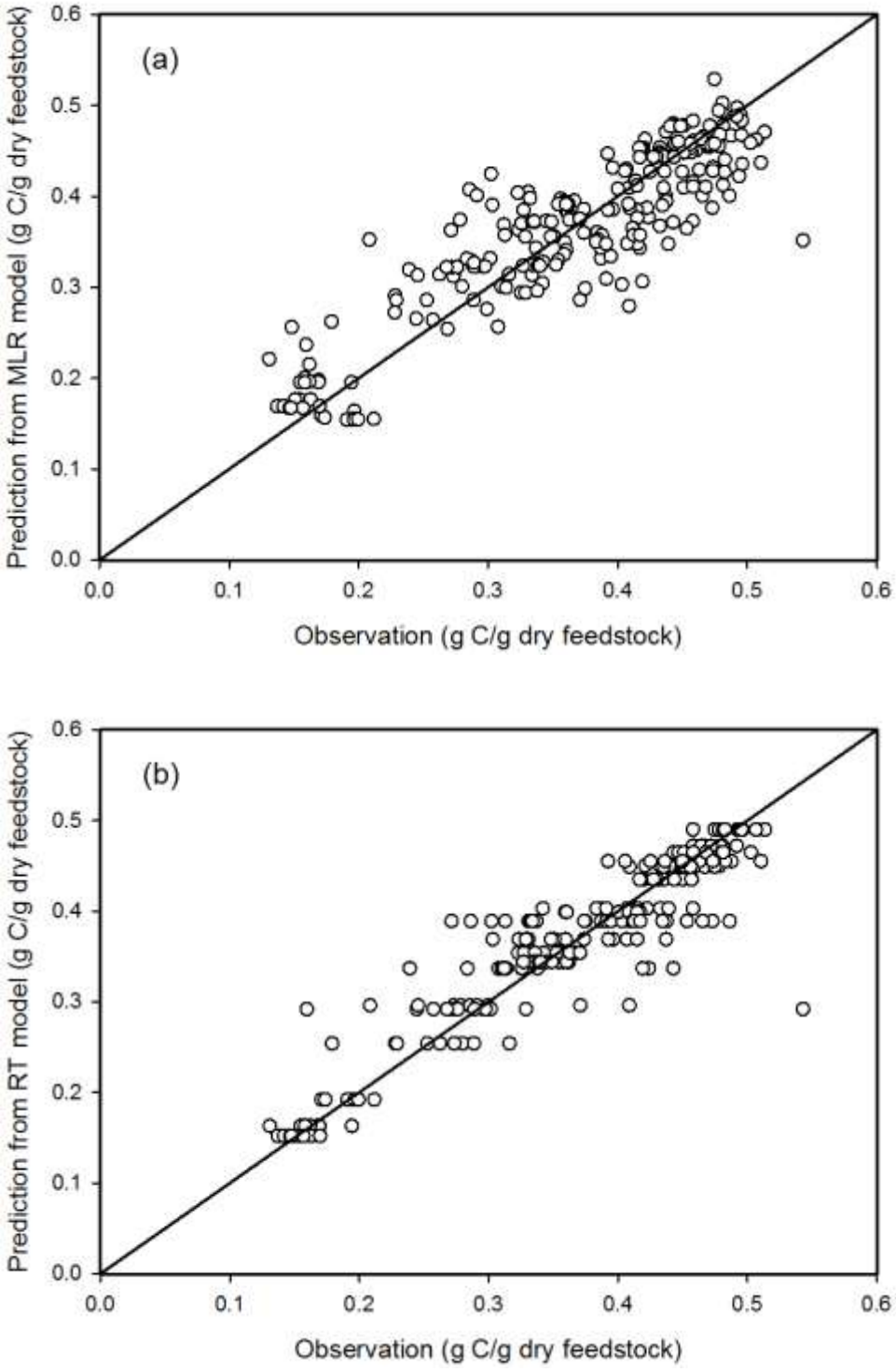

Figure 4.25 Comparison between observed normalized carbon in the solid and predicted normalized carbon in the solid from (a) multiple linear regression (MLR) model and (b) regression tree (RT) model.

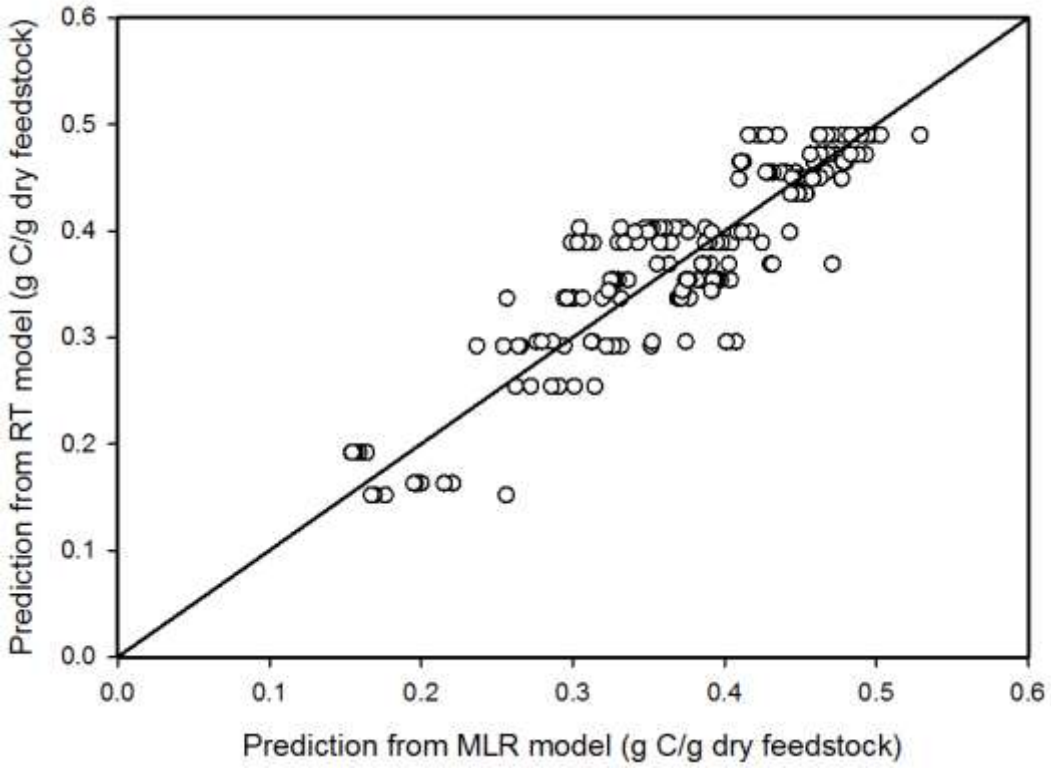

Figure 4.26 Comparison between predicted normalized carbon in the solid from regression tree (RT) model and multiple linear regression (MLR) model.

4.6.4 References

Abdelmoez, W., Nage, S.M., Bastawess, A., Ihab, A., Yoshida, H. 2014. Subcritical water technology for wheat straw hydrolysis to produce value added products. 70, 68-77.

Akalın, M. K., Tekin, K., Karagoz, S., 2012. Hydrothermal liquefaction of cornelian cherry stones for bio-oil production. Bioresour. Technol. 110, 682-687.

Alatalo, S.-M., Repo, E., Mäkilä , E., Salonen, J., Vakkilainen, E., Sillanpää , M., 2013. Adsorption behavior of hydrothermally treated municipal sludge & pulp and paper industry sludge. Bioresour. Technol. 147, 71-76.

Areeprasert, C., Zhao, P., Ma, D., Shen, Y., Yoshikawa, K., 2014. Alternative Solid Fuel Production from Paper Sludge Employing Hydrothermal Treatment. Energy Fuels 28, 1198-1206.

Asghari, F. S., Yoshida, H., 2006. Acid-catalyzed production of 5-hydroxymethyl furfural from d-fructose in subcritical water. Ind. Eng. Chem. Res. 45, 2163-2173.

Aydıncak, K., Yumak, T., Sınag, A., Esen, B., 2012. Synthesis and characterization of carbonaceous materials from saccharides (glucose and lactose) and two waste biomasses by hydrothermal carbonization. Ind. Eng. Chem. Res. 51, 9145-9152.

Becker, R., Dorgerloh, U., Helmis, M., Mumme, J., Diakite, M., Nehls, I., 2013. Hydrothermally carbonized plant materials: Patterns of volatile organic compounds detected by gas chromatography. Bioresour. Technol. 130, 621-628.

Berge, N. D., Ro, K. S., Mao, J., Flora, J. R. V., 2011. Hydrothermal carbonization of municipal waste streams. Environ. Sci. Technol. 45, 5696-5703.

Bhattacharjee, S., Sultana, A., Sazzad, M.H., Islam, M.A., Ahtashom, M.M., Asaduzzaman, Analysis of the proximate composition and energy values of two varieties of onion (Allium cepa L.) bulbs of different origin: A comparative study. Int. J. Food Sci. Nutr., 2, 246-253.

Blazso, M., Jakab, E., Vargha, A., Szekely, T., Zoebel, H., Klare, H., Keil, G., 1986. The effect of hydrothermal treatment on a merseburg lignite. Fuel 65, 337-341.

Brand, S., Hardi, F., Kim, J., Suh, D.J., 2014. Effect of heating rate on biomass liquefaction: Differences between subcritical water and supercritical ethanol. Energy, 68, 420-442.

Budai, A., Wang, L., Gronli, M., Strand, L.T., Antal, M.J., Abiven, S., Dieguez-Alonso, A., Anca-Couce, A., Rasse, D.P., 2014. Surface Properties and Chemical Composition of Corncob and Miscanthus Biochars: Effects of Production Temperature and Method. J. Agric. Food Chem. 62, 3791-3799.

Cao, X.; Ro, K. S.; Libra, J. A.; Kammann, C. I.; Lima, I.; Berge, N.; Li, L.; Li, Y.; Chen, N.; Yang, J.; Deng, B.; Mao, J., 2013. Effects of biomass types and carbonization conditions on the chemical characteristics of hydrochars. J. Agric. Food Chem. 61, 9401-9411.

Chang, S.; Zhao, Z.; Zheng, A.; Li, X.; Wang, X.; Huang, Z.; He, F.; Li, H., 2013. Effect of hydrothermal pretreatment on properties of bio-oil produced from fast pyrolysis of eucalyptus wood in a fluidized bed reactor. Bioresour. Technol. 138, 321-328.

Chen, W.-H., Ye, S.-C., Sheen, H.-K., 2012. Hydrothermal carbonization of sugarcane bagasse via wet torrefaction in association with microwave heating. Bioresour. Technol. 118, 195-203.

Danso-Boateng, E., Holdich, R. G., Shama, G., Wheatley, A. D., Sohail, M.; Martin, S. J., 2013. Kinetics of faecal biomass hydrothermal carbonisation for hydrochar production. Appl. Energy 111, 351-357.

Daneshvar, S., Salak, F., Ishii, T., Otsuka, K., 2012. Application of subcritical water for conversion of macroalgae to value-added materials. Ind. Eng. Chem. Res. 51, 77-84.

Demirbaş, A. 1997. Calculation of higher heating values of biomass fuels. Fuel 76, 431-434.

Dinjus, E., Kruse, A., Tröger, N., 2011. Hydrothermal carbonization – 1.Influence of lignin in lignocelluloses. Chem. Eng. Technol. 34, 2037-2043.

Du, Z., Hu, B., Shi, A., Ma, X., Cheng, Y., Chen, P., Liu, Y., Lin, X., Ruan, R., 2012a. Cultivation of a microalga chlorella vulgaris using recycled aqueous phase nutrients from hydrothermal carbonization process. Bioresour. Technol. 126, 354-357.

Du, Z., Mohr, M., Ma, X., Cheng, Y., Lin, X., Liu, Y., Zhou, W., Chen, P., Ruan, R., 2012b. Hydrothermal pretreatment of microalgae for production of pyrolytic bio-oil with a low nitrogen content. Bioresour. Technol. 120, 13-18.

Eibisch, N., Helfrich, M., Don, A., Mikutta, R., Kruse, A., 2013. Ellerbrock, R.; Flessa, H., Properties and degradability of hydrothermal carbonization products. J. Environ. Qual. 42, 1565-1573.

Energy Research Centre of the Netherlands, 2012. Database for biomass and waste. http://www.ecn.nl/phyllis2/Browse/Standard/ECN-Phyllis

Erlach, B., Harder, B., Tsatsaronis, G., 2012. Combined hydrothermal carbonization and gasification of biomass with carbon capture. Energy 45, 329-338.

Escala, M., Zumbuehl, T., Koller, C., Junge, R., Krebs, R., 2013. Hydrothermal carbonization as an energy-efficient alternative to established drying technologies for sewage sludge: A feasibility study on a laboratory scale. Energy Fuels 27, 454-460.

Eurotrade World Commerce, 1993. Certificate of analysis fructose. In Spain.

Falco, C., Baccile, N., Titirici, M.-M., 2011. Morphological and structural differences between glucose, cellulose and lignocellulosic biomass derived hydrothermal carbons. Green Chem. 13, 3273-3281.

Falco, C., Sieben, J. M., Brun, N., Sevilla, M., van der Mauelen, T., Morallón, E., Cazorla-Amorós, D., Titirici, M.-M., 2013. Hydrothermal carbons from hemicellulose-derived aqueous hydrolysis products as electrode materials for supercapacitors. ChemSusChem 6, 374-382.

Fiori, L., Basso, D., Castello, D., Baratieri, M., 2014. Hydrothermal carbonization of biomass: Design of a batch reactor and preliminary experimental results. Chem. Eng. Trans. 37, 55-60.

Flora, J. F. R., Lu, X., Li, L., Flora, J. R. V.; Berge, N. D., 2013. The effects of alkalinity and acidity of process water and hydrochar washing on the adsorption of atrazine on hydrothermally produced hydrochar. Chemosphere 93, 1989-1996.

Fujino, T., Calderon-Moreno, J. M., Swamy, S.; Hirose, T., Yoshimura, M., 2002. Phase and structural change of carbonized wood materials by hydrothermal treatment. Solid State Ionics 151, 197-203.

Funke, A., Reebs, F., Kruse, A., 2013a. Experimental comparison of hydrothermal and

vapothermal carbonization. Fuel Process. Technol. 115, 261-269.
Funke, A., Mumme, J., Koon, M., Diakite, M., 2013b. Cascaded production of biogas and hydrochar from wheat straw: Energetic potential and recovery of carbon and plant nutrients. Biomass Bioenergy 58, 229-237.
Gao, Y., Wang, X., Wang, J., Li, X., Cheng, J., Yang, H., Chen, H., 2013. Effect of residence time on chemical and structural properties of hydrochar obtained by hydrothermal carbonization of water hyacinth. Energy 58, 376-383.
He, C., Giannis, A., Wang, J.-Y., 2013. Conversion of sewage sludge to clean solid fuel using hydrothermal carbonization: Hydrochar fuel characteristics and combustion behavior. Appl. Energy 111, 257-266.
Heilmann, S. M., Davis, H. T., Jader, L. R., Lefebvre, P. A., Sadowsky, M. J., Schendel, F. J., von Keitz, M. G., Valentas, K. J., 2010. Hydrothermal carbonization of microalgae. Biomass Bioenergy 34, 875-882.
Heilmann, S. M., Jader, L. R., Harned, L. A., Sadowsky, M. J., Schendel, F. J., Lefebvre, P. A., von Keitz, M. G., Valentas, K. J., 2011. Hydrothermal carbonization of microalgae ii. Fatty acid, char, and algal nutrient products. Appl. Energy 88, 3286-3290.
Henry, W., Silliman, B., Buckingham, J.T., 1814. The elements of experimental chemistry (Volume 2). Thomas&Andrews, Boston.
Hoekman, S. K., Broch, A., Robbins, C., 2011. Hydrothermal carbonization (HTC) of lignocellulosic biomass. Energy Fuels 25, 1802-1810.
Hoekman, S. K., Broch, A., Robbins, C., Zielinska, B., Felix, L., 2013. Hydrothermal carbonization (HTC) of selected woody and herbaceous biomass feedstocks. Biomass Convers. Biorefin. 3, 113-126.
Hwang, I.-H., Aoyama, H., Matsuto, T., Nakagishi, T., Matsuo, T., 2012. Recovery of solid fuel from municipal solid waste by hydrothermal treatment using subcritical water. Waste Manage. 32, 410-416.
Jamari, S. S., Howse, J. R., 2012. The effect of the hydrothermal carbonization process on palm oil empty fruit bunch. Biomass Bioenergy 47, 82-90.
Kang, S., Li, X., Fan, J., Chang, J., 2012. Characterization of hydrochars produced by hydrothermal carbonization of lignin, cellulose, D-xylose, and wood meal. Ind. Eng. Chem. Res. 51, 9023-9031.
Kaur, A., Singh, N., Ezekiel, R., Guraya, H. S., 2007. Physicochemical, thermal and pasting properties of starches separated from different potato cultivars grown at different locations. Food Chem. 101, 643-651.
Karagöz, S., Bhaskar, T., Muto, A., Sakata, Y., 2005. Comparative studies of oil compositions produced from sawdust, rice husk, lignin and cellulose by hydrothermal treatment. Fuel 84, 875-884.
Karagöz, S., Bhaskar, T., Muto, A., Sakata, Y., 2006. Hydrothermal upgrading of biomass: Effect of K2CO3 concentration and biomass/water ratio on products distribution. Bioresour. Technol. 97, 90-98.
Khuwijitjaru, P., Watsanit, K., Adachi, S. 2012. Carbohydrate content and composition of product from subcritical water treatment of coconut meal. J. Ind. Eng. Chem. 18, 225-229.
Kim, D.S., Myint, A.A., Lee, H.W., Yoon, J., Lee, Y.W. 2013. Evaluation of hot compressed water pretreatment and enzymatic saccharification of tulip tree

sawdust using severity factors. Bioresour. Technol. 144, 460-466.
Knežević, D., van Swaaij, W., Kersten, S., 2010. Hydrothermal conversion of biomass. II. Conversion of wood, pyrolysis oil, and glucose in hot compressed water. Ind. Eng. Chem. Res. 49, 104-112.
Kobayashi, N., Okada, N., Hirakawa, A., Sato, T., Kobayashi, J., Hatano, S., Itaya, Y., Mori, S., 2008. Characteristics of solid residues obtained from hot-compressed-water treatment of woody biomass. Ind. Eng. Chem. Res. 48, 373-379.
Kong, L., Miao, P., Qin, J., 2013. Characteristics and pyrolysis dynamic behaviors of hydrothermally treated micro crystalline cellulose. J. Anal. Appl. Pyrolysis 100, 67-74.
Kumar, S., Loganathan, V. A., Gupta, R. B., Barnett, M. O., 2011. An assessment of U(VI) removal from groundwater using biochar produced from hydrothermal carbonization. J. Environ. Manage. 92, 2504-2512.
Lamoolphak, W., De-Eknamkul, W., Shotipruk, A., 2008. Hydrothermal production and characterization of protein and amino acids from silk waste. Bioresour. Technol. 99, 7678-7685.
Lilliestråle, A. 2007. Hydrothermal carbonization of biowaste - a step towards efficient carbon sequestration and sustainable energy production. Ph.D. Dissertation, Uppsala University, Uppsala.
Li, L., Diederick, R., Flora, J. R. V., Berge, N. D., 2013. Hydrothermal carbonization of food waste and associated packaging materials for energy source generation. Waste Manage. 33, 2478-2492.
Li, L., Mckenzie, H., Olsen, P., Berge, D. 2014. Using liquid waste streams as the moisture source during the hydrothermal carbonizaiton of municipal solid wastes. Waste Manage. 34, 2185-2195.
Liu, H.M. 2013. Cypress liquefaction in a water/methanol mixture: Effect of solvent ratio on products distribution and characterization of products. Ind. Eng. Chem. Res. 52, 12523-12529.
Liu, H.-M., Li, M.-F., Yang, S., Sun, R.-C., 2013. Understanding the mechanism of cypress liquefaction in hot-compressed water through characterization of solid residues. Energies 6, 1590-1603.
Liu, H. M., Li, M. F. 2014. Hydrothermal liquefaction of cypress: Effect of water amount on structural characteristics of the solid residues. Chem. Eng. Technol. 37, 95-102.
Liu, Z., Zhang, F.-S., Wu, J., 2010. Characterization and application of chars produced from pinewood pyrolysis and hydrothermal treatment. Fuel 89, 510-514.
Liu, Z., Quek, A., Balasubramanian, R., 2014. Preparation and characterization of fuel pellets from woody biomass, agro-residues and their corresponding hydrochars. Appl. Energy 113, 1315-1322.
Liu, Z., Quek, A., Hoekman, S.K., Balasubramanian, R., 2013a. Production of solid biochar fuel from waste biomass by hydrothermal carbonization. Fuel 103, 943-949.
Liu, Z., Quek, A., Parshetti, G., Jain, A., Srinivasan, M. P., Hoekman, S. K., Balasubramanian, R., 2013b. A study of nitrogen conversion and polycyclic aromatic hydrocarbon (PAH) emissions during hydrochar-lignite co-pyrolysis. Appl. Energy 108, 74-81.
Liu, Z., Balasubramanian, R., 2013. Upgrading of waste biomass by hydrothermal

carbonization (HTC) and low temperature pyrolysis (LTP): A comparative evaluation. Appl. Energy 114, 857-864.
Lu, L., Namioka, T., Yoshikawa, K., 2011. Effects of hydrothermal treatment on characteristics and combustion behaviors of municipal solid wastes. Appl. Energy 88, 3659-3664.
Lu, X., Jordan, B., Berge, N. D., 2012. Thermal conversion of municipal solid waste via hydrothermal carbonization: Comparison of carbonization products to products from current waste management techniques. Waste Manage. 32, 1353-1365.
Lu, X., Pellechia, P., Flora, J. R. V., Berge, N., 2013. Influence of reaction time and temperature on product formation associated with the hydrothermal carbonization of cellulose. Bioresour. Technol. 138, 180-190.
Lu, X., Flora, J., Berge, N., 2014. Influence of process water quality on hydrothermal carbonization of cellulose. Bioresour. Technol. 154, 229-239.
Luo, G., Shi, W., Chen, X., Ni, W., Strong, P. J., Jia, Y., 2011. Wang, H., Hydrothermal conversion of water lettuce biomass at 473 or 523 K. Biomass Bioenergy 35, 4855-4861.
Lynam, J. G., Coronella, C. J., Yan, W., Reza, M. T., Vasquez, V. R., 2011. Acetic acid and lithium chloride effects on hydrothermal carbonization of lignocellulosic biomass. Bioresour. Technol. 102, 6192-6199.
Lynam, J. G., Toufiq Reza, M., Vasquez, V. R., Coronella, C. J., 2012. Effect of salt addition on hydrothermal carbonization of lignocellulosic biomass. Fuel 99, 271-273.
Ministry of Education, Cultural, Sports, Science and Technology of Japan, 2011. Whole food catalog. http://wholefoodcatalog.info/nutrient/ash/fishes_and_shellfishes/
Miranda, T. 2008. Combustion analysis of different olive residues. Int J Mol Sci. 9, 512-525.
Miyazawa, T., Funazukuri, T., 2006. Noncatalytic hydrolysis of guar gum under hydrothermal conditions. Carbohydr. Res. 341, 870-877.
Mondal, M., Trivedy, K., Kumar, S.N., 2007. The silk proteins, sericin and fibroin in silkworm, bombyx mori linn., - A review. Caspian J. Env. Sci. 5, 63-76.
Möller, M., Harnisch, F., Schroder, U., 2013. Hydrothermal liquefaction of cellulose in subcritical water-the role of crystallinity on the cellulose reactivity. RSC Advances 3, 11035-11044.
Nikkhah, K., Bakhshi, N.N., MacDonald, D.G., 1993. Co-pyrolysis of various biomass materials and coals in a quartz semi-batch reactor. In: Proc. Energy from biomass and wastes XVI (Ed. D.L.Klass), pp. 857-902, Institute of Gas Technology, Chicago.
Nagamori, M., Funazukuri, T., 2004. Glucose production by hydrolysis of starch under hydrothermal conditions. J. Chem. Technol. Biotechnol. 79 , 229-233.
Nonaka, H., Funaoka, M., 2011. Decomposition characteristics of softwood lignophenol under hydrothermal conditions. Biomass Bioenergy 35, 1607-1611.
Ogden, C.A., Ileleji, K.E., Johnson, K.D., Wang, Q., 2010. In-field direct combustion fuel property changes of switchgrass harvested from summer to fall. Fuel Process Technol. 91, 266-271.
Oliveira, I., Blöhse, D., Ramke, H.-G., 2013. Hydrothermal carbonization of agricultural residues. Bioresour. Technol. 142, 138-146.

Pala, M., Kantarli, I.C., Buyukisik, H.B., Yanik, J., 2014. Hydrothermal carbonization and torrefaction of grape pomace: A comparative evaluation. Bioresour. Technol.161, 255-262.

Parikh, J.; Channniwala, S.A., Ghosal, G.K., 2007. A correlation for calculating elemental composition from proximate analysis of biomass materials. Fuel 86, 1710-1719.

Pari, G., Darmawan, S., Prihandoko, B. 2014. Porous Carbon Spheres from Hydrothermal Carbonization and KOH Activation on Cassava and Tapioca Flour Raw Material. Procedia Environ. Sci. 20, 342-351.

Parshetti, G. K., Liu, Z., Jain, A., Srinivasan, M. P., Balasubramanian, R., 2013a. Hydrothermal carbonization of sewage sludge for energy production with coal. Fuel 111, 201-210.

Parshetti, G. K., Kent Hoekman, S., Balasubramanian, R., 2013b. Chemical, structural and combustion characteristics of carbonaceous products obtained by hydrothermal carbonization of palm empty fruit bunches. Bioresour. Technol. 135, 683-689.

Pavlovic, I., Knez, Z., 2013. Skerget, M., Subcriticai water - a perspective reaction media for biomass processing to chemicals: Study on cellulose conversion as a model for biomass. Chem. Biochem. Eng. Q. 27, 73-82.

Pinkowska, H., Wolak, P., Złocinska, A., 2012. Hydrothermal decomposition of alkali lignin in sub- and supercritical water. Chem. Eng. J. 187, 410-414.

Pourali, O., Asghari, F. S., Yoshida, H., 2009. Sub-critical water treatment of rice bran to produce valuable materials. Food Chem. 115, 1-7.

Pourali, O., Asghari, F. S., Yoshida, H., 2010. Production of phenolic compounds from rice bran biomass under subcritical water conditions. Chem. Eng. J. 160, 259-266.

Ramsurn, H., Kumar, S., Gupta, R. B., 2011. Enhancement of biochar gasification in alkali hydrothermal medium by passivation of inorganic components using Ca(OH)2. Energy Fuels 25, 2389-2398.

Regmi, P., Garcia Moscoso, J. L., Kumar, S., Cao, X., Mao, J., Schafran, G., 2012. Removal of copper and cadmium from aqueous solution using switchgrass biochar produced via hydrothermal carbonization process. J. Environ. Manage. 109, 61-69.

Reza, M. T., Lynam, J. G., Uddin, M. H., Coronella, C. J., 2013a. Hydrothermal carbonization: Fate of inorganics. Biomass Bioenergy 49, 86-94.

Reza, M. T., Yan, W., Uddin, M. H., Lynam, J. G., Hoekman, S. K., Coronella, C. J., Vásquez, V. R., 2013b. Reaction kinetics of hydrothermal carbonization of loblolly pine. Bioresour. Technol. 139, 161-169.

Reza, M.T., Uddin, M.H., Lynam, J.G., Hoekman, S.K., Coronella, C.J., 2014a. Hydrothermal carbonization of loblolly pine: reaction chemistry and water balance. Biomass Conv. Bioref. 4, 311-321.

Reza, M.T., Becker, W., Sachsenheimer, K., Mumme, J., 2014b. Hydrothermal carbonization (HTC): Near infrared spectroscopy and partial least-squares regression for determination of selective components in HTC solid and liquid products derived from maize silage. Bioresour. Technol. 161, 91-101.

Román, S., Nabais, J. M. V., Laginhas, C., Ledesma, B., González, J. F., 2012. Hydrothermal carbonization as an effective way of densifying the energy content

of biomass. Fuel Process. Technol. 103, 78-83.
Salak, F., Daneshvar, S., Abedi, J., Furukawa, K., 2013. Adding value to onion (Allium cepa L.) waste by subcritical water treatment. Fuel Process Technol. 112, 86-92.
Sevilla, M., Fuertes, A. B., 2009a, The production of carbon materials by hydrothermal carbonization of cellulose. Carbon 47, 2281-2289.
Sevilla, M., Fuertes, A. B., 2009b. Chemical and structural properties of carbonaceous products obtained by hydrothermal carbonization of saccharides. Chem. Eur. J. 15, 4195-4203.
Sevilla, M., Maciá-Agulló, J. A., Fuertes, A. B., 2011. Hydrothermal carbonization of biomass as a route for the sequestration of CO2: Chemical and structural properties of the carbonized products. Biomass Bioenergy 35, 3152-3159.
Stemann, J., Putschew, A., Ziegler, F., 2013. Hydrothermal carbonization: Process water characterization and effects of water recirculation. Bioresour. Technol. 143, 139-146.
Sun, P., Heng, M., Sun, S.-H., Chen, J., 2011. Analysis of liquid and solid products from liquefaction of paulownia in hot-compressed water. Energy Convers. Manage. 52, 924-933.
SuÁrez, J., Luengo A., 2000. Thermochemical Properties of Cuban Biomass. Energy Sources, 22, 851-857.
Tchobanoglous, G., Theisen, H., Vigil, S., 1993. Integrated solid waste management: Engineering principles and management issues. McGraw-Hill Education: Columbus, p 36-65.
Tian, Y., Kumabe, K., Matsumoto, K., Takeuchi, H., Xie, Y., Hasegawa, T., 2012. Hydrolysis behavior of tofu waste in hot compressed water. Biomass Bioenergy 39, 112-119.
Toor, S.S., Reddy, H., Deng, S., Hoffmann, J., Spangsmark, D., Madsen, L.B., Holm-Nielsen, J.B., Rosendahl, L.A., 2013. Hydrothermal liquefaction of spirulina and nannochloropsis salina under subcritical and supercritical water conditions. Bioresour. Technol. 131, 413-419.
Tremel, A., Stemann, J., Herrmann, M., Erlach, B., Spliethoff, H., 2012. Entrained flow gasification of biocoal from hydrothermal carbonization. Fuel 102, 396-403.
TRI-K Industries, Inc., 2008. Product data sheet_silk protein.
Wang, S.H., Liu, J. L., Li, F., Dai, J. M., Jia, H. S., Xu, B. S., 2014. Study on converting cotton pulp fiber into carbonaceous microspheres. Fiber Polym. 15, 286-290.
Watchararuji, K., Goto, M., Sasaki, M., Shotipruk, A., 2008. Value-added subcritical water hydrolysate from rice bran and soybean meal. Bioresour. Technol. 99, 6207-6213.
Wiedner, K., Naisse, C., Rumpel, C., Pozzi, A., Wieczorek, P., Glaser, B., 2013. Chemical modification of biomass residues during hydrothermal carbonization - What makes the difference, temperature or feedstock? Org. Geochem. 54, 91-100.
Xiao, L.-P., Shi, Z.-J., Xu, F., Sun, R.-C., 2012. Hydrothermal carbonization of lignocellulosic biomass. Bioresour. Technol. 118, 619-623.
Xiao, L.-P., Shi, Z.-J., Xu, F., Sun, R.-C., 2013. Hydrothermal treatment and enzymatic hydrolysis of tamarix ramosissima: Evaluation of the process as a conversion method in a biorefinery concept. Bioresour. Technol. 135, 73-81.
Yan, W., Acharjee, T. C., Coronella, C. J., Vásquez, V. R., 2009. Thermal pretreatment

of lignocellulosic biomass. Environ. Prog. Sustain. Energy 28, 435-440.
Yin, S., Pan, Y., Tan, Z., 2011. Hydrothermal conversion of cellulose to 5-hydroxymethyl furfural. Int. J. Green Energy 8, 234-247.
Yoshida, H.; Terashima, M.; Takahashi, Y., 1999. Production of organic acids and amino acids from fish meat by sub-critical water hydrolysis. Biotechnol. Progr. 15, 1090-1094.
Zhang, J., Lin, Q., Zhao, X., 2014. The hydrochar characters of municipal sewage sludge under different hydrothermal temperatures and durations. J. Integr. Agr. 13, 471-482.
Zhao, P., Shen, Y., Ge, S., Yoshikawa, K. 2014. Energy recycling from sewage sludge by producing solid biofuel with hydrothermal carbonization. Energ. Convers. Manage. 78,815-821.

CHAPTER 5.

THE INFLUENCE OF FEEDSTOCK PROPERTIES AND PROCESS CONDITIONS ON HYDROCHAR YIELD AND CARBON CONTENT AND ENERGY CONTENT

5.1 INTRODUCTION

Hydrothermal carbonization (HTC) is a wet, low temperature thermal conversion process that is gaining significant attention for the sustainable generation of a value-added solid material (referred to as hydrochar) from waste materials (Berge et al., 2011; Libra et al., 2011; Titirici et al., 2007 and 2012). During HTC, wet waste materials are exposed to autogenic pressures at temperatures between 180 – 350 ^{o}C. As a result of these conditions, a series of simultaneous reactions, including dehydration, decarboxylation, aromatization, and condensation, occur and result in the generation of hydrochar (Funke et al., 2010; Sevilla and Fuertes, 2009; Titirici et al., 2007 and 2012; Reza et al., 2014). Hydrochar is a carbon-rich, energy-dense material with high surface area. The generation and use of this hydrochar has been well studied (Baccile et al., 2009; Cao et al., 2011; Falco et al., 2011; Fuertes et al., 2010; Hwang et a l., 2012; Kang et al., 2012). Potential applications of hydrochar include use as a soil amendment (Libra et al., 2011), solid fuel (Berge et al., 2011; Heilmann et al., 2010; Reza et al., 2014; Hrncic et al., 2016), adsorption for contaminant treatment (Román et al., 2012 and 2013; Jain et al., 2016) and energy storage (Falco et al., 2013).

Currently, carbonization of various feedstocks is being conducted over large ranges of process conditions (Berge et al., 2011; Falco et al., 2011; Kang et al., 2012; Li et al., 2013). Understanding the factors influencing generation and characteristics of the hydrochar would permit more informed carbonization study design and implementation. It has been reported that feedstock properties and process conditions influence hydrochar properties. Changes in reaction temperature have also been documented to influence hydrochar yield (Álvarez-Murillo et al., 2015; Becker et al., 2013; Benavente et al., 2015;

Basso et al., 2016), carbon content (Benavente et al., 2015; Hwang et al., 2012; Kong et al., 2013; Salak et al., 2013) and energy content (Álvarez-Murillo et al., 2015; Benavente et al., 2015; Basso et al., 2016). In general, with the increase of temperature, hydrochar yield decresases (Becker et al., 2013; Benavente et al., 2015; Basso et al., 2016; Du et al., 2012) while hydrochar carbon content (Benavente et al., 2015; Cao et al., 2013; Hwang et al., 2012; Pala et al., 2014) and energy content increase (Benavente et al., 2015; Basso et al., 2016; Kong et al., 2013; Pala et al., 2014). Feedstock initial solids concentration and reaction time have also been reported to influence the hydrochar properties (Heilmann et al., 2010 and 2011; Knežević et al., 2010; Li et al., 2013). However, the importance of these process conditions is unclear because conclusions from literature contradict one another. Lu et al. (2014), for example, suggest temperature and time have a large influence on cellulose carbonization at early times. Román et al. (2012) have reported that temperature and initial solids concentration are more influential on product formation than time. Some other studies also suggest reaction time has little influence on hydrochar characteristics (Heilmann et al., 2010; Mumme et al., 2011). Studies evaluating the influence of feedstock properties on hydrochar characteristics have also been conducted, with results often contradicting one another (Hoekman et al., 2011; Wiedner et al., 2013). These contradictions are likely a result of changes in process kinetics, which likely vary with feedstock type, reactor volume, and reactor heating mechanisms/rates.

Linear and non-linear statistical models also have been developed to describe and understand the relationships between process conditions and hydrochar properties (Álvarez-Murillo et al., 2015; Danso-Boateng et al., 2015; Kannan et al., 2017; Mumme et al., 2011; Sabio et al., 2016). Mumme et al. (2011) developed linear regression models

to study the hydrochar yield and carbon content obtained from the HTC of silage at different temperatures (190-270 ^{o}C), time (2-10 hr) and initial pH (3-7). Results from their work suggest temperature is the most influential factor on hydrochar carbon content. Non-linear models have also been developed using response surface methodology to identify the importance of process conditions on hydrochar yield and energy content obtained from HTC of tomato peel (Sabio et al., 2016). Sabio et al. (2016) indicate that both reaction temperature and time affect hydrochar yield and energy content and that temperature is more influential than time. Few models include feedstock properties. Li et al. (2015) developed linear and non-linear regression models based on data collected from HTC literature and determined process conditions have greater influence on hydrochar yields than feedstock properties, while feedstock properties are more influential on the hydrochar carbon content and energy content. However, the feedstock properties used in the work described by Li et al. (2015) were somewhat limited, as only the ultimate and proximate properties of feedstocks were considered.

It is important to determine the feedstock and process conditions that universally influence hydrochar characteristics. To evaluate this, linear and non-linear models were developed to describe hydrochar characteristics based on data collected from HTC-related literature. A global sensitivity analysis was subsequently conducted to identify the parameters that influence model output. The specific objectives of this work are to: (1) develop linear and non-linear statistical models (regression tree and random forest models) predicting hydrochar yield, carbon content and energy content as a function of feedstock properties and process conditions using data collected, (2) use Sobol analysis to evaluate the sensitivity of independent variables within each model, and (3) compare the

performance of the different models and identify the most influential parameters on the studied hydrochar properties.

5.2. METHODS

5.2.1 Data collection and extraction

Methods for data collection and extraction are the same as that described in Chapter 4. Briefly, studies reporting on hydrothermal carbonization occurring between 180-350 ^{o}C were collected. Literature searches were conducted in scientific databases using key words including hydrothermal carbonization, hydrothermal conversion, hydrothermal decomposition, subcritical water hydrolysis, hydrolysis, and hot compressed water. Literature available in these databases through June 2016 was collected. Feedstock properties, process conditions and carbonization product information from each study were tabulated. Feedstock properties include proximate analysis parameters (ash content, volatile matter and fixed carbon), ultimate analysis parameters (carbon, hydrogen and oxygen content), chemical compositions (cellulose, hemicellulose and lignin content), and polarity. The abbreviation of parameters investigated in this study is listed in Table 5.1.

Polarity index, which is calculated as the mass ratio of O+N to C is used to approximate feedstock polarity (Rutherford et al., 1992). Polarity index illustrates the hydrophobicity of the organic feedstocks (Wu et al., 2001). The smaller the polarity index, the more hydrophobic the feedstock is. Feedstock lignin content was also collected and used as reported. It should be noted that feedstock lignin content is reported as either: (1) Klason, (2) ADL, or (3) no reference to the technique used to determine the lignin content. Conversion between these types of lignin is not possible. Feedstock cellulose and

hemicellulose were also collected and these feedstock properties are not routinely reported in HTC-related studies. If feedstock cellulose, hemicellulose and lignin were not reported, literature searches were conducted to obtain these properties for the specific feedstock.

Process conditions collected for this study include: initial solids concentration, temperature, and time. In this study, reaction temperature is the final desired temperature. Reaction time includes the time it taken to heat the reactor to the desired temperature and the time maintained at the desired temperature. The time to cool the reactor is not considered.

Carbonization products investigated include: hydrochar yield (mass of dry recovered solids per mass of initial dry feedstock, % dry basis), solid-phase carbon content (carbon content in the recovered solids, % dry basis), and hydrochar energy content (MJ/kg). For hydrochar yield, carbon content and energy content, 613, 475 and 420 data points were collected, respectively.

5.2.2 Parameter selection

Parameter selection was conducted using correlation tests. Strongly correlated parameters, defined as those with a correlation coefficient greater than 0.8 (Divaris, et al., 2012; Beldjazia and Alaton, 2016), were identified. A series of models representing all possible combinations of non-correlated parameters were developed. Both linear and non-linear correlation tests were performed.

5.2.2.1. Pearson correlation

Correlated parameters associated with the linear models were determined using the Pearson correlation test. The Pearson correlation coefficient is used to measure the

strength of a linear relationship between two variables. Pearson correlation coefficient ranges from -1 to +1. -1 indicates a perfect negative linear relationship while +1 indicates a perfect positive linear relationship (Fujita et al., 2009). The Pearson correlation coefficient is defined as:

$$r = \frac{cov_{xy}}{\sigma_x \sigma_y} \quad (1)$$

where, cov_{xy} is the covariance between x and y, σ_x is the standard deviation of x, and σ_y is the standard deviation of y. The absolute value of the Pearson correlation coefficient above 0.8 was considered as a strong correlation.

5.2.2.2 Distance correlation

Distance correlation tests, which measure the dependence between two random variables, provides a measure of correlations associated with nonlinear relationships (Szekely et al., 2007; Szekely and Rizzo, 2009). The distance correlation coefficient ranges from 0 to 1 and can be defined as:

$$dCor(x, y) = \frac{dCov(x,y)}{\sqrt{dVar(x)dVar(y)}} \quad (2)$$

where, dCov(x,y) is the distance covariance between x and y, dVar(x) is the distance covariance of x, and dVar(y) is the distance covariance of y (Szekely et al., 2007). A distance correlation coefficient greater than 0.8 was considered as a strong correlation.

5.2.3 Model development

Both linear and non-linear models were developed to describe the relationship between the independent and dependent parameters. Multiple linear regression was used to describe linear relationships. In this study, multiple linear regression models were

developed using the "lm" function in the statistical software package R (version 3.1.0, R Development Core Team).

Non-linear relationships were described using regression tree and random forest models. Regression tree models are non-parametric models that produce binary trees through splitting dependent variables into nodes following recursive partitioning rules (Breiman et al., 1984). The advantages associated with regression tree models were described in Chapter 4. Regression tree models were developed using the "rpart" function of the ''rpart'' package in R.

Random forest models were also developed. Random forests are tree-based models, but differ from regression tree models in that a large collection of trees are developed (Breiman et al., 2001). The performance of the random forest model is the average of the trees. Random forest is a black box approach, since individual trees cannot be evaluated, but it is a robust method to the noise since tree diversity guarantees model stability (Bouchon-Meunier et al., 2010; Hastie et al., 2008). Random forest models were developed using the "randomForest" function of the "randomForest" package in R.

5.2.4 Model evaluation and comparison

For linear regression, coefficient of determination (R^2), adjusted R^2, mean absolute percentage error (MAPE), root mean squared error (RMSE) and Akaike information criterion (AIC) were used to evaluate the performance of the linear regression models. The adjusted R^2 is a modified version of R^2 (Cameron and Windmeijer, 1995) that accounts for the number of explanatory variables in linear regression and number of nodes in regression tree.

MAPE is a common measure of prediction accuracy that indicates the average absolute percentage error (Hyndman and Koehler, 2006). The calculation of MAPE is as follows:

$$MAPE = \frac{100}{n}\sum_{t=1}^{n}\left|\frac{Y_{pred,i}-Y_{obs,i}}{Y_{obs,i}}\right| \quad (3)$$

where, $Y_{pred,i}$ represents the prediction, $Y_{obs,i}$ represents the observation, and n represents n observations.

RMSE, which is an indication of mean distance between predictions and observations, was calculated according to equation 4 (Kobayashi and Salam, 2000):

$$\text{RMSE} = \sqrt{\frac{\sum_{i=1}^{n}(Y_{pred,i}-Y_{obs,i})^2}{n}} \quad (4)$$

where, $Y_{pred,i}$ represents the prediction, $Y_{obs,i}$ represents the observation, and n represents n observations. RMSE has the same unit as the dependent variable being estimated.

AIC, which is based on information theory, is a method used for model selection. This parameter evaluates the goodness of fit through the likelihood function (Bozdogan, 1987; Posada and Buckley, 2004). AIC is defined as:

$$AIC = -2(\ln(likelihood)) + 2K \quad (5)$$

Where, likelihood is the probability of the data give a model and K is the number of the input parameters in the model.

For regression tree, R^2, adjusted R^2, MAPE and RMSE were used to evaluate the performance of the models. For random forest models, R^2, MAPE, RMSE and out-of-bag (OOB) RMSE were used to evaluate the performance of the models. The OOB RMSE was calculated using the average predictions from the trees that are not trained with datasets including the corresponding observations.

The predictive ability of all models was determined using leave one out cross validation which was described in Chapter 4. Briefly, all observations except for one were used to build the model. The prediction for the left out observation was obtained from the model developed without it. This process is repeated until cross-validated predictions are obtained for all observations. RMSEcv was calculated based on the cross-validated predictions.

The 95% confidence intervals associated with the mean of MAPE, RMSE and RMSEcv were calculated according to equation 6:

$$\sigma^2 = \bar{\sigma}^2 \pm \sqrt{2} \times 1.96 \frac{\bar{\sigma}^2}{\sqrt{N-1}} \qquad (6)$$

where, n is the number of data points and $\bar{\sigma}$ is the mean of MAPE, RMSE and RMSEcv.

5.2.5 Sensitivity analysis

Sobol analyses were conducted to identify the parameters imparting the greatest influence on hydrochar properties. Sobol analysis is a Monte Carlo-based variance decomposition method that determines the contribution of each model input parameter and their interactions to the overall model output variance (Sobol, 1993; Saltelli, et al., 2008; Zhang et al., 2015).

In this work, the first order Sobol index (FSI) and total order Sobol index (TSI) were calculated using the "soboljansen" function of the "sensitivity" package in R. Monte Carlo analyses were performed to generate data for input parameters including feedstock properties and process conditions in the model. Data generated from the Monte Carlo simulations follow a uniform distribution and were generated using the "runif" function in R. Using this function, n uniform random numbers which lie within the interval of the

minimum and maximum values of the simulated parameter were generated. The minimum and maximum values of each parameter were obtained from the collected data. To evaluate convergence with respect to sample size (n), variation of Sobol values with respect to sample size was investigated. The test on models with most number of parameters included suggests 200,000 data points is an adequate sample size for this study. At this point, the TSI changes by less than 15% for three consecutive measurements for hydrochar yield results. This criterion is assumed to hold true for hydrochar carbon content and energy content results. To identify specific parameter-to-parameter interactions, second and third order sensitivity indices were calculated using the "Sobol" function of the "sensitivity" package in R.

5.3 RESULTS AND DISCUSSION

5.3.1 Char yield

Both linear (Danso-Boateng et al., 2015; Mumme et al., 2011) and non-linear (Kannan et al., 2017; Li et al., 2015; Sabio et al., 2016) models have been previously developed to describe char yield. A similar approach was used in this study. A series of multiple linear regression, regression tree and random forest models were developed based on data collected from the literature (as described previously). The parameters used in each model were based on results from linear and non-linear correlation tests, which indicate that feedstock ash content is highly correlated (>0.8) with volatile matter. Therefore, a series of models representing all possible combinations of non-correlated parameters were developed. Table 5.2 contains a summary of the models developed to describe char yield. Subsequent sections detail results from each model structure (e.g., linear regression, regression tree, random forest).

5.3.1.1 Linear regression

General parameters describing the linear models, including R^2, adjusted R^2, RMSE and MAPE are listed in Table 5.3 and indicate that model performance is similar. The R^2 and adjusted R^2 values associated with these models are less than 0.5, suggesting a linear model does not fit the majority of the data well. The MAPE values indicate that all models have an average absolute percentage error in excess of 20%. AIC and RMSEcv (Figure 5.1) are used to assess model predictive capability and indicate that the models similarly predict yield.

Results from the Sobol analysis are shown in Figure 5.2 and also suggest the models are similar. As expected with linear models, the FSI and TSI are the same, indicating no parameter-to-parameter interactions exist. The magnitude of the Sobol indices was used to define parameter sensitivity on char yield. Highly sensitive parameters are defined as those with Sobol indices greater than 0.1, which represent parameters that explain more than 10% of the variance associated with model predicted char yields. Sensitive parameters are defined as those that represent 1 – 10% (Sobol indices ranging from 0.01 – 0.1) of the predicted variance and slightly sensitive parameters are those in which the Sobol indices are less than 0.01, but greater than 0. Parameters that are insensitive are defined as those in which the Sobol index is 0 or the confidence interval associated with their index crosses 0. Results from this grouping are presented in Table 5.4.

The results from the Sobol analysis suggest that for all linear models, char yield is most sensitive to feedstock polarity and oxygen content. These results seem reasonable based on processes known to occur during HTC. Changes in feedstock polarity influence

feedstock solubility (Rutherford et al., 1992; Wu et al., 2001); The more polar the substance, the more soluble in water. Changes in feedstock solubility will influence its hydrolysis, which has been defined as the potential rate-limiting step of the HTC process (Reza et al., 2014). The influence of oxygen content on char yield is also reasonable and supported by the literature. Changes in oxygen content during HTC have been shown to be one of the major contributors to feedstock mass loss (Lu et al., 2013; Falco et al., 2011). This loss occurs as a result of deoxygenation, which occurs during both the dehydration and decarboxylation process (Lu et al., 2013). Char yield is also sensitive to many proximate analysis parameters, including initial solids concentration, temperature and feedstock hydrogen content. Although feedstock lignin content is defined as a sensitive parameter with respect to the Y-L1 model (not Y-L2 model), it only explains 1.1% of the variance associated with the model predicted char yields.

These Sobol results indicate that, if using linear models to describe and/or predict char yield, the most critical feedstock properties are not currently being measured and/or reported. No papers currently report feedstock polarity and only 66.8% of the papers report feedstock oxygen contents. Many of the sensitive parameters are reported, with the exception of lignin content (19.5%). The fraction of papers that report the individual parameters is included in Table5.5.

5.3.1.2 Regression tree

General parameters describing the regression tree models, including R^2, adjusted R^2, RMSE and MAPE are included in Table 5.6. These results indicate, much like the linear regression models, that model performance is similar. The R^2 results suggest both regression tree models explain 78% of the model predicted variance and fit the majority of the data well. The MAPE indicates that all models have an average absolute

percentage error less than 13%, which is significantly lower than that associated with the linear models. The RMSEcv results indicate the regression tree models similarly predict yield, with relatively low values (Figure 5.3).

Sobol results based on the regression tree models are presented in Figure 5.4. Unlike that observed with results from the linear regression models, the TSI and FSI indices resulting from these Sobol analyses differ for the majority of the model parameters. The difference between these indices provides a measure of parameter-to-parameter interactions. The results for both models indicate that char yield is most sensitive to initial solids concentration, which explains approximately 20% of the predicted variance by itself (FSI) and contributes to approximately 30% of predicted variance through its interaction with other parameters (TSI-FSI). Initial solids concentration is the most interactive parameter in both of the regression tree models (Table 5.7). To identify the interactions between initial solids concentration and other model variables, the "Sobol" function of the sensitivity package was applied. The top five interactions associated with are listed in Table 5.7.

The high degree of sensitivity on char yield with initial solids concentration, as well as the interactions associated with this variable is consistent with that reported in the HTC literature. Many HTC papers have reported the influence of initial solid concentration on char yield (Danso-Boateng et al., 2013; Heilmann et al., 2010 and 2011; Sabio et al., 2016). The importance associated with the interaction between initial solids concentration and temperature ranks as the first and second most sensitive interactions for models Y-RT1 and Y-RT2, respectively. This result suggests that temperature imparts a different influence on char yield at various initial solids concentrations. This conclusion

is also consistent with that reported in the literature (Heilmann et al., 2010 and 2011; Sabio et al., 2016; Sevilla & Fuertes, 2009). Initial solids concentration also has appreciable interactions with feedstock oxygen, polarity and ash (Table 5.7). Based on the current knowledge of the HTC process, such interactions are reasonable. It is possible, although not substantiated within the literature, that when carbonizing with high initial solids concentrations, for example, the polarity may have less influence on char yield because of smaller levels of possible feedstock dissolution, which may in turn potentially inhibit the hydrolysis process.

Polarity is also a highly sensitive and interactive parameter, contributing to 10-15% of the predicted variance individually (FSI) and 15-20% of the predicted variance through parameter-to-parameter interactions (Table 5.4, Figure 5.4). As described previously, polarity influencing char yield can be explained by current knowledge of the HTC process. Interactions between polarity and other model parameters (e.g., volatile matter, ash, hydrogen and initial solid concentration, see Table5.7) differ for each regression tree model.

According to the Sobol results, temperature is also highly interactive and contributes to approximately 15% of the predicted variance through interactions with other parameters. This interaction is likely predominantly through its interaction with initial solids concentration, which is highly ranked among all interactions. Feedstock hydrogen content, oxygen content and reaction time are also sensitive parameters based on both regression tree models. They influence char yield mainly by their interactions with other parameters. Char yield is also sensitive to feedstock carbon and cellulose contents in model Y-RT1, but not in model Y-RT2. It is also important to note that

polarity is the second most interactive parameter (Table5.7) and is involved in more interactions with other parameters based on model Y-RT1 than Y-RT2. It should be noted that interpretation of the magnitude of these interactions should be done so cautiously. The confidence intervals of some of these interactions are wide (> 20% of the average sensitivity indices) and the lower bounds of some of them cross zero, indicating these individual interactions may be insignificant.

These Sobol results indicate that, if using regression tree models to describe and/or predict char yield, the most influential parameters are initial solids concentration, feedstock polarity, feedstock ash or volatile matter content, and reaction temperature. Many of these parameters are currently being measured and/or reported, with exception of feedstock polarity (see Table 5.5).

5.3.1.3 Random forest

General parameters describing the random forest models, including R^2, RMSE and MAPE are listed in Table 5.8. As with the linear and regression tree models, these results suggest the two random forest models are similar. The R^2 values associated with both random forest models are the same, and are greater than 0.9, suggesting both random forest models fit the char yield data quite well, suggesting the relationship between char yield and feedstock and process conditions is non-linear. Many models describe a non-linear relationship between char yield and process conditions based on quadratic functions resulting from a design of experiment method (Álvarez-Murillo et al., 2015; Kannan et al., 2017; Nizamuddin et al., 2016; Sabio et al., 2016). Li et al., (2015) previously developed a model that describes a non-linear relationship between feedstock properties and process conditions with hydrochar yield using regression trees. Both the

out-of-bag RMSE and RMSEcv results (Figure 5.5) suggest both random forest models similarly predict char yield and suggest good predictive capability.

Sobol results based on the random forest models are presented in Figure 5.6. These Sobol results suggest initial solids concentration is the most influential parameter on char yield and the second most influential parameter is temperature. Many HTC papers have reported the importance of these two parameters on char yield (Basso et al., 2016; Benavente et al., 2015; Román et al., 2012; Sevilla & Fuertes, 2009), corroborating these results. Based on the differences between the TSI and FSI indices, both initial solids concentration and reaction temperature also exhibit some parameter-to-parameter interactions. According to the detailed interaction analysis (Table 5.9), the interaction between initial solids concentration and temperature is the most significant parameter-to-parameter interaction. Sobol results also indicate polarity is a sensitive parameter, which is consistent with the results obtained from the regression tree models. Feedstock lignin content is also a sensitive parameter, which explains 3% of the predicted variance by itself and contributes to an additional 2% of the predicted variance through its interaction with other parameters (Table5.9). It has been well documented that lignin is only mildly influenced when exposed to the HTC process (Falco et al., 2011), with char yields generally increasing with increasing feedstock lignin content (Kang et al., 2012; Karagöz et al., 2005).

Feedstock carbon and hydrogen contents and reaction time explain less than 1% of the predicted variance by themselves, but each interacts with other parameters (<3% of the predicted variance). According to the detailed interaction analysis, lignin and polarity interact with each other and both interact with initial solid concentration (Table 5.9). In

addition, temperature interacts with reaction time and feedstock hydrogen contents. Studies have reported that severity factor, which is a combination of temperature and time (Ruyter, 1982), can be used to describe the influence of process conditions on char yield (Suwelack et al. 2016a and 2016b), illustrating the existence and validity of this interaction. As described previously, the interpretation of the magnitude of these interactions should be done so cautiously.

In general, these Sobol results suggest that process conditions are more influential on char yield than feedstock properties, which is consistent with previously conducted studies (Li et al., 2015). The most influential parameters (initial solids concentration and reaction temperature) are being routinely reported in the literature (Table5.5). Some of the sensitive parameters, such as lignin and polarity, however, are reported less frequently (Table 5.5). Reporting or considering these parameters when conducting HTC studies that focus on achieving specific char yields should be practiced.

5.3.1.4 Model comparison

The predictive capability (based on RMSEcv) associated with the random forest models is superior to both the linear and regression tree models (Figure 5.7), suggesting a non-linear relationship is most appropriate for describing char yield. The Sobol analysis results also differ between models. There is not a single parameter defined as being highly sensitive that is highly sensitive for all model types (e.g., L, RT, and RF). This result suggests that parameter sensitivity is dependent on model structure and thus, likely, goodness of fit. Models that do not fit the data well likely result in the reporting of parameter sensitivities that may result from model error. This suggests that for char yield, the parameter sensitivities result from the RF models most accurately reflect the true

parameter relationships with char yield. Thus, when conducting HTC experiments with the goal of achieving a certain level of char yield, the following parameters are most influential: Initial solid concentration, temperature, feedstock lignin content, polarity, hydrogen content, carbon content, time and ash content.

5.3.2 Hydrochar carbon content

As described previously, a series of multiple linear regression, regression tree, and random forest models were developed. The feedstock properties and process conditions used in each model were based on results from linear and non-linear correlation tests. Results from linear correlation tests indicate that feedstock ash content is highly correlated (>0.8) with feedstock volatile matter. Results from non-linear correlation tests indicate that feedstock ash content is highly correlated (>0.8) with feedstock volatile mater and feedstock polarity is highly correlated with feedstock carbon content. Therefore, a series of models representing all possible combinations of non-correlated parameters were developed, as presented in Table 5.10. Subsequent sections detail results from each model structure (e.g., linear regression, regression tree, random forest).

5.3.2.1 Linear regression

General parameters describing the linear models, including R^2, adjusted R^2, RMSE and MAPE are shown in Table 5.11. These results suggest all linear models perform similarly, which is not surprising since the only difference between them is the removal of correlated parameters. The R^2 and adjusted R^2 values associated with these models are less than 0.55, like that with hydrochar yield, a linear model does not fit the majority of the data well. The MAPE values indicate all models have a percentage

average absolute error less than 15%. AIC and RMSEcv are shown in Figure 5.8 and indicate that the models similarly predict carbon content.

The results from the Sobol analysis suggest for all models, hydrochar carbon content is most sensitive to feedstock carbon content (Table 5.12, Figure 5.9). This result is consistent with previously published reports that indicate feedstock carbon content influences hydrochar carbon content (Titirici, 2008). In addition, these results indicate that polarity is also a highly sensitive parameter to hydrochar carbon content; polarity explains approximately 10.1% of the predicted variance in C-L1 model and 27.4% of the predicted variance in C-L2 model. As described previously, polarity may have influence on the hydrolysis process which may affect subsequent reactions (e.g., dehydration, decarboxylation and condensation). Hydrochar carbon content is also sensitive to temperature, feedstock ash content or volatile matter, feedstock hydrogen content and reaction time in both C-L1 and C-L2 models. Many HTC papers have reported the influence of temperature and time on hydrochar carbon content (Benavente et al., 2015; Cao et al., 2013; Pala et al., 2014). It is also possible that high feedstock ash content, which remains unconverted during the HTC process, ultimately results in low hydrochar carbon content. Feedstock volatile matter is highly correlated with ash content which makes the high sensitivity of volatile matter possible. Moreover, feedstock cellulose, hemicellulose are sensitive parameters in C-L1 model while feedstock oxygen content is a sensitive parameter in C-L2 model.

These Sobol results indicate that, if using linear models to describe and/or predict hydrochar carbon content, the most critical parameter is feedstock carbon content which is commonly reported (68.4% of the HTC papers, Table 5.5). Some of the sensitive

parameters, such as polarity, cellulose and hemicellulose, however, are reported less frequently (Table 5.5). Reporting and considering these parameters when selecting feedstocks for HTC studies that focus on achieving specific char carbon content should be practiced.

5.3.2.2 Regression tree

General parameters describing the regression tree models are included in Table 5.13. The R^2 results suggest both regression tree models explain approximately 78% of the model predicted variance and thus fit the majority of the data well. The MAPE indicates that all models have an average absolute percentage error less than 6.5%, which is slightly lower than that associated with the linear models. The RMSEcv results indicate the regression tree models similarly predict hydrochar carbon content, with relatively low values (Figure 5.10).

The results for all regression tree models indicate that hydrochar carbon content is highly sensitive to feedstock hydrogen content (Table5.12, Figure5.11). Dehydration is an important pathway during the HTC process (Funke et al., 2010; Libra et al., 2011; Reza et al., 2014). Feedstock hydrogen content, influences the dehydration process (Chheda and Dumesic, 2007), which may contribute to the formation of more condensed aromatic structure (decrease in the H/C and O/C atomic ratios), suggesting the high hydrochar carbon content. Feedstock carbon content is a highly sensitive parameter for regression tree models including it (models C-RT1 and C-RT2). Feedstock hydrogen and carbon content also exhibit large parameter-to-parameter interactions (Table 5.14). Feedstock hydrogen content has an appreciable interaction with carbon content in models including carbon content (model C-RT1 and C-RT2). Studies have reported that the

aromaticity of the organics can influence the condensation reaction (Tayade and Mishra, 2013). Hydrogen also interacts with other parameters, including lignin and reaction temperature in models C-RT1 and C-RT2. It is possible that at various feedstock hydrogen contents, temperature may impart a different influence on the dehydration process, which may result in the change of H/C and O/C ratios in hdyrochar (Reza et al., 2014). For model C-RT1 and C-RT2, hydrochar carbon content is sensitive to temperature. Lignin is also a sensitive parameter. The sensitivity associated with lignin occurs because of its interactions with other parameters The Sobol value associated with the lignin interaction (TSI-FSI) is 0.0664 in model C-RT1 and 0.0672 in model C-RT2.

The Sobol values associated with sensitive interactions in model C-RT3 and C-RT4 are smaller than that in C-RT1 and C-RT2, suggesting fewer but more impactful parameter-to-parameter interactions in C-RT1 and C-RT2. In absence of carbon content and volatile matter (model C-RT4), the feedstock ash content is defined as a highly sensitive and interactive parameter besides hydrogen content. As described previously, it is possible that feedstock ash content may lead to decreases in hydrochar carbon content. The interaction between ash and hydrogen content is significant since it ranks the first for model C-RT4.

These Sobol results indicate that, if using regression tree models to describe and/or predict hydrochar carbon content, the most critical parameter is feedstock hydrogen content. Feedstock carbon content and ash content are also highly influential parameters, depending on the model. These parameters are currently being measured and/or reported by more than 60% of the HTC papers (see Table 5.5).

5.3.2.3 Random forest

General parameters describing the random forest models are listed in Table 5.15. As with the linear and regression tree models, these results suggest random forest models investigated in this study are similar. The R^2 values associated with all these random forest models are the same, and are greater than 0.9, suggesting all these models fit the hydrochar carbon content data quite well, suggesting the relationship between hydrochar carbon content and parameters investigated (e.g., feedstock properties and process conditions) is non-linear. Li et al. (2015) previously developed a regression tree model that can fit the hydrochar carbon content data well and describe the non-linear relationship between hydrochar carbon content and feedstock properties, as well as process conditions. Both the out-of-bag RMSE and RMSEcv results (Figure 5.12) suggest all random forest models investigated similarly predict carbon content in hydrochar and suggest good predictive capability.

Sobol results based on the RF models are presented in Figure 5.13. These Sobol results suggest hydrochar carbon content is highly sensitive to feedstock hydrogen, carbon, and ash content. Feedstock hydrogen content appears to be the dominant parameter; it explains more than 60% of the predicted variance. As described previously, feedstock hydrogen content may affect the condensation of the hydrochar, suggesting its influence on hydrochar carbon content. Other sensitive parameters exist in each model (Table 5.12), but each explains less than 2% of the predicted variance.

Feedstock hydrogen, carbon and ash content are also interactive parameters and they are involved in various parameter-to-parameter interactions (Table 5.16). The interaction between feedstock carbon content and initial solids concentration is

significant since the Sobol value associated with this interaction ranks the first and the third in model C-RF1 and C-RF2, respectively. In the models including feedstock ash content (C-RF2 and C-RF4), the interaction between feedstock ash and hydrogen content is the most important interaction. Moreover, feedstock hydrogen also interacts with process conditions including temperature and time in all these random forest models. This result implies that feedstock hydrogen imparts a different influence on hydrochar carbon content at various temperatures and times.

In general, the Sobol results suggest the feedstock properties are more influential on hydrochar carbon content than process conditions, which is consistent with previously conducted studies (Li et al., 2015). The most influential parameters are feedstock hydrogen (in all studied random forest models), carbon (in model C-RF1 and C-RF2) and ash content (in model C-RF2 and C-RF4). More than 60% of the HTC papers have reported these parameters (see Table 5.5).

The predictive capability (based on RMSEcv) associated with the random forest models is superior to both the linear and regression tree models (Figure 5.14), suggesting a non-linear relationship is most appropriate for describing hydrochar carbon content. When included as a parameter, feedstock carbon content is highly sensitive for all model types. The significance of feedstock hydrogen content on hydrochar carbon content is only observed by the non-linear models. However, feedstock polarity is defined as being highly sensitive for linear models, but not for the non-linear models. As mentioned previously, this result suggests that parameter sensitivity is dependent on model structure and thus, likely, goodness of fit. This suggests that for hydrochar carbon content, the parameter sensitivities resulting from the random forest models most accurately reflect

the true parameter relationships with hydrochar carbon content. Thus, when conducting HTC experiments with the goal of achieving a certain amount of carbon in the hydrochar or feedstock selection, the following parameters are most influential and should be considered: feedstock hydrogen content, carbon content, initial solids concentration and ash content or volatile matter.

5.3.3 Hydrochar energy content

The parameters used in the linear regression, regression tree, and random forest models were based on results from linear and non-linear correlation tests, which indicate that feedstock ash content is highly correlated (>0.8) with volatile matter. Table 5.17 contains a summary of the models developed to describe hydrochar energy content. Subsequent sections detail results from each model structure (e.g., linear regression, regression tree, random forest).

5.3.3.1 Linear regression

General parameters describing the linear models are listed in Table 5.18 and indicate that model performance is similar. The R^2 and adjusted R^2 values associated with these models are less than 0.7, suggesting a linear model fits the hydrochar energy content data better than that associated with hydrochar carbon content and yield. The MAPE values indicate that all models have an average absolute percentage error less than 10%. AIC and RMSEcv (Figure 5.15) indicate that the models similarly predict hydrochar energy content.

Results from the Sobol analysis are shown in Figure 5.16. Hydrochar energy content is highly sensitive to feedstock polarity, oxygen content, hydrogen content and ash content or volatile matter (Table 5.19). Many studies have demonstrated that the

heating value of a fuel can be predicted using the elemental composition and/or proximate properties of the fuel (Table 5.20). Among most of these relationships, hydrogen content is the most influential parameter according to the regression coefficient. Polarity is also a highly sensitive parameter. It is possible that feedstock polarity influences feedstock hydrolysis (Rutherford et al., 1992), which may ultimately influence carbonization extent. More carbonization may lead to higher hydrochar energy content. . It is logical that energy content is highly sensitive to feedstock ash content since ash is non-combustible (Akowuah et al., 2012) and the increase of feedstock ash content may lead to the decrease of hydrochar energy content. Feedstock volatile matter is highly correlated with ash content which makes the high sensitivity of volatile matter possible.

Hydrochar energy content is sensitive to feedstock carbon, cellulose and hemicellulose content and each parameter explains less than 2.5% of the predicted variance. Feedstock fixed carbon is also a sensitive parameter in model E-L1 but not in E-L2. Besides the aformentioned feedstock properties, hydrochar energy content is also sensitive to temperature and time, which is consistent with previously published studies (Álvarez-Murillo et al., 2015; Benavente et al., 2015; Hoekman et al., 2011; Pala et al., 2014; Reza et al., 2014). It has been well documented that hydrochar energy content increases with temperature and time during HTC process (Danso-Boateng et al., 2013; Pala et al., 2014; Reza et al., 2014).

These Sobol results indicate that, if using linear models to describe and/or predict hydrochar energy content, the most critical feedstock properties are being measured and reported, with the exception of polarity and volatile matter. No papers currently report feedstock polarity and only 36.5% of the papers report feedstock volatile matter (Table

5.5). Many of the sensitive parameters are reported except for cellulose and hemicellulose content, which are reported by less than 20% of the HTC related papers.

5.3.3.2 Regression tree

General parameters describing the regression tree models are listed in Table 5.21. The R^2 results suggest both regression tree models explain less than 85% of the model predicted variance and thus fit the majority of the data well. The MAPE indicates that all models have an average absolute percentage error of approximately 6.3%, which is similar as that for the linear models. The RMSEcv results indicate the regression tree models similarly predict hydrochar energy content, with relatively low values (Figure 5.17). These values are similar to the linear regression models.

Sobol results based on the regression tree models are presented in Figure 5.18. The results for both models indicate that feedstock hydrogen content is the most influential parameter on hydrochar energy content. Feedstock carbon content is the second most influential parameter. Feedstock hydrogen content explains approximately 55% of the predicted variance by itself (FSI) and contributes to approximately 20% of predicted variance through its interaction with other parameters (TSI-FSI). Feedstock hydrogen content is involved in the interaction with feedstock carbon content, oxygen content and ash or volatile matter (Table 5.22) which indicates that with various feedstock hydrogen contents, the influence of feedstock carbon content, oxygen content and ash or volatile matter on hydrochar energy content changes. During combustion, some bonds among C, H and O atoms are broken and reformed, which may result in the interaction between hydrogen and carbon content as well as hydrogen and oxygen content. The second order empirical relationship associated with energy content suggested by

Grummel and Davis (Table 5.20) also indicates the possibility of the existence of interactions between hydrogen and carbon content as well as hydrogen and oxygen content.

Feedstock ash content or volatile matter are also sensitive parameters, mainly influencing hydrochar energy content by two-parameter and three-parameter interactions with feedstock hydrogen and carbon content (Table 5.22). Besides the interactions among feedstock properties, time also interacts with feedstock hydrogen content, suggesting hydrogen content may have a different influence on hydrochar energy content at various reaction times. Temperature is the fifth most interactive parameter (Table 5.22), however, interactions associated with temperature are not ranked among the top five, suggesting that temperature is involved in small interactions with many parameters.

In general, the Sobol results suggest the feedstock properties are more influential on hydrochar energy content than process conditions, which is consistent with previously conducted studies (Li et al., 2015). The top three most influential parameters are feedstock hydrogen, carbon and oxygen content and less than 70% of the HTC papers are currently being measured and/or reported (see Table 5.5). These results are reasonable, since many empirical relationships associated with energy content (Table 5.22) indicate the importance of the fuel source elemental composition ranks as follows: hydrogen > carbon > oxygen.

5.3.3.3 Random forest

General parameters describing the random forest models are provided in Table 5.23. As with the linear regression and regression tree models, these results suggest random forest models investigated in this study are similar. The R^2 values associated with

all these random forest models are the same, and are greater than 0.9. Both the out-of-bag RMSE and RMSEcv results (Figure 5.19) suggest all random forest models investigated similarly predict hydrochar energy content and suggest good predictive capability.

Sobol results based on the random forest models are presented in Figure 5.20. These Sobol results suggest feedstock hydrogen content is the most influential parameter on hydrochar energy content, similar to that described for the linear regression and regression tree models. Feedstock carbon content is the second most sensitive parameter; it is a highly sensitive parameter in model E-RF1 and a sensitive parameter in model E-RF2. Hydrogen is the most interactive parameter, according to the detailed interaction analysis (Table 5.24). Feedstock hydrogen content interacts with feedstock carbon, oxygen, and ash contents, as well as with reaction time. These interactions suggest with various feedstock hydrogen contents, feedstock carbon, oxygen and ash content, as well as reaction time have a different influence on hydrochar energy content. With various reaction times, the hydrogen content remains in hydrochar may be different and therefore influences hydrochar energy content differently. Feedstock ash content is defined as a sensitive parameter in model E-RF2. As mentioned previously, ash is non-combustible and the increase of feedstock ash content may lead to the decrease of hydrochar energy content.

These Sobol results indicate that, if using random forest models to describe and/or predict hydrochar energy content, the influential parameters are feedstock hydrogen, carbon, oxygen, and ash contents and reaction temperature and time. More than 60% of the HTC papers report these parameters (see Table 5.5).

5.3.3.4 Model comparison

Based on RMSEcv (Figure 5.21), the predictive capability associated with random forest models is better than the linear models, while random forest and regression tree models have similar predictive capabilities. Feedstock hydrogen content is highly sensitive in all models. The significance of feedstock carbon content on hydrochar energy content is captured. It can explain less than 2% of the predicted variance in each linear model and less than 30% of the predicted variance in each non-linear model. Feedstock polarity is defined as being highly sensitive for linear models but not for regression tree and random forest models. As mentioned previously, this result suggests that parameter sensitivity is dependent on model structure and thus, likely, goodness of fit. This suggests that for hydrochar energy content, the parameter sensitivities result from the random forest models most accurately reflect the true parameter relationships with hydrochar energy content. Thus, when conducting HTC experiments with the goal of achieving a certain level of hydrochar energy content, feedstock hydrogen content, carbon content, oxygen content, ash content, temperature and time are most influential parameters. This is consistent with the importance suggested by many relationships associated with energy content (Table 5.20).

5.4 CONCLUSION

The predictive capabilities associated with the nonlinear models are better than the linear models for describing hydrochar yield, carbon content and energy content. Parameter sensitivity is dependent on model structure and global sensitivity analysis results indicate that the most influential parameters are initial solid concentration, temperature, feedstock lignin content, polarity, hydrogen content, carbon content, time

and ash content when conducting HTC experiments with the goal of achieving a certain level of hydrochar yield. The most influential parameters to hydrochar carbon content are feedstock hydrogen content, carbon content, initial solids concentration and ash content or volatile matter. The most influential parameters to hydrochar energy content are feedstock hydrogen content, carbon content, oxygen content, ash content, temperature and time. If carbonizing to meet a specific hydrothermal carbonization objective, these influential parameters should be considered.

Table 5.1. Feedstock properties and process conditions investigated in this study.

Parameter	Unit	Abbreviation	Data Source
Ash	%, dry basis	Ash_{feed}	If available, taken from the individual study. If not available, literature searches were conducted to obtain the average ash content for that feedstock.
Volatile matter	%, dry basis	VM_{feed}	If available, taken from the individual study. If not available, literature searches were conducted to obtain the average volatile matter for that feedstock.
Fixed carbon	%, dry basis	FC_{feed}	If available, taken from the individual study. If not available, literature searches were conducted to obtain the average fixed carbon for that feedstock.
Carbon	%, dry basis	C_{feed}	If available, taken from the individual study. If not available, literature searches were conducted to obtain the average carbon content for that feedstock.
Hydrogen	%, dry basis	H_{feed}	If available, taken from the individual study. If not available, literature searches were conducted to obtain the average hydrogen content for that feedstock.
Oxygen	%, dry basis	O_{feed}	If available, taken from the individual study. If not available, literature searches were conducted to obtain the average oxygen content for that feedstock.
Polarity	-*	Pol_{feed}	Calculated value
Cellulose	%, dry basis	Cel_{feed}	If available, taken from the individual study. If not available, literature searches were conducted to obtain the average cellulose content for that feedstock.
Hemicellulose	%, dry basis	Hem_{feed}	If available, taken from the individual study. If not available, literature searches were conducted to obtain the average hemicellulose content for that feedstock.
Lignin	%, dry basis	Lig_{feed}	If available, taken from the individual study. If not available, literature searches were conducted to obtain the average lignin content for that feedstock.
Initial solid concentration	%, dry basis	$Solids_{initial}$	Taken from the individual study.
Temperature	^{o}C	T_{final}	Taken from the individual study.
time	min	t	Taken from the individual study.

*- represents that parameter is unitless

Table 5.2. Char yield models developed in this study.

Model ID	Model Type	Parameters Not Included in the Model
Y-L1	Linear regression	Ash_{feed}
Y-L2	Linear regression	VM_{feed}
Y-RT1	Regression tree	Ash_{feed}
Y-RT2	Regression tree	VM_{feed}
Y-RF1	Random forest	Ash_{feed}
Y-RF2	Random forest	VM_{feed}

Table 5.3. Performance of the linear regression models of hydrochar yield.*

Model ID	R^2	adjusted R^2	RMSE	MAPE
Y-L1	0.465	0.4547	13.01 (12.26-13.72)	27.69 (26.10-29.20)
Y-L2	0.491	0.481	12.69 (11.96-13.38)	26.71 (25.17-28.16)

*values in parentheses represent the 95% confidence interval.

Table 5.4. Summary of parameter sensitivities to char yield based on different models.*

Sensitivity	Linear regression		Regression tree		Random forest	
	Y-L1	Y-L2	Y-RT1	Y-RT2	Y-RF1	Y-RF2
Highly sensitivie	Pol_{feed} (0.4640) O_{feed} (0.2675)	Pol_{feed}(0.5047) O_{feed}(0.2831)	$Solids_{initial}$(0.4963) Pol_{feed}(0.4162) VM_{feed}(0.2974) T_{final}(0.1586)	$Solids_{initial}$(0.5347) Ash_{feed}(0.3480) Pol_{feed}(0.2733) T_{final}(0.1735)	$Solids_{initial}$(0.5433) T_{final}(0.3963)	$Solids_{initial}$(0.5339) T_{final}(0.3842)
Sensitive	VM_{feed}(0.0667) T_{final}(0.0628) FC_{feed}(0.0588) $Solids_{initial}$(0.0559) H_{feed} (0.0182)	Ash_{feed} (0.0647) T_{final}(0.0535) $Solids_{initial}$(0.0375) H_{feed}(0.0210) FC_{feed}(0.0137) Lig_{feed}(0.0114)	H_{feed}(0.0894) O_{feed}(0.0866) t(0.0121)	O_{feed} (0.0969) C_{feed}(0.0462) t(0.0209) Cel_{feed}(0.0204) H_{feed}(0.0172)	Lig_{feed}(0.0547) Pol_{feed},(0.0409) H_{feed}(0.0278) C_{feed}(0.0149) t(0.0137)	Lig_{feed}(0.0474) Pol_{feed}(0.0457) H_{feed}(0.0342) Ash_{feed}(0.0206) t(0.0146) C_{feed}(0.0126)
Insensitive	Lig_{feed} (0.0091) t (0.0061) C_{feed}(0.0033) Hem_{feed}(0.0007) Cel_{feed}(0.0002)	t (0.0064) C_{feed}(0.0016) Cel_{feed}(0.0006) Hem_{feed}(0.0004)	Cel_{feed}(0.0068) C_{feed}(0.0028) FC_{feed}(0.0015) Lig_{feed}(0.0010) Hem_{feed}(0.0004)	FC_{feed}(0.0043) Lig_{feed}(0.0021) Hem_{feed}(0.0003)	VM_{feed}(0.0061) O_{feed}(0.0042) Cel_{feed},(0.0038) FC_{feed}(0.0033) Hem_{feed}(0.0017)	FC_{feed}(0.0037) Cel_{feed}(0.0035) O_{feed} (0.0035) Hem_{feed},(0.0015)

*values in parentheses represent the TSI associated with that parameter.

Table 5.5 Overview of collected feedstock properties and process conditions from the literature.

Parameter	% of Papers Reporting
Ash (%, db)	64.2
Volatile matter (%, db)	36.5
Fixed carbon (%, db)	36.5
Carbon (%, db)	68.4
Hydrogen (%, db)	67.9
Oxygen (%, db)	66.8
Polarity	0
Cellulose (%, db)	19.5
Hemicellulose (%, db)	19.5
Lignin (%, db)	19.5
Initial solid concentration (%)	90.5
Temperature (oC)	100.0
Time (min)	100.0

Table 5.6. Performance of regression tree models*.

Model ID	R^2	adjusted R^2	RMSE	MAPE
Y-RT1	0.776	0.618	8.43 (7.94-8.88)	12.81 (12.07-13.51)
Y-RT2	0.775	0.588	8.45 (7.96-8.91)	12.49 (11.77-13.17)

*values in parentheses represent the 95% confidence interval.

Table 5.7. Sobol of the interactions based on regression tree models of hydrochar yield.*

Model ID	Degree of interaction		Interaction	
	1	$Solids_{initial}$ (0.2850)	1	VM_{feed}*Pol_{feed}
	2	Pol_{feed} (0.2538)	2	$Solids_{initial}$*T_{final}
	3	VM_{feed} (0.1839)	3	$Solids_{initial}$*O_{feed}
	4	T_{final} (0.1336)	4	H_{feed}*Pol_{feed}
Y-RT1	5	O_{feed} (0.0750)	5	$Solids_{initial}$*Pol_{feed}
	1	$Solids_{initial}$ (0.2881)	1	$Solids_{initial}$*T_{final}
	2	Ash_{feed} (0.1709)	2	Ash_{feed}*Pol_{feed}
	3	Pol_{feed} (0.1685)	3	$Solids_{initial}$*O_{feed}
	4	T_{feed} (0.1604)	4	Ash_{feed}*$Solids_{initial}$
Y-RT2	5	O_{feed} (0.0929)	5	$Solids_{initial}$*Pol_{feed}

* values in parentheses represent the average Sobol index

Table 5.8. Performance of random forest models of hydrochar yield.*

Model	R^2	RMSE	MAPE
Y-RF1	0.942	4.28 (4.03-4.51)	6.03 (5.68-6.36)
Y-RF2	0.942	4.27 (4.02-4.50)	6.03 (5.68-6.36)

*values in parentheses represent the 95% confidence interval

Table 5.9. Sobol of the interactions based on random forest models.

Model ID	Degree of interaction		Interaction	
Y-RF1	1	T_{final} (0.0575)	1	$Solids_{initial}$*T_{final}
	2	$Solids_{initial}$ (0.0555)	2	Lig_{feed}*Pol_{feed}
	3	Lig_{feed} (0.0246)	3	$Solids_{initial}$*Pol_{feed}
	4	Pol_{feed} (0.0239)	4	T_{final}*H_{feed}
	5	H_{feed} (0.0235)	5	Lig_{feed}*$Solids_{initial}$
Y-RF2	1	T_{final} (0.0556)	1	$Solids_{initial}$*T_{final}
	2	$Solids_{initial}$ (0.0470)	2	T_{final}*H_{feed}
	3	H_{feed} (0.0184)	3	$Solids_{initial}$*Pol_{feed}
	4	Pol_{feed}(0.0149)	4	Lig_{feed}*Pol_{feed}
	5	Lig_{feed} (0.0140)	5	Lig_{feed}*$Solids_{initial}$

* values in parentheses represent the average Sobol index.

Table 5.10. Hydrochar carbon content models developed in this study.

Model ID	Model Type	Parameters Not Included in the Model
C-L1	Linear regression	Ash_{feed}
C-L2	Linear regression	VM_{feed}
C-RT1	Regression tree	Ash_{feed} and Pol_{feed}
C-RT2	Regression tree	VM_{feed} and Pol_{feed}
C-RT3	Regression tree	Ash_{feed} and C_{feed}
C-RT4	Regression tree	VM_{feed} and C_{feed}
C-RF1	Random forest	Ash_{feed} and Pol_{feed}
C-RF2	Random forest	VM_{feed} and Pol_{feed}
C-RF3	Random forest	Ash_{feed} and C_{feed}
C-RF4	Random forest	VM_{feed} and C_{feed}

Table 5.11. Performance of the linear regression models of hydrochar carbon content.*

Model ID	R^2	adjusted R^2	RMSE	MAPE
C-L1	0.497	0.484	7.46 (6.93-7.95)	10.06 (9.35-10.72)
C-L2	0.517	0.504	7.31 (6.79-7.79)	9.81 (9.12-10.45)

*values in parentheses represent the 95% confidence interval.

Table 5.12. Summary of parameter sensitivities to hydrochar carbon based on different models.*

Sensitivity	Linear regression		Regression tree				Random forest			
	C-L1	C-L2	C-RT1	C-RT2	C-RT3	C-RT4	C-RF1	C-RF2	C-RF3	C-RF4
Highly sensitive (>0.1)	C_{feed} (0.4775) T_{final} (0.1354) Pol_{feed} (0.1007)	C_{feed} (0.3142) Pol_{feed} (0.2736) Ash_{feed} (0.1066)	C_{feed} (0.7845) H_{feed} (0.4527)	C_{feed} (0.7840) H_{feed} (0.4527)	H_{feed} (0.9657)	H_{feed} (0.6437) Ash_{feed} (0.4763)	H_{feed} (0.6245) C_{feed} (0.2977)	H_{feed} (0.6567) C_{feed} (0.1835) Ash_{feed} (0.1537)	H_{feed} (0.9723)	H_{feed} (0.8396) Ash_{feed} (0.1659)
Sensitive (0.01-0.1)	VM_{feed} (0.0836) H_{feed} (0.0801) t (0.0678) $Solid_{sinitial}$ (0.0244) Cel_{feed} (0.0132) Hem_{feed} (0.0125)	T_{final} (0.0852) H_{feed} (0.0682) O_{feed} (0.0629) t (0.0435)	Lig_{feed} (0.0664) T_{final} (0.0185)	Lig_{feed} (0.0672) T_{final} (0.0183)	$Solid_{sinitial}$ (0.0343) VM_{feed} (0.0221) Hem_{feed} (0.0192) O_{feed} (0.0160) t (0.0129)	Hem_{feed} (0.0319) t (0.0222) Pol_{feed} (0.0225)	$Solid_{sinitial}$ (0.0159) T_{final} (0.0132) VM_{feed} (0.0117) Cel_{feed} (0.0116)	Hem_{feed} (0.0148) $Solid_{sinitial}$ (0.0144) T_{final} (0.0129) t (0.0110)	VM_{feed} (0.0135) $Solid_{sinitial}$ (0.0122)	Hem_{feed} (0.0101) $Solid_{sinitial}$ (0.0108)
Insensitive(<0.01)	Lig_{feed} (0.0058) FC_{feed} (0.0014) O_{feed} (0)	Hem_{feed} (0.0099) FC_{feed} (0.0092) Lig_{feed} (0.0086) $Solid_{sinitial}$ (0.0079) Cel_{feed} (0.0057)	t (0.0087) $Solid_{sinitial}$ (0.0012) Cel_{feed} (0.0011) Hem_{feed} (0.0007) O_{feed} (0.0005) FCfeed (0.0004) VMfeed	t (0.0089) $Solid_{sinitial}$ (0.0011) Cel_{feed} (0.0010) Hem_{feed} (0.0009) O_{feed} (0.0005) FC_{feed} (0.0004) Ash_{feed}	T_{final} (0.0026) Pol_{feed} (0.0025) Cel_{feed} (0.0002) FC feed (0) Lig_{feed} (0)	T_{final} (0.0024) Cel_{feed} (0.0010) $Solid_{sinitial}$ (0.0062) O_{feed} (0.0006) FC_{feed} (0.0004) Lig_{feed} (0)	Hem_{feed} (0.0098) t (0.0086) Lig_{feed} (0.0009) O_{feed} (0.0008) FC_{feed} (0.0008)	Cel_{feed} (0.0080) Lig_{feed} (0.0010) FC_{feed} (0.0009) O_{feed} (0.0007)	T_{final} (0.0085) Hem_{feed} (0.0071) t (0.0055) Cel_{feed} (0.0014) Lig_{feed} (0.0008) Pol_{feed} (0.0008) O_{feed}	t (0.0093) T_{final} (0.0086) Cel_{feed} (0.0013) Pol_{feed} (0.0008) Lig_{feed} (0.0007) O_{feed} (0.0005) FC_{feed}

			(0)	(0)					(0.0005)	(0.0005)
									FC_{feed} (0.0002)	

*values in parentheses represent the TSI associated with that parameter

Table 5.13. Performance of the regression tree models of hydrochar carbon content.*

Model ID	R^2	Adjusted R^2	RMSE	MAPE
C-RT1	0.788	0.769	4.84 (4.50-5.16)	6.13 (5.70-6.54）
C-RT2	0.778	0.757	4.96 (4.61-5.28)	6.36 (5.91-6.77)
C-RT3	0.787	0.767	4.86 (4.52-5.18)	6.38 (5.93-6.79)
C-RT4	0.792	0.774	4.80 (4.46-5.11)	6.12 (5.69-6.52)

*values in parentheses represent the 95% confidence interval

Table 5.14. Sobol of the interactions based on regression tree models of hydrochar carbon content.*

Model ID	Degree of interaction			Interaction	
C-RT1	1	H	0.2767	1	C*H
	2	C	0.2614	2	Lignin*H
	3	Lignin	0.0664	3	Lignin*C*H
	4	Temp	0.0185	4	Temp*t
	5	t	0.0087	5	Temp*H
C-RT2	1	H	0.2769	1	C*H
	2	C	0.2615	2	Lignin*H
	3	Lignin	0.0672	3	Lignin*C*H
	4	Temp	0.0183	4	Temp*t
	5	t	0.0089	5	Temp*H
C-RT3	1	H	0.0494	1	VM*H
	2	Solid	0.0259	2	Solid*H
	3	VM	0.0208	3	H*O
	4	O	0.0150	4	Hem*H
	5	Hem	0.0138	5	Solid*O
C-RT4	1	Ash	0.1736	1	Ash*H
	2	H	0.1625	2	Ash*Polarity
	3	Hem	0.0276	3	Hem*Ash
	4	Polarity	0.0225	4	H*Polarity
	5	t	0.0196	5	t*H

* values in parentheses represent the average Sobol index.

Table 5.15. Performance of the random forest models on hydrochar carbon content.*

Model ID	R^2	RMSE	MAPE
C-RF1	0.935	2.68 (2.49-2.85)	3.12 (2.90-3.33)
C-RF2	0.935	2.68 (2.50-2.86)	3.14 (2.92-3.35)
C-RF3	0.934	2.70 (2.51-2.88)	3.17 (2.95-3.38)
C-RF4	0.934	2.70 (2.51-2.88)	3.17 (2.95-3.38)

*values in parentheses represent the 95% confidence interval

Table 5.16. Sobol of the interactions based on random forest models of hydrochar carbon content.*

Model ID	Degree of interaction			Interaction	
C-RF1	1	C	0.0216	1	Solid*C
	2	H	0.0202	2	C*H
	3	Solid	0.0118	3	t*H
	4	Temp	0.0088	4	Temp*H
	5	Cel	0.0065	5	Solid*H
C-RF2	1	Ash	0.0333	1	Ash*H
	2	H	0.0331	2	Hem*Ash
	3	C	0.0161	3	Solid*C
	4	Hem	0.0147	4	Temp*H
	5	Solid	0.0145	5	t*H
C-RF3	1	H	0.0177	1	Solid*H
	2	Solid	0.0092	2	Temp*H
	3	Temp	0.0055	3	Lignin*H
	4	t	0.0033	4	t*H
	5	Hem	0.0032	5	Temp*t
C-RF4	1	H	0.0343	1	Ash*H
	2	Ash	0.0338	2	Hem*Ash
	3	Solid	0.0108	3	Solid*H
	4	Hem	0.0101	4	Temp*H
	5	t	0.0093	5	t*H

Table 5.17. Hydrochar energy content models developed in this study.

Model ID	Model Type	Parameters Not Included in the Model
E-L1	Linear regression	Ash_{feed}
E-L2	Linear regression	VM_{feed}
E-RT1	Regression tree	Ash_{feed}
E-RT2	Regression tree	VM_{feed}
E-RF1	Random forest	Ash_{feed}
E-RF2	Random forest	VM_{feed}

Table 5.18. Performance of the linear regression models of hydrochar energy content.*

Model ID	R^2	adjusted R^2	RMSE	MAPE
E-L1	0.663	0.653	2.54 (2.37-2.71)	8.57 (7.97-9.13)
E-L2	0.662	0.652	2.55 (2.37-2.72)	8.64 (8.03-9.20)

*values in parentheses represent the 95% confidence interval

Table 5.19. Summary of parameter sensitivities to hydrochar energy content based on different models.

Sensitivity	Linear regression		Regression tree		Random forest	
	E-L1	E-L2	E-RT1	E-RT2	E-RF1	E-RF2
Highly sensitive	O_{feed} (0.2225) Pol_{feed} (0.2213) H_{feed} (0.2122) VM_{feed} (0.1774)	Pol_{feed} (0.2887) O_{feed} (0.2469) H_{feed} (0.2082) Ash_{feed} (0.1306)	H_{feed} (0.7633) C_{feed} (0.2484) O_{feed} (0.1088)	H_{feed} (0.7598) C_{feed} (0.2813)	H_{feed} (0.7298) C_{feed} (0.2339)	H_{feed} (0.8169)
Sensitive	T_{final} (0.0466) FC_{feed} (0.0299) t (0.0270) Cel_{feed} (0.0245) Hem_{feed} (0.0191) C_{feed} (0.0116)	T_{final} (0.0440) t (0.0251) Cel_{feed} (0.0177) C_{feed} (0.0148) Hem_{feed} (0.0116)	VM_{feed} (0.0552) t (0.0521) T_{final} (0.0426) Pol_{feed} (0.0129)	O_{feed} (0.0948) Ash_{feed} (0.0485) t (0.0454) T_{final} (0.0371) Pol_{feed} (0.0112)	T_{final} (0.0712) O_{feed} (0.0407) t (0.0347)	C_{feed} (0.0750) Ash_{feed} (0.0712) T_{final} (0.0542) O_{feed} (0.0386) t (0.0293)
Insensitive	$Solid_{sinitial}$ (0.0077) Lig_{feed} (0.0042)	FC_{feed} (0.0085) $Solid_{sinitial}$ (0.0047) Lig_{feed} (0.0015)	Cel_{feed} (0.0078) Hem_{feed} (0.0007) $Solids_{initial}$ (0.0003) FC_{feed} (0.0001) Lig_{feed} (0.0000)	Cel_{feed} (0.0068) Hem_{feed} (0.0006) $Solids_{initial}$ (0.0003) Fc_{feed} (0.0001) Lig_{feed} (0.0000)	Pol_{feed} (0.0099) VM_{feed} (0.0075) $Solids_{initial}$ (0.0024) Hem_{feed} (0.0012) Lig_{feed} (0.0010) Cel_{feed} (0.0006) FC_{feed} (0.0003)	Pol_{feed} (0.0076) $Solids_{initial}$ (0.0022) Hem_{feed} (0.0016) Cel_{feed} (0.0006) Lig_{feed} (0.0006) FC_{feed} (0.0002)

*values in parentheses represent the TSI associated with that parameter.

Table 5.20 Empirical relationship between the HHV of fuel and ultimate/proximate properties. (Yuan et al., 2009; Channiwala et al., 2002; Sheng et al., 2005; Parikh et al., 2005; Cordero et al., 2001)

Reference	Empirical Correlation
Dulong (1880)	$HHV = 0.3383 \cdot C + 1.443 \cdot (H - O/8)$
Strache and Lant (1924)	$HHV = 0.3406 \cdot C + 1.4324 \cdot H - 0.1532 \cdot O + 0.1047 \cdot S$
Grummel and Davis (1933)	$HHV = (0.0152 \cdot H + 0.9875)\ (C/3 + H - (O - S)/8)$
Gumz (1938)	$HHV = 0.3403 \cdot C + 1.2432 \cdot H + 0.0628 \cdot H^2 + 0.1909 \cdot S - 0.0984 \cdot O$
Sumegi (1939)	$HHV = 0.3391 \cdot (C - 0.75 \cdot O/2) + 1.444 \cdot (H - 0.125 \cdot O/2) + 0.1047 \cdot S$
Boie (1952)	$HHV = 0.3516 \cdot C + 1.16225 \cdot H + 0.1109 \cdot O + 0.0628 \cdot N + 0.10465 \cdot S$
Channiwala (2002)	$HHV = 0.3491 \cdot C + 1.178 \cdot H + 0.1005 \cdot S - 0.1034 \cdot O - 0.0151 \cdot N - 0.0211 \cdot ash$
Sheng and Azevedo (2005)	$HHV = 0.3137 \cdot C + 0.7009 \cdot H - 0.0318 \cdot O - 1.3675$ MJ/kg
Kucukbayrak (1991)	$HHV = 76.56 - (1.3 \cdot (VM + ash) - 7.03/1000 \cdot (VM + ash)^2)$
Cordero et al. (2001)	$HHV = 0.3543\ FC + 0.1708\ VM$
Parikh et al. (2005)	$HHV = 0.3536 \cdot FC + 0.1559 \cdot VM - 0.0078 \cdot ash$
Demirbas (1997)	$HHV = (313.3 \cdot (VM + FC))/1000 - 10814.08$ MJ/kg
Jimenez and Gonzales (1991)	$HHV = 14.119 + 0.196 \cdot FC$

Table 5.21. Performance of regression tree models of hydrochar energy content.*

Model ID	R^2	adjusted R^2	RMSE	MAPE
E-RT1	0.813	0.791	1.90 (1.76-2.02)	6.34 (5.90-6.76)
E-RT2	0.815	0.791	1.89 (1.75-2.01)	6.30 (5.86-6.72)

*values in parentheses represent the 95% confidence interval.

Table 5.22. Sobol of the interactions based on regression tree models of hydrochar energy content.*

Model ID	Degree of interaction			Interaction	
E-RT1	1	H	0.2089	1	C*H
	2	C	0.1379	2	H*O
	3	O	0.0707	3	VM*H
	4	VM	0.0455	4	VM*C*H
	5	Temp	0.0295	5	t*H
E-RT2	1	H	0.2133	1	C*H
	2	C	0.1584	2	H*O
	3	O	0.0667	3	Ash*C
	4	Ash	0.0456	4	Ash*C*H
	5	Temp	0.0316	5	t*H

* values in parentheses represent the average Sobol index

Table 5.23. Performance of random forest models of hydrochar energy content.*

Model ID	R^2	RMSE	MAPE
E-RF1	0.949	0.99 (0.92-1.06)	3.07 (2.85-3.27)
E-RF2	0.949	0.99 (0.92-1.05)	3.08 (2.86-3.28)

*values in parentheses represent the 95% confidence interval.

Table 5.24. Sobol of the interactions based on random forest models.*

Model ID	Degree of interaction			Interaction	
E-RF1	1	H	0.112015	1	C*H
	2	C	0.075972	2	H*O
	3	O	0.037334	3	t*H
	4	Temp	0.016364	4	C*Polarity
	5	t	0.014821	5	C*O
E-RF2	1	H	0.082741	1	Ash*H
	2	Ash	0.037571	2	C*H
	3	O	0.033659	3	H*O
	4	C	0.023497	4	t*H
	5	t	0.016746	5	Ash*Temp

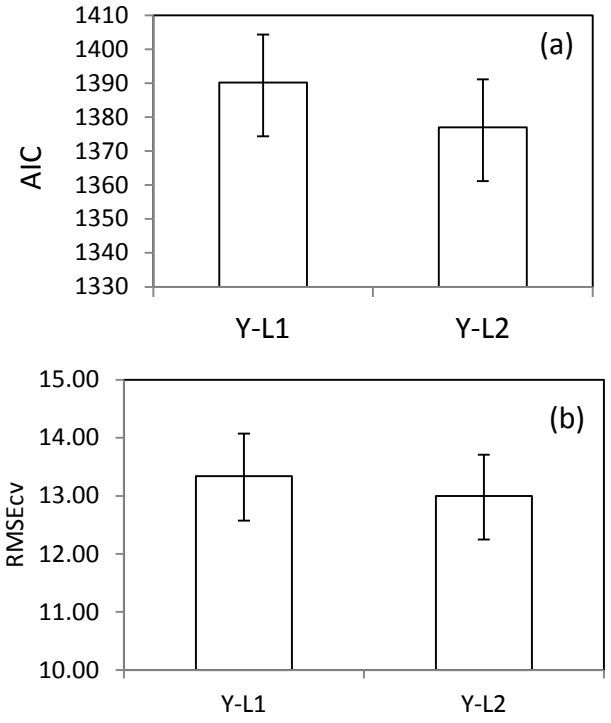

Figure 5.1. AIC (a) and RMSEcv (b) associated with the linear regression models of hydrochar yield.

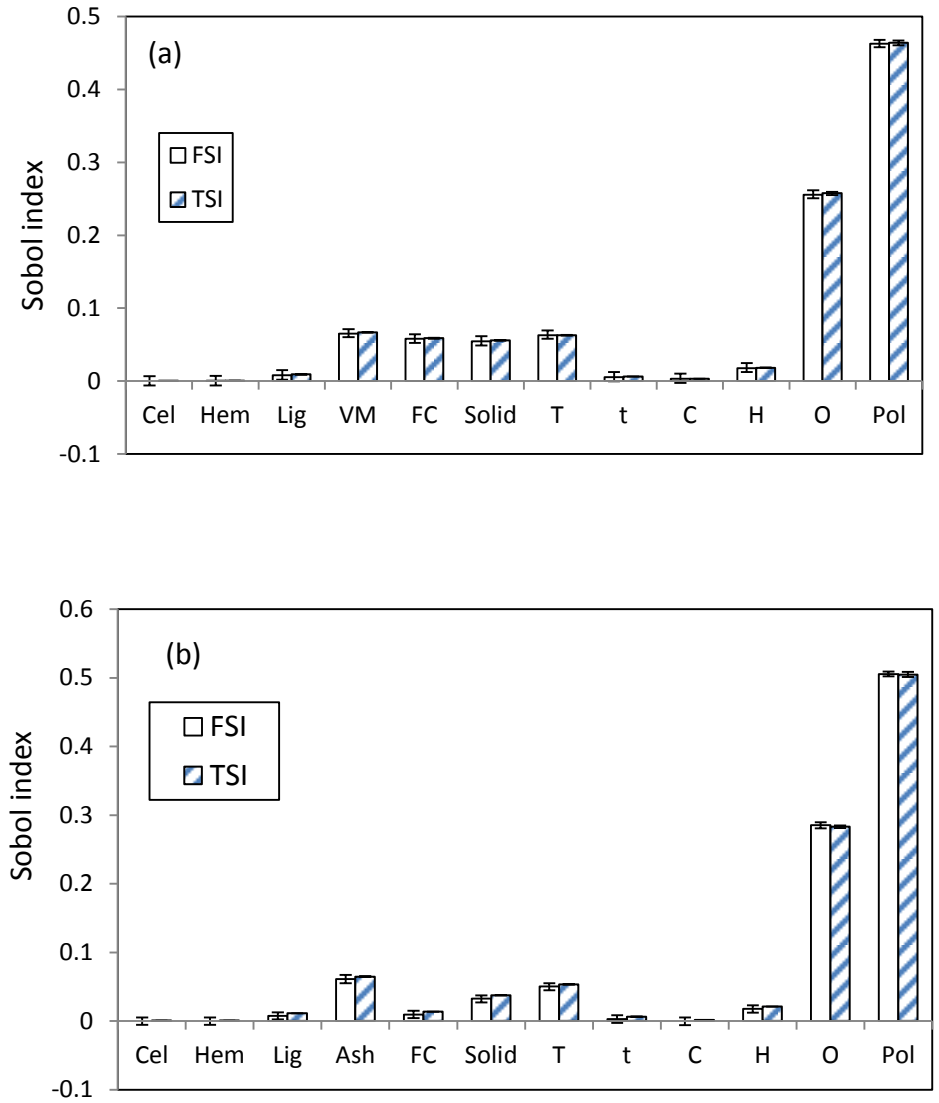

Figure 5.2. FSI and TSI of each parameter based on model Y-L1 (a) and Y-L2 (b).

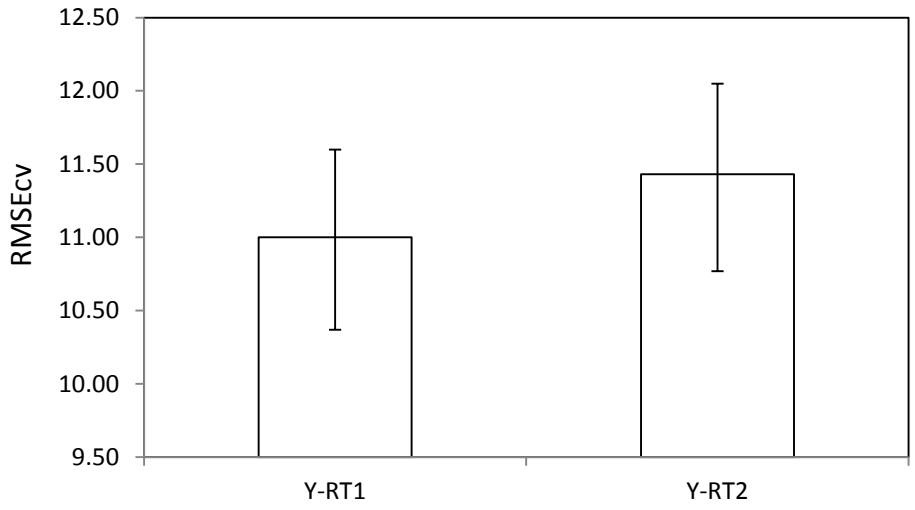

Figure 5.3. RMSEcv associated with regression tree models of hydrochar yield.

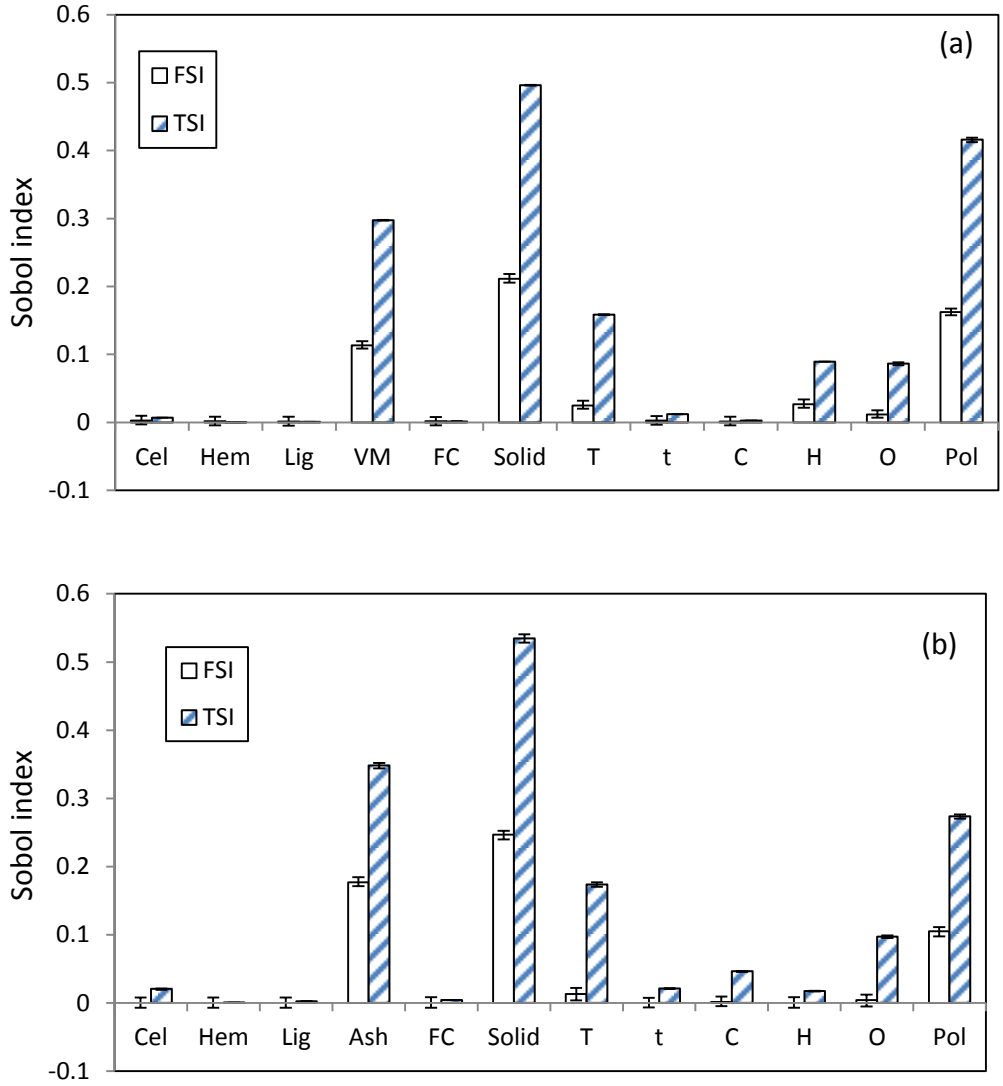

Figure 5.4. FSI and TSI of each parameter based on model Y-RT1 (a) and Y-RT2 (b).

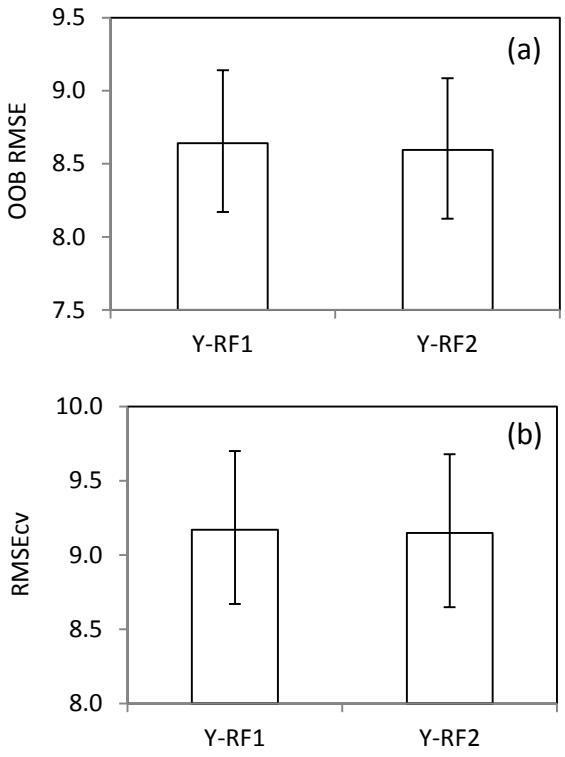

Figure 5.5. OOB RMSE (a) and RMSEcv (b) associated with random forest models of hydrochar yield.

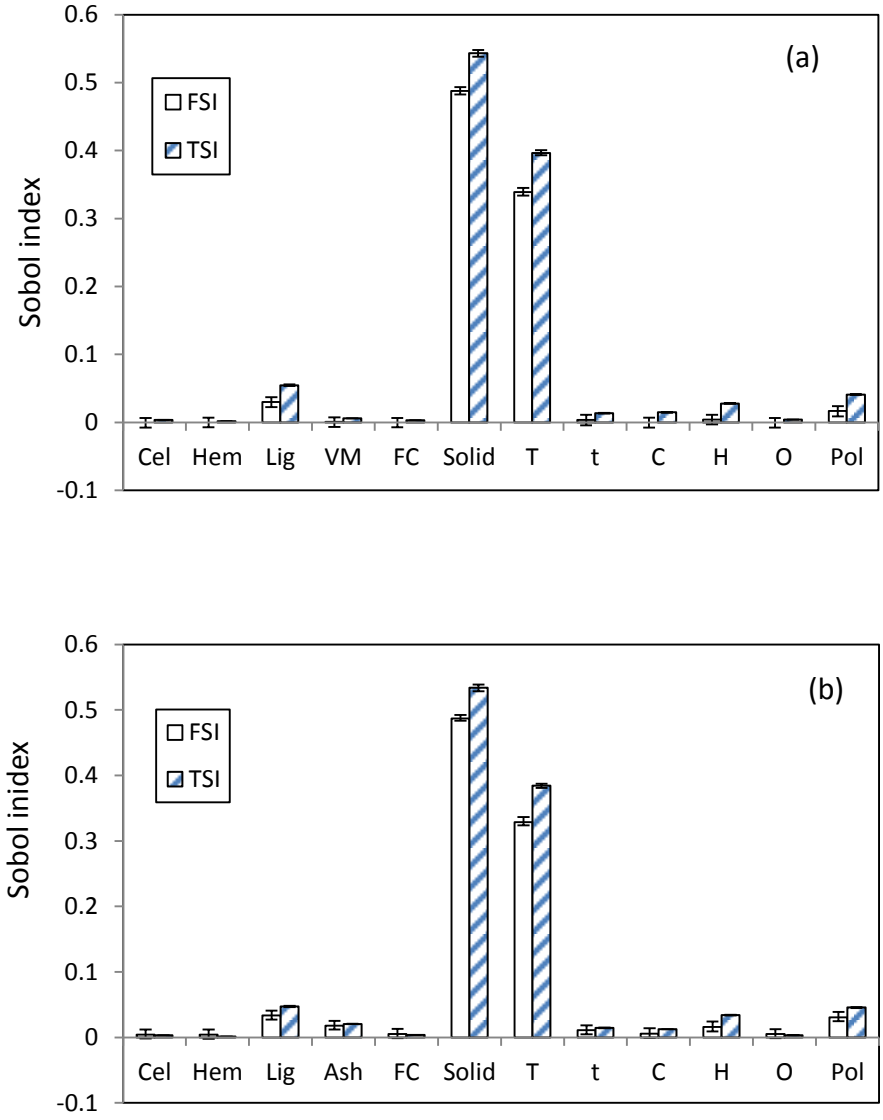

Figure 5.6. FSI and TSI of each parameter based on model Y-RF1 (a) and Y-RF2 (b).

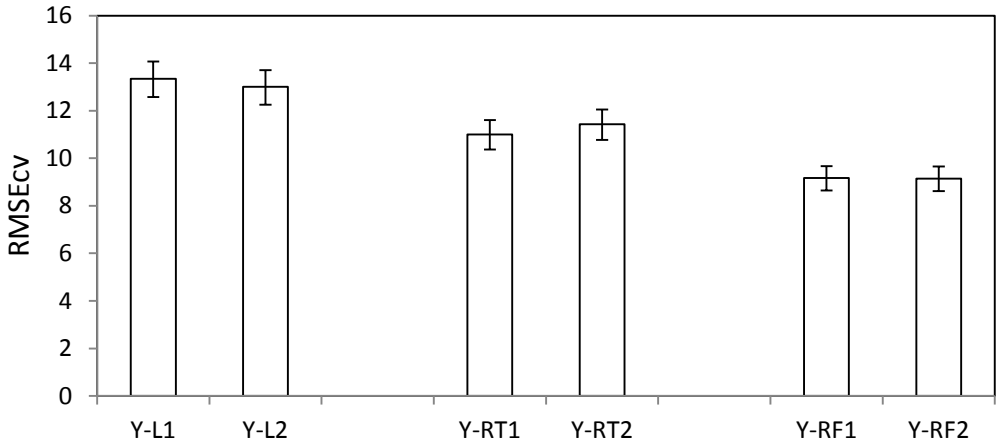

Figure 5.7. Comparison of the RMSEcv for linear, regression tree and random forest models of hydrochar yield.

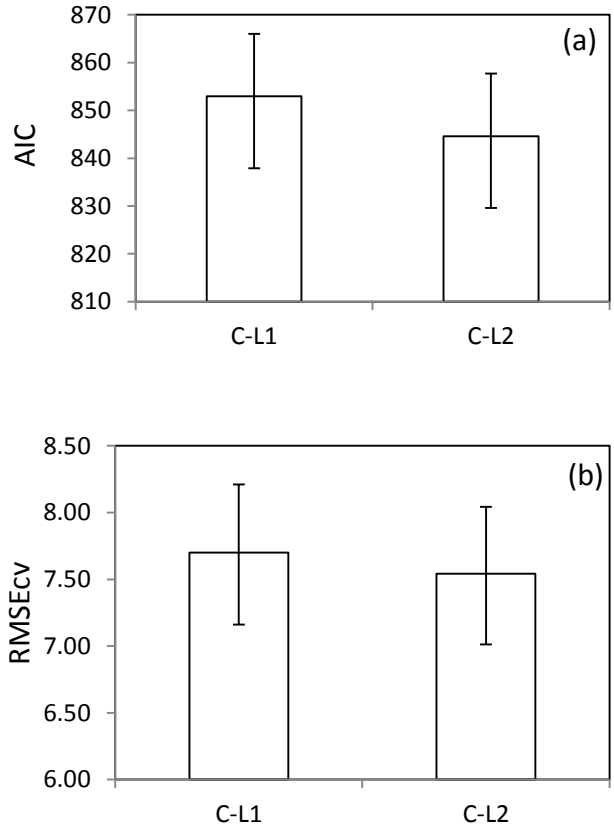

Figure 5.8. AIC (a) and RMSEcv (b) associated with linear regression models of hydrochar carbon content.

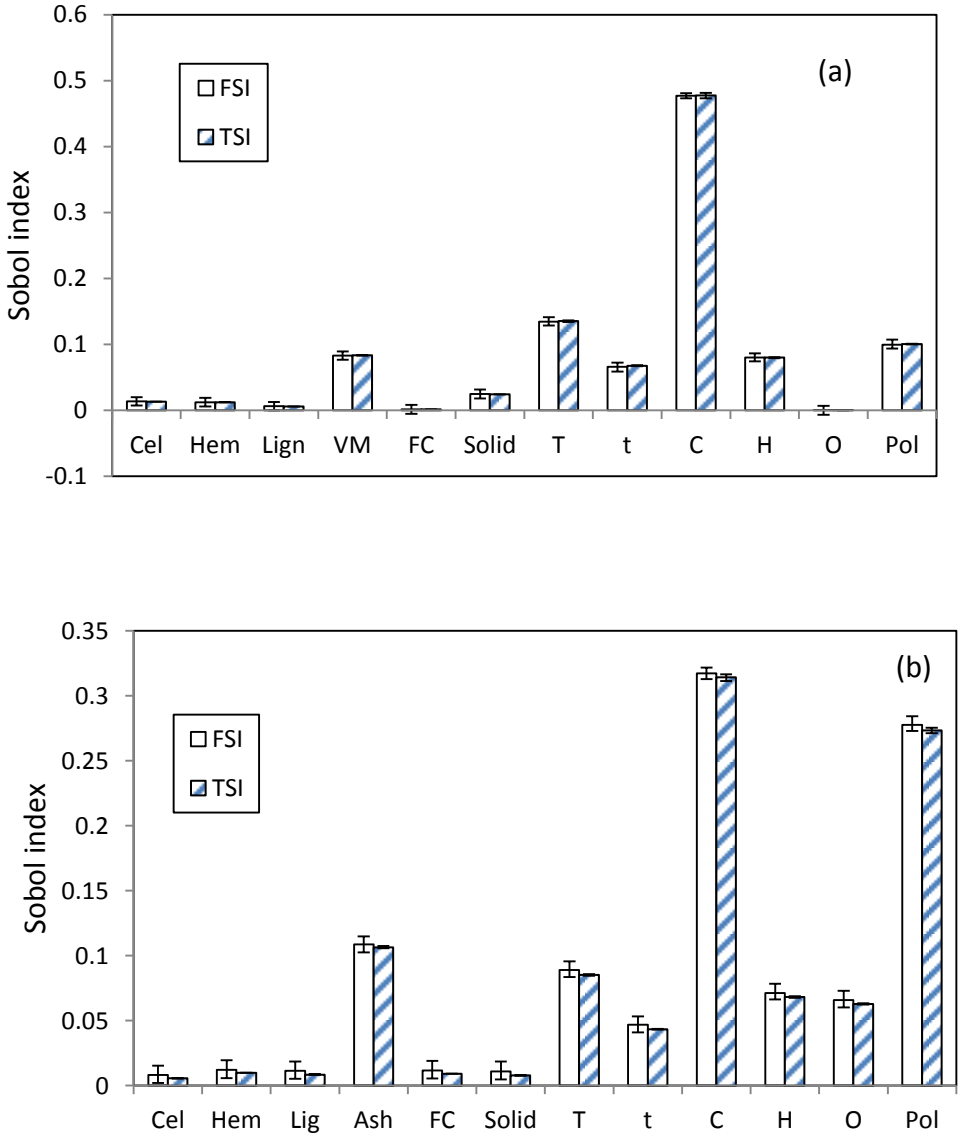

Figure 5.9. FSI and TSI of each parameter based on model C-L1 (a) and C-L2 (b).

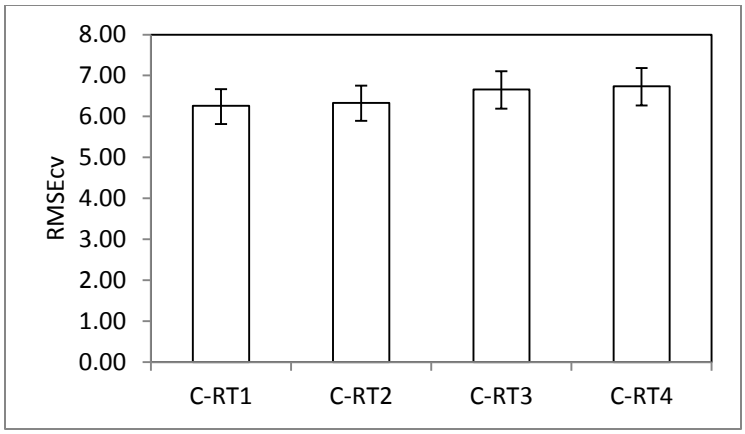

Figure 5.10. RMSEcv of regression tree models associated with hydrochar carbon content.

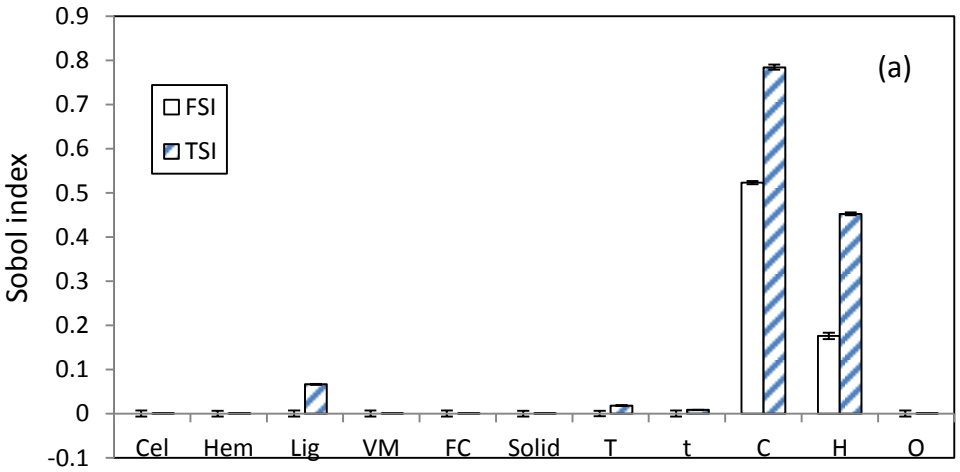
(a)
FSI
TSI
Sobol index
0.9
0.8
0.7
0.6
0.5
0.4
0.3
0.2
0.1
0
-0.1
Cel
Hem
Lig
VM
FC
Solid
T
t
C
H
O

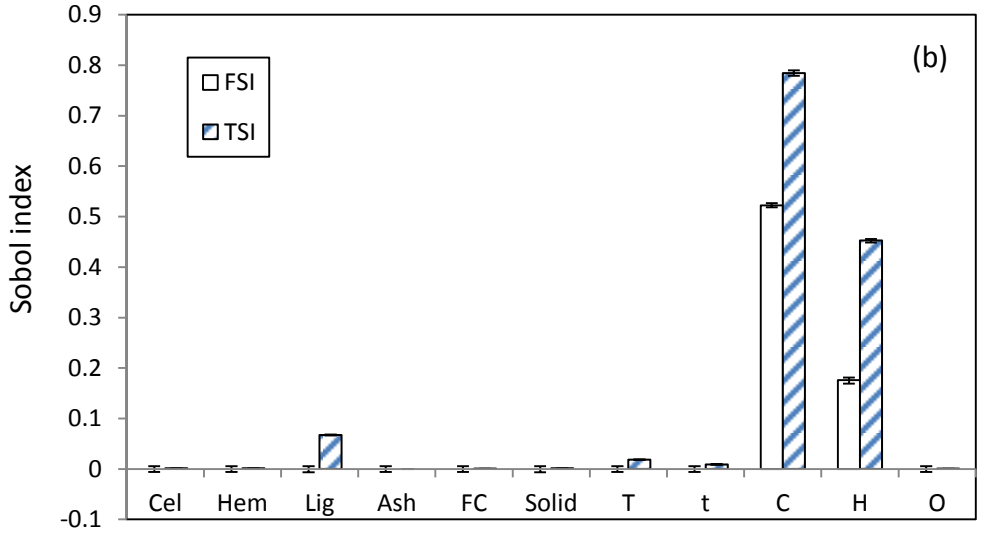
(b)
FSI
TSI
Sobol index
0.9
0.8
0.7
0.6
0.5
0.4
0.3
0.2
0.1
0
-0.1
Cel
Hem
Lig
Ash
FC
Solid
T
t
C
H
O

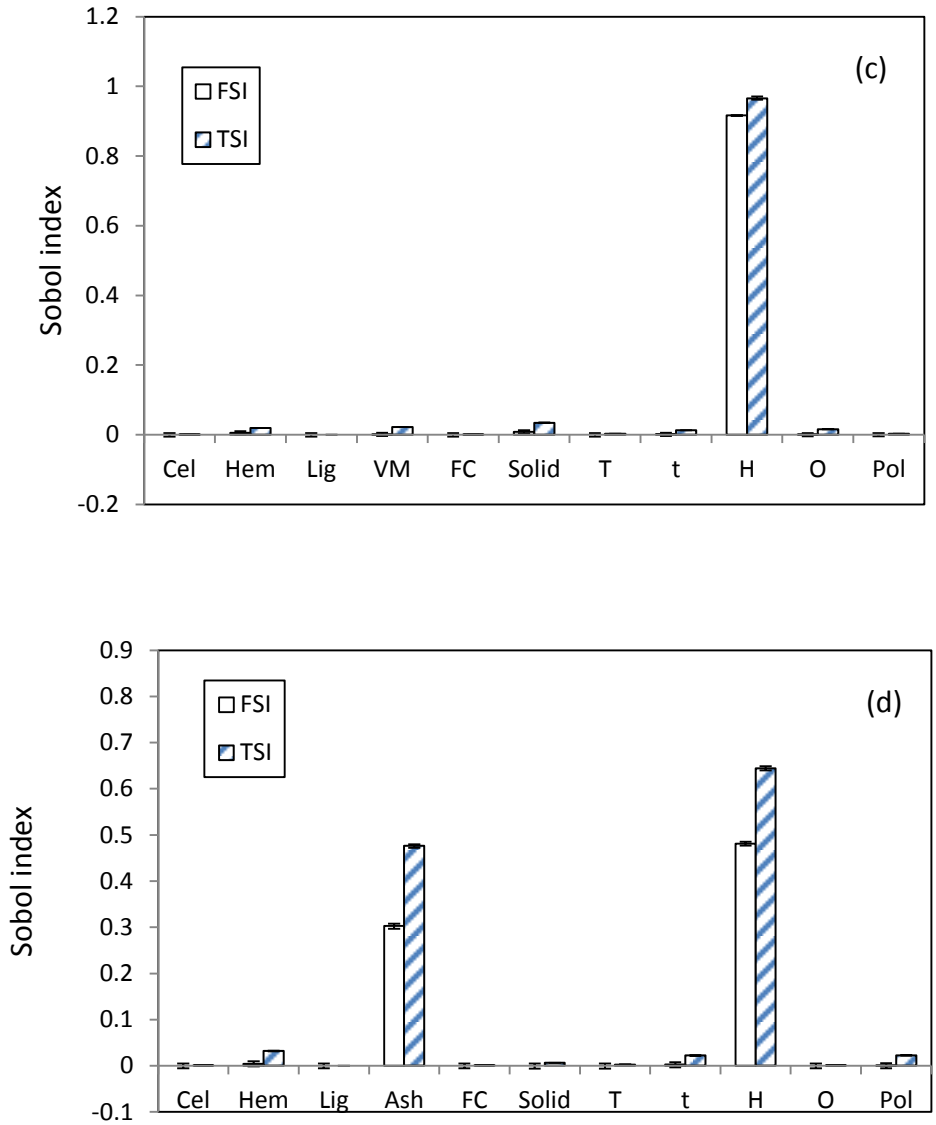

Figure 5.11. FSI and TSI of each parameter based on model C-RT1 (a), C-RT2 (b), C-RT3 (c) and C-RT4 (d).

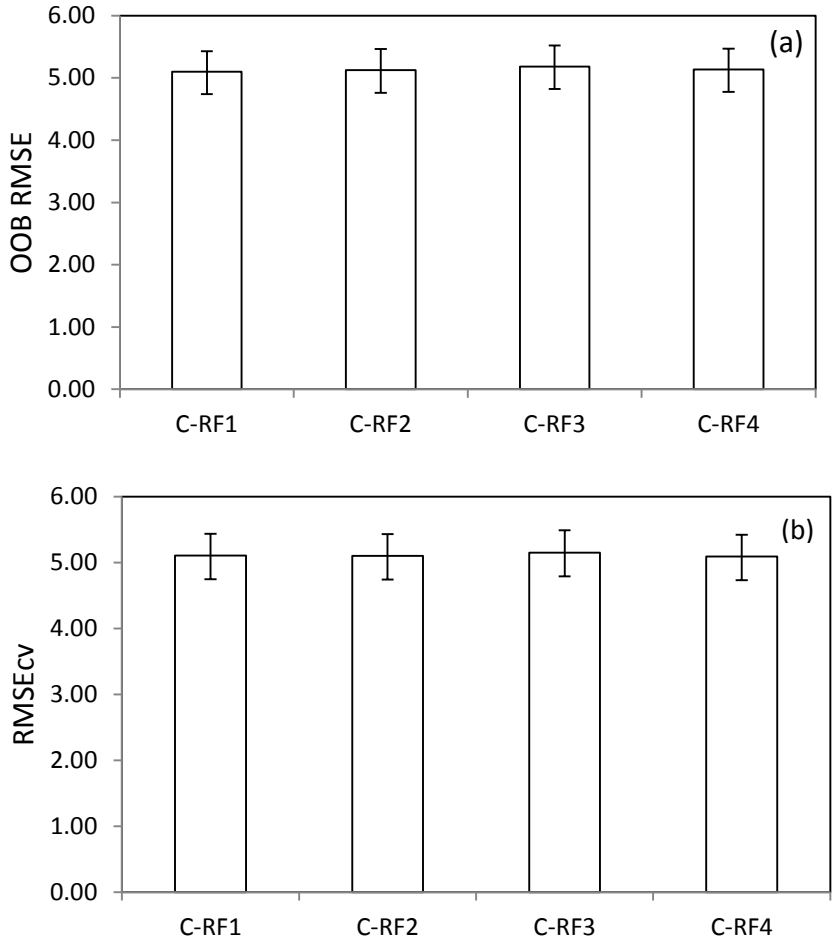

Figure 5.12. OOB RMSE (a) and RMSEcv (b) of random forest models on hydrochar carbon content.

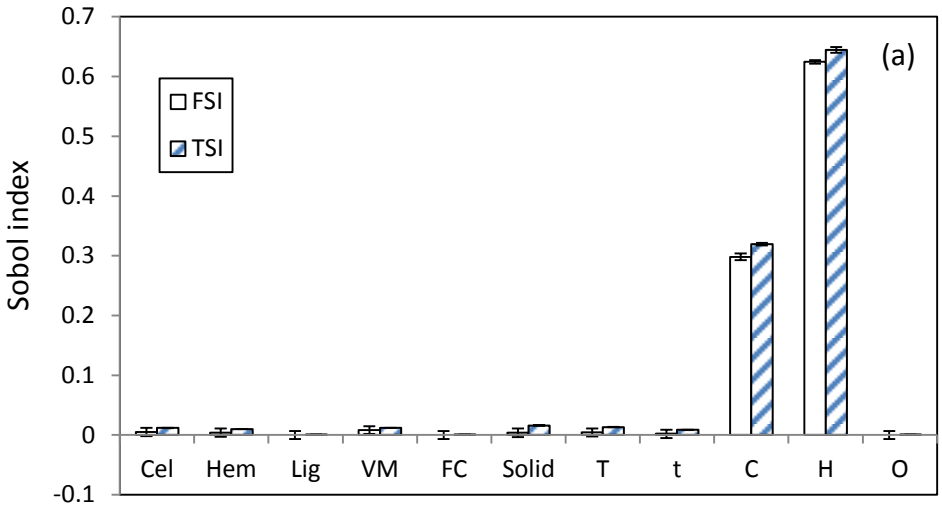
0.7
0.6
0.5
0.4
0.3
0.2
0.1
0
-0.1
Sobol index
FSI
TSI
(a)
Cel
Hem
Lig
VM
FC
Solid
T
t
C
H
O

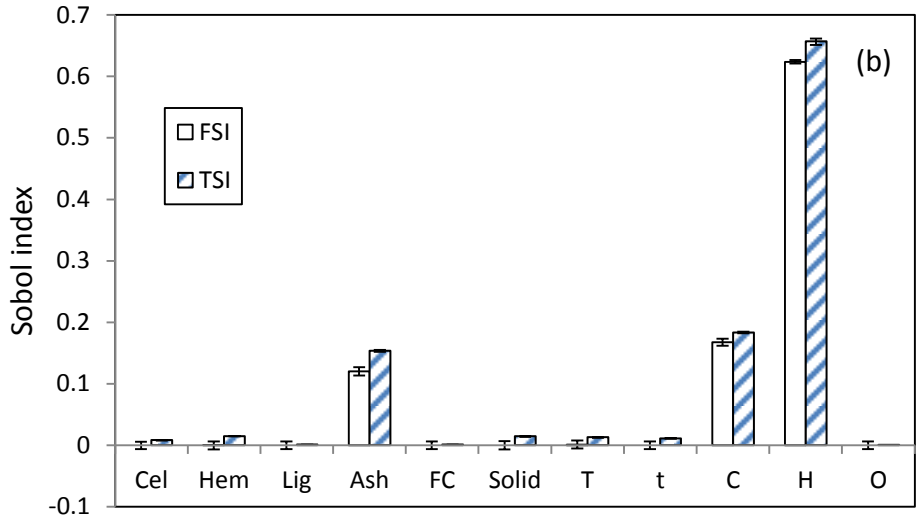
0.7
0.6
0.5
0.4
0.3
0.2
0.1
0
-0.1
Sobol index
FSI
TSI
(b)
Cel
Hem
Lig
Ash
FC
Solid
T
t
C
H
O

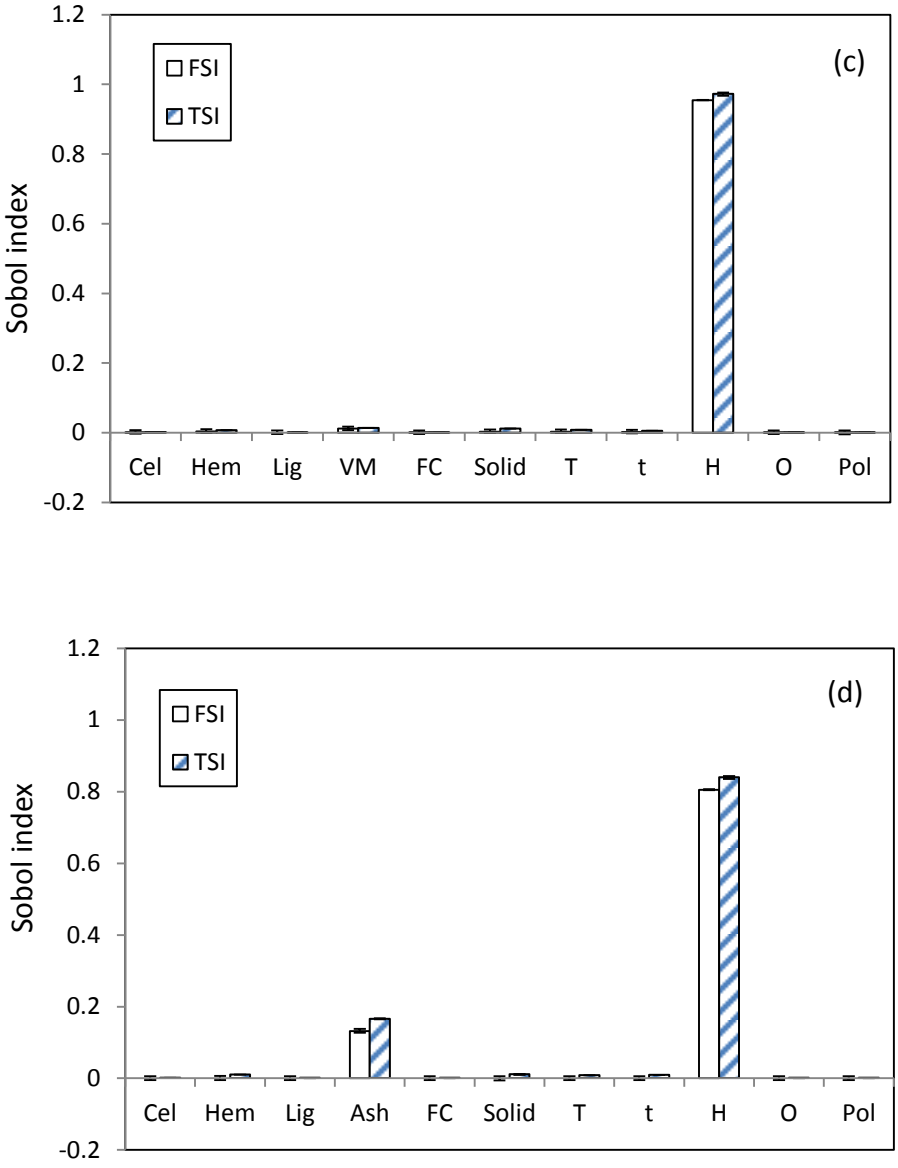

Figure 5.13. FSI and TSI of each parameter based on model C-RF1 (a), C-RF2 (b), C-RF3 (c) and C-RF4 (d).

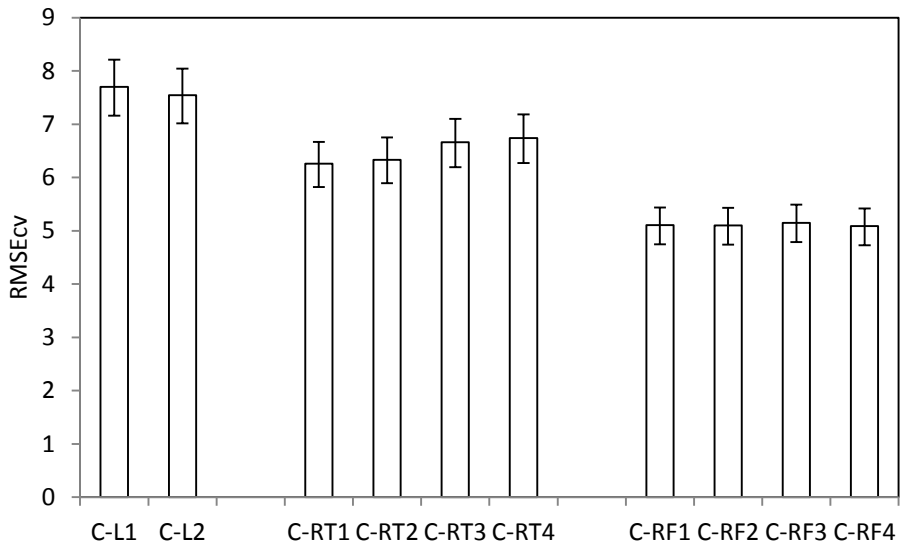

Figure 5.14. Comparison of the RMSEcv for linear, regression tree and random forest models of hydrochar carbon content.

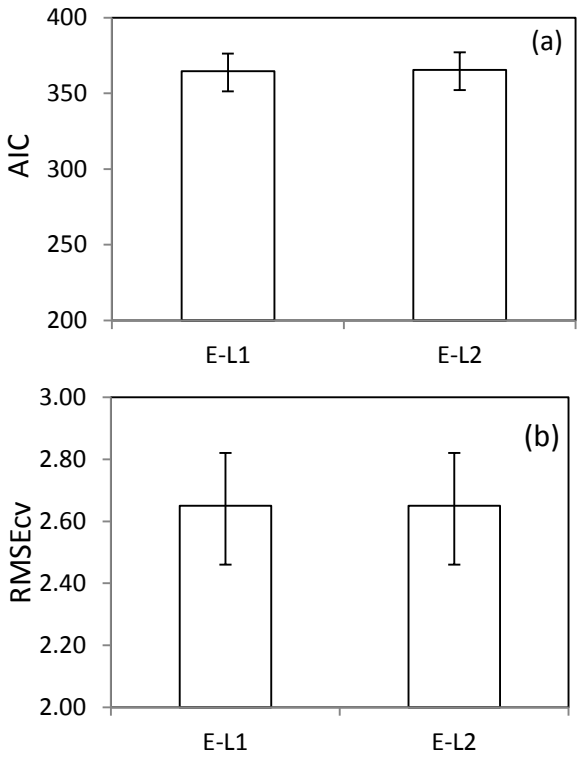

Figure 5.15. AIC (a) and RMSEcv (b) associated with the linear regression models of hydrochar energy content.

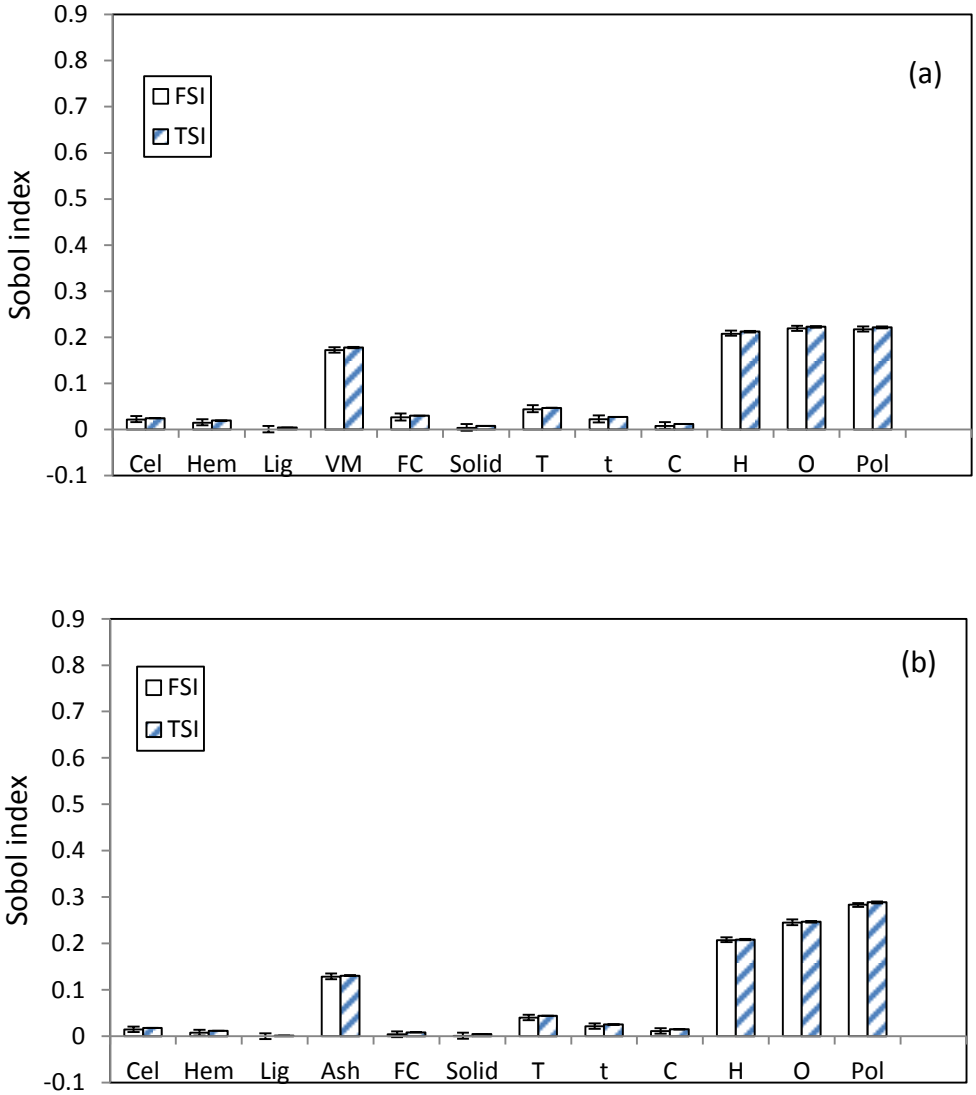

Figure 5.16. FSI and TSI of each parameter based on model E-L1 (a) and E-L2 (b).

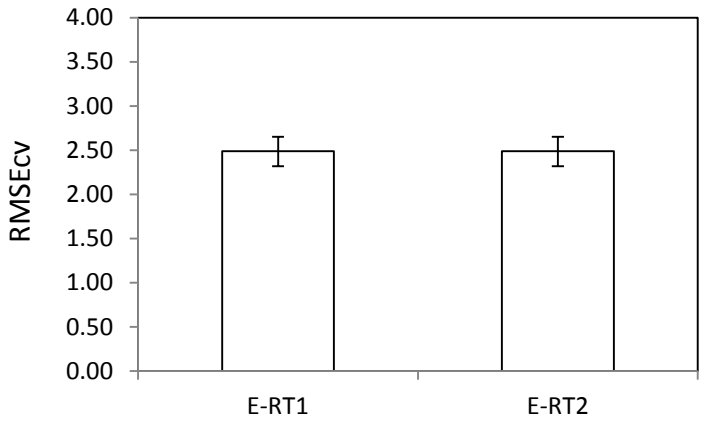

Figure 5.17. RMSEcv of regression tree models of hydrochar energy content.

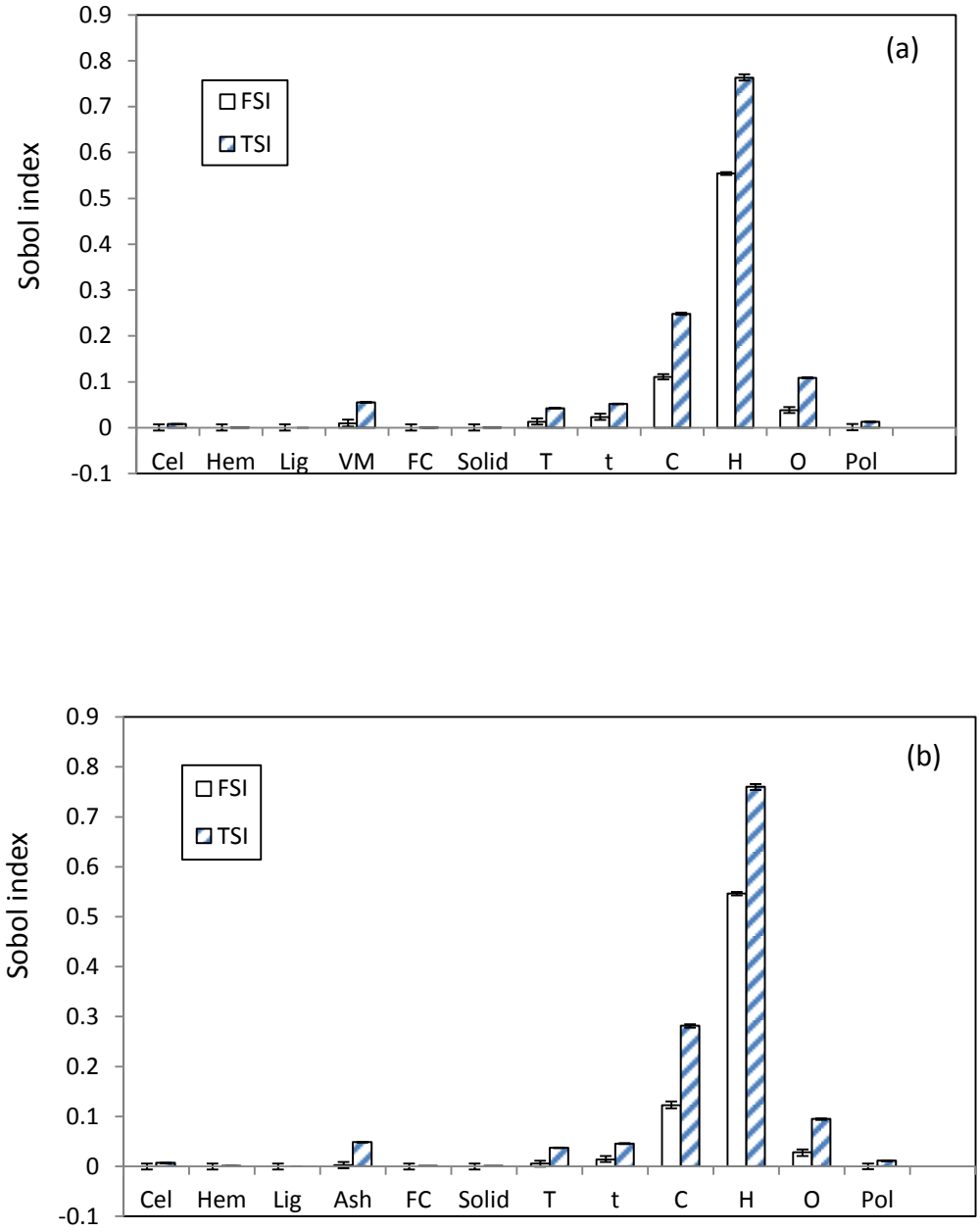

Figure 5.18. FSI and TSI based on model E-RT1 (a) and E-RT2 (b).

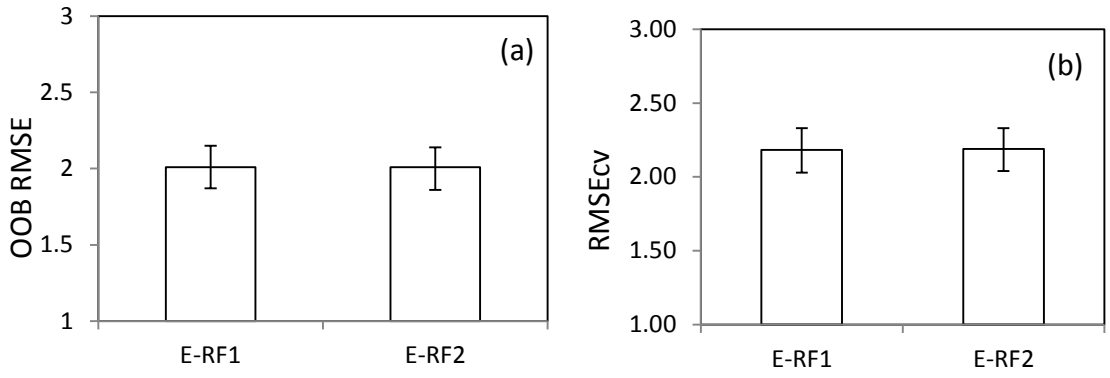

Figure 5.19. OOB RMSE (a) and RMSEcv (b) of random forest models of hydrochar energy content.

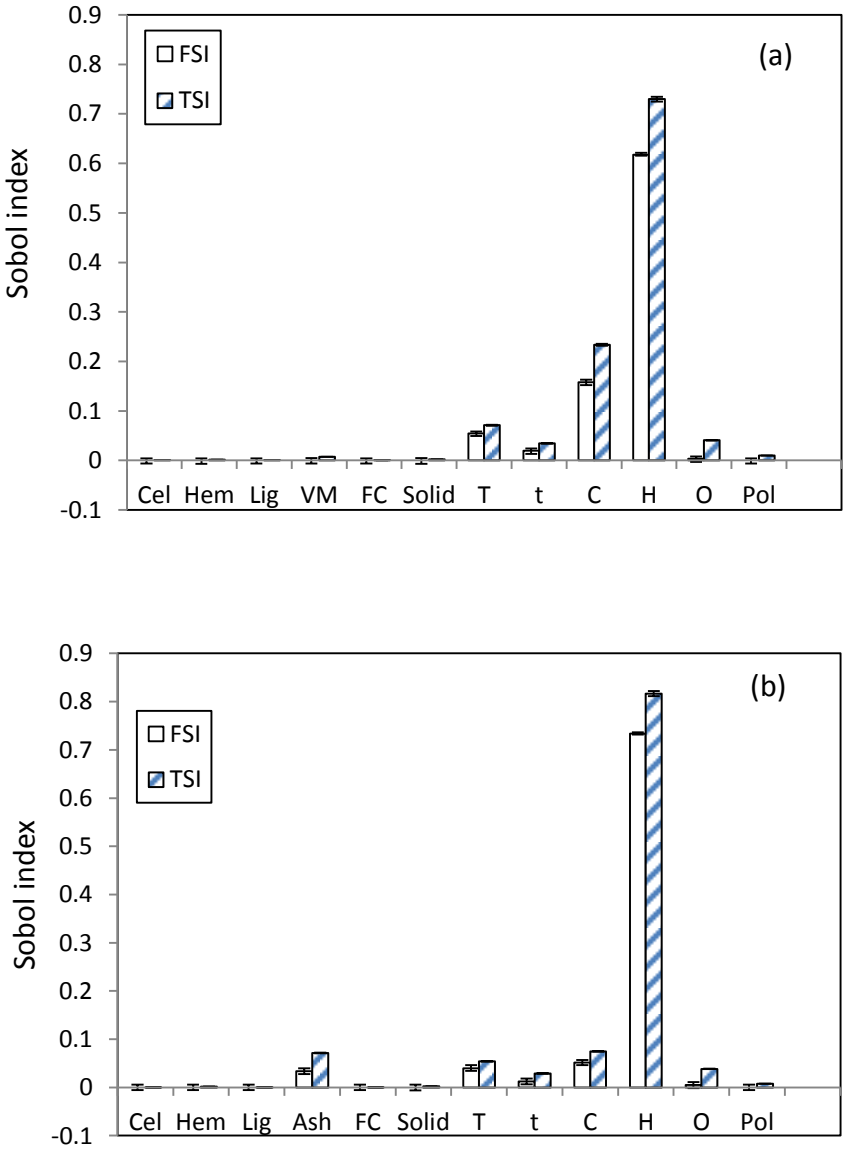

Figure 5.20. FSI and TSI based on random forest models of model E-RF1 (a) and E-RF2 (b).

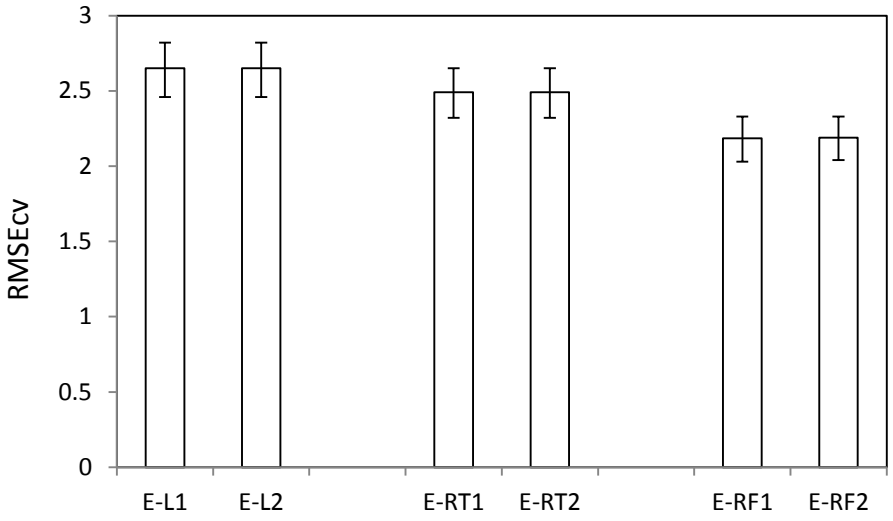

Figure 5.21. Comparison of the RMSEcv for linear, regression tree and random forest models of hydrochar energy content.

CHAPTER 6.

CONCLUSIONS AND RECOMMENDATIONS

6.1 CONCLUSION

Hydrothermal carbonization (HTC) is a more emerging thermal conversion process that has been shown to be an environmentally beneficial approach for the transformation of organic feedstocks, such as biomass, carbohydrates and organic components of waste streams, into value-added products. This study was conducted to: (1) determine the effect of specific feedstocks (e.g., paper, yard waste and food waste) and process conditions (e.g., temperature, time and initial solids concentration) on the carbonization product characteristics and determine whether interactions between feedstocks are present during carbonization;. (2) understand how liquid characteristics (e.g., pH, conductivity, COD and TOC) influence carbonization product characteristics and evaluate the significance of liquid characteristics in predicting these carbonization product characteristics (e.g., hydrochar yield, carbon content, energy content as well as the mass of carbon in the liquid and gas phase); and (3) develop statistical models to predict product characteristics when carbonizing a variety of feedstocks over a range of reaction conditions and to study the parameters significantly influencing the carbonization product characteristics using different methods. The main findings associated with this study include:

- Results from carbonization of food waste and packaging materials indicate initial solids concentration influences carbon distribution because of increased compound solubilization, while changes in reaction temperature imparted little change on carbon distribution. The presence of packaging materials significantly influences the energy content of the recovered solids. As the proportion of

packaging materials increase, the energy content of recovered solids decreases because of the low energetic retention associated with the packaging materials.

- Different moisture sources including activated sludge and landfill leachate impart minimal impact on the evaluated carbonization product characteristics including hydrochar yield, energy content, carbon content as well as the mass of carbon in the liquid and gas phase.
- Multiple linear regression and regression tree models were developed to describe the influence of process conditions and feedstock elemental and proximate properties on hydrochar yield, energy content and normalized carbon content in gas and the carbon content in the liquid and solid phase. Results from these models indicate that process conditions are more influential to the solid yields and liquid and gas-phase carbon contents, while feedstock properties are more influential on hydrochar carbon and energy contents, and the normalized carbon content of the solid.
- Both linear and nonlinear (e.g., regression tree and random forest) models can be used to describe the hydrochar yield, carbon content, and energy content. The predictive capabilities associated with the nonlinear models are generally better than the linear models for describing the characteristics of products generated from the hydrothermal carbonization of organic feedstocks. When using these models, parameter sensitivity is dependent on model structure and global sensitivity analysis results indicate that the most influential parameters are initial solid concentration, temperature, feedstock lignin content, polarity, hydrogen content, carbon content, time and ash content when conducting HTC experiments

with the goal of achieving a certain level of hydrochar yield. The most influential parameters to hydrochar carbon content are feedstock hydrogen content, carbon content, initial solids concentration and ash content or volatile matter. The most influential parameters to hydrochar energy content are feedstock hydrogen content, carbon content, oxygen content, ash content, temperature and time.

6.2 RECOMMENDATIONS FOR FUTURE WORK

The statistical models that can predict the characteristics of products generated from the hydrothermal carbonization of organic feedstocks have been developed and the most influential parameters on the product characteristics are identified in this work. Besides feedstock properties and process conditions investigated in this study, catalysts may also have an impact on HTC product characteristics and required additional study.

Additionally, HTC products can be used in a variety of applications such as a soil amendment, energy source, and environmental sorbent. The critical parameters associated with the specific application objective are unknown. Developing statistical models to predict hydrochar performance associated with each specific application and identifying the critical parameters with each application would be beneficial. This would allow for the predetermination of the suitable feedstock and operational conditions required to meet the desired product application. Furthermore, development of mechanistic models associated with the complex HTC process would be beneficial and should be investigated in future studies.

REFERENCES

Al-Meshan, M.A. and Mahrous, F., 2001. Recycling of municipal solid waste in the State of Kuwait. *Arabian Journal for Science and Engineering, 27*(2), pp.3-10.

Akalın, M.K., Tekin, K. and Karagoz, S., 2012. Hydrothermal liquefaction of cornelian cherry stones for bio-oil production. *Bioresource Technology, 110*(0), pp.682-687.

Akiya, N. and Savage, P.E. 2002., Roles of water for chemical reactions in high temperature water. *Chemical Reviews, 102*(8), pp.2725-2750.

Alenezi, R., Leeke, G.A., Santos, R.C.D. and Khan, A.R., 2009. Hydrolysis kinetics of sunflower oil under subcritical water conditions. *Chem. Eng. Res. Des. 87*, pp.867-873.

Álvarez-Murillo, A., Román, S., Ledesma, B. and Sabio, E. 2015. Study of variables in energy densification of olive stone by hydrothermal carbonization. *Journal of Analytical and Applied Pyrolysis, 113*, pp.307-314.

Amini, H.R. and Reinhart, D.R., 2011. Regional prediction of long-term landfill gas to energy potential. *Waste Management 31*, pp.2020-2026.

Appels, L., Lauwers, J., Degrève, J., Helsen, L., Lievens, B., Willems, K., Van Impe, J. and Dewil, R., 2011. Anaerobic digestion in global bio-energy production: Potential and research challenges. *Renewable and Sustainable Energy Reviews, 15*, pp.4295-4301.

Asghari, F.S. and Yoshida, H., 2006. Acid-catalyzed production of 5-hydroxymethyl furfural from D-fructose in subcritical water. *Industrial & Engineering Chemistry Research, 45*, 2163-2173.

Baccile, N., Laurent, G., Babonneau, F., Fayon, F., Titirici, M.-M. and Antonietti, M., 2009. Structural characterization of hydrothermal carbon spheres by advanced solid-state MAS 13C NMR investigations. *Journal of Physical Chemistry C 113*(22), pp.9644 – 9654.

Banks, C.J., Chesshire, M., Heaven, S. and Arnold, R., 2011. Anaerobic digestion of source-segregated domestic food waste: Performance assessment by mass and energy balance. *Bioresource Technology 102*, pp.612-620.

Basso, D., Patuzzi, F., Castello, D., Baratieri, M., Rada, E.C., Weiss-Hortala, E. and Fiori, L. 2016. Agro-industrial waste to solid biofuel through hydrothermal carbonization. *Waste Management, 47*, Part A, pp.114-121.

Becker, R., Dorgerloh, U., Helmis, M., Mumme, J., Diakite, M. and Nehls, I., 2013. Hydrothermally carbonized plant materials: Patterns of volatile organic

compounds detected by gas chromatography. *Bioresource Technology, 130*(0), pp.621-628.

Beldjazia, A. and Alatou, D., 2016. Precipitation variability on the massif forest of Mahouna (North eastern-Algeria) from 1986 to 2010. *International Journal of Management Sciences and Business Research, 5*(3), pp.21-28.

Benavente, V., Calabuig, E. and Fullana, A. 2015. Upgrading of moist agro-industrial wastes by hydrothermal carbonization. *Journal of Analytical and Applied Pyrolysis, 113,* pp.89-98.

Berge, N.D., Ro, K.S., Mao, J. and Flora, J.R.V., 2011. Hydrothermal Carbonization of Municipal Waste Streams. *Environmental Science & Technology 45,* pp.5696-5703.

Bernstad, A. and la Cour Jansen, J., 2012. Separate collection of household food waste for anaerobic degradation - Comparison of different techniques from a systems perspective. *Waste Management 32,* pp.806-815.

Bouchon-Meunier, B., Magdalena, L., Ojeda-Aciego, M., Verdegay, J.L. and Yager, R.R., eds., 2010. *Foundations of reasoning under uncertainty* (Vol.249). Springer.

Bozdogan, H., 1987. Model selection and Akaike's information criterion (AIC): The general theory and its analytical extensions. *Psychometrika, 52*(3), 345-370.

Breiman, L., Friedman, J.H., Olshen, R.A. and Stone, C.J., 1984. Classification and regression trees. Belmont, Chapman and Hall (Wadsworth, Inc.), New York, USA.

Breiman, L., 2001. Random forests. *Machine learning, 45*(1), 5-32.

Büyüksönmez, F., 2012. Full-Scale VOC Emissions from green and food waste windrow composting, *Compost Science & Utilization, 20*(1), pp.57-62.

CalRecycle, 2010. Climate change and solid waste management-organics. http://www.calrecycle.ca.gov/climate/Organics/default.htm.

Cameron, A.C. and Windmeijer, F.A.G., 1996. R-squared measures for count data regression models with applications to health-care utilization. *Journal of Business & Economic Statistics, 14*(2), pp.209-220.

Cao, X., Ro, K. S., Chappell, M., Li, Y. and Mao, J., 2011. Chemical structures of swine-manure chars produced under different carbonization conditions investigated by advanced solid-state 13C nuclear magnetic resonance (NMR) spectroscopy. *Energy Fuels 25*, pp.388-397.

Cao, X.Y., Ro, K.S., Libra, J.A., Kammann, C.I., Lima, I., Berge, N., Li, L., Li., Y., Chen, N., Yang, J., Deng, B. and Mao, J.D. 2013. Effects of biomass types and carbonization conditions on the chemical characteristics of hydrochars. *Journal of Agricultural and Food Chemistry, 61*, pp.9401-9411.

Channiwala, S.A., Parikh, P.P., 2002. A unified correlation for estimating HHV of solid, liquid and gaseous fuels. *Fuel, 81*, pp.1051-1063.

Chheda, J.N., Dumesic, J.A., 2007. An overview of dehydration, aldol-condensation and hydrogenation processes for production of liquid alkanes from biomass-derived carbohydrates. *Catalysis Today, 123*(1), pp.59-70.

Chuntanapum, A., Matsumura, Y., 2010. Char formation mechanism in supercritical water gasification process: A study of model compounds. *Industrial & Engineering Chemistry Research, 49,* pp.4055-4062.

Cordero, T., Marquez, F., Rodriguez-Mirasol, J. and Rodriguez, J.J. 2001. Predicting heating values of lignocellulosics and carbonaceous materials from proximate analysis. *Fuel, 80*(11), pp.1567-1571.

Danso-Boateng, E., Holdich, R. G., Shama, G., Wheatley, A. D., Sohail, M. and Martin, S. J., 2013. Kinetics of faecal biomass hydrothermal carbonisation for hydrochar production. *Applied Energy, 111,* pp.351-357.

Danso-Boateng, E., Shama, G., Wheatley, A.D., Martin, S.J., Holdich, R.G. 2015. Hydrothermal carbonisation of sewage sludge: Effect of process conditions on product characteristics and methane production. *Bioresource Technology, 177,* pp.318-327.

DEFRA, 2011. Waste Data Overview. Department for Enviornment Food and Rural Affairs, 1-31.

Divaris, K., Vann Jr., W.F., Baker, A.D. and Lee, J.Y., 2012. Examining the accuracy of caregivers' assessments of young children's oral health status. *Journal of the American Dental Association, 143*(11), pp.1237-1247.

Du, Z., Mohr, M., Ma, X., Cheng, Y., Lin, X., Liu, Y., Zhou, W., Chen, P., Ruan, R. 2012. Hydrothermal pretreatment of microalgae for production of pyrolytic bio-oil with a low nitrogen content. *Bioresource Technology, 120*(0), pp.13-18.

EPA, U., 2011. Municipal Solid Waste in the United States: 2010 Facts and Figures. . EPA-530-F-11-005.

EU Council, 1999. Council Directive 1999/31/EC on the Landfill of Waste. 1-19.

European Commission, 2010. Preparatory Study of Food Waste across EU 27.

Falco, C., Baccile, N. and Titirici, M.-M., 2011. Morphological and structural differences between glucose, cellulose and lignocellulosic biomass derived hydrothermal carbons. *Green Chemistry, 13,* pp.3273-3281.

Falco, C., Sieben, J. M., Brun, N., Sevilla, M., van der Mauelen, T., Morallón, E., Cazorla-Amorós, D. and Titirici, M.-M., 2013. Hydrothermal carbons from hemicellulose-derived aqueous hydrolysis products as electrode materials for supercapacitors. *ChemSusChem, 6,* pp.374-382.

Favoino, E., 2000. The development of composting in Italy: Programs for source separation, features and trends of quality composting and biological treatment of restwaste. In Proc. National Conference, La Rioja, Spain, pp.1-19.

Flora, J.F.R., Lu, X., Li, L., Flora, J.R.V. and Berge, N.D. 2013. The effects of alkalinity and acidity of process water and hydrochar washing on the adsorption of atrazine on hydrothermally produced hydrochar. *Chemosphere, 93*(9), pp.1989-1996.

Fujita, A., Sato, J.R., Demasi, M.A., Sogayar, M.C., Ferreira, C.E. and Miyano, S., 2009. Comparing Pearson, Spearman and Hoeffding's D measure for gene expression association analysis. *J. Bioinform. Comput. Biol., 7*(4), pp.663-684.

Funke, A., Reebs, F., Kruse, A. 2013. Experimental comparison of hydrothermal and vaopthermal carbonization. *Fuel Processing Technology, 115,* pp.261-269.

Funke, A. and Ziegler, F., 2010. Hydrothermal carbonization of biomass: A summary and discussion of chemical mechanisms for process engineering. *Biofuels Bioproducts & Biorefining 4,* pp.160-177.

Goto, M., Obuchi, R., Hirose, T., Sakaki, T. and Shibata, M., 2004. Hydrothermal conversion of municipal organic waste into resources. *Bioresource Technology, 93,* pp.279-284.

Hájeková, E., Špodová, L., Bajus, M. and Mlynková, B., 2007. Separation and characterization of products from thermal cracking of individual and mixed polyalkenes. *Chemical Papers, 61,* pp.262-270.

Hanrot, F., Ablitzer, D., Houzelot, J.L. and Dirand, M., 1994. Experimental Measurement of the True Specific Heat Capacity of Coal and Semicoke during Carbonization. *Fuel, 73,* pp.-309.

Hastie, T., Tibshirani, R. and Friedman, J.H., 2001. The elements of statistical learning. New York: Springer series in statistics.

Hatakeyama, T., 1982. Studies on Heat Capacity of Cellulose and Lignin by Differential Scanning Calorimetry. *Polymer, 23,* pp.1801-1804.

Heilmann, S.M., Davis, H.T., Jader, L.R., Lefebvre, P.A., Sadowsky, M.J., Schendel, F.J., von Keitz, M.G. and Valentas, K.J., 2010. Hydrothermal carbonization of microalgae. *Biomass Bioenergy, 34,* pp.875-882.

Heilmann, S.M., Jader, L.R., Sadowsky, M.J., Schendel, F.J., von Keitz, M.G. and Valentas, K.J., 2011. Hydrothermal carbonization of distiller's grains. *Biomass Bioenergy, 35* (7), pp.2526-2533.

Hoekman, S.K., Broch, A., Robbins, C., 2011. Hydrothermal Carbonization (HTC) of Lignocellulosic Biomass. *Energy & Fuels, 25,* pp.1802-1810.

Hrnčič, M. K., Kravanja, G. and Knez, Ž., 2016. Hydrothermal treatment of biomass for energy and chemicals. *Energy, 116,* pp.1312-1322.

Hwang, I.-H., Aoyama, H., Matsuto, T., Nakagishi, T. and Matsuo, T., 2012. Recovery of solid fuel from municipal solid waste by hydrothermal treatment using subcritical water. *Waste Management 32,* pp.410-416.

Hyndman, R.J. and Koehler, A.B., 2006. Another look at measures of forecast accuracy. *International Journal of Forecasting, 22*(4), pp.679-688.

Ike, M., Inoue, D., Miyano, T., Liu, T.T., Sei, K., Soda, S. and Kadoshin, S., 2010. Microbial population dynamics during startup of a full-scale anaerobic digester treating industrial food waste in Kyoto eco-energy project. *Bioresource Technology, 101,* pp.3952-3957.

Jain, A., Balasubramanian, R. and Srinivasan, M.P., 2016. Hydrothermal conversion of biomass waste to activated carbon with high porosity: A review, *Chemical Engineering Journal, 283,* pp.789-805.

Jambeck, J.R., Farrell, E.W. and Cleaves, S.M., 2006. Food Scraps to Composting....And Back to Food. *BIocycle, 47,* pp.49.

Jia, Y., Huang, J., Wang, Y., 2004. Effects of calcium oxide on the cracking of coal tar in the freeboard of a fluidized bed. *Energy & Fuels, 18,* pp.1625-1632.

Kamio, E., Takahashi, S., Noda, H.; Fukuhara, C., Okamura, T., 2008. Effect of heating rate on liquefaction of cellulose by hot compressed water. *Chemical Engineering Journal, 137,* pp.328-338.

Kang, S., Li, X., Fan, J., Chang, J., 2012. Solid fuel production by hydrothermal carbonization of black liquor. *Bioresource Technology, 110,* pp.715-718.

Kang, S.M., Li, X.H., Fan, J., Chang, J., 2012. Characterization of hydrochars produced by hydrothermal carbonization of lignin, cellulose, D-xylose, and wood meal. *Industrial & Engineering Chemistry Research, 51,* pp.9023-9031.

Kannan, S., Gariepy, Y. and Raghavan, G.S.V., 2017. Optimization and characterization of hydrochar derived from shrimp waste. *Energy & Fuels, 31*(4), pp.4068-4077

Kelleher, M., 2007. Anaerobic digestion outlook for MSW streams. *Biocycle,* pp.51-56.

Kieseler, S. Neubauer, Y. and Zobel, N., 2013. Ultimate and proximate correlations for estimating the higher heating value of hydrothermal solids. *Energy Fuels, 27,* pp.908-918.

Knežević, D., van Swaaij, W.P.M. and Kersten, S.R.A., 2009. Hydrothermal conversion of biomass: I, glucose conversion in hot compressed water. *Industrial & Engineering Chemistry Research, 48,* pp.4731-4743.

Knežević, D., van Swaaij, W. and Kersten, S., 2010. Hydrothermal conversion of biomass. II. Conversion of wood, pyrolysis oil, and glucose in hot compressed water. *Industrial & Engineering Chemistry Research, 49,* pp.104-112.

Knežević, D., van Swaaij, W.P.M. and Kersten, S.R.A., 2009. Hydrothermal conversion of biomass: I, Glucose conversion in hot compressed water. *Industrial & Engineering Chemistry Research, 48,* pp.4731-4743.

Kobayashi, K. and Salam, M.U., 2000. Comparing simulated and measured values using mean squared deviation and its components. *Agron. J. 92,* pp.345-352.

Kong, L., Miao, P. and Qin, J. 2013. Characteristics and pyrolysis dynamic behaviors of hydrothermally treated micro crystalline cellulose. *Journal of Analytical and Applied Pyrolysis, 100*(0), pp.67-74

Levis, J.W. and Barlaz, M.A., 2011. Is biodegradability a desirable attribute for discarded solid waste? Perspectives from a national landfill greenhouse gas inventory model. *Environmental Science & Technology, 45,* pp.5470-5476.

Levis, J.W., Barlaz, M.A., Themelis, N.J. and Ulloa, P., 2010. Assessment of the state of food waste treatment in the United States and Canada. *Waste Management, 30,* pp.1486-1494.

Libra, J.A., Ro, K.S., Kammann, C., Funke, A., Berge, N.D., Neubauer, Y., Titirici, M.-M., Fühner, C., Bens, O. and Emmerich, J.K.K.-H., 2011. Hydrothermal carbonization of biomass residuals: a comparative review of the chemistry, processes and applications of wet and dry pyrolysis. *Biofuels, 2,* pp.89-124.

Li, L., Diederick, R., Flora, J.R.V. and Berge, N.D. 2013. Hydrothermal carbonization of food waste and associated packaging materials for energy source generation. *Waste Management, 33*(11), pp.2478-2492.

Li, L., Flora, J.R.V., Caicedo, J.M. and Berge, N.D. 2015. Investigating the role of feedstock properties and process conditions on products formed during the hydrothermal carbonization of organics using regression techniques. *Bioresource Technology, 187,* pp.263-274.

Lilliestråle, A., 2007. Hydrothermal carbonization of biowaste - A step towards efficient carbon sequestration and sustainable energy production. *Dissertation in the Biotechnology Propgramme,* Uppsala University, Uppsala.

Lu, X., Jordan, B. and Berge, N.D., 2012. Thermal conversion of municipal solid waste via hydrothermal carbonization: Comparison of carbonization products to products from current waste management techniques. *Waste Management 32,* pp.1353-1365.

Lundie, S. and Peters, G.M., 2005. Life cycle assessment of food waste management options. *Journal of Cleaner Production 13,* pp.275-286.

Lu, X., Pellechia, P.J., Flora, J.R.V. and Berge, N.D., 2013. Influence of reaction time and temperature on product formation associated with the hydrothermal carbonization of cellulose. *Bioresource Technology, 138,* pp.180-190.

Luo, G., Shi, W., Chen, X., Ni, W., Strong, P.J., Jia, Y. and Wang, H., 2011. Hydrothermal conversion of water lettuce biomass at 473 or 523 K. *Biomass Bioenergy, 35*(12), pp.4855-4861.

Lynam, J.G., Coronella, C.J., Yan, W., Reza, M.T. and Vasquez, V.R., 2011. Acetic acid and lithium chloride effects on hydrothermal carbonization of lignocellulosic biomass. *Bioresource Technology, 102*(10), pp.6192-6199.

Lynam, J.G., Reza, M.T., Vasquez, V.R. and Coronella, C.J., 2012. Effect of salt addition on hydrothermal carbonization of lignocellulosic biomass. *Fuel, 99*(0), pp.271-273.

Miyazawa, T. and Funazukuri, T., 2006. Noncatalytic hydrolysis of guar gum under hydrothermal conditions. *Carbohydr. Res. 341* (7), pp.870-877.

Mumme, J., Eckervogt, L., Pielert, J., Diakité, M., Rupp, F. and Kern, J., 2011. Hydrothermal carbonization of anaerobically digested maize silage. *Bioresource Technology, 102,* pp.9255-9260.

McKendry, P., 2002. Energy production from biomass (Part 1): Overview of biomass. *Bioresource Technology 83,* pp.37-46.

Moore, R. and Edgar, E.W.R., 2008. Greenhouse gas emissions reduction accounting from recycling, composting, and biomass feedstock energy production. *Proposed Recycling and Waste Diversion Reporting Project Protocol,* pp.1-11.

Morikawa, J. and Hashimoto, T., 2011. Estimation of frequency from a temperature scanning rate in differential scanning calorimetry at the glass transition of polystyrene. *Polymer, 52,* pp.4129-4135.

Möller, M., Harnisch, F. and Schroder, U., 2013. Hydrothermal liquefaction of cellulose in subcritical water-the role of crystallinity on the cellulose reactivity. *RSC Advances, 3,* pp.11035-11044.

Mumme, J., Eckervogt, L., Pielert, J., Diakité, M., Rupp, F. and Kern, J., 2011. Hydrothermal carbonization of anaerobically digested maize silage. *Bioresour. Technol. 102,* pp.9255-9260.

Namkoong, W., Hwang, E.Y., Cheong, J.G. and Choi, J.Y., 1999. A Comparative Evaluation of Maturity Parameters for Food Waste Composting. *Compost Science & Utilization, 7,* pp.55.

Nathans, L.L., Oswald, F. and Nimon, K., 2012. Interpreting multiple linear regression: A guidebook of variable importance. *Practical Assess., Res. Eval. 17,* pp.1-19.

Nizamuddin, S., Baloch, H.A., Griffin, G.J., Mubarak, N.M., Bhutto, A.W., Abro, R., Mazari, S.A. and Ali, B.S., 2017. An overview of effect of process parameters on hydrothermal carbonization of biomass. *Renewable and Sustainable Energy Reviews, 73,* pp.1289-1299.

Nizamuddin, S., Mubarak, N.M., Tiripathi, M., Jayakumar, N.S., Sahu, J.N. and Ganesan, P. 2016. Chemical, dielectric and structural characterization of optimized hydrochar produced from hydrothermal carbonization of palm shell. *Fuel, 163,* pp.88-97.

NRDC, 2012. Wasted: How America Is Losing Up to 40 Percent of Its Food from Farm to Fork to Landfill. http://www.nrdc.org/food/wasted-food.asp.

Parikh, J., Channiwala, S.A., and Ghosal, G.K. 2005. A correlation for calculating HHV from proximate analysis of solid fuels. *Fuel, 84*(5), pp.487-494.

Pinkowska, H., Wolak, P. and Złocinska, A., 2012. Hydrothermal decomposition of alkali lignin in sub- and supercritical water. *Chemical Engineering Journal, 187,* pp.410-414.

Pala, M., Kantarli, I.C., Buyukisik, H.B. and Yanik, J., 2014. Hydrothermal carbonization of grape pomace: A comparative evaluation. *Bioresource Technology, 161*(0), pp.255-262.

Posada, D. and Buckley, T.R., 2004. Model selection and model averaging in phylogenetics: advantages of Akaike information criterion and Bayesian approaches over likelihood ratio tests. *Systematic biology*, *53*(5), pp.793-808.

Ramke, H.G., Blöhse, D., Lehmann, H.J. and Fettig, J., 2009. Hydrothermal carbonization of organic waste. 20th International Waste Management and Landfill Symposium.

Ren, L.H., Nie, Y.F., Liu, J.G., Jin, Y.Y. and Sun, L., 2006. Impact of hydrothermal process on the nutrient ingredients of restaurant garbage. *Journal of Environmental Sciences*, *18*, pp.1012-1019.

Reza, M.T., Lynam, J.G., Uddin, M.H. and Coronella, C.J., 2013a. Hydrothermal carbonization: Fate of inorganics. *Biomass Bioenergy 49*, pp.86-94.

Reza, M.T., Yan, W., Uddin, M.H., Lynam, J.G., Hoekman, S.K., Coronella, C.J., and Vásquez, V.R., 2013b. Reaction kinetics of hydrothermal carbonization of loblolly pine. *Bioresour. Technol. 139*, pp.161-169.

Reza, M.T., Andert, J., Wirth, B., Busch, D., Pielert, J., Lynam, J.G. and Mumme, J., 2014. Hydrothermal carbonization of biomass for energy and crop production. *Appl. Bionergy*, *1*, pp.11-29.

Rodriguez, R.P., Rodrigo, M.E. and Kelly, P., 1995. A calorimetric method to determine specific heats of prepared foods. *Journal of Food Engineering*, *26*(1), pp.81-96.

Román, S., Nabais, J.M.V., Laginhas, C., Ledesma, B. and González, J.F., 2012. Hydrothermal carbonization as an effective way of densifying the energy content of biomass. *Fuel Processing Technology*, *103*, pp.78-83.

Román, S., Valente Nabais, J.M., Ledesma, B., Gonzalez, J.F., Laginhas, C. and Titirici, M.M. 2013. Production of low-cost adsorbents with tunable surface chemistry by conjunction of hydrothermal carbonization and activation processes. *Microporous and Mesoporous Materials*, *165*(0), pp.127-133.

Rutherford, D.W., Chiou, C.T. and Kile, D.E., 1992. Influence of soil organic matter composition on the partition of organic compounds. *Environmental Science&Technology*, *26*, pp.336-340.

Ruyter, H.P., 1982. Coalification model. *Fuel*, pp.1182-1187.

Sabio, E., Alvarez-Murillo, A., Roman, S. and Ledesma, B., 2016. Conversion of tomato-peel waste into solid fuel by hydrothermal carbonization: Influence of the processing variables. *Waste Management*, *47*, pp.122-132.

Salak, F., Daneshvar, S., Abedi, J. and Furukawa, K. 2013. Adding value to onion (Allium cepa L.) waste by subcritical water treatment. *Fuel Processing Technology*, *112*, pp.86-92.

Saltelli, A., Ratto, M., Andres, T., Campolongo, F., Cariboni, J., Gatelli, D., Saisana, M. and Tarantola, S. 2008. Global sensitivity analysis: The primer. John Wiley & Sons.

Sandler, S.I., 2006. Chemical, Biochemical, and Engineering Thermodynamics, 4th edition, John Wiley and Sons, New York.

Sevilla, M. and Fuertes, A.B., 2009. The production of carbon materials by hydrothermal carbonization of cellulose. *Carbon, 47,* pp.2281-2289.

Sevilla, M. and Fuertes, A. B., 2009a. Chemical and structural properties of carbonaceous products obtained by hydrothermal carbonization of saccharides. *Chem. Eur. J. 15,* pp.4195-4203.

Sevilla, M. and Fuertes, A. B., 2009b. The production of carbon materials by hydrothermal carbonization of cellulose. *Carbon, 47,* pp.2281-2289.

Sheng, C., and Azevedo, J.L.T. 2005. Estimating the higher heating value of biomass fuels from basic analysis data. *Biomass and Bioenergy, 28*(5), pp.499-507.

Siskin, M. and Katritzky, A.R. 2001. Reactivity of organic compounds in superheated water: General background. *Chemical Reviews, 101*(4), pp.825-835.

Sobol, I.M., 1993. Sensitivity estimates for nonlinear mathematical models. *Mathematical Modelling and Computational Experiments, 1*(4), pp.407-414.

Stemann, J., Putschew, A. and Ziegler, F. 2013. Hydrothermal carbonization: process water characterization and effects of water recirculation. *Bioresource Technology, 143,* pp.139-146.

Sujauddin, M., Huda, S.M.S. and Hoque, A.T.M.R., 2008. Household solid waste characteristics and management in Chittagong, Bangladesh. *Waste Management 28,* pp.1688-1695.

Sullivan, D., 2010. College students initiate food waste diversion. *Biocycle 51,* 65.

Suwelack, K.U., Wüst, D., Fleischmann, P. and Kruse, A. 2016b. Prediction of gaseous, liquid and solid mass yields from hydrothermal carbonization of biogas digestate by severity parameter. *Biomass Conversion and Biorefinery, 6*(2), pp.151-160

Suwelack, K., Wüst, D., Zeller, M., Kruse, A. and Krümpel, J. 2016a. Hydrothermal carbonization of wheat straw—prediction of product mass yields and degree of carbonization by severity parameter. *Biomass Conversion and Biorefinery, 6*(3), pp.347-354.

Székely, G.J., Rizzo, M.L. and Bakirov, N.K., 2007. Measuring and testing dependence by correlation of distances. *Ann. Statist., 35*(6), pp.2769-2794.

Székely, G.J., Rizzo, M.L., 2009. Brownian distance covariance. *Ann. Appl. Stat., 3*(4), pp.1236-1265.

Takata, M., Fukushima, K., Kino-Kimata, N., Nagao, N., Niwa, C. and Toda, T., 2012. The effects of recycling loops in food waste management in Japan: Based on the environmental and economic evaluation of food recycling. *Science of the Total Environment, 432,* pp.309-317.

Tayade, K.N. and Mishra, M., 2013. A study on factors influencing cross and self-product selectivity in aldol condensation over propylsulfonic acid functionalized silica. *Catalysis Science & Technology, 3*(5), pp.1288-1300.

Tian, Y., Kumabe, K., Matsumoto, K., Takeuchi, H., Xie, Y. and Hasegawa, T., 2012. Hydrolysis behavior of tofu waste in hot compressed water. *Biomass Bioenergy, 39* (0), pp.112-119.

Titirici, M.-M. and Antonietti, M., 2010. Chemistry and materials options of sustainable carbon materials made by hydrothermal carbonization. *Chemical Society Reviews 39,* pp.103-116.

Titirici, M.-M., Antonietti, M. and Baccile, N., 2008. Hydrothermal carbon from biomass: a comparison of the local structure from poly- to monosaccharides and pentoses/hexoses. *Green Chemistry, 10,* pp.1204-1212.

Titirici, M.-M., Thomas, A. and Antonietti, M., 2007a. Back in the black: hydrothermal carbonization of plant material as an efficient chemical process to treat the CO_2 problem? *New Journal of Chemistry, 31,* pp.787-789.

Titirici, M. M., Thomas, A., Yu, S.-H., Möller, J.-O. and Antonietti, M., 2007b. A direct synthesis of mesoporous carbons with bicontinuous pore morphology from crude plant material by hydrothermal carbonization. *Chem. Mater., 19,* pp.4205-4212.

Titirici, M.M., White, R.J., Falco, C. and Sevilla, M. 2012. Black perspectives for a green future: hydrothermal carbons for environment protection and energy storage. *Energy & Environmental Science, 5*(5), pp.6796-6822.

Turns, S.R., 2000. An Introduction to Combustion: Concepts and Applications. 2nd edition. McGraw-Hill, New York.

Wantanabe, M., Sato, T., Inomata, H., Smith, R., Arai, K., Kruse, A. and Dinjus, E. 2004. Chemical reactions of C1 compounds in near critical and supercritical water. *Chemical Reviews, 104,* pp.5803-5821.

Watchararuji, K., Goto, M., Sasaki, M. and Shotipruk, A., 2008. Value-added subcritical water hydrolysate from rice bran and soybean meal. *Bioresour. Technol., 99* (14), pp.6207-6213.

Weiner, B., Baskyr, I., Poerschmann, J. and Kopinke, F.D. 2013. Potential of the hydrothermal carbonization process for the degradation of organic pollutants. *Chemosphere, 92*(6), 674-680.

Wiedner, K., Naisse, C., Rumpel, C., Pozzi, A., Wieczorek, P. and Glaser, B., 2013. Chemical modification of biomass residues during hydrothermal carbonization - What makes the difference, temperature or feedstock? *Org. Geochem. 54,* pp.91-100.

Wirth, B., Mumme, J. and Erlach, B., 2012. Anaerobic treatment of HTC wastewater. Presented at the 2012 US Biochar Conference, Sonoma State University, Rohnert Park, CA, July 29-Aug. 1, 2012.

Witt, C., 2011. Costco example: Food waste diversion through composting. http://codywitt.wordpress.com/2011/02/25/costco-example-food-waste-diversion-through-composting/.

Wu, B., Taylor, C.M., Knappe, D.R.U., Nanny, M.A. and Barlaz, M.A., 2001. Factors controlling alkylbenzene sorption to municipal solid waste. *Environ. Sci. Technol., 35*, pp.4569-4576.

Yuan, X.Z., Tong, J.Y., Zeng, G.M, Li, H. and Xie, M., 2009. Comparative Studies of Products Obtained at Different Temperatures during Straw Liquefaction by Hot Compressed Water, *Energy Fuels*, *23*(6), pp 3262–3267

Yespan, R., 2009. US Residential food waste collection and composting. *Biocycle 50*, 35.

Zhang, X.Y., Trame, M.N., Lesko, L.J. and Schmidt, S., 2015. Sobol sensitivity analysis: a tool to guide the development and evaluation of systems pharmacology models. *CPT: Pharmacometrics & Systems Pharmacology*, *4*(2), 69-79.

Zhong, M., Zhang, Z., Zhou, Q., Yue, J., Gao, S. and Xu, G., 2012. Continuous high-temperature fluidized bed pyrolysis of coal in complex atmospheres: Product distribution and pyrolysis gas. *Journal of Analytical and Applied Pyrolysis, 97*, 123-129.

APPENDIX A.

MANUSCRIPT PERMISSION

ELSEVIER LICENSE
TERMS AND CONDITIONS

Jun 28, 2017

This Agreement between Liang Li ("You") and Elsevier ("Elsevier") consists of your license details and the terms and conditions provided by Elsevier and Copyright Clearance Center.

License Number	4137770757450
License date	Jun 28, 2017
Licensed Content Publisher	Elsevier
Licensed Content Publication	Waste Management
Licensed Content Title	Hydrothermal carbonization of food waste and associated packaging materials for energy source generation
Licensed Content Author	Liang Li,Ryan Diederick,Joseph R.V. Flora,Nicole D. Berge
Licensed Content Date	Nov 1, 2013
Licensed Content Volume	33
Licensed Content Issue	11
Licensed Content Pages	15
Start Page	2478
End Page	2492
Type of Use	reuse in a thesis/dissertation
Portion	full article
Format	both print and electronic
Are you the author of this Elsevier article?	Yes
Will you be translating?	No
Order reference number	
Title of your thesis/dissertation	INVESTIGATING THE FEEDSTOCK PROPERTIES AND PROCESS CONDITIONS INFLUENCING THE CHARACTERISTICS OF PRODUCTS GENERATED FROM THE HYDROTHERMAL CARBONIZATION OF ORGANIC FEEDSTOCKS
Expected completion date	Jul 2017
Estimated size (number of pages)	250
Elsevier VAT number	GB 494 6272 12
Requestor Location	Liang Li 301 Main Street COLUMBIA, SC 29201 United States Attn: Liang Li
Publisher Tax ID	98-0397604
Total	0.00 USD

ELSEVIER LICENSE
TERMS AND CONDITIONS

Jun 28, 2017

This Agreement between Liang Li ("You") and Elsevier ("Elsevier") consists of your license details and the terms and conditions provided by Elsevier and Copyright Clearance Center.

License Number	4137771290736
License date	Jun 28, 2017
Licensed Content Publisher	Elsevier
Licensed Content Publication	Waste Management
Licensed Content Title	Using liquid waste streams as the moisture source during the hydrothermal carbonization of municipal solid wastes
Licensed Content Author	Liang Li,McKenzie Hale,Petra Olsen,Nicole D. Berge
Licensed Content Date	Nov 1, 2014
Licensed Content Volume	34
Licensed Content Issue	11
Licensed Content Pages	11
Start Page	2185
End Page	2195
Type of Use	reuse in a thesis/dissertation
Intended publisher of new work	other
Portion	full article
Format	both print and electronic
Are you the author of this Elsevier article?	Yes
Will you be translating?	No
Order reference number	
Title of your thesis/dissertation	INVESTIGATING THE FEEDSTOCK PROPERTIES AND PROCESS CONDITIONS INFLUENCING THE CHARACTERISTICS OF PRODUCTS GENERATED FROM THE HYDROTHERMAL CARBONIZATION OF ORGANIC FEEDSTOCKS
Expected completion date	Jul 2017
Estimated size (number of pages)	250
Elsevier VAT number	GB 494 6272 12
Requestor Location	Liang Li 301 Main Street COLUMBIA, SC 29201 United States Attn: Liang Li

ELSEVIER LICENSE
TERMS AND CONDITIONS

Jul 18, 2017

This Agreement between Liang Li ("You") and Elsevier ("Elsevier") consists of your license details and the terms and conditions provided by Elsevier and Copyright Clearance Center.

The publisher has provided special terms related to this request that can be found at the end of the Publisher's Terms and Conditions.

License Number	4152040275279
License date	Jul 18, 2017
Licensed Content Publisher	Elsevier
Licensed Content Publication	Bioresource Technology
Licensed Content Title	Investigating the role of feedstock properties and process conditions on products formed during the hydrothermal carbonization of organics using regression techniques
Licensed Content Author	Liang Li,Joseph R.V. Flora,Juan M. Caicedo,Nicole D. Berge
Licensed Content Date	Jul 1, 2015
Licensed Content Volume	187
Licensed Content Issue	n/a
Licensed Content Pages	12
Start Page	263
End Page	274
Type of Use	reuse in a thesis/dissertation
Intended publisher of new work	other
Portion	full article
Format	both print and electronic
Are you the author of this Elsevier article?	Yes
Will you be translating?	No
Order reference number	
Title of your thesis/dissertation	INVESTIGATING THE FEEDSTOCK PROPERTIES AND PROCESS CONDITIONS INFLUENCING THE CHARACTERISTICS OF PRODUCTS GENERATED FROM THE HYDROTHERMAL CARBONIZATION OF ORGANIC FEEDSTOCKS
Expected completion date	Jul 2017
Estimated size (number of pages)	250
Elsevier VAT number	GB 494 6272 12
Requestor Location	Liang Li 301 Main Street